MYC transcriptional functions controlling epidermal stem cell self-renewal and differentiation

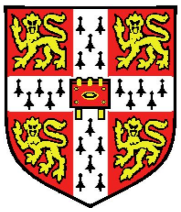

Elisabete Nascimento

Darwin College

University of Cambridge

A dissertation submitted for the degree of

Doctor of Philosophy

September 2011

This dissertation is dedicated to my mum, dad and brother.

Declaration

This dissertation is the result of my own work and includes nothing which is the outcome of work done in collaboration except where specifically indicated in the text.

The work described was carried out at the Wellcome Trust Centre for Stem Cell Research, University of Cambridge, and the Cancer Research UK Cambridge Research Institute under supervision of Dr. Michaela Frye and Dr. Duncan Odom.

The length of this thesis does not exceed 60,000 words, not including figures, photographs, tables, appendices and bibliography, as specified by the Biology Degree Committee.

This dissertation is not substantially the same as any that I submitted for a degree or diploma or other qualification at any other University.

Furthermore, I state that no part of this dissertation has been, or is concurrently being, submitted for any degree, diploma, or other qualification.

Elisabete Nascimento
September 2011

Abstract

The oncoprotein MYC has long been recognized as an important stem cell regulator, yet its direct biological contributions have been difficult to determine. MYC activation can induce pleiotropic phenotypes and mediates cellular functions as opposing as cell growth and proliferation, metabolism, differentiation and apoptosis. In addition, functional redundancy with MYCL and MYCN proteins as well as dose dependency, complicates the identification of the most relevant biological functions. Studies in tissues with high proliferative capacity and rapid turnover have shown that MYC is a key regulator of homeostasis by balancing stem cell self-renewal, proliferation and differentiation processes. In skin, MYC induces the exit of epidermal stem cells from their niche, increases proliferation of progenitor cells and subsequently stimulates lineage specific differentiation into interfollicular epidermis and sebaceous glands; yet the direct transcriptional roles of MYC in these processes remained elusive. To gain insight into the transcriptional roles of MYC in epidermal stem cell homeostasis, I performed chromatin immunoprecipitation on microarrays (ChIP-on-Chip) using mouse proximal promoter arrays combined with mRNA expression data that was generated using epidermal cells from wild-type and transgenic K14MycER mice, treated in a time-course from zero to six days with tamoxifen, to induce the *Myc* transgene expression in the basal undifferentiated layers of the epidermis. Data analysis revealed that 2187 genes, which corresponds to 15% of the promoter regions covered, were directly regulated by MYC. To identify genes uniquely regulated by MYC in skin, I performed gene expression studies on mouse skin in which MYC was conditionally deleted in the basal layer of the epidermis. Remarkably, I found that 45% of all repressed genes were related to epidermal maintenance and differentiation. To better understand the mechanism of how MYC induces keratinocytes to differentiate specifically into lineages of sebaceous glands and interfollicular epidermis, I analyzed whether MYC might have directly regulated genes involved in skin differentiation. Here, I focused my studies on a single 2.2 Mb locus located on mouse chromosome 3 designated as the epidermal differentiation complex (EDC). To assess how activation of MYC could influence the expression of genes localized to the EDC, I performed ChIP-on-Chip for MYC, H3K4me3, H3K27me3,

as well as transcription factors, which have been described to regulate terminal differentiation in skin, such as CEBPα, OVOL-1, KLF4, TCFAP2-γ and SIN3A, among others. I demonstrated that MYC recruits a specific set of tissue-specific transcription factors to the EDC, (e.g. KLF4 and OVOL-1) and thereby prevents binding of a different and distinct set of genomic regulators, (e.g. CEBPα, MXI1 and SIN3A). Using a combination of mouse models and systems biology tools, I then identified SIN3A as a key regulator in this MYC-dependent transcriptional network. I found that MYC and SIN3A form a negative feedback loop, which is required to balance proliferation and differentiation in epidermis, and both factors are essential to maintain skin homeostasis.

Acknowledgements

I would like to thank Michaela Frye for giving me the oportunity to join her lab and for believing in my capabilities to carry out this project. Michaela's guidance, great optimism and enthusiasm inspired me to become a more mature, focused and independent scientist and challenged me to pursue research as my path over the next years. I feel it has been a privilege to work with her.

Thank you to all Frye lab members for providing a healthy and collaborative environment to work, especially to Sandra Blanco for our interesting scientific discussions but most of all for the friendship we developed and for keeping me motivated at all times.
Thank you to the CSCR Biofacility, Histology, Imaging, Genotyping and Tissue Culture facilities, as well as the Genomic core facility from CRI, in particular James Hatfield and Michelle Osborne for help in the Illumina microarray preparation and hybridization. I would also like to thank Nigel Miller from the Pathology Department for his assistance during my flow cytometry experiments.

I'm forever grateful to Duncan Odom, for all the support he provided in terms of resources, as well as his continuous efforts to try to keep me focused in order to conclude my project. Thank you to Stewart MacArthur and Matthew Trotter for their work and dedication helping me during microarray data analysis.

This dissertation was financially supported by a Cancer Research UK scholarship.

To a more personal level, I would also like to thank my dear friends Tiago, David, Ornella, Daniel, Yifan, Priyanka, Sandra, and Ole with whom I carried out my Cambridge experience. Thank you for putting a smile in my face everytime we would meet and for keeping me down to earth and emotionally balanced.
Finally, I have to express my endless appreciation to my parents and brother for their love, support and words of encouragement and for always being present for me and continously remind me of what is really important.

List of abbreviations

BMP Bone Morphogenic Protein
bHLHz basic Helix-Loop-Helix zipper
bp base pair
BSA Bovine Serum Albumin
CDK Cyclin Dependent Kinase
cDNA Complementary Deoxyribonucleic Acid
CE Cornified envelope
CHIP Chromatin Immunoprecipitation
CNE Non Coding Elements
cRNA Complementary Ribonucleic Acid
CSNK2 Caseine Kinase 2
Cy3 Cyanine 3
Cy5 Cyanine 5
DAPI 4',6-Diamidino-2-Phenylindole
DMEM Dulbecco's Modified Eagle's Medium
DMSO Dimethyl Sulphoxide
DNA Deoxyribonucleic Acid
dNTP Deoxynucleotide Triphosphate
DP Dermal papilla
ECL Electrochemiluminescence
ECM Extra Cellular Matrix
EDC Epidermal Differentiation Complex
EDTA Ethylenediaminetetraacetic Acid
EGF Epidermal Growth Factor
EPU Epidermal Proliferative Unit

ER oestrogen receptor
ERAS ES cell expressed Ras
ES Embryonic Stem Cell
GAPDH Glyceraldehyde 3-Phosphate Dehydrogenase
GFP Green fluorescent protein
GSK3 Glycogen Synthase Kinase 3
EGFR Epidermal Growth Factor Receptor
ERK Extracellular-Signal-Regulated Kinase
EV Empty Vector
FAD F12 + Adenine + DMEM
FBW7 F-box Protein 7
FCS Foetal Calf Serum
FLG Filaggrin
H2B Histone H2B
H&E Hematoxilin and eosin
HAT Histone acetyltransferase
HSC Hematopoietic stem cell
HDAC Histone deacetylase
HF Hair Follicle
HG Hair Germ
HSC Hematopoietic Stem Cell
HRP Horseradish Peroxidase
HUWE1 HECT, UBA and WWE domain containing 1
HS Hair shaft
HSP19 Heat Shock Protein 19
IF Intermediate Filaments
IFE Interfollicular Epidermis
IHH Indian Hedgehog
IKK IκB kinase
IP Immunoprecipitation
IRS Inner Root Sheet
ISH *In Situ* hybridisation
IV Ichthyosis vulgaris

ITGB1 β1-Integrin
IVL Involucrin
IVT *In Vitro* Transcription
JAK Janus Kinase
JNK c-Jun N-terminal Kinase
Kb Kilobase
KRT Keratin
LCE Late Cornified Envelope
LGR5 Leucine-rich repeat containing G protein-coupled receptor 5
LGR6 Leucine-rich repeat containing G protein-coupled receptor 6
LOR Loricrin
LRIG1 Leucine-rich repeat and Immunoglobulin-like domain protein 1
LRC Label-Retaining Cell
MAPK Mitogen-Activated Protein Kinase
MCSP Melanoma Chondroitin Sulphate Proteoglycan
MEK1 MAPK/ERK Kinase 1
MTAP4 Microtubule associated protein 4
mRNA Messenger Ribonucleic Acid
mTOR Mammalian Target of Rapamycin
MM Molecular marker
MW Molecular Weight
NF-κB Nuclear Factor κB
4-OHT 4-hydroxy-tamoxifen
ORS Outer Root Sheath
PAGE Polyacrylamide Gel Electrophoresis
PBS Phosphate-buffered Saline
PCR Polymerase Chain Reaction
PE Phycoerythrin
PI3K Phosphatidylinositol 3-Kinase
PIN1 Peptodylprolyl cis/trans Isomerase, NIMA-interacting 1
PP2A Protein Phosphatase 2A
PPAR Peroxisome Proliferator Activated Receptor
PRKC Protein Kinase C

QPCR Quantitative Polymerase Chain Reaction
RAR Retinoic Acid Receptor
RIPA Radio-Immunoprecipitation Assay
RNA Ribonucleic Acid
RNAi Ribonucleic Acid interference
rRNA ribosomal RNA
SCC Squamous Cell Carcinoma
SCF SKP1-CUL1-F-box protein
SDS Sodium Dodecyl Sulphate
SKP1 S-phase kinase-associated protein 1
SKP2 S-phase kinase-associated protein 2
SHH Sonic Hedgehog
SG Sebaceous Gland
SPRR Small Proline Rich
STAT Signal Transducer and Activator of Transcription
TA Transit-Amplifying
TAE Tris-acetic acid-EDTA
TPA 12-O-tetradecanoylphorbol-13-acetate
TBS Tris-buffered Saline
TCHH Trichohyalin
TGF Transforming Growth Factor
TGM Transglutiminase
tRNA transfer RNA
TSS Transcription start site
TU α-Tubulin
UV UltraViolet
UVB UltraViolet B
Wai Wai acidic protein
WCE Whole cell extract
RT Real time

Mouse Lines

f/f floxed alleles
Δ/Δ deleted alleles

Microarray Data Accession Numbers

Data deposited under ArrayExpress accession numbers described below.
Data can be accessed via http://www.ebi.ac.uk/microarray-as/ae/:

Experiment name: Transcriptional profiling of wild-type and K14MycER mice.
ArrayExpress accession: E-MTAB-553

Experiment name: Transcriptional profiling of K14Sin3a$^{\Delta/\Delta}$ and related lines.
ArrayExpress accession: E-MTAB-554

Experiment name: ChIP-on-chip of wild-type and K14MycER in mouse genome-wide proximal promoter regions.
ArrayExpress accession: E-MTAB-555

Experiment name: ChIP-on-chip of wild-type at mouse chromosome 3.
ArrayExpress accession: E-MTAB-556

Contents

List of Figures

List of Tables

Chapter 1

Introduction

1.1 Anatomy of the skin

The skin serves as a protective barrier against environmental insults potentially harmful to the organism. It prevents the body from dehydration, microbial infection and UV radiation; while also providing temperature regulation and tactile sensitivity. This protective function is supported by the acquisition of appendages, such as hair follicles (HFs), sebaceous glands (SGs), sweat glands and nails that are formed through a sequence of complex epithelial-mesenchymal interactions during development [Fuchs, 2007]. Mammalian adult skin can be divided into two main layers: the epidermis (ectoderm origin) and the dermis (mesoderm and neural crest origins) (Figure 1.1). The epidermis, also designated as interfollicular epidermis (IFE), is the outermost layer of the skin, covers the whole surface of the body and is separated from the dermis by a basement membrane. Lying on top of this membrane sits a basal layer of mitotically active epidermal cells, also known as keratinocytes. These cells express keratins, produce and secrete extracellular matrix (ECM) proteins and growth factors. Basal keratinocytes provide support to the suprabasal cells, which have already initiated terminal differentiation and therefore detached from the basement membrane, withdraw the cell cycle and moved upwards to the skin surface [Pincelli and Marconi, 2010]. This sequence of events generates spinous and granular layers, culminating in a cornified envelope that contains transcriptionally inactive, flattened, dead keratinocytes

that will eventually be shed from the skin surface by inner cells moving upwards [Candi et al., 2005]. It is the balance between keratinocyte's proliferation and differentiation that maintains skin homeostasis. This equilibrium must depend on a source of long-lived, high proliferative cells with regenerative potential, in other words putative stem cells [Fuchs, 2009a].

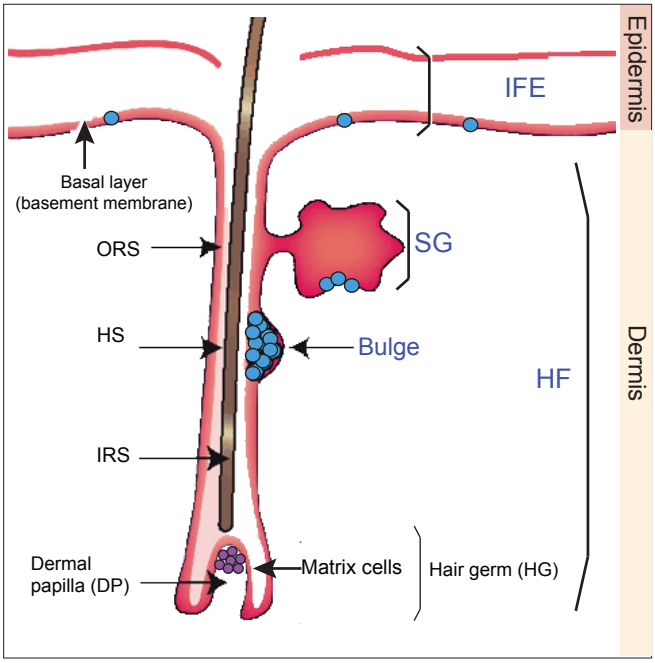

Figure 1.1: Schematic illustration of the murine skin. The skin is subdivided into two layers: epidermis and dermis. The interfollicular epidermis (IFE) is interdispersed with appendages such as hair follicles (HF) and sebaceous glands (SG). These structures are maintained throughout the life of the organism and are constinuously self-renewed due to the presence of stem cells (depicted in blue). These cells are located in niches in the basal layer of the epidermis and sebaceous glands and in the bulge region of the hair follicle. In addition, other structures of the hair follicle are shown such as: ORS - outer root sheath, IRS - inner root sheath, DP - dermal papilla, HG - hair germ, HS - hair shaft and the matrix. This figure was adapted and modified from Khavari [2004].

1.2 Stem cells, transit amplifying cells and committed progenitors

Stem cells are currently defined through functional criteria by the ability to continuously self-renew and generate daughter cells, or committed progenitors, with potential to undergo terminal differentiation [Lajtha, 1979; Schofield, 1983]. During mammalian development, embryonic stem cells are able to divide and give rise to all differentiated cell types in the embryo. In contrast, highly dynamic tissues such as the skin, hematopoietic system or intestinal gut, require adult stem cells to maintain tissue integrity after cell death or injury; these however are restricted to generate progenitors and differentiated cells within that lineage [Hall and Watt, 1989]. The skin constitutes an attractive model to study stem cell biology, not only because of its dynamic nature and self-regenerative capacity, but also due to its high cell turnover and accessibility. Epidermal stem cells are believed to divide rarely in order to preserve their proliferative potential (i.e. clonogenicity) and genomic DNA integrity. They can divide and generate transit amplifying (TA) or committed progenitor cells with a more restricted proliferative potential. TA cells will inevitably initiate a terminal differentiation program and exhaust their proliferative capacity in order to maintain normal homeostasis.

The slow-cycling nature of keratinocyte stem cells is shown by their ability to retain modified DNA precursors [e.g. tritiated thymidine (3H-T) or bromodeoxyuridine (BrdUrd)] or chromatin labels (e.g. H2B-GFP) in label-retaining assays [Bickenbach, 1981; Bickenbach and Chism, 1998; Tumbar et al., 2004]. In these experiments, TA or progenitor cells with a high division rate, will dilute the dye, whereas stem cells will preserve it. These studies, combined with the fact that label retaining cells (LRCs) exhibit high clonogenicity *in vitro*, recognized LRCs as epidermal stem cells, located in three distinct locations or niches: HF bulge, SGs and basal layer of the IFE. In normal physiological conditions it is believed that each stem cell niche gives rise to its own progeny and, only under the appropriate stimuli (e.g. wounding), an epidermal stem cell will generate progeny in the three different lineages [Ghazizadeh and Taichman, 2001].

1.3 Epidermal stem cell niches

1.3.1 Hair follicle

The hair follicle is a skin appendage that undergoes continuous cycles of growth (anagen), regression (catagen) and rest (telogen) [Hardy, 1992] (Figure 1.2). During anagen, slow-cycling LRCs residing in the murine and human bulge region and produce rapid, but transiently, proliferating matrix keratinocytes [Akiyama et al., 2000; Cotsarelis et al., 1990; Lyle et al., 1998; Tumbar et al., 2004]. In mice, matrix cells divide in the hair bulb after receiving signals from the dermal papilla (DP); a region in the HF that aggregates dermal cells and capillaries. Their progeny moves upwards and differentiates into the seven different lineages that will constitute the hair shaft (HS) and inner root sheet (IRS). As soon as catagen begins, the DP regresses through apoptosis and starts moving upwards. Consequently, matrix cells stop receiving signals from the mesenchymal cells of the DP, cease to proliferate and the HF enters a dormant phase known as telogen (reviewed in [Blanpain and Fuchs, 2009; Braun and Prowse, 2006; Fuchs, 2009b]).

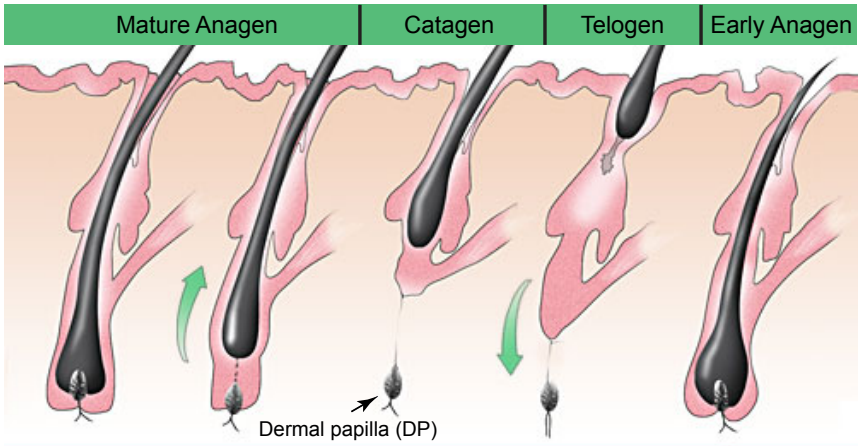

Figure 1.2: Hair follicle cycles. Scheme of the different cycles of hair follicle regeneration. Anagen, the growth phase of the hair cycle (mature and early), the regression phase where the dermal papilla (DP) is pushed upwards closer to the interfollicular epidermis (catagen) and the resting phase (telogen). This figure was adapted and modified from http://hairline.ge/photos/uploads/sub-about-hs-eng-01.jpg.

The mechanisms regulating HF regeneration remain poorly understood, however there is evidence for crosstalk between epidermal and dermal cells [Fuchs and Horsley, 2008].

Currently, the HF bulge constitutes the best defined epidermal stem cell niche. Located at the site of attachment of the *musculus arrector pili*, this region concentrates the higher number of LRCs within the appendage. Nevertheless, bulge LRCs can be stimulated to proliferate under stress conditions, for example, upon treatment with 12-O-tetradecanoylphorbol-13-acetate (TPA) or as a consequence of physical injury [Cotsarelis et al., 1990; Jaks et al., 2010; Morris and Potten, 1999]. In mice, the majority of LRCs overlaps, both locally and in terms of gene expression, with bulge cells expressing the cell surface marker CD34 [Trempus et al., 2003] (Figure 1.3). CD34 expressing keratinocytes display high proliferation potential *in vitro* and are able to fully reconstitute HF and IFE *in vivo* - functional characteristics of epidermal stem cells [Blanpain et al., 2004; Trempus et al., 2003; Tumbar et al., 2004]. This population of stem cells overlaps with other stem cell marker which has been identified in the region covering the bulge and upper region of the hair germ (HG), keratin 15 (KRT15). Keratinocytes expressing KRT15 have a gene expression profile identical to the one presented for $CD34^+$ bulge cells [Morris et al., 2004; Trempus et al., 2007] (Figure 1.3). Interestingly, $CD34^+$ and $KRT15^+$ keratinocytes express high levels of leucine-rich repeat-containing heterotrimeric guanine nucleotide-binding protein (G protein)-coupled receptor 5, LGR5 (Figure 1.3). In contrast to the markers previously described, LGR5 marks actively cycling keratinocytes in the HG at the onset of anagen, as well as a rare number of bulge LRCs [Jaks et al., 2008] (Figure 1.3). Despite the fact that the $LGR5^+$ cell population does not comply with the historic definition of a stem cell population, $LGR5^+$ keratinocytes can originate functional HFs *in* and *ex vivo*; supporting a model in which the HF is maintained by quiescent as well as actively cycling stem cells [Li and Clevers, 2010]. The regions located above the bulge region (namely, infundibulum and isthmus) also arbour highly clonogenic keratinocytes, fully able to reconstitute the HF. In the upper isthmus, keratinocytes expressing the thymus stem cell marker PLET1, which is recognized by the monoclonal antibody MTS24, are able to fully differentiate in HF and IFE lineages, as multipotent of stem cells would [Jensen et al.,

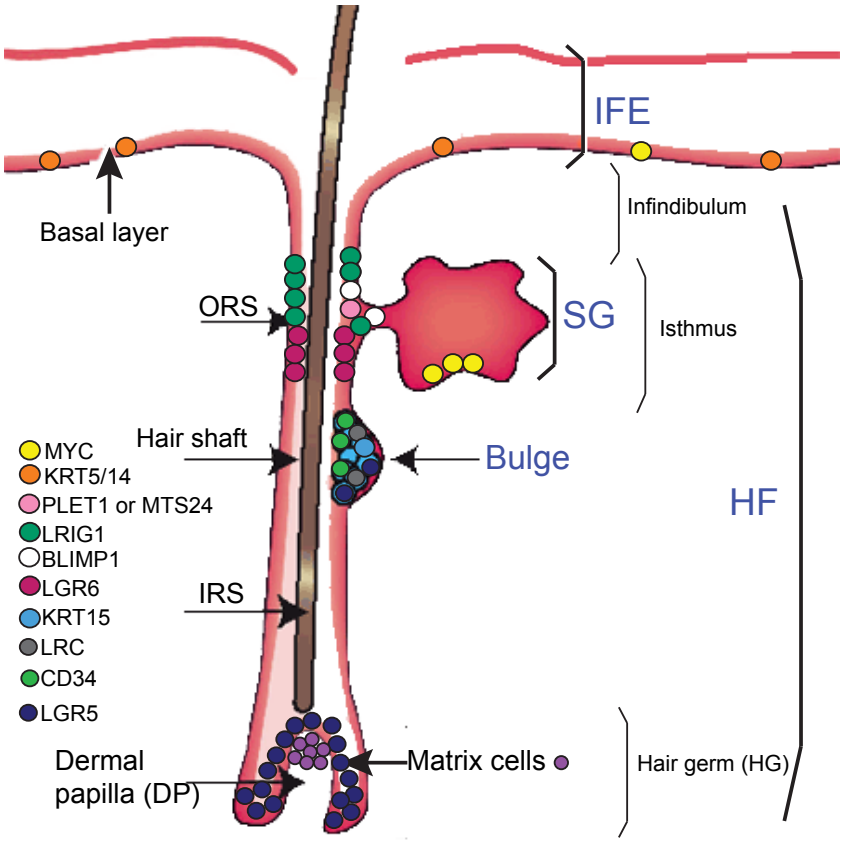

Figure 1.3: Stem cell markers in murine skin. Stem cell populations have been identified in the hair follicle (HF), sebaceous glands (SG) and interfollicular epidermis (IFE) and are represented according to their gene/protein expression or promoter activity: LGR5 (dark blue, hair germ and bulge), CD34 (light green, bulge), KRT15 (light blue, bulge), LGR6 (magenta, lower isthmus), BLIMP1 (white, sebaceous gland opening), LRIG1 (dark green, isthmus), PLET1 or MTS24 (pink, isthmus), KRT5/14 (orange, basal layer of epidermis) and MYC (yellow, basal layer of epidermis and sebaceous gland). Slow diving label retaining cells, LRCs (grey, bulge). This figure was adapted from Jaks et al. [2010] and Khavari [2004].

2008]. These cells do not express CD34, but do express low levels of integrin alpha 6, ITGα6 and the infundibulum marker, stem cell antigen 1, LY6A. Moreover, another population of quiescent HF cells has been identified in the upper region of the isthmus and lower infundibulum; this population expresses the leucine-rich immunoglobin-like protein, LRIG1 marker [Jensen et al., 2009] (Figure 1.3). Finally, in the region between $CD34^+$ bulge cells and MTS24/LRIG1 expressing cells, another subpopulation of highly clonogenic keratinocytes was also identified, marked by LGR6. Similarly to the LGR5 population, $LGR6^+$ keratinocytes do not retain labels; nevertheless, these cells fulfil all functional criteria that define an epidermal stem cell, being able to supply the IFE and SG lineages [Snippert et al., 2010]. Interestingly, LGR5, LGR6 and LRIG1 are co-expressed during development at embryonic day 18.5 (E18.5) with SOX9, a marker expressed during hair morphogenesis, suggesting the existence of a common precursor for HF stem cells in the adult [Jaks et al., 2008, 2010; Jensen et al., 2009; Nowak et al., 2008; Snippert et al., 2010; Vidal et al., 2005]. Early murine bulge LRCs also express other transcription factors associated with *stemness*, such as: TCF3, LHX2 and NFATC1 [Nowak et al., 2008].

The majority of previous studies identified stem cell populations in the murine HF. The main reason for this is that in humans, the bulge region is difficult to identify morphologically; and only, few stem cell markers have been identified, due to the understandable inability to conduct lineage tracing experiments in humans. Still, it has been possible to demonstrate that human HF bulge keratinocytes are quiescent and express high levels of KRT15, similarly to mouse bulge keratinocytes. However, the expression pattern does not overlap with CD34 because in humans KRT15 is expressed in the lower ORS of the HF [Cotsarelis, 2006; Lyle et al., 1998; Ohyama et al., 2006]. Gene expression profiling of human HF bulge cells revealed CD200 as a new marker for quiescent HF cells; but it also confirmed the existence of different stem cell populations between mouse and human [Ohyama et al., 2006]. Although murine and human bulge stem cells express different markers, the signalling pathways that govern HF stem cell maintenance, induction, cell fate and differentiation processes appear to be conserved, and therefore mouse models are a useful model to study skin stem cells, as reviewed in Pincelli and Marconi [2010].

The bulge region of the HF constitutes a protective microenvironment that maintains stem cells quiescent and sheltered from external stimuli. The factors that regulate quiescence are poorly understood, but one of the pathways that is known to affect the cell cycle of bulge stem cells is WNT/β-catenin. Indeed, when β-catenin is conditional deleted in adult skin, hair follicle loss is observed. On the other hand, when β-catenin is activated it results in *de novo* hair morphogenesis [Braun and Prowse, 2006; Gat et al., 1998; Huelsken et al., 2001; Merrill et al., 2001], whereas transient expression of β-catenin prompts HFs to enter anagen earlier, and induces formation of ectopic HFs [LoCelso et al., 2004; Silva-Vargas et al., 2005; VanMater et al., 2003].

BMP signalling is also important in bulge stem cell activation. When this pathway is impaired, either by deletion of its receptor *Bmp1r*, or by overexpression of *Nog* (encodes a protein that inactivates BMP) [Kulessa et al., 2000], it causes formation of cysts within the HF structure [Andl et al., 2004] or impaired differentiation in the matrix [Kobielak et al., 2003], respectively.

In summary, bulge cell fate decisions can be manipulated in response to environmental signals, suggesting that quiescence is not an intrinsic property of the stem cells, but a response that is mediated by intrinsic factors and external stimuli. This allows the co-existence of epidermal and non-epidermal stem cells in the same tissue, such as: melanocyte [Nishimura et al., 2002], neural crest [Sieber-Blum et al., 2004] and nestin-positive, keratin-negative stem cells [Amoh et al., 2005].

1.3.2 Sebaceous gland

The sebaceous gland's main function is to provide hair lubrication and prevent microbial infection through secretion of lipids and sebum which are produced by sebocytes [Stewart and Downing, 1991]. For this reason, SGs are frequently seen as HF appendages, in the sense that in some instances it is possible to lose their structure concomitantly to HF loss [Selleri et al., 2006]; yet there is evidence that a single population of SG stem cells is able to maintain homeostasis of this skin appendage. Studies where epidermal cells were retrovirally labelled have shown that SGs can arise and be maintained by a single population of cells unrelated

to the HF [Ghazizadeh and Taichman, 2001; LoCelso et al., 2008]. Furthermore, transgenic mice lacking HFs, still present SGs, and these persist in skin lacking HFs (e.g. footpad epidermis) [Allen et al., 2003; Nakamura et al., 2001]. Sebaceous gland stem cells are thought to be located in the basement membrane of the gland (Figure 1.3). The cells in this region present a high proliferative capacity as well as high levels of *Myc* expression. In fact, overexpression of *Myc* or deletion of *Rac1* in different mouse models, causes hyperplasia, suggesting a role in sebocyte differentiation [Arnold and Watt, 2001; Benitah et al., 2005; Braun et al., 2003; Bull et al., 2005; Frye et al., 2003; Waikel et al., 2001]. BLIMP1 (also known as PDRM1), a known *Myc* repressor, has been described as a marker of sebaceous gland progenitors (Figure 1.3). Lineage tracing experiments have shown that BLIMP1 positive cells can generate sebaceous glands and that when *Blimp1* is mutated, sebaceous gland homeostasis is affected [Horsley et al., 2006]. LRIG1 also has been shown to contribute, during homeostasis, to the population of SG BLIMP1$^+$ cells located in the junctional zone between the infundibulum and SG [Jensen et al., 2009]. These cells are thought to maintain their quiescence state due to BLIMP1 and LRIG1 negative regulation over *Myc* expression [Horsley et al., 2006; Jensen et al., 2009]. LGR6$^+$ HF stem cells also contribute to the sebaceous gland lineage under homeostatic conditions [Snippert et al., 2010] and Sonic hedgehog (SHH) signalling was also shown to have an effect in sebocyte proliferation. Activation of SHH through expression of a mutant smoothen receptor induces ectopic sebocyte development [Allen et al., 2003]. *In vitro* treatment of sebocytes with Indian hedgehog (IHH) increases sebocyte differentiation [Niemann et al., 2003]. Conversely, inhibition of this pathway through a dominant-negative mutant of GLI2, suppresses sebocyte development [Allen et al., 2003; Fuchs and Horsley, 2008]. Inhibition of WNT signalling through expression of a dominant negative form of LEF1, ΔNLEF1, results in sebocyte differentiation at the expense of HF formation [Gat et al., 1998; LoCelso et al., 2004; VanMater et al., 2003]. Confirming these results, degradation of β-catenin through increased expression of *Smad7* also results in SG hyperproliferation [Han et al., 2006]. Nevertheless, the fact that overexpression of *Tcf3* results in suppression of sebocyte formation [Nguyen et al., 2006], seems to point to the fact that a proper balance between WNT and SHH signalling needs to be established during

SG development [Fuchs and Horsley, 2008]. Sebocyte differentiation is also regulated by the adipogenic transcription factor peroxisome proliferator-activated receptor-γ, PPARγ. This was shown in studies using embryonic stem cells *null* for *Ppar*γ which contributed poorly to sebaceous glands formation in chimaeric mice [Horsley et al., 2006; Rosen et al., 1999]. Additional supporting evidence for these observations comes from studies where skin was treated with PPARγ ligands. These treatments increase sebocyte differentiation *in vitro* and sebum production in humans [Trivedi et al., 2006].

1.3.3 Interfollicular epidermis

The interfollicular epidermis is a stratified squamous epithelium, structurally organized with a basal layer of mitotically active keratinocytes, and suprabasal layers with progressively decreased self-renewal potential. The basal layer secretes ECM proteins such as laminin 5, and uses $\alpha 3\beta 1$-integrin as part of the ECM [Blanpain and Fuchs, 2006]. As cells migrate from basal to suprabasal layers, a series of events starts to take place, such as withdrawal of the cell cycle, decreased integrin and laminin expression and initiation of a terminal differentiation program. The epidermis also contains a high content of keratins; these are obligate heterodimers which form 10 nm intermediate filaments that interact with desmosomes containing $\alpha 6\beta 4$ integrin [Blanpain and Fuchs, 2006]. These interactions form a stable network that is attached to the ECM through desmosomal cadherins. Typically, the basal layer of the adult IFE expresses keratins 5 and 14 (KRT5 and KRT14) (Figure 1.3), the spinous layer expresses keratins 1 and 10 (KRT1 and KRT10) and the granular layer produces filaggrin and loricrin structural proteins. In the IFE, terminal differentiation is controlled by specific transcription factors, such as: JUN, TCFAP2, CEBPs, KLFs, PPARs and NOTCH [Dai and Segre, 2004]. The molecular mechanisms governing epidermal differentiation will be discussed later in Section 1.7.

The IFE stratification process is thought to be initiated when basal epidermal cells detach from the basement membrane and neighbouring keratinocytes are pushed upwards into the spinous layer, through delamination [Vaezi et al., 2002]. There is some evidence that stratification might depend on the orientation of

the mitotic spindle orientation of basal cells regarding the basement membrane where these are attached. In other words, if the mitotic spindle is perpendicular to the basement membrane, it will immediately place one of the daughter cells in the suprabasal layer. Studies in embryonic murine epidermis seem to favour this hypothesis [Lechler and Fuchs, 2005]. Namely, because asymmetric segregation of cell fate determinants might play an important role in differentiation, as seen in stem cells in other organisms such as *Drosophila melanogaster* or *Caenorhabditis elegans* [Cowan and Hyman, 2004; Wodarz, 2005].

Evidence for the existence of stem cells in the IFE is illustrated by the ability to culture human epidermal keratinocytes *in vitro* [Rheinwald and Green, 1975] and subsequently perform transplantation in patients with severe skin burns [Gallico et al., 1984]. These autografts show regenerative capacity after many generations in culture and are able to completely restore the burned skin [Rochat et al., 1994]. The grafts can also persist on the patients for several years, even when hairless skin biopsies are used [Pellegrini et al., 1999]. This healing process relies on epidermal stem cells as these cell populations alone are sufficient to maintain the IFE. In fact, when epidermal stem cells are grown in culture at clonal density, large actively growing colonies (holoclones) are formed whereas, when more committed progenitors or differentiated cells are grown in culture, these tend to form irregular, slow-dividing abortive colonies (meroclones and paraclones), which will eventually undergo terminal differentiation after few rounds of division [Barrandon and Green, 1987].

In humans, the epidermis is thicker and forms ridges. Human epidermal stem cells are thought to lie on top of these ridges and to divide less frequently, when compared to what is observed in mouse skin [Lavker and Sun, 1982]. When cultured *in vitro*, human epidermal stem cells express high levels of $\beta 1$ integrin and show high clonogenicity [Jones and Watt, 1993]. These observations led to another hypothesis in which these cells might be located at the tips of the dermal papilla and TA cells would migrate to the ridges. Attempts to try to establish a specific genetic signature for human IFE stem cells have shown that, IFE putative stem cells express high levels of integrin $\alpha 6$, melanoma chondroitin sulphate (MCSP), KRT15, and low levels of the transferrin receptor, CD71 [Jones and Watt, 1993; Legg et al., 2003; Li et al., 1998; Tani et al., 2000; Webb et al.,

2004]. However, none of these markers has been proven to be specific only for IFE stem cells *in vivo*, due to the inevitable heterogeneity observed in the fluorescence-activated cell sorted populations used in the experiments. In addition, deletion of integrin molecules in the IFE does not lead to a stem cell depletion phenotype [López-Rovira et al., 2005] consequently, the search for stem cell markers in the IFE still continues. Single cell profiling however, is a useful experimental tool that might be able to address the heterogeneity problem and therefore provide increased sensitivity. LRIG1, a key marker of stem cell quiescence, was identified using this method [Jensen and Watt, 2006].

1.4 Epidermal stem cell plasticity

The stem cell populations of the HF, IFE and SG are interconvertible. This means that even though cell autonomous regulators (such as: transcription factors, asymmetric division determinants, clock genes [Lin et al., 2009]) restrict stem cells to a specific lineage, these signals can be modulated by extrinsic signals such as cytokines, growth factors or morphogens, direct contact with neighbouring cells, availability to oxygen and nutrients and even stretch forces [Connelly et al., 2010; Spradling et al., 2001; Watt and Hogan, 2000]. The combination of these forces on an epidermal stem cell will dictate the specific differentiation pathway. For example, dermal papilla cells, when in contact with the basal layer of adult epidermis can induce HF formation, suggesting that communication between IFE keratinocytes with dermal papilla cells reprograms the previous lineage commitment to HF morphogenesis [Reynolds and Jahoda, 1992]. Also, overexpression of the gene encoding the transcription factor, ZIPRO1, deletion of *Rxrα* or the vitamin D receptor in adult mouse epidermis originates cysts with absent or abnormal HFs. Presumably, these results reflect the induction of an IFE differentiation phenotype [Li et al., 2000b, 1997; Niemann and Watt, 2002]. Moreover, activation of β-catenin in the basal layer of the epidermis, under control of the *Krt4* promoter, induces ectopic formation of hair follicles in the IFE [Gat et al., 1998; LoCelso et al., 2004; VanMater et al., 2003]; whereas, inhibition of this gene or overexpression of a N-terminally truncated form of LEF1, ΔNLEF1, which lacks the β-catenin binding site, induces hair loss and formation

of dermal cysts [Niemann and Watt, 2002]. These studies confirm the importance of environmental cues dictating epidermal stem cell fate, and denote a role for β-catenin in activating HF differentiation.

Similarly, manipulation of the microenvironment through activation of MYC in basal undifferentiated layers of the epidermis, stimulates differentiation of epidermal stem cells into the IFE and sebaceous glands, at the expense of HFs (Figure 1.7) [Frye et al., 2003; Gebhardt et al., 2006; Waikel et al., 2001]. Increased differentiation is measured, for example, by an increase in epidermal suprabasal layers expressing KRT10 and involucrin (IVL). Furthermore, when cells from the IFE are subjected to mesenchymal stimuli, these can differentiate into the HF and SG lineages [Ferraris et al., 1997; Reynolds and Jahoda, 1992].

Epidermal stem cell plasticity can also be observed during wound healing response, when multipotent bulge stem cells are able to regenerate the IFE [Ito et al., 2005; Levy et al., 2005; Taylor et al., 2000; Tumbar et al., 2004]. These studies demonstrate that epidermal stem cells from the IFE, HF and SG are all multipotent and able to regenerate the tissue where they reside.

1.5 Models of skin homeostasis and repair

Skin homeostasis requires a perfect balance between cell proliferation and differentiation. For several years, a hierarchical model has been used to describe this process in which a single quiescent stem cell would be activated to asymmetrically divide and give rise to a new stem and TA cell that after a few rounds of division would differentiate. This model was designated as the epidermal proliferative unit (EPU) model, where the epidermis was thought to be maintained by EPU units, each containing one stem cell that would divide asymmetrically, giving rise to mitotically active progenitors or TA cells and later to differentiated cells overlaying it [Lechler and Fuchs, 2005; Mackenzie, 1970; Potten and Booth, 2002] (Figure 1.4).

Stem cell symmetric division was tought to only occur during tissue expansion or damage. In recent years this model has been challenged by lineage tracing experiments *in vivo* in murine epidermis where stem cells and TA cells are tracked during clonal expansion of individual cells [Clayton et al., 2007; Snippert et al.,

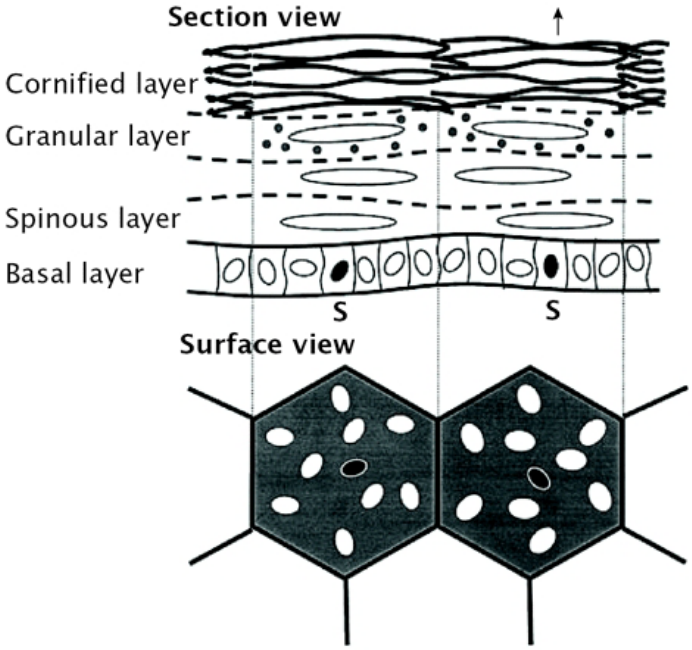

Figure 1.4: Epidermal proliferative unit (EPU) model. Model for skin renewal in the mouse based on Potten's model of epidermal proliferative units. This model considers that one in ten basal cells are stem cells (S). The neighboring basal cells and all cells in the suprabasal layers would have derived from the single stem cell in a typical stem cell-transit amplifying cell model. The surface view shows that each unit derived from a single stem cell forms a hexagonal shape that encompasses about ten basal cells –the epidermal unit –. Each black cell denotes the single stem cell in each unit. Taken from Potten and Booth [2002].

2010]. Data analysis using the EPU model would predict that, if a TA cell was labelled (using the LACZ or GFP), the label would be lost due to differentiation; whereas in the case of a stem cell, this would result in increased expansion of a labelled clone, because stem cells rarely divide in the classical definition; and when division would take place it would be asymmetric. Consequently the resultant expansion of the clonal area would originate an epidermal unit [Mackenzie, 1970]. Unexpectadly, what has been observed is that labelled clones are continuously lost and replaced by neighbouring clones, with the overall number of labelled cells being kept constant over time [Clayton et al., 2007]. This observation suggests a stochastic model where stem cell division can lead to one of three different outcomes: it can originate two stem cells, two TA cells or one stem cell and one TA cell [Clayton et al., 2007; Jones et al., 2007; Klein et al., 2007]. Stochasticity also assumes that, at the single cell level, the stem cell fate cannot be predicted but, at the population level, the average fate can be set to be one stem cell originating one TA cell [Simons and Clevers, 2011]. These results have led to the conclusion that the murine epidermis is maintained by a unipotent population of progenitor cells in homeostatic conditions. Nevertheless, the stochastic model does not exclude the possibility of a second, more dormant, stem cell population, which would only be activated upon injury. In fact, there is evidence for such population in the upper region of the murine HF [Jensen et al., 2009; Snippert et al., 2010]. Furthermore, when this model is used to predict the fate of human epidermal stem cells *in vitro*, it seems to favour the existence of cell division heterogeneity as well as the notion that maintenance of homeostasis within the human epidermis might require different stem cell populations, expressing different levels of stem cell markers (e.g. $\beta 1$ integrin, LRIG1). This suggests that LRCs are far more common than what was initially predicted, and that stem cell quiescence is not a necessary requisite for *stemness*. In fact, comparison of stem cell's proliferation rates in tissues with high cell turnover such as, the intestine, HF bulge and mammary gland, all point to the fact that label retention is a property of some stem cells, but not all. It seems that stem cells might adjust their cell cycle properties in response to the microenvironment around them. A good example for this idea, comes from studies where slow-cycling bulge stem cells are depleted from the HF and the more active-cycling cells of the HG repopulate and regenerate

the bulge niche [Fuchs, 2009a; Ito et al., 2004].

Considerable progress has been made to try to understand the key regulators of epidermal stem cell maintenance, activation and lineage determination. In the following sections I will summarize some of the key aspects of epidermal stratification and the transcriptional regulators of stem cell activation and terminal differentiation in normal IFE, as well as in disease.

1.6 Morphological aspects of epidermal differentiation

As previously mentioned, the differentiation of the IFE is a multistep process where, basal proliferative keratinocytes detach from the basement membrane and commit to differentiation by migrating upwards through the suprabasal layers. This sequence of events is known as cornification and implies changes in keratin intermediate filaments (IFs), appearance of keratohyalin granules and formation of a cornified envelope (CE). The morphological changes accompanying this process have been well documented. Briefly, as basal keratinocytes migrate to the spinous layer, they exit from the cell cycle and start synthesizing structural proteins essential for keratinization, such as KRT1 and KRT10, replacing the initial keratins, KRT5 and KRT14. Subsequently, keratinocytes start to accumulate granules containing profilaggrin (a precursor of filaggrin, FLG) and other structural proteins are also synthesized (e.g involucrin, loricrin, trichohyalin, S100 calcium binding proteins, late cornified envelope proteins-LCEs, small proline rich proteins-SPRRs) [Candi et al., 2005] (Figure 1.5). These proteins are cross-linked by transglutaminases (TGMs) forming the CE structure. Lipids (e.g. ceramides) covalently bond to the newly formed isopeptides, form lamellar granules that are extruded into the extracellular space, conferring impermeability to the epidermal barrier [Candi et al., 2005]. Cornification is a highly regulated process where the majority of the genes encoding for structural proteins important for establishment of the CE are clustered in a region of the mammalian genome designated as the epidermal differentiation complex (EDC).

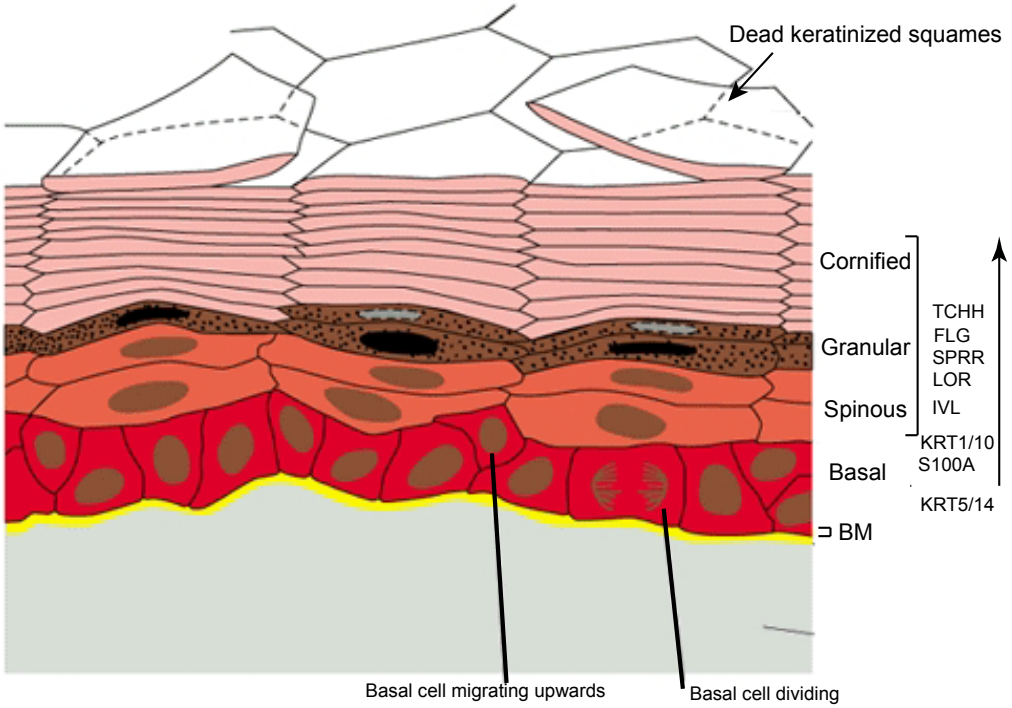

Figure 1.5: Cornification process in the epidermis. As basal epidermal cells [marked by KRT5 and KRT14 (KRT5/14)] divide, detachment from the basement membrane (BM) triggers them to move upwards to the suprabrasal layers of the epidermis, namely the spinous, granular and cornified layers. Throughout this process epidermal cells initiate the expression of genes encoding for KRT1 and KRT10 (KRT1/10), as well as other structural proteins, such as S100A calcium binding proteins, involucrin (IVL), loricrin (LOR), small proline rich proteins (SPRRs), filaggrin (FLG) and trichohyalin (TCHH). As soon as a cell reaches the epidermal surface, it has already lost its nucleus and its structure changed from round to flat, due to cytoskeleton rearrangements. At this point this cell constitutes a dead keratinized squame that will eventually be shed from the surface and replaced by inner cells, in a continuous process throughout the lifetime of the organism. This image was adapted from http://www.ncbi.nlm.nih.gov/books/NBK26865/bin/ch22f2.jpg. Information for the mRNA expression pattern of the differentiation related genes in the epidermis was taken from Williams et al. [2002].

1.6.1 The epidermal differentiation complex (EDC)

The epidermal differentiation complex (EDC; 1q21 in human, 3q2.1 in mouse and 2q34 in rat) clusters around 61 genes which encode the main substrates of TGMs important for the keratinocyte differentiation pathway [Brown et al., 2007; Williams et al., 2002]. EDC genes are organized into four different families: cornified envelope precursor proteins (involucrin, loricrin and SPRRs), filaggrin-like proteins (FLG and TCHH), calcium binding proteins (S100A) and late cornified envelope proteins (LCE) [Marshall et al., 2001; Mischke et al., 1996]. The expression pattern of EDC genes during keratinocyte differentiation is represented in (Figure 1.5). Spatial constrain of these genes, over billions of years and across species, suggests that EDC genes possibly share regulatory elements, to tightly and temporally control transcription during epidermal differentiation [Mischke et al., 1996; Williams et al., 2002; Zhao and Elder, 1997]. One possible model for coordinate expression would involve cis-regulatory elements. Indeed, 48 conserved non-coding elements (CNEs) have been identified *in silico* and two have been experimentally confirmed to possess *in vivo* enhancer activity and capable of dynamically regulating the expression of *LCE3C* and *LCE3B* genes during differentiation and proliferation [DeGuzmanStrong et al., 2010]

The coordinate arrangement and transcription of the EDC genes, creates a region extremely attractive for lineage commitment studies, particularly in the IFE. It would be interesting to understand which signalling pathways control keratinocyte differentiation, as well as what are the genetic alterations that might predispose to skin diseases such as psoriasis or cancer. Below, I will describe some of the key features and roles of selected epidermal structural proteins encoded at the EDC.

1.6.2 Involucrin - IVL

Involucrin, IVL, is a soluble precursor of the epidermal CE. It presents several glutamine reactive sites that are used to establish isopeptide covalent bonds with other structural proteins present in the envelope [Eckert et al., 2004]. This structural protein acts as an amine receptor in transglutaminase enzymatic reactions [Watt, 1983] and this allows it to be used as a scaffold for other precursors of the

CE. Involucrin expression usually starts in the early formed spinous layer and it is maintained through the granular layer, however the protein itself, is only incorporated in the transition zone between the two layers. In addition, *Ivl* expression, and consequently keratinocyte differentiation, is regulated by extrinsic factors such as: calcium [Bikle et al., 2001; Deucher et al., 2002], vitamin A [Poumay et al., 1999] protein kinase C (PRKC) [Welter, 1995] retinoids [Monzon et al., 1996] and antioxidants [Balasubramanian et al., 2002]. This protein is not exclusively expressed in the stratified squamous epithelium of the skin, but it is also present in other epithelia: esophageal, lingual, conjunctival and corneal [Banks-Schlegel and Green, 1981; Eckert et al., 1993]. Surprisingly, overexpression of *Ivl* or deletion in transgenic mice does not induce major defects in epidermis [Candi et al., 2005; Crish et al., 1993; Djian et al., 2000].

1.6.3 Loricrin - LOR

Loricrin, LOR, is the most abundant protein of the CE, covering 75% of its protein content. Its structure is predicted to be disorganized and enriched in glycine, serine and cysteine residues and the lack of ordered structure is thought to contribute to the elastic properties of the CE. In general, the majority of isopeptide bonds established are LOR-LOR interactions, although binding to SPRRs and profilaggrin is also observed [Candi et al., 2005]. In humans, there is evidence that LOR is firstly deposited with profillagrin in the granular layer, where keratohyalin granules are released [Yoneda and Steinert, 1993] to an already established scaffold containing IVL, desmosomal proteins and S100 calcium binding proteins. Loricrin is also a substrate for transglutaminases, TGM1, TGM2, TGM3 and TGM5 [Candi et al., 1995]. Surprisingly, overexpression of the human *LOR* gene or deletion in mice yields a normal phenotype; suggesting that this is not an essential gene and it can be substitute by other structural proteins, such as SPRRs [Jarnik et al., 2002; O'Driscoll et al., 2002]. Overexpression in transgenic mice also does not interfere with normal assembly of the CE; confirming that LOR is deposited later into the pre-existing scaffold [Yoneda and Steinert, 1993]. *In vitro* studies show that *LOR* expression is increased by calcium and phorbol ester and decreased by retinoic acid [Dlugosz and Yuspa, 1993; Hohl et al.]. Defects in

the *LOR* gene have been linked to two skin diseases: Vohwinkel syndrome and progressive symmetric erythrokeratodermia (PSEK). The first is characterized by hyperkeratosis of the palms and soles, which in some instances can lead to amputation; while the second is characterized by erythematous plaques over the entire body and palmoplantar hyperkeratosis [Armstrong et al., 1998; Ishida-Yamamoto et al., 1997; Korge et al., 1997].

1.6.4 Filaggrin - FLG

Filaggrin, FLG, is a dephosphorylated form of profilaggin (a filaggrin precursor). In its phosphorylated form, this protein accumulates in keratohyalin granules along with LOR, throughout the granular layers of the epidermis. *In vitro*, FLG is able to form aggregates with keratin intermediate filaments, establishing ordered arrays. These interactions are thought to cause some of the drastic morphological changes observed when keratinocytes move from a round to a more flattened shape, possibly due to their effect in the cytoskeleton [Candi et al., 2005]. Mutations in the *FLG* gene are linked to the disease Ichthyosis vulgaris (IV). Patients carrying this mutation, show low levels of FLG, mild hyperkeratosis and a diminished granular layer [Segre, 2006]. In mice, a mutated form of FLG induces a phenotype designated as flaky tail, also establishing a link with IV. These mice express an abnormal form of profilaggrin and present similar phenotype to what have been observed in humans patients with IV [Hoffjan and Stemmler, 2007; Presland et al., 2000]. In addition, mutations in *FLG* seem to constitute a predisposed factor for atopic dermatitis [Palmer et al., 2006; Smith et al., 2006].

1.6.5 Trichohyalin - TCHH

Trichohyalin, TCHH, is a keratin-intermediate filament associated protein that is also expressed in the granular cells of the epidermis. Its biochemical structure is very similar to FLG; both proteins present calcium binding domains at the N-terminus, similar to the ones observed in S100 calcium binding proteins (discussed below) [Ishida-Yamamoto et al., 1997]. TCHH structure suggests that *TCHH* gene expression might be dependent on calcium concentration. This protein is

present in small amounts in keratohyalin granules in the epidermis, and it is expressed at much higher extent in the HF, when compared to the IFE [Lee et al., 1993; Rothnagel and Rogers, 1986; Tarcsa et al., 1997].

1.6.6 Small-proline rich proteins - SPRRs

The family of *Sprr* genes was first identified in response to UV radiation [Fischer et al., 1996]. However, these genes are normally expressed during normal epidermal differentiation. *Sprr* genes encode small (6-18kDa) proline-rich proteins, in which the structure consists of variable, subclass specific, internal repeats, flanked by conserved amino carboxy terminus [Candi et al., 1995]. These repeats contain domains rich in glutamine and lysine and the amino- and carboxy- terminals share many features with the domains observed in *Ivl* and *Lor*, suggesting that all must have diverged from the same ancestral gene [Gibbs et al., 1993]. However, contrarily to its neighbour genes, *Sprrs* function appears to have evolved to constitute a mechanism that allows modification of the physical properties of the CE. For example, the ratio of SPRR to LOR varies from 1:100 to 1:3 if one compares the structure of the CE in the IFEs of lip and sole epidermis to stomach; each subtype of skin epithelium presents different flexibility requirements [Candi et al., 1995]. In addition to being expressed differentially in different stratified epithelia, SPRR proteins are also induced in response to different environmental cues, such as: epidermal injury [Gibbs et al., 1993; Kartasova et al., 1988], inflammation [Yaar et al., 1995], hyperproliferation [Hohl et al., 1995], keratinization disorders, tumourigenesis [Lohman et al., 1997] and also during normal aging skin [Garmyn et al., 1992].

1.6.7 S100A calcium binding proteins - S100A

The *S100A* genes encode for a family of proteins that act as messengers of calcium response in a variety of tissues, including the brain [Donato, 1999; Heizmann et al., 2002]. In human epidermis, as well as, *in vitro* cultivated keratinocytes, at least eleven out of the more than twenty known S100A proteins are expressed in the cytoplasm of basal and spinous layers of the IFE, but transported laterally into the cell during differentiation. These genes are also expressed in the HF,

where they seem to play a role in regeneration [Ito and Kizawa, 2001; Leśniak et al., 2007]. Structurally, S100 proteins present two EF hands (helix-loop-helix calcium binding proteins), separated by an hinge region and flanked by amino- and carboxy- terminals [Eckert et al., 2004]. In the cell they exist as anti-parallel homo- or heterodimers with monomers linked together by non-covalent interactions which are used as a substrate for TGMs [Zimmer and Dubuisson, 1993]. The S100A structure suggests a role in reorganization of the CE, probably linked to transmembrane influx of calcium. Furthermore, some proteins such as S100A7, have been shown to interact with E-FABP, an epidermal fatty acid binding protein, also suggesting a role for lipid metabolism during epidermal differentiation [Hagens et al., 1999]. These proteins function has also been linked to the inflammatory response [Jinquan et al., 1996]. For example, human heterodimer S100A8/S100A9 acts as a chemostatic molecule in inflammation [Newton and Hogg, 1998], S100A4 presents angiogenic potential [Ambartsumian et al., 2001] and S100A12 is involved in the host-parasite response [Marenholz et al., 2004]. Alteration of S100A protein levels has been described in a variety of illnesses, such as: heart disease, diseases from the central nervous system, inflammatory diseases such as psoriasis and cancer [Alowami et al., 2003; Broome et al., 2003; Marenholz et al., 2004; Shrestha et al., 1998].

1.6.8 Late cornified envelope proteins - LCE

The LCE proteins contain an N-terminal region similar to the one observed for SPRR proteins, also harbouring glycine-serine-cysteine rich motifs comparable to the ones observed in LOR. In fact, in *Lor-null* mice, the expression of *Lce* genes increases, suggesting functionally redundancy [Koch et al., 2000a,b]. Genome-wide association studies have shown that mutations in certain *LCE* genes, such as the ones encoding for LCE3C/LCE3B are associated to psoriatic skin [Zhang et al., 2009].

1.7 Transcriptional control of epidermal differentiation

The morphological changes occurring during epidermal maturation are known and have been well described in the literature, however, information regarding the signalling pathways that govern stem cell activation and differentiation in the IFE is lacking. Recently, mouse genetics has shed light to some of the mechanisms, highlighting the role of transcription factors JUN,TCFAP2, CEBPs, KLFs, MYC, TRP63, OVOL1, amongst others, in these processes. In this section I am going to summarize the main findings regarding the role of these trascription factors in either stem cell activation or lineage determination (terminal differentiation) in the epidermis.

1.7.1 Epidermal stem cell activation

The transcription factor (TF) TRP63 is expressed in the basal layer of the IFE and has been involved in the switch from basal to spinous layer. *In vivo*, mice lacking *Trp63* do not progress to skin morphogenesis beyond embryonic development; the epidermis fails to stratify, leaving embryos with few and poorly differentiated layers [Blanpain and Fuchs, 2009; Laurikkala et al., 2006]. Several studies have shown that TRP63 is not only required for initiating the stratification programme but also for maintenance of the self-renewal capacity of the stem cells. There have been identified two splicing variants of *Trp63* which appear to have opposing effects. Overexpression of Δ*TRP63* in cultured keratinocytes blocks calcium induced differentiation [King et al., 2003], suggesting a role in proliferation, whereas ectopic expression of another splicing variant, *Tap63*, converts a normal epithelium positive for KRT18 into a KRT14 and KRT5 expressing squamous epithelium [Koster et al., 2004], indicating a role in lineage specification. Overall, studies suggest that TAP63 has a role in epidermal stratification and ΔTRP63 is important for progenitors proliferation. The proper balance of both splicing forms needs to be established for normal homeostasis [Koster and Roop, 2008].

Another TF with important functions in epidermal stem cell regulation is

MYC. Also, expressed in the basal layer of the epidermis, its expression has been shown to induce keratinocyte differentiation [Gandarillas and Watt, 1997]. MYC expression drives stem cells to enter the TA compartment where keratinocytes proliferate for a short period before engaging into a terminal differentiation program. A mouse model where *MYC* is overexpressed in the basal layers of the epidermis, under the control of the *Krt14* promoter, induces extensive hyperproliferation, hair loss, impaired wound healing and significant expansion of the TA compartment at the expense of SC loss [Arnold and Watt, 2001; Waikel et al., 2001]. The mechanism suggested for the physiological role of MYC in epidermis, postulates that this TF affects the stem cell-niche interactions because increased expression of *Myc* causes a decrease in the levels of integrin proteins and other ECM components. In addition, ectopic expression of *Myc* stimulates IFE and SG lineage differentiation at the expense of the HFs, raising the possibility that MYC might have a role in epidermal lineage determination [Frye et al., 2003]. In the IFE it has been suggested that MYC regulates the switch from basal to suprabasal not only by repressing ECM components but also by inducing global histone modifications associated with an active chromatin state [Frye et al., 2007]. Histone modifications have been shown to impact IFE differentiation; for example, when EZH2 a component of the PRC2 complex [Cao et al., 2002] is targeted for deletion in the epidermis causing removal of trimethylated lysine 27 of histone H3, H3K27me3 (histone mark associated with gene repression), premature activation of epidermal differentiation specific genes is observed [Ezhkova et al., 2009].

1.7.2 Epidermal lineage commitment

Among the factors which have been shown to be important for epidermal lineage commitment is retinoblastoma protein 1, RB1. Targeted deletion of *Rb1* in the epidermis results in increased proliferation of basal and suprabasal keratinocytes, which ultimately leads to loss of the stem cell pool. In culture, depletion of *Rb1* triggers keratinocytes to re-enter the cell cycle even when the differentiation program has been initiated [Ruiz et al., 2003].

Other important regulator of epidermal differentiation is the OVOL1 zinc

finger protein. This protein is expressed in differentiated keratinocytes and is activated in response to β-catenin/LEF1 signalling. Epidermis lacking *Ovol1* shows increased proliferation and upregulation of TFs MYC and ID2, as well as defects in terminal differentiation. There is also evidence that OVOL1 acts as a repressor of *Myc*, *Id2* and *Lor* by direct binding to the promoter region of these genes [Nair et al., 2006, 2007]. In addition, ID2 may also regulate epidermal stem cell maintenance since it has been observed that a quarter of the mice lacking *Id2* present defects in the epidermal barrier [Yokota et al., 1999].

OCT1, OCT6 and OCT11 proteins belong to the POU family of TFs and are all expressed in the epidermis. Skin specific overexpression of *Oct11 in vivo* prompts keratinocytes to differentiate, whereas deletion of both *Oct6* and *Oct11* induces expression of the basal stem cell marker KRT14 in the suprabasal layers of the epidermis [Andersen et al., 1997]. It appears that these TFs might be important for repression of genes in basal undifferentiated cells, as well as important activators of epidermal specific differentiation genes [Dai and Segre, 2004].

JUN and TCFAP2 TFs have long been considered key players in IFE maturation. *In silico* analysis has revealed binding sites for both proteins in promoters of genes encoding epidermal structural proteins [Eckert et al., 2004; Jang and Steinert, 2002; Sark et al., 1998]. *In vivo* studies show that inactivation of JUN in the suprabasal layers of murine epidermis causes hyperproliferation and hyperkeratinosis [Rorke et al., 2010]. In addition, targeted deletion of *Tcfap2*α and *Tcfap2*γ in the basal layer of murine epidermis leads to defects in epidermal stratification. Namely, at embryonic day 17.5, E17.5, the epidermis of the double-knockout (DKO) mice does not present granular layer or stratum corneum, failing to terminally differentiate, and to increase terminal differentiation markers expression such as *Krt1*, *Krt10*, *Ivl* and *Lor*. Interestingly, the basal layer of these mice remains unaffected, with normal expression of *Krt5*/*Krt14* basal markers, suggesting that loss of both TCFAP2 proteins only affects commitment of IFE keratinocytes from basal to suprabasal [Wang et al., 2008]. Furthermore, expression of CEBPα/CEBPβ TFs, which is important for gene regulation in the suprabasal layers, is also affected.

CEBPα/CEBPβ are expressed in the basal layer of the epidermis and are upregulated during keratinocyte commitment to differentiate. These TFs are

required for *Krt1* and *Krt10* expression, as well as for downregulation of Δ*Trp63*. Mice lacking *Cebpα*/*Cebpβ*, fail to exit the cell cycle and accumulate stem cell gene expression signatures such as, persistent expression of *Krt14* in the upper layers of the IFE [Lopez et al., 2009].

Kruppel-like factor 4, KLF4, is a TF expressed in the suprabasal layers of the IFE and required for maintenance of the epidermal barrier. Loss of *Klf4* in the epidermis results in misexpression of EDC genes required for formation of the CE, namely *Sprr* genes, such as *Sprr2a* [Segre et al., 1999].

Another TF that appears to regulate IFE differentiation is Distal less-3, DLX3. This protein is expressed in the suprabasal layers of the epidermis and ectopic expression in mouse basal keratinocytes causes precocious activation of IFE related differentiation genes, such as loricrin and profilaggrin in the basal keratinocytes [Morasso, 1996].

Finally, FOXN1 is also another regulator of IFE differentiation. Overexpression of *Foxn1* in differentiated keratinocytes induces gene activation of early differentiated markers (*Krt1*) and suppresses the expression of later genes (*Flg*, *Lor* and *Ivl*). FOXN1 seems to be necessary for the temporal control of epidermal lineage commitment [Baxter and Brissette, 2002].

A full understanding of the transcriptional control occurring during epidermal differentiation is still lacking. In particular, it is not known how the different signalling pathways activated through the described TFs integrate in order to promote epidermal homeostasis. Genetic approaches using transgenic mouse models to assess the effects of gain- and loss- off function of specific epidermal transcription regulators, for example, targeted to specific layers of the epidermis and the combination of double and even triple mutants to understand if such regulators act individually or in cooperation, the use of genomic approaches to map TF binding sites, such as chromatin immunoprecipitation [Odom et al., 2004] and crosstalk with genetic profiling, seem invaluable strategies necessary to understand the signalling networks underlying stem cell activation and commitment at the IFE, as discussed in Dai and Segre [2004].

1.8 *Myc*: oncogene and stem cell regulator

In my project I focused on the question of whether the oncogene *Myc* had a direct role in epidermal stem cell activation and lineage determination. For more than 30 years now, MYC has been extensively studied in normal tissues as well as cancer, with no consensus being made on the primary functions of this TF in a normal physiological context [Eilers and Eisenman, 2008]. The underlying reasons for this seem to rely lie in the fact that MYC assumes pleiotropic functions, sometimes as antagonistic as metabolism, growth and proliferation, differentiation and apoptosis. In addition, it has been difficult to fully dissect MYC primarily functions due to redundancy with other members of the MYC family, mainly MYCL and MYCN [Watt et al., 2008]. Nevertheless, knockout studies in tissues with rapid cell turnover such as, skin, intestine, blood and testis, as well as genome wide studies using expression arrays, SAGE (serial analysis of gene expression), chromatin IP, promoter scanning and whole cell proteomic approaches, to identify MYC target genes, are starting to unravel other functions of MYC in addition to proliferation [Sodir and Evan, 2009]. In fact, due to its role as a weak transcriptional factor, it is astonishing how MYC is able to regulate as much as 15% of the genes in mammalian genomes, converting MYC primarily to a modulator of context-specific biological functions. In this section, I am going to describe MYC's role as an activator as well as repressor, its expression and function in different tissues, as well as, the general mechanisms that control MYC activity in the specific contexts of epidermal homeostasis and cancer.

1.8.1 MYC structure and gene targets

MYC belongs to a family of basic helix-loop-helix leucine zipper (bHLH) proteins that also comprises MYCL and MYCN. During embryonic development, *Myc* is highly expressed in the extraembryonic tissues, while *Mycn* is more abundant in the primitive streak and other regions of the embryonic mesoderm [Downs et al., 1989] and *Mycl* is expressed in the developing kidney, lung, brain and neural tube [Hatton et al., 1996]. At later developmental stages and through adulthood, MYC proteins are expressed in highly proliferative cell populations, in general decreasing the levels throughout differentiation. Collectively, deregulation of the

proteins encoded by these genes has been associated with specific types of tumours in humans, such as Burkitt lymphoma (*MYC*), small-cell lung carcinoma (*MYCL*) and neuroblastoma (*MYCN*) [Atchley and Fitch, 1995; Watt et al., 2008].

MYC proteins are thought to require obligate heterodimerization with the binding partner MAX in order to activate the majority of its target genes. Transactivation occurs through binding to promoters of genes containing the E-box canonical DNA motif CACA/GTG; whereas repression involves interaction with other TFs, such as MIZ-1 or recruitment of dimethyltransferase DNMT3A [Adhikary and Eilers, 2005; Eilers and Eisenman, 2008] (Figure 1.6).

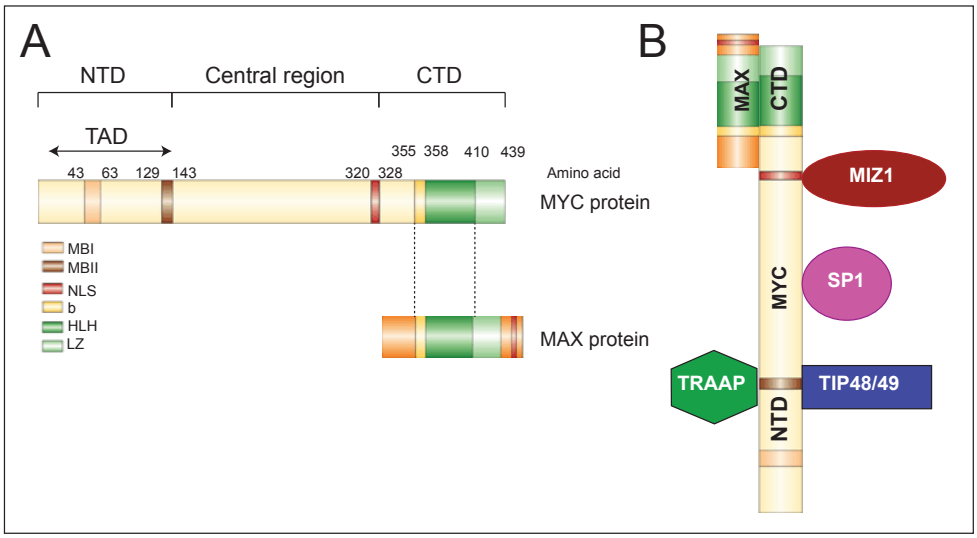

Figure 1.6: Myc protein domains and interactions. (A) Structure of the MYC protein. Illustrated is the carboxy-terminal domain (CTD), the central region of the protein and the amino terminal domain (NTD) which contains conserved *MYC Boxes* I and II (MBI and MBII) that are essential for the transactivation of MYC target genes. (B) Proteins shown to interact with MYC include: co-activator TRAAP (transformation/transcription domain associated protein), part of a complex that contains histone acetyltransferase (HAT) activity. TRAAP interacts with MBII region mediating chromatin remodeling on histones; TIP48 and TIP49 interact with NTD and are also implicated in chromatin remodeling. MIZ-1 interacts with CTD and affects MYC transcriptional activity being responsible for MYC mediated repression; SP1 interacts with the central region of MYC. Modified from Pelengaris et al. [2002b].

Gene expression profiling in settings where *Myc* is overexpressed led to the

unified conclusion that MYC modulates the expression of thousands of genes in the genome, predominantly upregulating genes involved in cell growth, ribosome biogenesis, metabolism, protein translation and mitochondrial function, as it has been discussed in several reviews [Dang et al., 2006; Eilers and Eisenman, 2008; Zeller et al., 2003]. However, as previously mentioned, MYC also acts as a repressor, downregulating genes involved in cell adhesion, cell-cell communication, cytoskeleton [Frye et al., 2003; Gebhardt et al., 2006; Wilson et al., 2004] and cell cycle arrest [Knoepfler et al., 2002; Staller et al., 2001]. In recent years, TF binding location in the genome using promoter or genome-wide arrays (ChIP-on-Chip) or high-throughput sequencing (ChIP-Seq) have been used to try to identify direct gene targets of MYC. In summary, the majority of these studies confirmed that MYC functions are broad and cover almost all biological processes found in genome wide expression studies. Furthermore, the majority of the genes bound by MYC were also transcriptional modulated by the protein. Overall, these studies confirmed that MYC-MAX heterodimers bind to E-box elements [Berberich and Cole, 1992; Blackwell et al., 1993; Blackwood et al., 1992; Littlewood et al., 1992] to promote gene activation [Amati et al., 1992; Amin et al., 1993; Kretzner et al., 1992] and that MYC binding covers 10-15% of the whole genome in mammalian cells [Fernandez et al., 2003; Rahl et al., 2010]. ChIP-Seq techniques uncovered that Myc binding sites are not exclusively associated with coding regions, but are also associated with enhancer regions for cooperative regulation in cell specific developmental contexts (e.g. epidermal differentiation [Watt et al., 2008] or β - cell differentiation [Lawlor et al., 2006]). Moreover, these sites could also represent non-coding RNAs that regulate transcription, such as miRNAs [Chang et al., 2008; O'Donnell et al., 2005] or RNA polymerase III products (tRNAs or 5S rRNA) [Gomez-roman et al., 2003], which seem to correspond to MAX-independent MYC functions. An elegant study in *Drosophila melanogaster* where *dMyc* and *dMax* null-alleles, transgenic RNAi and overexpression where employed, provided strong evidence for MYC activity independent of MAX binding being linked to activation of RNA polymerase III transcripts and synthesis of small non-coding RNAs [Gallant and Steiger, 2009; Steiger et al., 2008]. In addition, other MYC binding sites might correlate with recruitment to core-promoter regions by interaction, for example, with MIZ-1. Remarkably, because some of

these core-promoters do not present MIZ-1 binding, they uncover the exciting possibility of MYC mediated repression via interaction with other proteins such as: SP1, nuclear-factor Y (NFY), transcription factor II-I (GTF2I), SMAD2/3 and yingyang-1 (YY1) [Adhikary and Eilers, 2005; Feng et al., 2002]. A great effort has been made to try to dissect both activator and repressor MYC functions. Identifying mutants that either disrupt the MYC-MAX or the MYC-MIZ-1 interaction has been a challenge. However, one of the first mutants to be identified was MycV394D, which has been shown unable of MYC-MIZ1 binding as well as MYC's ability to repress genes [Herold et al., 2002]. Other MYC mutants that lack the transactivation domain have been generated, but these affected MYC transcriptional activity.

1.8.2 Regulators of MYC transcriptional activity

The observed widespread binding of MYC in the genome, favours the idea that binding of this oncogene must somehow be directed and regulated across the genome. Indeed, genome-wide studies using mouse embryonic stem cells (ES) seem to embrace this idea, suggesting that chromatin marks, such as histone methylation are key determinants of MYC binding [Kim et al., 2010]. MYC appears to select regions in the genome with high levels of histone H3 lysine 4 (H3-K4) and lysine 79 (H3-K79) methylation, normally associated with active transcription, when compared to lysine 27 (H3-K27) (repressive mark) [Guccione et al., 2006]. In general, these studies have shown that MYC preferentially binds to regions that are or have already been actively transcribed, also modulating the transcriptional process itself. In fact, it is known that MYC interacts with proteins of the RNA transcriptional machinery, such as transcription elongation factor, P-TEFb. This interaction mediates phosphorylation of the C-terminal domain of RNA polymerase II, contributing to its pause-release and therefore to elongation [Cowling and Cole, 2007; Eberhardy and Farnham, 2002; Rahl et al., 2010]. Lastly, MYC also contributes to mRNA cap methylation [Cowling and Cole, 2007].

On the other hand, MYC binding to the genome can be restricted by competition with members of the MNT/MAD family of transcriptional repressors,

namely MXD1 (MAD1), MXI1 (MAD2), MXD3 (MAD3), MXD4 (MAD4), MNT and MGA [Ayer et al., 1993; Hurlin et al., 1995, 1997; Meroni et al., 1997; Zervos et al., 1993]. These proteins contain a basic helix-loop-helix leucine zipper (bHLHz) domain, identical to the one present in MYC proteins, and therefore compete for their common heterodimer protein, Max, as well as for available binding sites [Grinberg et al., 2004]. Repression by MAD-MAX heterodimers is mediated through interaction with the co-repressor proteins SIN3A and SIN3B, which are multiprotein complexes that recruit histone deacetylases (HDACs), among other proteins [Ayer et al., 1995; Hurlin et al., 1995, 1997; Schreiber-Agus et al., 1995]. HDACs are ultimately involved in chromatin remodelling and induction of heterochromatin states, usually associated with transcriptional silencing [Alland et al., 1997; Hassig et al., 1997; Laherty et al., 1997]. Consequently, MXD functions are antagonistic of MYC, which is known to recruit acetyltransferases GCN5 and TIP60 via TRAAP and CBP/EP300 activator proteins in order to promote a more permissive/transcriptional active euchromatic state [Frank et al., 2003; McMahon et al., 1998, 2000; Vervoorts et al., 2003]. Several lines of evidence suggest that MXD and MNT function as antagonists of MYC activity. Studies in *Drosophila melanogaster* comparing binding sites of DMYC, DMNT and DMAX, have shown that these proteins share binding sites which tend to vary in number with protein concentration [Orian et al., 2003]. In addition, MYC and MNT have opposite roles in cell growth [Loo et al., 2005]. Also, mouse embryonic fibroblasts (MEFs) null for *Mnt*, phenotypically resemble *Myc* overexpressing cells [Hurlin et al., 2003; Nilsson et al., 2004; Walker et al., 2005]. Deletion of *Mxd1* delays terminal differentiation of granulocytes, as well as, deletion of *Mxi1*; both favouring proliferation [Foley et al., 1998; Schreiber-Agus et al., 1998]. *Mxd* genes are also preferentially expressed in differentiated cell populations [Ayer et al., 1993; Hurlin et al., 1995; Quéva et al., 1998; Västrik et al., 1995] as well as quiescent cells [Marcotte et al., 2003], contrarily to *Myc* which is downregulated during differentiation and absent in the G0 phase of the cell cycle, only to be expressed upon mitogenic stimulation (e.g. WNT/β-catenin, NOTCH, RTK/RAS signalling) or ectopic expression [Eilers et al., 1991; Kelly et al., 1983; Rabbitts et al., 1985]. The MYC protein has an extremely rapid turnover, with a half-life of 20 minutes, that correlates with an increase during the G1 phase of

the cell cycle and rapid decline in the S phase, upon mitogens withdrawal [Kelly et al., 1983; Rabbitts et al., 1985]. These observations therefore comply with a model where *Mxd* proteins, being more expressed in differentiated cells, are up-regulated when levels of *Myc* are downregulated during differentiation or exit of the cell cycle [Hooker and Hurlin, 2006]. However, it is not entirely clear what is the limiting step controlling the balance between MXD/MNT-MAX and MYC-MAX heterodimers, and what ultimately controls the balance between activation and repression of MYC target genes. Since the half-life for MXD, MNTt and MYC is much lower than MAX ($t^{1/2} = 24$ hours) [Blackwood et al., 1992], MAX does not seem to be the limitating factor. Nevertheless, it has been observed that the proportion of MNT-MAX heterodimers decreases upon *Myc* induction, even though *Mnt* levels remain constant [Walker et al., 2005]. This observation can either explain that more molecules of MYC are present to compete with MXD or MNT for MAX or that during MYC activation, MXD or MNT proteins are transiently post-translationally modified in a way that interferes with their binding to MAX. The later hypothesis is more attractive as MNT proteins have been shown to interact with SIN3A upon phosphorylation [Popov et al., 2005], so in theory, similar protein modifications are possible and might prevent binding of these proteins to MAX.

1.8.3 Life cycle of MYC

Deregulation of the MYC protein can arise through direct alterations in the *MYC* gene, such as: chromosomal translocations (Burkitt lymphoma), gene amplifications (colon cancer), viral integrations (human papilloma virus cervical cancer) and mutations in cis-regulatory regions or, as a consequence of an increase in mRNA or protein stability. In addition, failure to induce MYC's auto-repressive mechanism can also have a deleterious impact in cells [Levens, 2010; Murphy et al., 2008; Nesbit et al., 1999]. Hence, it appears reasonable to assume that mutations or misregulation of the pathways involved in regulation of MYC activity, can potentially promote tumorigenesis. MYC is induced by multiple signal transduction pathways, such as: WNT, RAS/RAF/MAPK, JAK/STAT, TGFβ and NF-kB. Several of these pathways are also deregulated in cancer cells, of-

ten contributing to enhanced MYC expression [Vervoorts et al., 2006]. Thus, MYC is subjected to several and interdependent post-transcriptional and post-translational modifications (e.g phosphorylation, acetylation, ubiquitination) that allow tight control of its activity.

The protein itself presents several phosphorylation sites; two of them, in the acidic domain, are substrates for the protein casein kinase 2, CSNK2 [Lüscher et al., 1989]. Two additional sites locate in the N-terminal region of the protein, within the transactivation domain (TAD) and are targets for glycogen synthase kinase (GSK3β) and proline directed kinases [Sears, 2004]. The consequences of CSKN2 phosphorylation remain unknown, although some studies suggest a role in increasing MYC stability [Channavajhala and Seldin, 2002], others suggest a role modulating MYC/MAX and MAX/MAX complexes and regulation of the activity of caspases during apoptosis [Berberich and Cole, 1992; Krippner-Heidenreich et al., 2001]. Additional MYC phosphorylation sites are found in the Mycbox I region, specifically in threonine 58 and serine 62 (Thr58 and Ser62). However, phosphorylation at Ser62 is necessary for subsequent phosphorylation at Thr58. Serine 62 can be phosphorylated by several kinases, such as c-JUN N-terminal kinase (JNK), cyclin dependent 1 kinase (CDK1) and mitogen-activated kinase (MAPK); this modification seems to stabilize MYC activity [Vervoorts et al., 2006]. The Ras signalling pathway is known to be involved in the process, through activation of MAP kinases that phosphorylate Ser62. At this point, Thr58 is a substrate for GSK3β phosphorylation, triggering a cascade of reactions with the ultimate goal of MYC degradation [Sears, 2004; Vervoorts et al., 2006]. In addition, RAS inhibits GSK3β through the PI3K pathway, stabilizing MYC. The importance of the phosphorylation of both Thr58 and Ser32 in MYC's degradation is shown by the recognition of PIN1 prolyl isomerase, that subsequently facilitates the access of protein phosphatase 2A (PP2A) to dephosphorylates Ser62. Threonine 58 phosphorylation, desestabilizes MYC and once it is recognized by F-box protein 7 (FBW7), a subunit of the SKP1-Cul1-F-box protein (SCF) ubiquitin ligase that stimulates ubiquitination, the protein is targeted to proteasomal degradation [Adhikary and Eilers, 2005]. These post-translation modifications are essential for normal homeostasis as, mutations in Thr58 and amino acids in its vicinity are frequently associated with Burkitt lymphoma. When MYC is mu-

tated at Thr58, it fails to activate the expression of BH3-only protein BCL2L11, a pro-apoptotic gene like *Bcl2*, reducing apoptosis and enhancing self-renewal of the transformed cells. This response seems independent of the pro-apoptotic effects of MYC through CDKN2A, an inhibitor of MDM2 E3 ligase that leads to TP53 stabilization [Hemann et al., 2005; Vervoorts et al., 2006; Zindy et al., 1998]. In addition to SCF-FBW7, other proteins have been shown to be involved in MYC's degradation, such as SCF-SKP2 and HUWE1. The first, is required for MYC transactivation; but, MYC is also used as a substrate of SCP-SKP2, indicating that ubiquitination of MYC is probably required for MYC activation [Lehr et al., 2003]. Furthermore, HUWE1 seems to be important for MYC recruitment of other acetyltransferases such as CBP/EP300 to the far N-terminal part of the protein. Ubiquitinases also seem to enhance the recruitment of Mediator complexes [Eberhardy and Farnham, 2002] as well as elongator factor, P-TEFb [Kanazawa et al., 2003]. In addition, MYC also recruits several cofactors containing histone acetyltransferase activity (HATs), such as CBP/EP300, GCN5 and TIP60 [Bouchard et al., 2001; Dang et al., 2006; Frank et al., 2003]. These HATs are used to trigger acetylation at the promoters of MYC target genes; yet the MYC protein itself can also be modified by these enzymes at several potential lysine sites. Interestingly, acetylation at particular sites confers increased stability of the protein *in vitro* [Patel et al., 2004]. Although some sites appear to overlap with ubiquitination potential sites, it will be interesting to understand how strongly connected these two modifications are and what is the impact in MYC function, particularly in its degradation but also in the recruitment of other cofactors.

1.8.4 Physiological functions of MYC in normal tissues

The physiological functions of MYC have been difficult to dissect. MYC acts as a weak transcription factor and modulates a plethora of biological processes. In fact, one could say that MYC primarily acts as a coordinator, fine-tuning the action of additional TFs with enhanced transcriptional activity. Nevertheless, *in vivo* and *in vitro* gain and loss-of-function studies, in different model organisms, have contributed extensively to a better understanding of the role of MYC in

normal tissues. It also helped shaping the current view that MYC biological functions are broad but context-specific. Conditional excision of genes (e.g. Cre recombinase system), as well as use of inducible systems using the oestrogen receptor (ER) that responds oestrogens related molecules such as tamoxifen (4-OHT), is a valuable tool that has been used to address the biological roles of MYC *in vivo* as well as *in vitro*.

In vitro experiments using Rat1 fibroblast cells, with undetectable levels of MYCL and MYCN, have shown that these cells can remain viable after targeted deletion of *Myc* through recombination. However, these studies revealed extensive doubling times due to defects in the cell cycle as well as a delay in the activity of cyclin CDK complexes. This data directly attributed to MYC the role of cell cycle regulator [Mateyak et al., 1997].

Experiments using conditional excision enable the generation of *Myc* null mice, but excision of the gene causes death at E9.5 with embryos presenting hematopoietic, vascular and placental defects. These experiments indicated that Myc is crucial for development beyond this developmental stage [Baudino et al., 2002]. *Mycn* deficient mice are also embryonic lethal, but at E10.5 [Davis et al., 1993], whereas *Mycl* mice are able to survive [Hatton et al., 1996], indicating that *Myc* and *Mycn* are essential genes during embryonic morphogenesis. In these studies, the *Myc* genes where excised using the Cre-LoxP system. This system uses Cre (Cyclization Recombination), a sequence specific DNA recombinase that recognizes specific stretches of DNA, Lox-P (Locus of X-over P1) sites, and excises these when flanking a particular DNA region of interest. As deletion of *Myc* is embryonic lethal, subsequent studies aimed to target the excision of this gene in adult tissues using tissue specific promoters. In the gastrointestinal gut, *Myc* was deleted using a Cre-oestrogen receptor (ER) fusion transgene driven by a intestine-specific villi promoter, *Cyp1a*. The deletion resulted in growth inhibition of the intestinal crypts [Muncan et al., 2006].

In the mammary gland, Cre was induced with the promoter *Wap* (Wap Whey acidic protein) to target deletion of *Myc* in the luminal alveolar cells of the mammary gland during mid-pregnancy and through lactation. When *Wap*Cre transgenic mice are crossed with $Myc^{fl/fl}$ mice, pregnant mothers exhibit lower milk production, mainly because the terminal end buds required for the alveoli fail to

develop. Subsequent pregnancies increase the phenotype and demonstrate that mRNA translation, proliferation and maturation of the alveolar cells is compromised upon *Myc* deletion [Sodir and Evan, 2009; Stoelzle et al., 2009].

In hematopoietic stem cells (HSCs), deletion of *Myc* results in accumulation of these cells in the niche, increased anaemia and failure to differentiate. Absence of *Myc* in this context does not interfere with the proliferation of progenitor cells, as in the intestine or mammary gland, but rather interferes with the interactions of the HSCs and their niche [Malynn et al., 2000]. Also, when an additional deletion of *Mycn* is added to the system, the combinatorial effects result in HSCs lethality, suggesting that both proteins are absolutely required for HSC proliferation, differentiation and survival [Laurenti et al., 2008; Wilson et al., 2004]. Similar results were observed in neural stem and precursor cells [Hatton et al., 2006; Knoepfler et al., 2002].

Knockout of *Myc* in the epidermis leads to an exhaustion of the epidermal stem cell compartment, leading to a dramatic reduction in keratinocyte's cell size, growth and endoreplication. As a consequence, the epidermis shows lack of elasticity, tears off in areas of mechanical friction and displays impaired wound healing [Zanet et al., 2005].

In the pancreas, conditional inactivation of *Myc* impairs development of the exocrine pancreas [Nakhai et al., 2008] and in the bone marrow, results in accumulation of megakaryocyte and erythroid progenitors [Guo et al., 2009]. MYC has also been described as a modulator of the renal stem cell progenitor population, as deletion of *Myc* impacts late renal differentiation/maturation and homeostasis [Couillard and Trudel, 2009]. The combination of these studies suggests a role for MYC in lineage determination, in addition to proliferation and cell cycle regulation.

Finally, overexpression of a dominant negative form of MYC that efficiently blocks the transactivation activity of MYC, MYCL and MYCN (OMOMYC) also affects adult tissues the skin, bone marrow and testis, by reducing the proliferation rate of these tissues. However, no cell death is observed. In less-proliferative tissues such as pancreas, liver, lungs and kidney these effects where not observed [Soucek et al., 2004].

Tamoxifen inducible systems have also been generated to study MYC biology.

This approach relies on the fusion of the MYC protein to the hormone-binding domain of estrogen receptor (ER). The fused protein forces MYC functions to depend on the ER ligand β-estradiol. This ligand displaces ER from its inactive form when associated with the heat shock protein 90 (HSP90), and promotes translocation of the recombinant protein to the nucleus. Mutant ERs have been generated which do not respond to physiological estrogens but only to the synthetic ligand, 4-hydroxy-tamoxifen (4-OHT), MYCER [Indra et al., 1999; Littlewood et al., 1995]. The advantages of using such system are that 4-OHT inducible proteins are activated within minutes and their activation is reversible upon withdrawal of the synthetic compound. In addition, expression of the recombinant protein can be induced in any tissue by use of a specific promoter and the levels of protein, rather than its transcription, are controlled and relatively easy to predict.

Induction of the *MYCER* construct in the suprabasal layer of the epidermis, by the *Ivl* promoter, triggers post mitotic differentiated cells to enter the cell cycle and induces the formation of papillomas. Nonetheless, this phenotype is completely reversible upon removal of 4-OHT [Pelengaris et al., 1999]. Conversely, when *MycER* is targeted to the basal layer of the epidermis, using the *Krt14* promoter, the epidermal stem cells exit the niche and amplify as TA cells, differentiating into IFE and SG lineages (Figure 1.7). In this system, the phenotype cannot be restored upon MYCER deactivation [Arnold and Watt, 2001].

In pancreatic β cells, MYCER activation, driven by an insulin (*Ins2*) promoter, drives entry into the cell cycle, but ultimately causes cell death by apoptosis [Pelengaris et al., 2002a]. Interestingly, time-course expression profiling of β pancreatic cells following MYCER activation and deactivation confirms that MYC regulates genes involved in cell-cycle, cell growth and metabolism, but also genes which are cell-type specific. Several genes specific for pancreatic β cells were repressed upon MYC activation [Lawlor et al., 2006].

These studies, highlight the fact that the consequences of MYC activation are cell-type specific and also dependent on the threshold of MYC *in vivo* [Murphy et al., 2008].

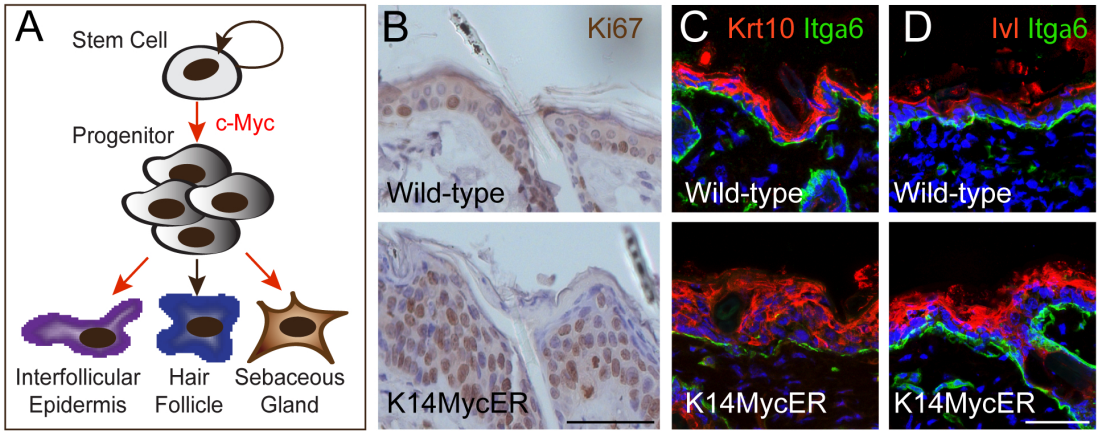

Figure 1.7: Epidermal morphological changes upon MYC activation. (A) MYC activation in epidermal stem cells is thought to promote stem cell's exit from the niche, proliferation of the progenitor's pool and differentiation into interfollicular epidermis and sebaceous gland lineages. (B) Proliferation is observed by an increase in KI67 positive keratinocytes in K14MycER mice (MYC was induced in the basal layer of the epidermis) and (C.D) differentiation is shown by the increased number of suprabasal layers positive for keratin 10, KRT10 (C, red) and involucrin, IVL (D, red) in K14MycER mice compared to wild-type. Expression of the extracellular component integrin $\alpha 6$, ITG$\alpha 6$, is shown in green. Scale bar: 50 μm.

1.9 *In vivo* studies of MYC in skin

In the epidermis, seven mouse models have been generated to understand the function of the stem cell regulator MYC in the epidermis [Watt et al., 2008]. Ectopic expression of the *Myc* gene in LOR positive cells, targeting the basal and suprabasal layers of the epidermis, induces hyperproliferation, hyperkeratinosis and sensitivity to UVB-induced apoptosis [Waikel et al., 1999]. Inducible expression of *Myc* in the suprabasal layers of the epidermis, under the *Ivl* promoter, induces reversible tumour formation [Pelengaris et al., 1999]; whereas expression in basal undifferentiated Krt15$^+$ keratinocytes triggers hyperproliferation and irreversible keratinocyte tumour transformation [Rounbehler et al., 2001]. Ectopic expression of Myc in the basal Krt14$^+$ keratinocytes, as previously discussed, has shown to exhaust the stem cell pool [Waikel et al., 2001], while inducible *Myc* expression directs differentiation into the IFE and SG lineages [Arnold and Watt, 2001]. Furthermore, deletion of *Myc* in the basal layer from the epidermis, depending on the mouse model used, either affects the epidermis by impairing wound healing and the epidermal barrier [Zanet et al., 2005], or does not seem to have a substantial effect in epidermal homeostasis [Oskarsson et al., 2006]. In these studies, the use of mouse models has revealed that the effects of MYC in differentiated cells are reversible, but not in basal undifferentiated keratinocytes. This suggests that deregulation of MYC in the stem cell compartment might potentially cause for skin cancer [Watt et al., 2008].

1.10 MYC in normal and tumorigenic skin

As an organ subjected to continuous regeneration, the epidermis maintains a tight control of keratinocytes proliferation and differentiation. This implies a continuous balance between division of epidermal stem cells and subsequent commitment of the daughter cells. Disruption of any of these processes, as a consequence of deregulation of the underlying signalling pathways, can disrupt normal epidermal homeostasis and lead to disease. Because the suprabasal, differentiated keratinocytes are continuously shed from the surface of the skin and replaced by the inner cells, it has been hypothesized that epidermal stem cells are the

cells more likely to accumulate genetic mutations and more prone to tumorigenesis, due to their continuous self-renewal and long tissue residence [Honeycutt et al., 2004; Owens and Watt, 2003; Perez-Losada and Balmain, 2003; Youssef et al., 2010]. MYC has been shown to be involved in both proliferation and differentiation processes within the epidermis, and deregulation of its expression is known to contribute to skin cancer (e.g. non-melanoma skin cancer, basal and squamous cell carcinoma). For example, 50% of the squamous cell carcinomas (SCCs) express high levels MYC across the entire tumour mass and this is caused by amplification of the *MYC* gene [Watt et al., 2008]. Deregulation of MYC is found in many other tumours types including breast [Nass and Dickson, 1997], colon [Kopnin, 1993] and lung [Gazdar]. The key role of MYC in tumorigenesis relates with its ability to induce cell proliferation, specifically in the G1 to S transition of the cell cycle. MYC has been shown to control the expression of cell cycle regulators: CCNB2, CDK4, MCM7 and CDKN2B [Bouchard et al., 1999; Fernandez et al., 2003; Hermeking et al., 2000; Honeycutt et al., 2004; Staller et al., 2001]. However, deregulation of MYC alone does not seem sufficient to induce cancer. Ectopic expression of *Myc* in fibroblasts, in the absence of survival factors, induces apoptosis indicating that for a putative tumour cell to emerge it must evade apoptosis [Evan et al., 1992; Pelengaris et al., 2002a]. Therefore, in light of these studies, in order for MYC to induce tumorigenesis, its deregulation has to cooperate with either overexpression of anti-apoptotic proteins (e.g. BCL2, BCL2L1) or loss of tumour suppressors (e.g CDKN2A, TP53). Studies of lymphomagenesis in transgenic mice corroborate both ideas [Adams and Cory, 1985; Blyth et al., 1995; Elson et al., 1995; Pelengaris et al., 2002a; Strasser et al., 1990]. In epidermis, MYC induced differentiation is thought to act as a fail-safe mechanism, similar to apoptosis, to prevent tumorigenesis [Jensen and Watt, 2006]. Undeniably, both processes share many features such as, expression of TGMs, loss of ECM interactions as well as cell nucleus [Gandarillas et al., 1999]. However, since keratinocytes are known to be resistant to apoptosis [Pincelli and Marconi, 2010], MYC expressing cells need to acquire additional oncogenic mutations in order to induce tumours such as SCCs. Deregulation of MYC and overexpression of the anti-apoptotic gene *Bcl2l1*, suppressed MYC ability to induce apoptosis, allowing tumour formation [Pelengaris et al., 2002a]. Similarly,

analysis of mammary gland tumours suggest cooperative transformation between BCL2L1 and MYC [Nass et al., 1996] and in fact, human SCCs have been shown to express high levels of BCL2L1 [Delehedde et al., 1999]. It is interesting to note that human SCCs express many markers characteristic of normal, actively cycling stem cells, such as melanoma associated *CSPG4*, while downregulating markers required for stem cell dormancy, such as *LRIG1* and *MAP4* [Jensen et al., 2008]. These observations are in agreement with the fact that activation of MYC in actively-cycling stem cells induces a transcriptional program that shares many similarities with the one observed for cancer cells [Kim et al., 2010; Wong et al., 2008]. Finally, mutations in *TP53* and deregulation of RAS have also been related to SCCs development [Brash and Pontén, 1998; Dajee et al., 2003]. Mammary tumours where *Myc* is transiently deleted, rapidly relapse after *Myc* re-expression, presenting mutations in the encoded RAS protein, ERAS [D'Cruz et al., 2001]. Other studies also suggest that epidermis lacking *Myc* is less susceptible to RAS induced tumorigenesis [Oskarsson et al., 2006], indicating that MYC induces genomic instability and potentiates the emergence of mutations in the cells. In skin, even though *Myc* overexpression by itself does not seem to induce epidermal SCCs, MYC might facilitate the emergence and survival of cells that have sustained additional oncogenic mutations [Adhikary and Eilers, 2005].

1.11 Genome-wide approaches for the study of epidermal cell fate commitment

Epidermal differentiation is thought to be coordinated by a group of highly regulated TFs that, responding to environmental cues, regulate gene expression forcing cells to maintain or alter a specific state. A number of TFs (e.g. TRP63, MYC, OVOL1, KLF4, TCFAP2), as well as miRNAs (e.g. miR-203), has emerged as strong determinants of epidermal stem cell lineage commitment [Blanpain and Fuchs, 2009; Dai and Segre, 2004]. Most of these studies have used genetically modified mice where the TF of interest was either overexpressed or depleted. Alterations in these transgenic mice were then analysed at the gene level, using microarray gene expression arrays, quantitative real-time PCR or immunohisto-

chemistry/immunofluorescence. Although these approaches are useful to infer TF functions in the epidermis, the differential gene expression that results from the gain or loss a TF, does not necessarily correlate with the direct regulation of a gene. For example, MYC is known as a potent regulator of epidermal stem cell decisions, and overexpression of *Myc* in the epidermal stem cells produces hyperplasia, hair loss and enlargement of the sebaceous glands [Frye et al., 2003]. The use of microarrays for cells isolated with one and four days of MYC activation using the K14MYCER mouse model [Arnold and Watt, 2001] involved MYC in a variety of processes that had already been previously described such as, cell growth, proliferation and differentiation [Eisenman, 2001; Frye et al., 2003]. However, some of these gene expression changes might have occurred as a cause of secondary effects, due to direct interaction of MYC with the promoter of intermediate genes. In addition, information of whether MYC was directly regulating IFE and SG lineage specific genes was lacking, as well as the knowledge of whether MYC transcriptional function was isolated or in cooperation with other TFs already known to have important roles in epidermis maturation. It seems therefore crucial to combine mouse genetics models with gene expression arrays, as well as techniques that are able to map TF binding to the study of epidermal stem and progenitor cell commitment. Chromatin immunoprecipitation (ChIP) is a useful tool that allows identification of the physical interactions between proteins (e.g TFs) and DNA in the context of chromatin. It involves chemical cross-linking of DNA-protein interactions in living cells to capture TFs at their binding sites on the genome. The cross-linked chromatin is then fragmented either enzymatically, using DNA nucleases, or mechanically, using sonicators and the protein-DNA complexes are enriched by immunopurification with antibodies specific for the protein of interest. DNA-protein cross-links are then reversed and the enriched DNA is purified and subjected to one of the three different approaches. Firstly, the DNA fragments can be amplified and subsequently hybridized to whole-genome promoters or customized DNA microarrays, in a technique designated as ChIP-on-Chip [Buck and Lieb, 2004; Iyer et al., 2001; Ren et al., 2000]. Here, the analysis takes into consideration a ratio of the fluorescent signal intensity of ChIP-DNA over control DNA, and this reflects the relative enrichment of the TF at the genomic binding sites. Secondly, ChIP-DNA fragments

can be cloned in a plasmid library and then be sequenced. This method is designated as ChIP-PET (paired ends di-tags) and it overcomes the problems found in hybridization, such as probe performance or genome coverage, as the binding site where the TF is located can be sequenced [Wei et al., 2006]. Lastly, ChIP-seq (sequencing), which is a technique that brought several advantages over the previous two mentioned. Here, ChIP-DNA is size-selected, amplified and deep sequenced. ChIP-Seq is far more advantageous than the previous two approaches as it requires small amounts of ChIP-DNA; it has deeper coverage and is more efficient [Robertson et al., 2007; Valouev et al., 2008]. Initially costly and less available than ChIP-on-Chip or ChIP-PET, nowadays ChIP-Seq is increasingly becoming the method of choice for TF binding location analysis, especially for example, for rare populations of somatic cells, such as epidermal stem or progenitor cells. These TF location methods are also useful for identification of putative interactors, including epigenetic regulators (e.g repressors) or components of the chromatin (e.g modified histones). In the epidermis for example, the use of ChIP has helped in the identification of a member of the polycomb repressor complex, EZH2, which is expressed in basal epidermal progenitors during development and is essential to prevent precocious differentiation and recruitment of other epidermal differentiation regulators such as JUN [Ezhkova et al., 2009]. In another study, ChIP-Seq was used to profile the epigenetic landscape of HF stem cell populations [Lien et al., 2011]. The global transcription landscape required for maintenance or cell fate commitment of epidermal stem cells is poorly understood. One explanation might be due to the difficulty in obtaining a large number of homogeneous *bona fide* somatic stem cells and progenitors *in vitro* for analyses. Unipotent and multipotent stem or progenitor cells of several tissues can be isolated and cultured *in vitro*, however their proliferative potential in culture is limited to a few rounds of divisions (e.g. human primary keratinocyte cultures) due to limited knowledge of the optimal medium conditions. The role of TFs either as regulators of epidermal stem cell maintenance or differentiation is of immense interest, because it will contribute to our understanding of normal epidermal homeostasis as well as skin disease. Therefore, mapping the epidermal stem cell transcription network will provide valuable clues. Nevertheless, a drawback of genome-wide ChIP studies is the fact that not every single TF

target gene can analysed functionally for its biological relevance, as this would be technically extremely challenging. In an attempt to overcome this limitation, global TF mapping has been correlated with microarray gene expression. This approach has revealed that not all genes are directly regulated by one single TF, and that association with additional TFs, binding to enhancers, or recruitment of cofactors, is also important to induce a transcriptional response. This is also true for the epigenetic state of the chromatin, as it can also determine binding location of TFs. For example, MYC is thought to potentially modify the chromatin architecture in order to be more permissive for the binding of OCT4 and SOX2 during reprogramming, via recruitment of HATs and therefore affecting global histone acetylation (histone modification associated with active transcription) [Takahashi and Yamanaka, 2006]. In summary, few studies have been performed to dissect transcriptional networks that control epidermal stem cell maintenance and differentiation. A combination of mouse models, where specific TFs are overexpressed or deleted, following by mapping of putative regulators of the process and gene expression analysis (preferably including coding and non-coding regions), might provide invaluable information regarding these processes.

1.12 Research aims

Activation of MYC in the epidermis appears to induce a global chromatin structure permissive for TF binding, where the occurrence TF binding in the genome is cell-context specific. To test this hypothesis I set myself to answer the following questions in the specific context of an epidermal stem/progenitor cell:

1. Is MYC directly regulating the genes involved in cell adhesion and proliferation responsible for triggering epidermal cell fate commitment in skin?
2. Does MYC directly regulate the expression of skin-specific differentiation genes?
3. How does MYC binding affect tissue-specific transcriptional networks to trigger lineage differentiation specifically into the IFE and SG lineages?

To answer to these questions I induced MYC-specific differentiation in the epidermis by expressing an inducible construct of *Myc* in the basal undifferentiated layers of the epidermis, using the previously described transgenic mouse model K14MycER [Arnold and Watt, 2001]. Following activation of MYC, murine epidermal cells were isolated and subjected to genome-wide assays such as genome-wide gene expression and ChIP assays, following functional validation.

Chapter 2

Material and Methods

2.1 Mouse lines

During the course of this work all mouse breeding and experimental protocols used were subjected to ethical approval and performed under the terms of a United Kingdom Government Home Office Project and Personal Licenses. All mouse lines were bred to a mixed genetic background of CBA x C57BL/6J. K14MycER line was kindly provided by Professor Fiona Watt [Arnold and Watt, 2001]. The Krt14-cre/Esr1 (The Jackson laboratory) line was crossed with mice carrying floxed alleles for *Sin3a* (K14Sin3a$^{f/f}$) and *Myc* (K14Myc$^{f/f}$). Mice were genotyped according to published protocols: K14MycER [Arnold and Watt, 2001], Sin3a$^{f/f}$ [Dannenberg et al., 2005] and Myc$^{f/f}$ [Alboran et al., 2001].

2.1.1 Treatment with 4-hydroxy-tamoxifen (4-OHT)

Mice were treated with 1 mg of 4-OHT (Sigma-Aldrich) diluted in acetone. Tamoxifen was topically applied to a shaved area of the dorsal mouse skin and, if not stated otherwise, the treatment was followed for a period of four days, in K14MycER mice, for expression of the *Myc* transgene in KRT14 positive basal cells of the epidermis. Mouse lines K14Sin3a$^{f/f}$ and K14Myc$^{f/f}$K14Sin3a$^{f/f}$ (generated and kindly provided by Claire Cox) were treated for 14 days and K14Myc$^{f/f}$ mice for 21 days, in order to induce excision of the floxed alleles by Cre recombinase. Following 4-OHT treatment, the mice were sacrified for removal of the

dorsal skin. All mouse lines were either compared to 4-OHT treated wild-type or vehicle (acetone) transgenic littermates.

2.1.2 Isolation of epidermal cells from mouse skin

Primary mouse keratinocytes were isolated from 4-OHT or acetone treated dorsal skin of transgenic and non-transgenic mice. The shaved dorsal skin was cut and washed in 10% (v/v) betadine solution (20 ml in 180 ml sterile water), following one wash in 70% (v/v) ethanol and two washes in phosphate buffer saline (PBS) (PAA Laboratories). The dermal side of the skin was thoroughly scraped with a scalpel to remove excess fat. The tissue was trypsinized for 2 hours at 37 °C or overnight at 4 °C floating (epidermal side up) in 0.25% (v/v) trypsin with no EDTA (Invitrogen), to separate the dermis from the epidermis. The epidermis was subsequently scraped from the dermis, cut in small pieces and re-suspended in 30 ml of FAD(-Ca) medium [1 part Ham's F12 medium, 3 parts Dulbecco's modified Eagle's medium (DMEM), 1.8x10^{-4} M adenine] (custom made by PAA Laboratories) supplemented with 10% fetal calf serum (FCS) (Sigma-Aldrich) and a cocktail of 0.5 μg/ml hydrocortisone (Fisher Scientific), 5 μg/ml insulin (Sigma Aldrich), 10^{-10} M cholera toxin (Enzo Life Sciences) and 10 ng/ml epidermal growth factor, EGF (Peprotech), as previously described [Jensen et al., 2010]. The cell suspensions were filtered through a 70 μm cell strainer (BD Biosciences) and centrifuged for 7 minutes at 1500 rpm (Eppendorf, 5702). Cell pellets were resuspended in 3 ml of complete FAD(-Ca) media and kept on ice until further processing.

2.2 ChIP-on-Chip Protocol

2.2.1 Formaldehyde crosslinking of keratinocytes

Epidermal cells grown in culture or isolated from mouse skin were washed in PBS (PAA Laboratories) and cross-linked by addition of 1% (v/v) formaldehyde (Sigma Aldrich) solution in PBS for 10 minutes. Cross-linking was terminated by addition of 2.5 M of glycine in water and incubation for 5 minutes. Cell pellets

were recovered by centrifugation at 1350 x g for 5 minutes at 4 °C or flash-frozen in dry ice and stored at -80 °C until further processing.

2.2.2 Pre-blocking and binding of antibodies to magnetic beads

A volume of 100 μl of protein G magnetic beads (Dynabeads, Invitrogen), was used for each ChIP. Protein G beads were dissolved in 1 ml of blocking solution [0.5 % (w/v) of bovine serum albumin, BSA (Sigma Aldrich) in PBS (PAA Laboratories)] and subsequently collected using a magnetic stand (Invitrogen), for removal of the supernatant. After two additional washes, the beads were resuspended in 250 μl of blocking solution and 10-15 μg of antibody specific to transcriptional regulator in study were added. Beads were incubated with the antibody overnight at 4 °C in a rotating platform specific for microcentrifuge tubes. All antibodies used for ChIP-on-chip/Seq are listed in Table 2.1.

Antibody	Catalogue #	Clone	Host	Source
c-MYC	sc-764	N-262	Rabbit pc	Santa Cruz
H3K4me3	ab71998	na	Mouse mc	Abcam
H3K27me3	07-449	na	Rabbit pc	Millipore
CEBPα	sc-9314	C-18	Goat pc	Santa Cruz
CEBPβ	sc-150	C-19	Rabbit pc	Santa Cruz
SIN3A	sc-994	K-20	Rabbit pc	Santa Cruz
KLF4	sc-20691	H118	Rabbit pc	Santa Cruz
OVOL1	na	na	Rabbit pc	gift from X. Dai [Nair et al., 2006]
OVOL2	na	na	Rabbit pc	gift from X. Dai [Wells et al., 2009]
TCFAP2γ	05-909	6E4/4	Mouse mc	Millipore
MXI1	sc-1042	G-16	Rabbit pc	Santa Cruz
RBP2	na	1416	Rabbit pc	gift from E.V. Benevolenskaya [Lopez-Bigas et al., 2008]

Table 2.1: Antibodies used for chromatin immunoprecipitation experiments: pc, polyclonal; mc, monoclonal; na, information not available.

2.2.3 Cell sonication

Formaldehyde fixed cell pellets were resuspended in 10 ml of cold Lysis Buffer 1 [50 mM Hepes-KOH, pH 7.5, 140 mM NaCl, 1 mM EDTA, 10% (v/v) glycerol, 0.5% (v/v) NP-40 and 0.25% (v/v) Triton X-100 in distilled water]. The resuspended cell pellet was incubated during 10 minutes at 4 °C in a rotating platform, followed by centrifugation for 5 minutes at 4 °C and 1350 x *g*. The newly recovered cell pellet was resuspended in 10 ml of Lysis Buffer 2 [200 mM NaCl, 1 mM EDTA, 0.5 mM EGTA and 10 mM Tris pH 7.5 in distilled water] and incubated at 4 °C in a rotating platform for 5 minutes. Cells were again collected by centrifugation at 4 °C and 1350 x *g* and resuspended in 3 ml of Lysis Buffer 3 [1 mM EDTA, 0.5 mM EGTA, 10 mM Tris-HCl pH 7.5, 0.1% (w/v) Na-deoxycholate and 0.5% (w/v) N-lauroyl sarcosine in distilled water]. Lysis buffers 1, 2 and 3 all contained

protease inhibitor cocktail tablets (Complete mini EDTA free, Roche). Cells were sonicated using an automatic sonicator (Misonix 3000), cycles of 30 seconds were applied with an output of 27-30 W and 1 minute intervals, with a total processed time of 12 minutes. The cell lysate was kept in an ice water bath during sonicaton. Cell extracts were transferred to 1.5 ml microcentrifuge tubes where 1/10 volume of 10%(v/v) Triton X-100 solution in water was added. Cell debris was removed by centrifugation at 2500 x g for 10 minutes at 4 °C in a table top centrifuge. After clearing, 50 μl of each sonicated fraction, corresponding to the whole cell extract (wce) supernatant (background reference/ input control) were transferred to 1.5 ml microcentrifuge tubes, and diluted in 150 μl of Elution buffer [50 mM Tris pH 8.0, 1 mM EDTA, 1% (w/v) SDS in distilled water] and stored at -20 °C. The remaining samples were used for chromatin immunoprecipitation.

2.2.4 Chromatin immunoprecipitation

Pre-cleared sonicated fractions were incubated with 100 μl of antibody prebound protein G magnetic beads at 4 °C, overnight on a rotating platform. The beads had been previously washed three times with 1 ml of the BSA blocking solution, in order to remove the excess of unbound antibody.

2.2.5 Wash, elution, and cross-link reversal

Following ChIP, the beads were washed four times with cold RIPA buffer [50 mM Hepes pH 7.6, 1 mM EDTA, 0.7% (w/v) Na-deoxycholate, 1% (v/v) NP-40 and 0.5 M LiCl in distilled water], and once with cold TE buffer [50 mM Tris pH 8.0, 1 mM EDTA and 1% (w/v) SDS in distilled water]. All washing steps were performed in a cold room at 4 °C, using a magnetic stand (Invitrogen) to recover the beads. The DNA-protein complexes were then eluted in 200 μl of Elution buffer [50 mM Tris-HCl pH 8.0, 10 mM EDTA and 1% (w/v) SDS in distilled water] after incubation at 65 °C for 10 to 15 minutes with brief vortexing every 2 minutes. At this step, the immunoprecipitate (IP) as well as wce samples (previously kept at -20 °C), were reverse cross-linked overnight at 65 °C.

2.2.6 Digestion of cellular protein and RNA

Following reverse-crosslinking, the 200 μl of IP and wce samples were centrifuged at 20000 x g and the supernatant was recovered and diluted in 200 μ of TE buffer. Samples were incubated for 30 minutes with 8 μl of 1 mg/ml of RNase A (Ambion) at 37 °C, in order to digest RNA molecules. Subsequently, 4 μl of 20 mg/ml of proteinase K (Invitrogen) were added to each sample in order to digest all proteins. Samples were incubated for 1 hour at 55 °C, and DNA was isolated using one volume of phenol: chlorophorm: isoamyl alcohol (Sigma-Aldrich) following centrifugation at 20000 x g for 5 minutes. The aqueous layer from each sample was collected and transferred to a new 1.5 μl microcentrifuge tube in which 16 μl of 5 M NaCl (Sigmal-Aldrich) and 1 μl of glycoblue (Ambion) were added. DNA was precipitated with 800 μl of 100% (v/v) ethanol by centrifugation at 20000 x g at 4 °C for 15 minutes. The DNA pellets were washed with 500 μl 80% (v/v) of ethanol and centrifugated at 20000 x g at 4 °C during 10 minutes, air-dried (following supernatant removal) and resuspended in 60 μl of 10 mM Tris-HCl pH 8.0. The DNA concentration of the wce sample was normalised to 100 ng/μl using a Nanodrop spectrophotometer (ND-1000, Nanodrop Technologies). In addition, 2 μl of each IP and wce samples were kept and analyzed in a 2% (w/v) agarose gel for fragment size verification (see preparation of agarose gel below).

2.2.7 End Repair to add 'A' bases to 3' Ends of DNA

To perform 3' end repair of the DNA fragments, the following reagents were mixed directly into PCR tubes kept on ice:

30 μl IP or 50 ng of wce DNA sample
5.0 μl of 10x NEB2 buffer (New England Biolabs)
1.0 μl of dNTP mix (10 mM) (New England Biolabs)
2.5 μl of T4 DNA polymerase, 3 U/ μl (New England Biolabs or Enzymatics)
1.0 μl of Klenow fragment (New England Biolabs or Enzymatics)
1.0 μl of polynucleotide kinase (PNK) (New England Biolabs or Enzymatics)
33 μl of ultrapure water (Ambion)

The IP and wce reaction mixtures were incubated for 30 minutes at 12 °C and the DNA samples were purified using DNA Clean Concentrator-5 columns (Zymo Research, USA). DNA was eluted with 32 μl of ultrapure water at 50 °C and the following mixture was prepared to add 'A' bases:

32 μl IP or wce DNA sample
5.0 μl of NEB2 buffer (New England Biolabs)
10 μl of dATP (1 mM) (New England Biolabs)
2.0 μl of exo-Klenow (Invitrogen or Enzymatics)

following incubation for 30 minutes at 37 °C and purification with DNA Clean Concentrator-5 columns (Zymo Research). DNA was eluted with 8 μl of ultrapure water and blunt-ended ligation was perform by addition of:

12.5 μl of ligase buffer (Invitrogen or New England Biolabs)
3.0 μl of annealed linkers 102+/103 [1]
1.0 μl of T4 ligase (Invitrogen or New England Biolabs)

The mixture was incubated overnight at 16 °C in a thermoblock (BioRad) and samples were purified with DNA Clean Concentrator-5 columns (Zymo Research, USA) and eluted in 25 μl ultrapure water at 50 °C. A reaction mixture was prepared with the following reagents:

25 μl of the blunt-ended IP or wce DNA sample
5.0 μl of 10x Thermopol buffer (New England Biosciences)
5.0 μl of dNTPs (2.5 mM dNTPs) (New England Biolabs)
2.0 μl oligo102+ primer (40 μM)
12 μl of ultrapure water (Ambion)
1.0 μl of AmpliTaq (Applied Biosystems, Roche)

[1] 375 μl of oligo 102+ G*CGGTGACCCGGGAGATCTGAATTCT (40 μM) were annealed to 375 μl of oligo103 G*AATTCAGATC (40 μM) in 250 μl of Tris-Hcl (1M), pH 9.0 after heating the oligos for 95°C during 5 minutes, following 70°C and subsequent cooling; * denotes phosphorothioate modification.

to perform the first DNA amplification (LM-PCR15) of the ligated IP and wce DNA fragments. The PCR program used was the following: 1 cycle (2' at 95 °C), 14 cycles (30" at 95 °C, 30" at 60 °C and 1' at 72 °C) and 1 cycle (1' at 72 °C). Ten microliters of the LM-PCR15 amplified products were added to a new reaction mixture containing:

5.0 μl of 10x Thermopol buffer (New England Biolabs)
5.0 μl of dNTPs (2.5 mM dNTPs) (New England Biolabs)
2.0 μl oligo102+ primer (40 μM)
27 μl of ultrapure water (Ambion)
1.0 μl of AmpliTaq (Applied Biosystems, Roche)

A second amplification step was performed, LM-PCR25 with the following program: 1 cycle (2' at 95 °C), 24 cycles (30" at 95 °C, 30" at 60 °C and 1' at 72 °C) and 1 cycle (5' at 72 °C). Finally, the DNA was purified using a QiAquick PCR purification kit (Qiagen), following the manufacturer's protocol. DNA was resuspended in 50 μl of Qiagen elution buffer and the concentration was normalised to 100 ng/μl using a Nanodrop spectrophotometer (ND-1000, Nanodrop Technologies).

2.2.8 Cy3/Cy5 labelling of IP and wce DNA amplified fragments

One microgram of IP or wce sample was diluted in 24 μl of ultrapure water (Ambion) and 26 μl of 2.5X random primer solution (Invitrogen Bioprime labeling kit). Samples were boiled for 5 minutes in a heatblock, following incubation in an ice water bath for 5 minutes. Eight microliters of 10x low T dNTP mix (1.2 mM dATP, dCTP, dGTP each and 0.6 mM dTTP), 1 μl of high concentration exo-Klenow (40 U/ml, Invitrogen Bioprime labeling kit) and 1 μl of cy5-dUTP (Enzo Life Sciences) or 0.5 μl of cy3-dUTP (Enzo Life Sciences) and 0.5 μl of sterile water, were added to the IP and wce fractions, respectively. Samples were incubated overnight in the dark at 21-25 °C. Subsequently, labelled IP and wce samples were purified with a QiAquick PCR purification kit, precipitated

with 25 μl of ammonium acetate and 300 μl of 100% (v/v) cold ethanol. The DNA pellets were air-dried and resuspended in 50 μl of Tris (Sigma-Aldrich) pH 8.0 solution. Cyanine 3 and cy5 incorporation was analyzed using a Nanodrop spectrophotometer (ND-1000, Nanodrop Technologies).
Note: The protocol just described has been published by Ren et al. [2000].

2.2.9 Hybridization on Microarrays

Equal amounts of wce-cy3 and IP-cy5 labeled DNA were combined (6-10 μg of total DNA) and hybridized overnight at 65°C to mouse proximal promoter microarrays (Agilent, G4490A) or mouse whole genome chromosome 3 (Amadid 15317), using the oligo CGH/ChIP-on-Chip hybridization kit (Agilent) and following the manufacturer's suggested protocol.

Arrays were scanned using a microarrays scanner (Agilent G2565CA) and data was extracted using the Feature Extraction software (Agilent, v10.5). A minimum of two biological independent replicates was used for each experiment. One biological replicate consisted of biological material containing, either, isolated mouse keratinocytes pooled from seven mice, or human primary keratinocytes with a total number of 5 x 10^7 - 1 x 10^8 cells.

2.2.10 Microarray scanning and data analysis

ChIP-on-chip data analysis of mouse whole genome proximal promoter arrays was performed in collaboration with Matthew Trotter [1]. ChIP-on-chip analysis of mouse whole genome chromosome 3 was performed in collaboration with Stewart MacArthur [2]. Both analyses were carried out using *R* and Bioconductor, namely the *Ringo* [Toedling et al., 2007], *RColorBrewer*, *WGCNA*, *limma* and *xtable* packages. To generate scatterplots for the ChIP-on-chip raw data, known mouse binding events for MYC were used as targets to center each window. A half size window corresponding to 3000 bp was defined and a minimum number

[1] Laboratory of Regenerative Medicine, LRM - University of Cambridge
[2] Bioinformatics core, Cancer Research UK - Cambridge Research Institute. Currently at Illumina Cambridge Limited

of 3 probes was set to consider a binding event. Targets were predicted using a 0.90 or 0.99 quantile and genomic regions between 1.0 Kb upstream and 0.3 Kb downstream of the TSS of annotated genes (Genome built used: NCBI37/mm9) .

ChIP-on-chip data access:
Data from ChIP-on-Chip mouse proximal promoter arrays for MYC and H3K4me3 were submitted to the ArrayExpress Database (http://www.ebi.ac.uk/arrayexpress/) under the accession number E-MTAB-555.
Data from ChIP-on-Chip in mouse whole genome chromosome 3 arrays for all TFs used were submitted to the ArrayExpress Database under the accession number E-MTAB-556.

2.3 Modification of the ChIP-on-chip protocol to enable sequencing (ChIP-Seq)

All previous steps of the ChIP-on-chip protocol described, until DNA ligation, were the same as for ChIP-Seq. If sequencing of the IP or wce fragments was desired then ligation overnight was performed with Illumina oligo adapters rather than linkers 102+/103.

2.3.1 Ligation of Illumina sequencing adapters to DNA fragments

Following digestion of the cellular protein and RNA from IP and wce samples the following reagents were mixed in 1.5 ml microcentrifuge tubes:

8.0 μl IP or 50 ng of wce DNA sample
12.5 μl DNA ligase buffer (New England Biolabs)
2.0 μl Adapter Oligo mix (Illumina)
2.5 μl DNA ligase (New England Biolabs)

Samples were incubated overnight at 16 °C in a thermocycler PCR machine or

water bath. Subsequently, the ligated DNA fragments were purified using DNA Clean Concentrator-5 columns (Zymo Research). DNA samples were eluted with 23 μl of pre-heated at 50 °C Qiagen elution buffer (QIAquick PCR purification kit) and samples were kept on ice until furhter processing.

2.3.2 Enrichment of adapter modified DNA by PCR

After the ligation step, the following reagents were added to pre-cooled PCR tubes:

23 μl of IP or wce DNA sample
25 μl Phusion DNA Polymerase 2x mastermix (Illumina)
1.0 μl PCR primer 1.1 (Illumina)
1.0 μl PCR primer 1.2 (Illumina)

in order to perform amplification of the adapter modified IP or wce DNA. The PCR program used was the following: 1 cycle (30" at 98 °C), 17 cycles (10" at 98 °C, 30" at 65 °C and 30" at 72 °C) and 1 cycle (5' at 72 °C). Amplified DNA fragments were purified with the QIAquick PCR purification kit (Qiagen) and eluted with 33.5 μl of pre-heated (50 °C) Qiagen elution buffer. One microliter of eluted IP or wce DNA was mixed with 9 μl of elution buffer and stored at -20 °C (Solexa 18 sample). The remainder sample of 32.5 μl was stored as SolexaPreGel sample. **Note**: Solexa18 was an aliquot that could be used for reamplification and microarray or real-time PCR analysis. SolexaPreGel was the sample which was ready for sequencing after Gel purification.

2.3.3 Reamplification of Solexa 18 for ChIP-on-chip or ChIP-qPCR

Two microliters of Solexa 18 IP or wce samples were mixed in PCR with:

5.0 μl 10x Thermopol buffer (New England Biolabs)
0.5 μl dNTP mix (25 mM each) (New England Biolabs)
2.5 μl Primer 1.2 for reamplification (10 μM) (Illumina)
2.5 μl Primer 2.2 for reamplification (10 μM) (Illumina)
1.0 μl AmpliTaq (Applied Biosystems, Roche)

Primer sequences used were the following:
Primer 1.2 for reamplification (5'AATGATACGGCGACCACCGAGATCTA CACTCTTTCCCTACACGACGCTCTTCCGATCT3') (Illumina)
Primer 2.2 for reamplification (5' CAAGCAGAAGACGGCATACGAGCTCTTC-CGATCT3') (Illumina)
Primers 1.1 and 1.2 are from the Genomic DNA sequencing kit (Illumina).

The PCR program for reamplification used was the following: 1 cycle (2' at 95 °C), 24 cycles (30" at 95 °C, 30" at 65 °C and 1' at 72 °C) and 1 cycle (5' at 72 °C). Amplified DNA fragments were purified with QIAquick PCR purification kit (Qiagen) and eluted with 25 μl pre-heated (50 °C) Qiagen elution buffer. The IP and wce amplified DNA samples were measured with NanoDrop (NanoDrop Technologies). At this point the samples were ready for further microarray processing, such as Cy3 and Cy5 labelling or RT-qPCR.

2.3.4 Gel purification of SolexaPreGel for ChIP-Seq

A 50 ml 2% (w/v) agarose (BioRad) TAE gel with 1x SYBR Safe (Invitrogen) was cast onto a BioRad gel electrophoresis tank. Meanwhile, a DNA ladder (NEB, cat. # N3233) was prepared by adding 3 μl of 50% (v/v) glycerol solution to 8 μl of the DNA ladder. In addition, 10 μl of 50% (v/v) glycerol solution were also added to the SolexaPreGel samples (only one sample was run per agarose gel). Both ladder and DNA sample were loaded into the wells of the agarose

gel. The gel was run at 120 V for 45 minutes and DNA fragments of 200-300 bp were excised on a Dark Reader and purified with the MinElute Gel Extraction kit (Qiagen) following the manufacturer's instructions. Purified DNA was eluted with 15 μl of pre-heated (50 °C) Qiagen elution buffer. DNA libraries were run on a Bioanalyzer (Agilent) for estimation of the concentration the IP and wce samples, which were submited for sequencing at the Cancer Research Institute (CRI) - Cambridge Research Institute Genomics Facility.

2.3.5 ChIP-Seq analysis

The analysis of the ChIP-Seq data was performed in collaboration with Sabine Dietmann[1]. Sequence tags of 36 nucleotides were aligned to the human reference genome (UCSCGRCh37/hg19) using the BOWTIE software (hht://bowtie-bio.source.net). After quality inspection the first 5' base were trimmed from the sequence tags. Mapping of the sequences, at not more than three genomic locations, and with more than two mismatches in a seed of lenght equal to 28, was used for data analysis. ChIP-Seq enriched regions were determined using MACS [Zhang et al., 2008] and CCAT [Xu et al., 2010] software packages for peak calling. A false discovery rate (FDR) of 0.1 and 0.05 was used to determine enriched peaks with a maximum of 10 reads aligning at the same position.

2.4 Confirmation of IP enrichment by nucleolin-specific PCR

2.4.1 Preparation of PCR amplification reaction

To confirm the protein of interest was bound to the *Ncl* promoter I performed PCR using the following reagents:

2.0 μl of IP and wce (in a dilution series, e.g 20 ng, 60 ng) DNA sample
2.0 μl of 5 μM Forward *Ncl* primer: 5'-GGCTGGAAGCGAGAGAAAG-3'

[1]Bioinformatics facility, Wellcome Trust Centre for Stem Cell Research - University of Cambridge

2.0 μl of 5 μM Reverse *Ncl* primer: 5'-TCACCTCTTAAAGCAGCCCA-3'
13.6 μl of ultrapure water (Ambion)
0.2 μl of dNTPs (New England Biolabs)
2.0 μl of 10x Thermopol buffer (New England Biolabs)
0.2 μl of AmpliTaq (Applied Biosystems, Roche)

The PCR program used for amplification of the *Ncl* promoter was: 1 cycle (2' at 94 °C), 28 cycles (45" at 94 °C, 1' at 56 °C and 1' at 72 °C) and 1 cycle (10' at 72 °C).

2.4.2 Loading of PCR amplified DNA samples in an agarose gel

A 50 ml of a 2% (w/v) agarose (Invitrogen) gel in 1 x TAE buffer (Invitrogen) with 3 μl of ethidium bromide (Solarbio), were poured in a gel electrophoresis tank (Mupid-One Gel Electrophoresis Unit from Anachem). A set of 13 combs was added to allow the formation of wells where the PCR samples could be loaded following gel polymerization. Six microliters of 6x DNA loading dye (0.25% (w/v) Orange G (Sigma-Aldrich) and 15% (v/v) (Ficoll-400 (Sigma-Aldrich)) were added to 20 μl of each PCR reaction and samples were loaded into each of the wells formed in the gel. In one of the wells a mixture of 3 μl of 1 Kb DNA ladder (Invitrogen, cat # 15615-016) and 6 μl of DNA loading dye were loaded. The gel was run for 150 V for 45 minutes and visualized under UVP Imaging system.

2.4.3 ChIP-qPCR

Semi-quantitative qPCR was used on to confirm enrichment in IP samples (ChIP-qPCR). Two microliters of IP or wce DNA (previously normalised to 100 ng/μl) were diluted in a 20 μl qPCR reaction mixture containing 12.5 μl of Fast SYBR Green (2x) (Applied Biosystems), 0.6 μl of forward and reverse primers (600 nM each) and 12 μl of ultrapure water. The qPCR reaction and preliminary analysis was performed using a 7900HT Fast Real-Time PCR System (Applied

Biosystems). Quantification of IP enrichment was performed using Ct values of IP relative to wce. The primers used for ChIP-qPCR were designed to target the promoter of genes bound by MYC and the corresponding sequences are listed below in Table 2.2

Primer	**Sequence**
Ncl forward	GGCTGGAAGCGAGAGAAAG
Ncl reverse	TCACCTCTTAAAGCAGCCCA
Suz12 forward	AATAGGTCGCTCCCTTTCGT
Suz12 reverse	GATCCCGAGACTGTGTGGTC
Ezh2 forward	ACCTACCCCTGGAGATTTGG
Ezh2 reverse	TGGTGACAGGTGCTAACGAA
Id2 forward	GGCAGAGTCCGGTGATGTAG
Id2 reverse	TGCAGGGCAGAGTCCTTCT
Hdac2 forward	ACCCCTTCGGTCCTCAGAT
Hdac2 reverse	CGTGCCATGTCCATCTCCT
Sprr1a forward	AGGGCTCGGGTGCCTTGGG
Sprr1a reverse	CAGCAGCAGGTGAAGCAGCCTTG
S100a1 forward	AGCGTTGGTTCGGTAGCTCCAGT
S100a1 reverse	CCCACTCTCGCCCAGCCCTT

Table 2.2: SYBR-green PCR primer sequences for ChIP-qPCR.

2.5 Gene expression microarrays

2.5.1 Biological material

A minimum of three biological samples were used for the mouse K14MycER line for each time point of 4-OHT treatment (0, 1, 2, 4 and 6 days), with corresponding wild-type controls. For mouse lines K14Sin3a$^{\Delta/\Delta}$, K14Myc$^{\Delta/\Delta}$K14Sin3a$^{\Delta/\Delta}$ and K14Myc$^{\Delta/\Delta}$ a minimum of four biological replicates were used treated with 4-OHT or acetone for 14 or 21 days, as previously described.

2.5.2 Extraction of total RNA

Samples from dorsal skin of transgenic and non-transgenic mice treated with 4-OHT or acetone were cut and flash-frozen in liquid nitrogen until further processing. Frozen tissues were added to nalgene centrifuge 50 ml tubes, previously rinsed with *RNAaseZap* solution (Ambion) and containing 3 ml of Trizol reagent (Invitrogen). Tissues were macerated using a homogeneizer (this step, and all involving Trizol usage were performed under a chemical hood). Tissue suspensions were incubated for 5 minutes at 21-25 °C and 0.6 ml of choroform were added. Samples were run in a vortex for 15 seconds and incubated for 15 minutes at 21-25 °C following centrifugation at 12000 x *g* for 30 minutes at 4 °C. The aqueous supernatant was removed and RNA was kept for 30 minutes on ice while precipitating in 1.5 ml of 2-propanol. RNA pellets were collected by centrifugation at 12000 x *g* for 30 minutes at 4 °C and were washed with 500 μl of 70% (v/v) ethanol by centrifugation at 12000 x *g* for 5 minutes. RNA samples were air-dried and diluted in 500 μl of ultrapure water and the concentration content was assessed using a Nanodrop spectrophotometer (ND-1000, Nanodrop Technologies). Concentrations were normalised to 25 ng/μl and sent to CRI Genomics Core facility for assessment of RNA integrity (RIN) using a Bioanalyzer (Agilent). From this step onwards only samples with a RIN = 9 were further processed.

2.5.3 Microarray sample preparation and hybridization

Microarray sample preparation and hybridization was performed in collaboration with Michelle Osborne [1]. A sample of 250 ng of total RNA was converted to complementary RNA (cRNA) target using a Illumina TotalPrep-96 Kit (Ambion 4397949). Briefly, total RNA was reverse transcribed and converted to double-stranded cDNA using a T7 promoter-Oligo(dT) primer and purified with magnetic oligo(dT) beads. This reaction formed the template for an *in vitro* transcription (IVT) reaction which included a biotinylated nucleotide/ribonucleotide mix for both cRNA amplification and biotin labeling. Quality control using a Bioanalyzer (Agilent) and normalisation was performed and the cRNA was hybridized to arrays (3 Sentrix BeadChip Array MouseWG-6 v2 Part #11278593). Hybridization, washing, staining and scanning were performed according to standard Illlumina protocols (Illumina WGGX DirectHyb Assay Guide 11286331 RevA).

2.5.4 Microarray data analysis

Microarray data analysis was performed in collaboration with Stewart MacArthur. Analysis involved the use of scripts written in *R* (R Development Core Team 2008; www.r-project.org) and Bioconductor (www.bioconductor.org) [Gentleman et al., 2004]. Differential gene expression analysis was performed using *limma* Smyth [2005] and time course analysis using the *timecourse* package [Tai and Speed, 2009]. The microarray data was clustered using Euclidian distance and the *complete* agglomeration method. Clusters were visualized in *R* software, using the *gplots* package (http://CRAN.R-project.org/package=gplots) [Warnes et al.]. Visualization of the time course of expression for individual genes was also performed in *R*. A more detailed description of the analysis follows below.

The raw beadlevel data was imported and processed using the *beadarray* package and differential expression was carried by applying linear models using the *limma* package. Following import of the data, a range of quality control (QC) steps were performed in order to see if there were any spatial effects during hybridization that might confound the data analysis. The *BASH* package was used to help

[1] Genomics core, Cancer Research UK - Cambridge Research Institute, CRI

remove spatial aberrations on the arrays. Positve and negative control spots on the arrays behaved normally during QC analysis.
Data was quantile normalised and log2 transform to remove small differences between arrays (Figure 2.1).

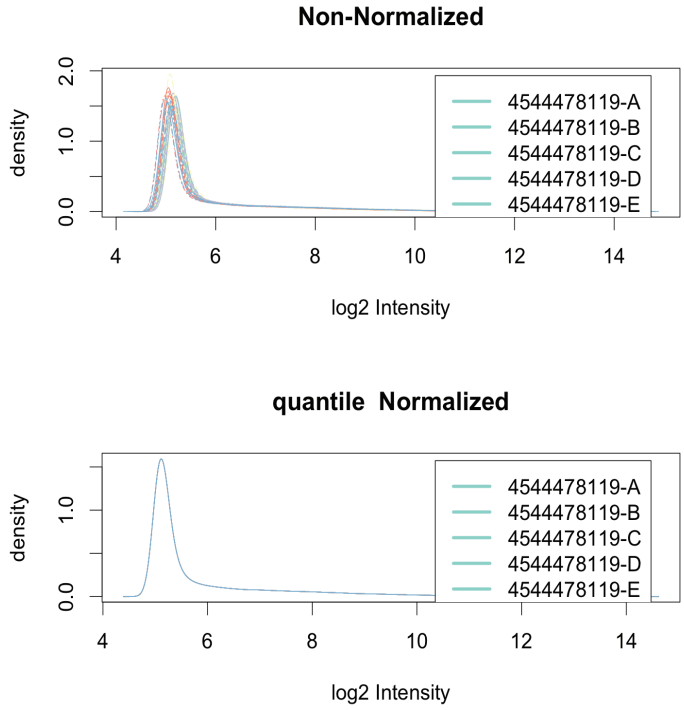

Figure 2.1: Density plot of log expression values. Data was quantile normalised to remove small differences between arrays. Numbers 4544478119A-E represent examples of samples hybridized.

Clustering was performed in order to try to see if there was a problem with sample mis-labelling or other confounding problems. Clustering of the arrays was based either on all probes or on the most variable probes (above the third quantile of variance) and the euclidian distance and complete method were used. Clustering should not be seen by other groups (e.g gender, age) other than genotype and treatment. In the rare cases that the arrays did not follow this presumption, samples history was tracked by histological analysis.

Annotation information for the Mousev2 beadarrays platform was obtained from the Cambridge Computational Biology Group's Illumina BeadChip Probe Re-annotation data. Identification of genes statistically differentially expressed was performed using linear models from the *limma* package. In some arrays where poor correlation between replicates was observed, these were weighted by how well replicates matched a fitted linear model.

Base packages used in this analysis:
Base
datasets
grDevices
graphics
methods
stats
tools
utils

Other packages used:
AnnotationDni 1.4.2
Biobase 2.2.1
RColorBrewer 1.0-2
WGCA 0.79-1
annotate 1.201
beadarray 1.11.3
dynamicTreeCut 1.20
fields 5.02
flashClust 0.10
gdata 2.4.2
geneplotter 1.20.0
gplots 2.6.0
gtools 2.5.0
hwriter 0.93

1.14.0
lattice *0.17.17*
limma *2.16.3*
sma 0.5.15
spam 0.15-3
x-table 1.5-4.
Loaded via a namespace: DBI 0.2-4, KernSmooth 2.22-22, RSQLite 0.7-1, grid 2.8.1.

R version used: R version 2.8.1/ 2008-12-22
Microarray mRNA expression data access:
Data from mRNA gene expression microarrays for wild-type and K14MycER time-course treated from 0 to 6 days with 4-OHT were submitted to the ArrayExpress Database under the accession number E-MTAB-553 (released date 2012-02-25).
Data from mRNA gene expression microarrays for K14Sin3a$^{\Delta/\Delta}$, K14Myc$^{\Delta/\Delta}$ and K14Myc$^{\Delta/\Delta}$K14Sin3a$^{\Delta/\Delta}$ treated for 14 and 21 days with 4-OHT were submitted to the ArrayExpress Database under the accession number E-MTAB-554 (released date 2012-02-25).

2.6 RT-qPCR for mRNA expression analysis

Total RNA samples were extracted as previously described. Double stranded cDNA was generated from 1 μl of RNA using Superscript III reverse transcriptase (Invitrogen) enzyme following manufacturer's instructions. Reverse transcription quantitative PCR (RT-qPCR) and analysis was conducted using the 7900HT Real-Time PCR System (Applied Biosystems). The standard amplification protocol was used with pre-designed probe sets and TaqMan Fast Universal PCR Master Mix (2) (Applied Biosystems). A list of the pre-designed probes used is shown in Table 2.3. A *Gapdh* probe (4352932E) was used to normalize samples using the ΔCt method.

Gene	Taqman Probe ID
Itgα6	Mm01333831_m1
Ivl	Mm00515219_s1
Myc	Mm00487803_m1
Sin3a	Mm00488255_m1
Ncl	Mm01290591_m1
Suz12	Mm013041352_m1
Hdac2	Mm00515108_m1
Sprr1a	Mm01962902_s1
Id2	Mm00711781_m1
S100a1	Mm00845129_g1
S100a11	Mm00845129_g1
Lce1e	Mm00783163_s1
S100a16	Mm00509522_m1
Lce1g	Mm00787694_s1
Lce3f	Mm02605425_s1
Ovol1	Mm00498263_m1
Klf4	Mm00516104_m1
Cebpα	Mm01265914_s1
S100a10	Mm00501457_m1
Lce1a2	Mm00783433_s1
MYC	Hs00153408_m1

Table 2.3: List of probes used for reverse transcription quantitative PCR (RT-pPCR).

2.7 Flow cytometry

Following the mouse epidermal keratinocytes isolation protocol, above described, cells were resuspended in PE-conjugated ITGα6 antibody (Clone GoH3, eBiosciences). After incubation for 45 minutes at 4 °C, cells were washed twice in PBS (PAA Laboratories). Cells were gated using forward *versus* side scatter to eliminate debris. Cell doublet discrimination was carried out using pulse width. The non viable cells, stained with DAPI (4',6-diamidino-2-phenylindole, dihydrochloride) DNA staining reagent (Sigma-aldrich) were then gated for their exclusion using a 450/65 nm filter. ITGα6 PE stained cells were detected using a 580/30 nm filter. Cells were then sorted based on ITGα6 expression (fluorescence detected using a 580/30 nm filter), after gating out dead cells (based on DAPI staining) with a MoFlo high-speed sorter (Beckman Coulter). This work was performed in collaboration with Nigel Miller [1].

2.8 Immunohistochemistry

Skin tissue samples were fixed in 4% (w/v) formaldehyde and paraffin embedded and sectioned at 5 to 10 μm for H&E staining at the Histology facility with the help of Margaret Mcleish[2]. Immunohistochemistry was performed using Ventana Discovery (Ventana Medical Systems, Inc) on paraffin embedded tissues, following manufacturer's guidelines. Antigen retrieval was performed using Ventana Cell Conditioning 1 solution (Roche) for 40 minutes at 99 °C. Primary antibody incubation was performed for 54 minutes at 37 °C. Secondary antibody incubation (Donkey anti-rabbit or anti-goat Ig biotinylated, Jackson) was performed for 30 minutes at 37 °C. Antibody detection was performed using the DAB Map detection kit (Ventana) and sections were counterstained using hematoxylin and bluing reagent (Roche). Primary antibodies used are listed in Table 2.4. All antibodies were used at a 1:100 dilution.

[1] Department of Pathology, University of Cambridge
[2] Histology Facility, Wellcome Trust Centre for Stem Cell Research - University of Cambridge

Antibody	Catalogue #	Clone	Host	Source
c-MYC	sc-764	N-262	Rabbit pc	Santa Cruz
CEBPα	sc-9314	C-18	Goat pc	Santa Cruz
SIN3A	sc-767	AK-11	Rabbit pc	Santa Cruz
KLF4	sc-20691	H118	Rabbit pc	Santa Cruz
KI67	VP-RM04	SP6	Rabbit mc	Vector Labs

Table 2.4: Primary antibodies used for immunohistochemistry: pc, polyclonal; mc, monoclonal

2.9 Immunofluorescence

Skin tissue cryosections of 5 to 10 μm, previously embedded in Optimal Cutting Temperature (OCT) solution (Raymond A Lamb) and fixed with 4% (w/v) paraformaldehyde were incubated for 5 minutes with a 0.2% (v/v) solution of Triton X-100 and subsequently blocked with blocking solution [10% (v/v) fetal calf serum (FCS), 0.05% (w/v) Na-azide in PBS]. Tissue sections were incubated with primary antibodies overnight at 4 °C (antibodies diluted in blocking solution). Subsequently, sections were washed three times with PBS (PAA Laboratories) for 10 minutes and incubated with secondary antibodies (antibodies diluted in blocking solution) in addition to DAPI (4',6-diamidino-2-phenylindole, dihydrochloride) DNA staining reagent (Sigma-aldrich) (1:1000 dilution) at 21-25 °C for 1 hour. Sections were washed three times with PBS for 5 minutes and mounted with Mowiol mounting media. The primary and secondary antibodies used are listed in Table 2.5:

Antibody	Dilution	Clone	Host	Source
KRT10	1:500	PRB-159	Rabbit pc	Covance
ITGα6	1:250	SP6	Rat pc	Serotec
IVL	1:500	ERLI-3	Rabbit pc	gift from Li ([Li et al., 2000a])
Rabbit IgG whole molecule Alexa 594	1:1000	na	Goat pc	Molecular Probes
Rat IgG whole molecule Alexa 488	1:1000	na	Goat pc	Molecular Probes

Table 2.5: Primary and secondary antibodies used for immunofluorescence: pc, polyclonal; na, information not available

2.9.1 Preparation of Mowiol Mounting media

Mowiol was prepared by using 24 g analytical grade glycerol (Sigma-aldrich), 9.6 g Mowiol 4-88 (Sigma-Aldrich), 24 ml distilled water and 48 ml 0.2 M Tris buffer, pH 8.5 were combined and homogeneized with a stir bar on a hot plate on 60 °C for at least 4-5 hours until dilution of the Mowiol powder in the solution. The solution was centrifuged at 5000 x g for 15 minutes and the supernatant was stored in aliquots at -20 °C for a maximum of 12 months. Mowiol was used at 21-25 °C.

2.9.2 Image acquisition

Microscopic white field images were acquired using an Olympus IX80 microscope and a DP50 camera. All the images were processed with Photoshop CS4 (Adobe) software.

2.10 Cell culture

All mammalian cell culture was performed using aseptic technique under a laminar flow hood. Cells were maintained at 37 °C in a humidified incubator with a 5% CO2 atmosphere. Cells were grown on plastic dishes or flasks of tissue culture grade (Falcon). Medium renewal was performed every two to three days and, when necessary cells were frozen in 1 ml aliquots containing 10^6 cells per mililiter in freezing medium (FCS and 10% (v/v) DMSO). Cell were first subjected to freezing in a *Mr. Frosty* freezing container (Nalgene) and kept one day at -80 °C following transfer to a liquid nitrogen container used as a cell bank.

2.10.1 Cell lines

HEK-293 cells were obtained from ATCC and maintained in DMEM (Invitrogen) supplemented with 10% (v/v) FCS serum (Sigma-Aldrich), 100 U/ml penicillium (PAA laboratories), 100 μg /ml streptomycin (PAA laboratories) and splitted 1:8 once a week according to ATCC guidelines.

COS-7 cells were obtained from ATCC and maintained in DMEM (Invitrogen) supplemented with 10% FCS serum (Sigma-Aldrich), 100 U/ml penicillium (PAA laboratories), 100 μg /ml streptomycin (PAA laboratories) and splitted 1:5 once a week according to ATCC guidelines.

3T3 J2 cells were generated from the J2 clone of random-bred Swiss mouse 3T3 cells which was selected to provide optimal feeder support of keratinocytes [Rheinwald and Green, 1975]. These cells were maintained in DMEM (Invitrogen) supplemented with 10% (v/v) bovine calf serum (BS) (Invitrogen), 100 IU/ml penicillin (PAA Laboratories), 100 μg/ml streptomycin (PAA Laboratories). Cells were passaged nearly confluency and re-seeded at a density of approximately 3,000/cm^2. Cells were maintained for up to 12 passages after thawing, after which a new stock of low passage number feeder cells was thawed to replace the old stock. Feeder cells were mitotically inactivated by incubation with 4 μg/ml mitomycin C (Sigma-Aldrich) for 2 hours at 37 °C to inhibit mitosis. These were washed twice with PBS to remove the mitomycin C and incubated in fresh FAD medium before used as feeders for keratinocytes. Cells were splitted 1:5 once a week.

3T3 J2-puro cells were stably transfected with pBabePuro retroviral vector to render them resistant to puromycin [Levy et al., 1998]. These were handled in the same way as J2-3T3 cells, in addition to the fact that the culture media was supplemented with 2 μg/ml of puromycin (Sigma-Aldrich). Cells were splitted 1:5 once a week.

Phoenix E ecotropic packaging cells were obtained from ATCC with approval of G. Nolan (Standford University, USA) [Swift et al., 2001]. Cell maintenance included cultivation in DMEM (Invitrogen) supplemented with 10% FCS (Sigma-Aldrich), 100 U/ml penicillium (PAA laboratories), 100 μg /ml streptomycin (PAA laboratories). Prior thawing, the culture dishes needed coating with a 1:100 solution of collagen (BD Biosciences) in PBS at 37 °C for a minimum of 30 minutes, as these cells are very sensitive and tend to detach from the plasticware. Cells were splitted 1:5 every 3 days.

AM12 amphotropic packaging cells first described by [Markowitz et al., 1988] were cultured in DMEM (Invitrogen) supplemented with 10% FCS serum (Sigma-Aldrich), 100 U/ml penicillium (PAA laboratories), 100 μg /ml streptomycin (PAA laboratories). Cells were splitted 1:5 every 3 days.

Primary human keratinocytes

Simon Broad [1] and Salvador Aznar Benitah [2] kindly provided vials of human keratinocytes (at passage 0) which had been isolated from neonatal foreskin and were maintained on J2-3T3 mouse feeder cells. These cells were maintained in complete FAD medium (FAD + FCS + HICE) which included one part Ham's F12 medium and three parts Dulbecco's modified Eagle's medium (DMEM), supplemented with 1.8 x 10^{-4} M adenine (FAD); 10% (v/v) FCS (Sigma-Aldrich); 0.5 μg/ml hydrocortisone (Fisher Scientific), 5 μg/ml insulin (Sigma-Aldrich), 10^{-10} M cholera toxin (Sigma-Aldrich), 10 ng/ml EGF (Peprotech) (HICE). Before passaging the keratinocytes, the J2-3T3 feeder cells were removed by incubation in versene (Gibco) for 5 minutes. Keratinocytes were dissociated by incubation in a 1:4 dilution of 0.25%v/v) trypsin solution with no EDTA (Invitrogen) in PBS (PAA Laboratories) for 5 minutes. Complete FAD medium was added and the cells were recovered by centrifugation at 1000 x g for 5 minutes. Keratinocytes were resuspended in complete FAD medium and replated at a density of 4,000/cm^2 on inactivated J2-3T3 feeder cells.

2.11 Transient transfection of HEK-293 cells for luciferase reporter assay

HEK-293 cells were grown in 6-well plates and plated in 24-well plates for transfection at a confluence of 50-60% using the Attractene Transfection Reagent (Qiagen) following manufacture's instructions. Cells were transfected with a total

[1] Fiona Watt Lab, Cancer Research UK - Cambridge Research Institute

[2] Head of Epithelial Homeostasis and Cancer, Center of Genomic Regulation(CRG), Barcelona

of 450 ng of plasmid DNA from the *Cignal c-Myc Reporter* luciferase assay from Qiagen (cignal reporter, cignal negative control and cignal positive control plasmids) as well as a wild-type Myc and a mutant *Myc* construct, K323/417R which cannot be methylated at lysines 323 and 417 by GCN5. The two *Myc* constructs were kind gifts of S. McMahon [Patel et al., 2004]. During transfection the cells were kept in OptiMEM media (Invitrogen) containing 5% (v/v) FCS (Sigma-Aldrich). Following transfection, the cells were recovered in complete growth media containing DMEM (Invitrogen), 10%(v/v) FCS (Sigma-Aldrich), 0.1 mM non essential amino-acids (NEAA) (PAA laboratories), 1 mM sodium pyruvate (PAA laboratories), 100 U/ml penicillium (PAA laboratories), 100 μg /ml streptomycin (PAA laboratories).

2.12 Transient transfection of Cos-7 cells for acetylation analysis

For MYC co-immunoprecipitation and acetylation assays the following constructs were cloned into eukaryotic expression vectors: estrogen receptor domain fused to a Flag-tag (ER-Flag), human MYC fused to ER and Flag-tag (MycER-Flag), and full length cDNA for *SIN3A*. The cytomegalovirus-driven expression vector containing *TIP60* was a kind gift from S. Khochbin [Legube et al., 2002], *GCN5* was kindly provided by S. Dent. Constructs were transfected using Cos-7 cells which were grown in 150 mm^2 dishes and transfected at 50% confluence with the empty vector, or *MYC*, *TIP60*, *GCN5* and *SIN3A* constructs with Lipofectamine LTX and Plus Reagent (Invitrogen) and harvested after 24 hours.

2.13 Retroviral infection of human keratinocytes

Twenty micrograms of the retroviral constructs pBabe-puro [Morgenstern and Land, 1991] and pBabeMYCER [Littlewood et al., 1995] were used transfect Phoenix E cells by calcium-phosphate precipitation as described previously [Morgenstern and Land, 1991]. Two days after transfection 2 μg/ml of puromycin (Sigma-Aldrich) were added to the normal culture media to select retrovirus pro-

ducing cells. Once stable Phoenix E transfected cells had been obtained, these were rinsed and incubated in puromycin-free medium overnight. The medium conditioned in this way was then harvested, filtered with a 40 μm filter to remove cell debris, and supplemented with 8 μg/ml of Polybrene. AM12 packaging at 60% confluency, were grown in the filtered conditioned media overnight. The following day, fresh conditioned media from Phoenix E cells was added to the infected AM12 cells and two days later 2 μg/ml of puromycin (Sigma-Aldrich) were added to normal AM12 media for selection of retrovirus-producing cell lines. Selection was perform for at least five days until AM12 puromycin resistent could be used to infect human keratinocytes. AM12 were then treated with 4 μg/ml mitomycin C (Sigma-Aldrich) for 2 hours at 37 °C to inhibit mitosis, washed twice with PBS (PAA Laboratories) and once with FAD^{++} culture medium (FAD + FCS + HICE) culture medium, and used as feeders for infection of human keratinocytes, which were seeded at normal passaging and density (4,000 cells/cm^2). After three to four days, when keratinocytes colonies were formed, puromycin selection was performed by adding 2 μg/ml of puromycin (Sigma-Aldrich) to keratinocyte's normal growth medium. Cells were then expanded in T175cm^2 flasks containing 3T3-J2-Puro feeder cells (previously mitomycin C treated), which were then removed by treatment with versene (Invitrogen) prior trypsinization and collection for ChIP-Seq experiments.

2.14 Biochemistry

2.14.1 Protein extraction from mouse skin tissue

Samples of frozen tissue were added to 1.5 ml of lysis buffer , RIPA [0.05% (w/v) SDS (Sigma-Aldrich), 0.1% (w/v) Na-deoxycholate (Sigma-Aldrich), 0.5% NP-40 (v/v) (Sigma-Aldrich) in PBS] containing tablets of complete Mini EDTA-free Protease Inhibitor Cocktail (Roche) and mixed using a homogeneizer. The cell lysate was transfered to 1.5 ml microcentrifuge tubes and incubated on ice for 30 minutes. Samples were centrifuged at 4600 rpm (Eppendorf 5424R) for 10 minutes at 4°C.The supernatant was kept, but when still cloudy, due to skin fat, it was centrifuged several times until it became completely clear. Protein sample

from the cell lysates was diluted in SDS sample buffer [40% (v/v) of glycerol, 0.8% (v/v) of SDS and 40 mM of DTT] after protein concentration was quantified using the Pierce bicinchoninic (BCA) Protein Assay Kit (Thermo Fisher Scientific), according to the manufacturer's instructions. Protein concentration was measured using a Spectrophotometer and the Softmax program for protein quantification. Samples were aliquoted and kept at -80°C with no more than two cycles of freezing and thawing.

2.14.2 Protein extraction from cell lines

Transfected cells lines or cells treated with cycloheximide (50μg/μl) (Sigma-Aldrich) were lysed in RIPA buffer, previously described, and the protein content was quantified using Pierce bicinchoninic (BCA) Protein Assay Kit (Thermo Fisher Scientific), according to the manufacturer's instructions. Samples were aliquoted and kept at -80°C with no more than two cycles of freezing and thawing.

2.14.3 Western-blotting

Cell protein lysates were homogeneized in SDS sample buffer [40% (v/v) of glycerol, 0.8% (v/v) of SDS and 40 mM of DTT], containing bromophenol blue and heated between 60-90 °C for 5 minutes before loading onto 10% BioRad pre-cast polyacrylamide gels. Gels were run in SDS Running buffer [14g Glycine, 3g Tris base, 1g SDS diluted to 100 ml of ultrapure water] at 200 V for 40 minutes, after which the proteins were transferred onto a nitrocellulose membrane (GE Healthcare) in Transfer buffer [14g glycine, 3 g of Tris-base diluted in 100 ml of ultrapure water containing 10% (v/v) methanol] for 2 hours at 4 °C. Membranes were blocked in 5% (w/v) non-fat milk in TBS-T (0.05% (v/v) Tween-20 in Tris-Buffered Saline, TBS) for 1 hour at 21-25 °C and incubated with primary antibody in blocking solution overnight at 4 °C. Primary antibodies used detected either MYC (sc-764, N-262, Santa Cruz) (1:500 dilution), TIP60 (sc-5725, N-17, Santa Cruz) (1:500 dilution), GCN5 (sc-6303, N-18, Santa Cruz) (1:500 dilution), SIN3A (sc-994, K-20, Santa Cruz) (1:500 dilution), mouse monoclonal anti-acetyllysine (Cell Signalling Technology) (1:1000) or rabbit polyclonal tubulin (T3526,

Sigma-Aldrich) (1:2000). Prior, incubation with Horseradish peroxidase (HRP)-labeled secondary antibodies (GE Healthcare) (diluted 1:5000), the membranes were washed three times with TBS. The HRP was detected using the Amersham ECL detection system (GE Healthcare).

2.14.4 Co-immunoprecipitation assays

Cells were lysed in lysis buffer consisting of PBS without Ca^{2+} and Mg^{2+} (PAA Laboratories), 0.5% (v/v) NP-40, 0.1% (w/v) sodium deoxycholate, 0.05% (w/v) SDS, and protease inhibitor tablets (Roche). Lysates were centrifuged at 13,000 rpm (Eppendorf 5424R) for 10 minutes at 4 °C and the supernatant was then added to Protein G Dynabeads (Invitrogen) which had been pre-incubated with 50 μg of rabbit polyclonal anti-c-Myc antibody (sc-764, N-262,; Santa Cruz) for 1 hour at 4 °C. Following 2 hours incubation at 4 °C, the beads were washed five times with lysis buffer and the immunoprecipitated protein was then eluted with SDS sample buffer at 70 °C. The protein supernatant was collected and ran in a polycrylamide gel as previously described.

2.15 Luciferase Reporter assay

Cells, grown in 24-well plates, were previously transfected with plasmid DNA for the protein of interest (wild-type Myc and a *Myc* mutant construct K323/417R) and from the *Cignal c-Myc Reporter* kit (cignal reporter, cignal negative control and cignal positive control plasmids), were gently washed with PBS (PAA Laboratories) to prevent detachment of the cells from the plate. The plate was frozen at -80 °C. The following day, cells lysates were obtained using a Lysis buffer solution from the Dual Luciferase Reporter Assay (Promega). Cells were treated with Renilla and Firefly containing solutions according to the manufacturer's suggested protocol. Luciferase and Renilla were measured using a microplate luminometer (Veritas).

2.16 List of suppliers and distributors

Abcam, Cambridge, UK.
Ambion, Applied Biosystems, Foster City, CA, USA.
Applied Biosystems, Foster City, CA, USA.
BD Biosciences, Franklin Lakes, NJ, USA.
BD PharMingen, San Diego, CA, USA.
Beckman Coulter Instruments, Palo Alto, CA, USA.
Bio-Rad, Hercules, CA, USA.
Cell Signaling Technology Inc, Danvers, MA, USA.
DAKO, Glostrup, Denmark.
Eppendorf, Histon, Cambridge, UK.
Enzymatics, Beverly, USA.
Falcon, part of Nunc A/S, Roskilde, Denmark.
Fisher Scientific, Loughborough, Leicestershire, UK.
GE Healthcare, Buckinghamshire, UK.
Illumina, Little Chesterford, UK.
Invitrogen, Paisley, UK.
Millipore, Harrow, Middelsex, UK.
Molecular Probes, Leiden, Netherlands.
New England BioLabs, Ispwich, UK.
PAA Laboratories GmbH, Pasching, Austria.
Peprotech EC Ltd, London, UK.
Pierce, Thermo Fisher Scientific, Waltham, MA, USA.
Promega UK Ltd, Southampton, UK.
Qiagen Ltd, Crawley, UK.
Roche, Lewes, East Sussex, UK.
Sigma-Aldrich, St. Louis, MO, USA.
Stratagene, Agilent Technologies, Santa Clara, CA, USA.
Takara Bio Inc, Shiga, Japan.
Thermo Fisher Scientific, Waltham, MA, USA.
Zymo Researh, Irvine, USA.

Chapter 3

Identification of transcriptional target genes of MYC in epidermis

Published observations have established that MYC induces a variety of biological responses within a cell. When activated specifically in epidermal stem cells, MYC has been shown to promote exit of stem cells from the niche and division of progenitors following differentiation into the IFE and SG lineages [Frye et al., 2003]. The effect of MYC activation in basal undifferentiated epidermal keratinocytes is shown by treatment of K14MycER mice with topical application of 4-OHT on the shaved dorsal skin for four days (Figure 3.1, A-C). Histological analysis of H&E stained skin sections from these mice, confirmed that MYC activation induces thickening of the IFE as well as an enlargement of the SGs, as previously shown [Frye et al., 2003]. RT-qPCR analysis confirmed that the phenotype observed was due to an increase in *Myc* expression levels upon 4-OHT treatment (Figure 3.1, A-C).

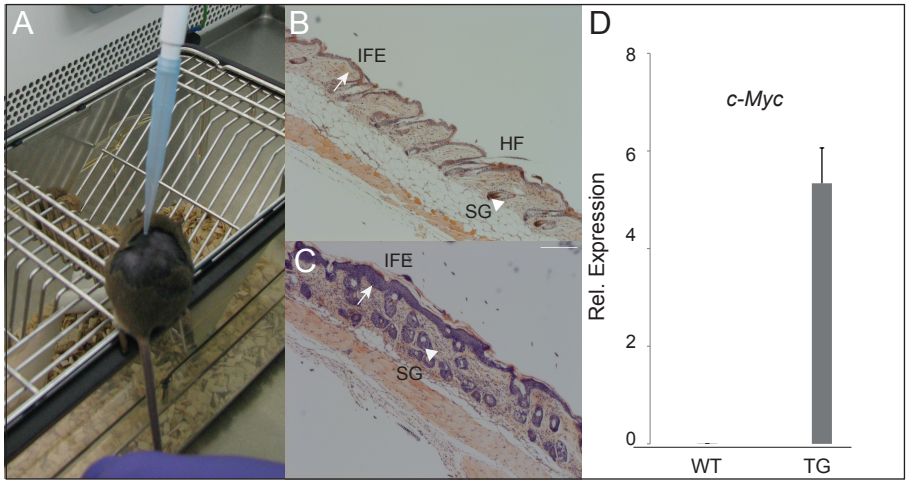

Figure 3.1: Effect of MYC activation in murine epidermis. (A) MYC was induced in basal undifferentiated keratinocytes of K14MycER (TG) mice by topical application of tamoxifen (4-OHT) for 4 days onto shaved dorsal skin resulting in hyperproliferation of the interfollicular epidermis, IFE (B,C - arrows) and enlargment of the sebaceous glands, SG (B,C - arrow heads) compared to wild-type (WT). The effects observed resulted from increased in *Myc* expression (D). HF denotes hair follicle.

3.1 Experimental design for ChIP-on-chip

To assess how MYC mechanistically regulates the genes involved in regulating epidermal stem cell fate, I established an experimental design (Figure 3.2) which included chromatin immunoprecipitation combined with promoter tiling arrays (ChIP-on-Chip), to identify MYC occupancy in activated epidermal stem cells. ChIP-on-chip experiments were combined with a time-course experiment, in which MYC activation was induced from zero to six days by 4-OHT treatment. Evaluation of the skin phenotype was performed by examination of histological skin samples stained with H&E, prior mRNA hybridization.

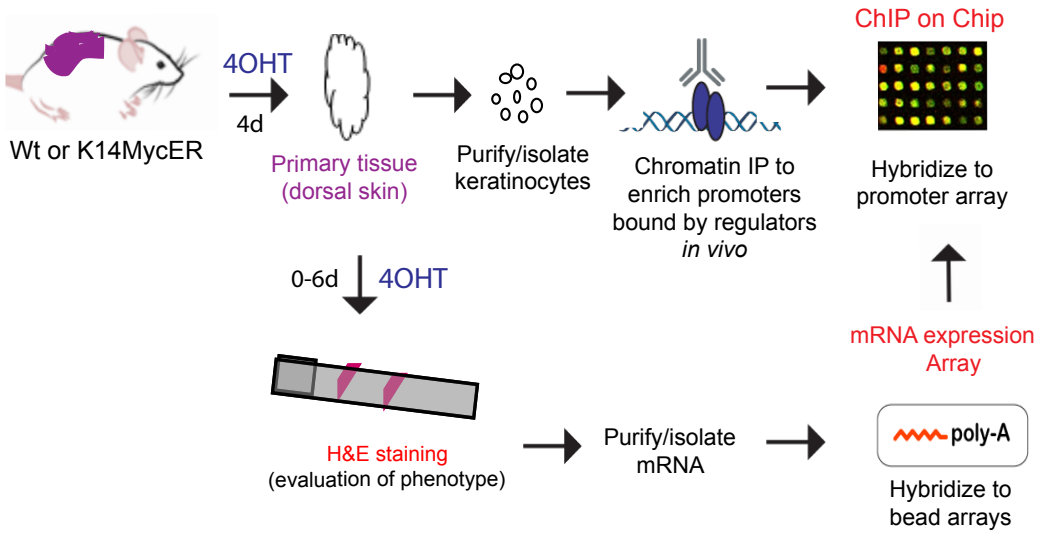

Figure 3.2: Genome-wide analysis of MYC transcriptional functions in murine epidermis. Mouse epidermal keratinocytes were isolated from dorsal skin of wild-type (WT) and K14MycER mice, following treatment with tamoxifen (4-OHT) for 4 days (4d), as previously described [Jensen et al., 2009]. Epidermal cells were fixed with 1% (v/v) formaldehyde to covalently link transcription regulators to DNA sites of interaction. Cells were harvested and chromatin in cell lysates was sheared by sonication. The regulator-DNA complexes were enriched by ChIP with specific antibodies, crosslinks were reversed, and enriched or control DNA fragments were amplified by ligation mediated polymerase chain reaction. The amplified DNA was labeled with distinct fluorophores - cyanine 3 (cy3) or 5 (cy5), combined and hybridized onto promoter microarrays (ChIP-on-Chip). In addition, mice were treated with tamoxifen in a time-course from 0 to 6 days (0-6d), the phenotype was evaluated by hematoxilin and eosin (H&E) staining and mRNA was extracted and hybridized onto bead arrays (mRNA expression Array) for gene expression analysis. ChIP-on-chip was compared to mRNA gene expression data for functional analysis.

3.2 Optimisation of ChIP parameters for genome wide studies

An important step of the ChIP-on-chip protocol is optimisation of the sonication conditions needed to shear the chromatin. Effective hybridization on probes from Agilent promoter arrays relies on genomic DNA fragments of 500 bp [Sandmann et al., 2006]. For this reason, following keratinocyte's isolation and fixation, I performed a time-course experiment, in which isolated, crosslinked keratinocytes were sonicated at different processed times to identify the optimal chromatin shearing conditions for hybridization (Figure 3.3). The sheared chromatin samples were treated with RNAse A and proteinase K (PNK) for RNA and protein degradation and the genomic DNA fragments were isolated, following reverse crosslinking at 65 °C, using phenol-chloroform extraction. Samples were run in a 2% (v/v) agarose gel. The optimal sonication processed time was found to be 12 minutes, as it yielded a smear of DNA with a peak of fragments at aproximately 500 bp. Experiments were repeated at least five times with consistent results.

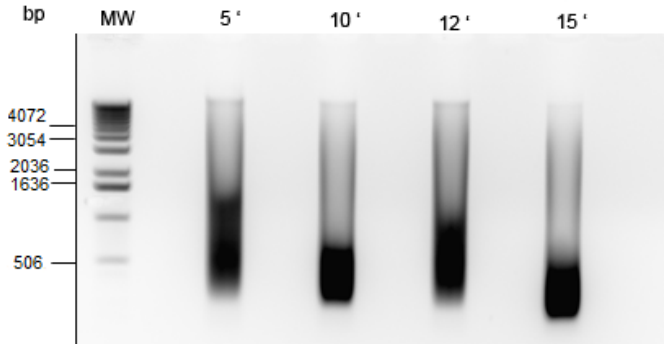

Figure 3.3: Optimization of sonication conditions for shearing genomic DNA in mouse epidermal keratinocytes. Keratinocytes were fixed with 1% (v/v) formaldehyde and crosslinked chromatin was sheared by sonication for 5, 10, 12 and 15 minutes using cycles of 30 seconds followed by 1 minute intervals. To verify the average sequence length, within different batches of sheared chromatin, 50 μl of chromatin were treated with RNAse A and proteinase K and the covalent crosslinks partially reversed at 65 °C. DNA was purified by phenol-chlorophorm extraction and ethanol precipitation and ran on this 2% (w/v) agarose gel by eletrophoresis. The size of genomic DNA fragments decreased during the time-course. The optimal fragment size was observed at 12 min where there is a peak around 500 base pairs (bp). MW stands for the 1 Kb (Kilobase) molecular DNA marker.

Enrichment of genomic DNA fragments bound by MYC was evaluated by PCR amplification of the murine *Ncl* promoter. Comparison of the intensity of the 344 bp band obtained for the immunoprecipitate (IP) and whole cell extract (wce) samples revealed an increase of at least two fold in genomic DNA fragments bound by MYC in K14MycER mice, when compared to wild-type littermates. Enrichment for trimethylation of histone H3 at lysine 4 (H3K4me3) was observed in both mouse strains (Figure 3.4).

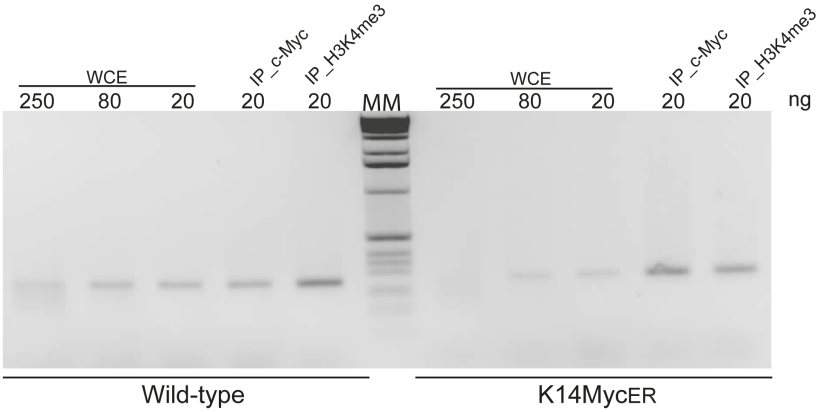

Figure 3.4: Chromatin immunoprecipitation (ChIP) experiments show interaction of MYC and H3K4me3 at the *Ncl* promoter. PCR analysis of genomic DNA from ChIP performed with MYC (IP c-Myc) and H3K4met3 (IP - H3K4me3) specific antibodies and lysates of crosslinked keratinocytes (wce), isolated from wild-type and K14MycER mice. A primer set specific to the *Ncl* promoter was used. Samples of 20 ng of immunoprecipitated DNA (IP) or whole cell extracts (wce)s /input DNA in a dilution series from 250, 80 to 20 ng were used. The higher intensity for the 344 bp amplified band was observed in the IP samples (compared to wce control) and demonstrate enrichment in DNA fragments containing MYC and H3K4me3 solely observed for K14MycER samples. Wild-type samples only show enrichment for H3K4me3 at the. MM stands for molecular DNA marker.

Subsequent experiments for enrichment of genomic DNA for validation of MYC target genes were performed by ChIP-qPCR as presented later in this chapter.

3.3 Genome-wide location of MYC in epidermis

Once MYC enrichment was confirmed by gene specific PCR, ChIP-on-chip experiments were performed against MYC and H3K4me3 on mouse proximal promoter arrays. The histone mark H3K4me3 was used as a positive control, as it is known to bind to enriched in regions close to the TSS of genes [Hampsey and Reinberg, 2003]. I used Agilent mouse proximal promoter arrays, that cover 17000 known transcripts, with promoter sequences located 5.5 Kb upstream or 2.5 Kb downstream the TSS (NCBI35/mm7). Preliminary analysis of the ChIP-on-chip data using the feature extraction software from Agilent identified thousands of MYC binding sites in K14MycER isolated keratinocytes (Figure 3.5, B) when compared to wild-type (Figure 3.5, A). Scatterplots represent the signal intensity between IP (rBGSubsignal) and wce (gBGSubsignal) and show greater enrichment for MYC in K14MycER mice, with more than 50% of the probes being bound.

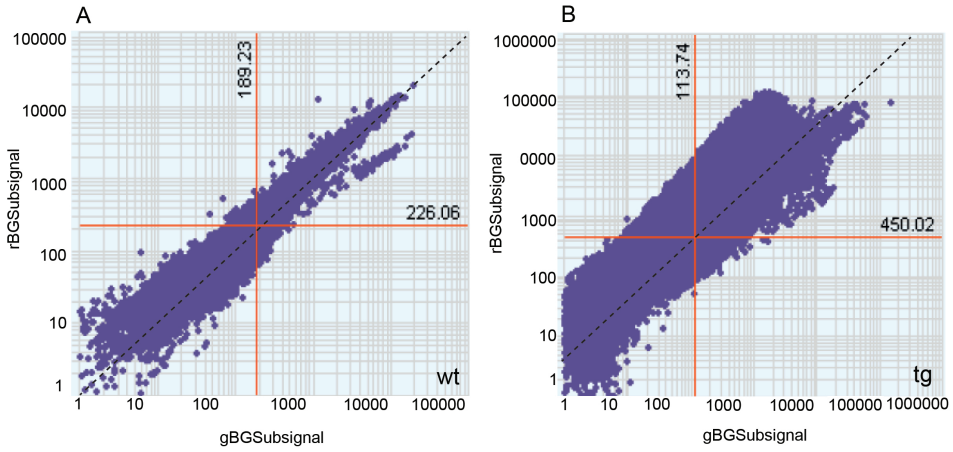

Figure 3.5: ChIP-on-chip analysis shows enrichment for MYC in K14MycER mice. ChIP data from wild-type, wt (A) and K14MycER, tg (B) mouse keratinocytes was obtained using Agilent promoter arrays and analyzed with the Agilent Feature extraction software (v10.5). Scatterplots represent background normalized signal level intensities for the immunoprecipitate (IP) sample (rBGSubsignal) relative to whole cell lysate (wce) control (gBGSubsignal) for all genes 17000 transcripts (features) spotted on the arrays. Each feature on the array is represented by a purple dot in the scatter plot. Scatterplots show greater enrichment for MYC in K14MycER mice, compared to wild-type. Signal intensities are shown in a log10 scale; rBG = red background (cyanine 3), gRG = gBGSubsignal (cyanine 5).

Following data analysis, 47 genes were identified as bound by MYC in wild-type epidermal keratinocytes (Figure 3.6, A) compared to 7174 genes in K14MycER mice (Figure 3.6, B). This result demonstrated that the endogenous expression levels of *Myc* in the wild-type cells were noticeably low to enable identification of its target genes (Figure 3.1, D). Both mouse strains were strongly enriched for H3K4me3, overlapping in more than 8000 sites, (i.e. more than 80% of enriched sites) (Figure 3.6, C), demonstrating that H3K4me3 enrichment was unchanged upon *Myc* overexpression. MYC binding strongly correlated with H3K4me3 in more than 90% of the sites, confirming previous reports [Guccione et al., 2006].

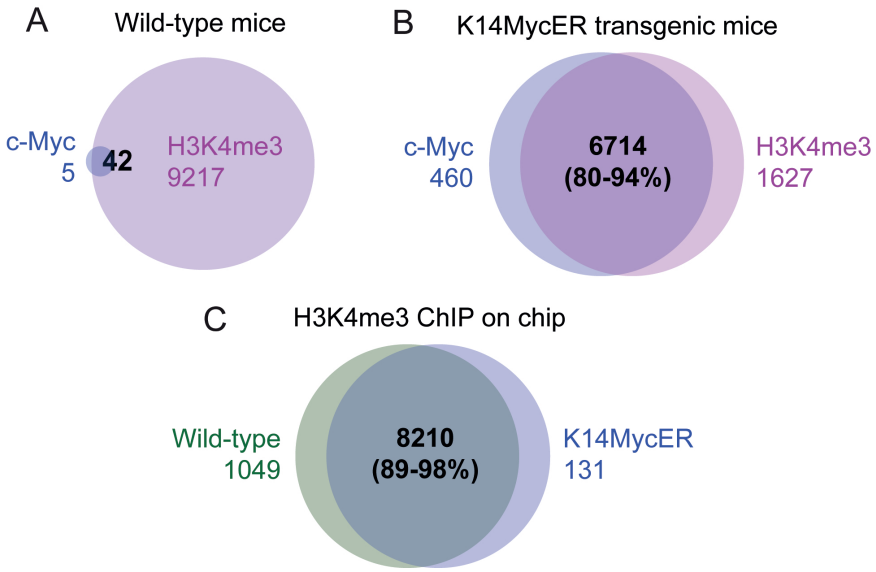

Figure 3.6: H3K4me3 correlates with MYC-binding and is unchanged in response *Myc* overexpression. Venn diagrams for occurrence of H3K4me3 and MYC in wild-type (A) and K14MycER transgenic mice (B). Occurrence of H3K4me3 highly overlaps in wild-type and K14MycER mice (89-98%, C). Data was obtained from proximal promoter ChIP-on-chip assays using keratinocytes isolated from wild-type and K14MycER treated for 4 days with tamoxifen (4-OHT).

3.3.1 Genomic distribution of MYC binding events

MYC binding in close proximity to the TSS was observed for 40-60% of the sites (Figure 3.7). However, MYC occupancy was widespread and also associated with a significant number of regions 0.8 Kb upstream the TSS in wild-type keratinocytes. In addition, at least 10% of the genes located 0.2 Kb downstream the TSS were also shown to be bound by MYC and enriched for H3K4me3 in the wild-type. In K14MycER mouse keratinocytes, the distribution of H3K4me3 enriched sites correlated with MYC binding almost at 100%. Furthermore, since proximal promoter arrays were used, it was not possible to assess whether MYC was also located at introns or intergenic regions; potential non-coding RNA targets [Chang et al., 2008]. The discrepancy in the distribution of binding events in wild-type compared to K14MycER mice is likely to be due to the low number of binding events detected in wild-type epidermal cells using this method.

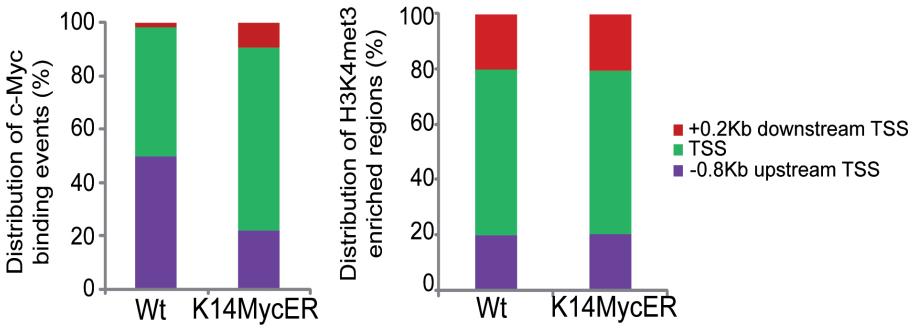

Figure 3.7: MYC preferentially binds to the transcription start site (TSS). The distribution of MYC and H3K4me3 location across the mouse genome, in particular in K14MycER mice, shows that 60% of the bound regions are located at the transcription start site (TSS), with the remaining 40% of genes bound being located either 0.2 kilobases (Kb) upstream or 0.8 Kb dowstream. In wild-type mice, 50% of the genes bound by MYC were also located upstream the TSS. In general, there is a high correlation fo MYC binding with H3K4me3 in K14MycER mice, that is not observed in wild-type mice.

Examples of MYC and H3K4me3 enriched regions in epidermal cells from wild-type and K14MycER mice are provided in Figure 3.8. As previously mentioned, H3K4me3 is highly enriched in both mouse strains but stronger MYC

binding is only observed in K14MycER mice. I found MYC was bound to the promoter region of *Ncl* and Polycomb genes *Ezh2* and *Suz12*, as previously reported [Goodliffe et al., 2005; Greasley et al., 2000]. In addition, MYC was identified in the promoter region of genes encoding cornified structural proteins, such as S100A1 and S100A11. The interaction of MYC with epidermal differentiation related genes has not been reported and it is particularly interesting as it might indicate a role for MYC controlling epidermal differentiation. Finally, MYC was also shown to bind to the promoter of *Hdac2*, a gene encoding for a protein involved in transcriptional repression through deacetylation of the histones [Nagy et al., 1997].

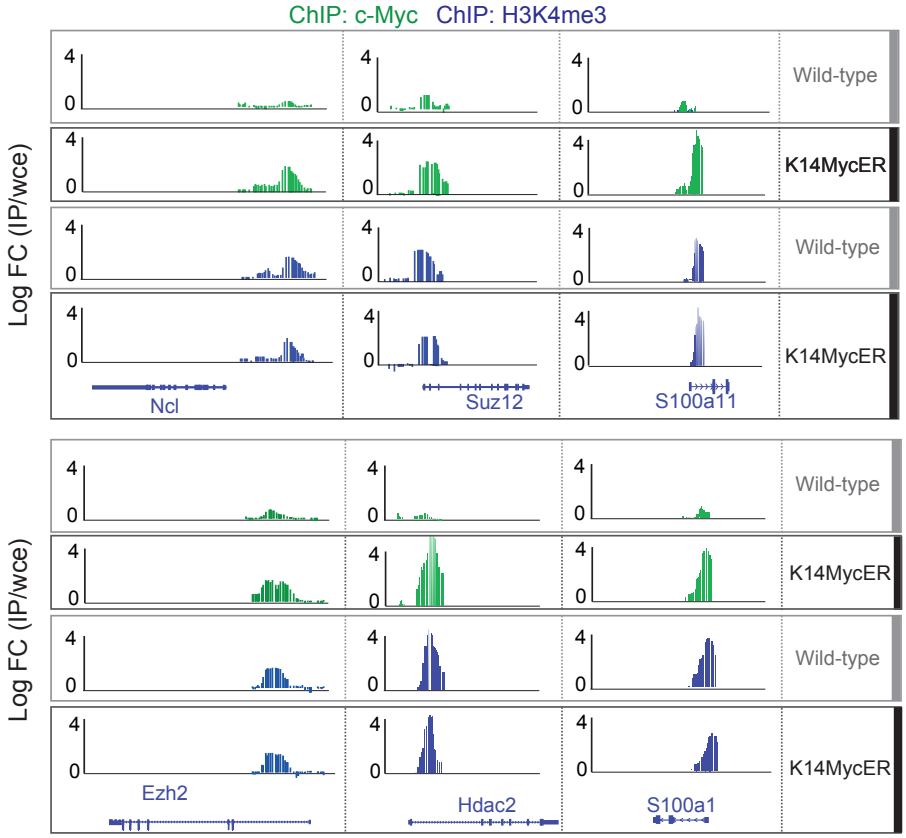

Figure 3.8: Examples of genes bound by MYC. All genes (*Ncl*, *Suz12*, *S100a11*, *Ezh2*, *Hdac2* and *S100a1*) show higher MYC (green peaks) binding in K14MycER mice compared to endogenous *Myc* levels in wild-type. However, promoter regions in both strains show the same levels of H3K4me3 (blue peaks). Enrichment was calculated by the Log2 fold ratios (Log FC) of the signal intensities obtained for immunoprecipitated fractions (IP) relative to whole cell lysate (wce) controls.

Confirmation of the interaction of MYC with the promoter regions of some of the genes shown was confirmed by ChIP semi-quantitative PCR (ChIP-qPCR) (Figure 3.9). As expected, enrichment for MYC binding was mainly observed in K14MycER mice (grey bars), with more than 25 fold increase of MYC levels at the promoter of *Ncl* and *Suz12*, when compared to wild-type (white bars). In addition, binding of MYC to the promoter of *Ezh2*, *Id2*, *Sprr1a*, *S100a1* and *Hdac2* was also confirmed.

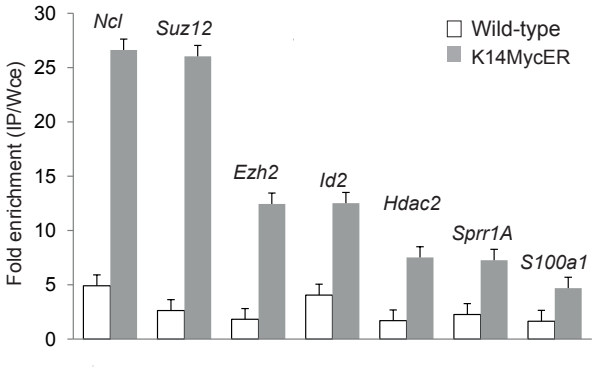

Figure 3.9: MYC binds to a diverse set of promoters in K14MycER mice. Chromatin immunoprecipitation semi-quantitative PCR (ChIP-qPCR) was performed to confirm the interaction of MYC with the promoter regions of the genes shown in wild-type (white bars) and K14MycER (grey bars) mice. c-Myc enrichment was confirmed in K14MycER mice for all genes shown. Data represents the mean values for two biological replicates (n = 2) and bars the standard deviation of the mean.

3.3.2 Identification of functional MYC target genes

To assess whether MYC binding induced changes at the transcriptional level, I performed RT-qPCR in a selected number of genes previously shown to be bound by MYC (*Ncl*, *Suz12*, *Sprr1a*, *Ezh2*, *Id2*, *S100a11* and *Hdac2*). In K14MycER mice, MYC binding correlated with a two to three fold increase in the expression levels of its target genes at day 4 of 4-OHT treatment (MYC activation). More importantly, MYC mediated upregulation was already observed after 1 day of MYC activation (Figure 3.10) for more than half of the genes.

MYC is known to bind to 15% of all active genes in the genome of a cell [Rahl et al., 2010]. For this reason, it became essential to identify which binding events, from the approximately 7000 genes targeted by MYC in the K14MycER mice, produced effects at the transcriptional level. To identify functional MYC binding sites, I performed a time-course experiment where I treated wild-type and K14MycER mice from zero to six days with 4-OHT. The phenotype of the mice was evaluated by H&E stainings of skin samples and mRNA samples were also collected for gene expression analysis. As expected, MYC activation resulted in

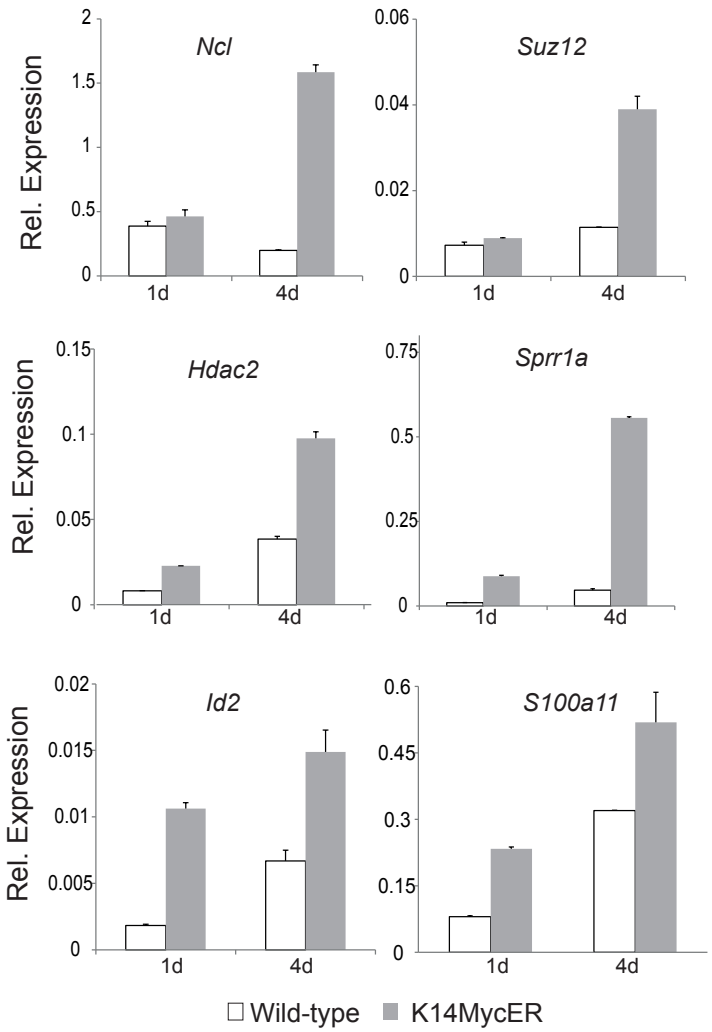

Figure 3.10: mRNA expression data for putative MYC target genes. mRNA expression profiles of selected MYC bound genes shows increased expression (aproximately 2-3 fold) upon c-Myc activation after 4 day (4d) tamoxifen treatment in K14MycER mice (grey bars) when compared to wild-type (white bars). mRNA expression values were measured relative to *Gapdh*. Data represents the mean values for three biological replicates (n = 3) and bars the standard deviation of the mean.

thickening of the IFE, a phenotype that progressively increased with the number of days of 4-OHT treatment (Figure 3.11).

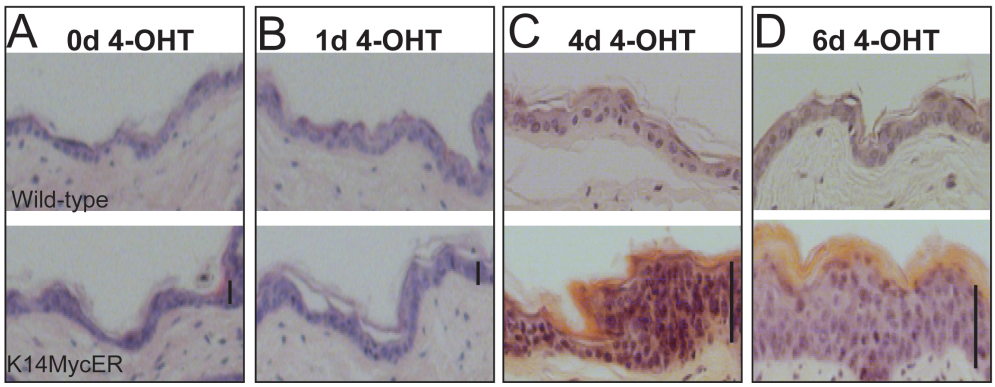

Figure 3.11: Morphological changes in the epidermis upon MYC activation. Tamoxifen (4-OHT) treated epidermis of wild-type and K14MycER mice over 6 days. K14MycER mice show progressive thickening of the epidermis, an effect that was not observed in wild-type littermates. Mouse dorsal skin was treated for 0, 1, 4 and 6 days (d) with 4-OHT (A-D).

To identify which set of genes were responsible for the epidermal phenotype observed upon MYC activation, I performed gene expression microarrays using skin samples treated with 4-OHT at the different time-points. Hierarchical clustering of the gene expression data shows that the most variable changes in expression occurred between treated K14MycER mice and wild-type/untreated K14MycER mice (Figure 3.12).

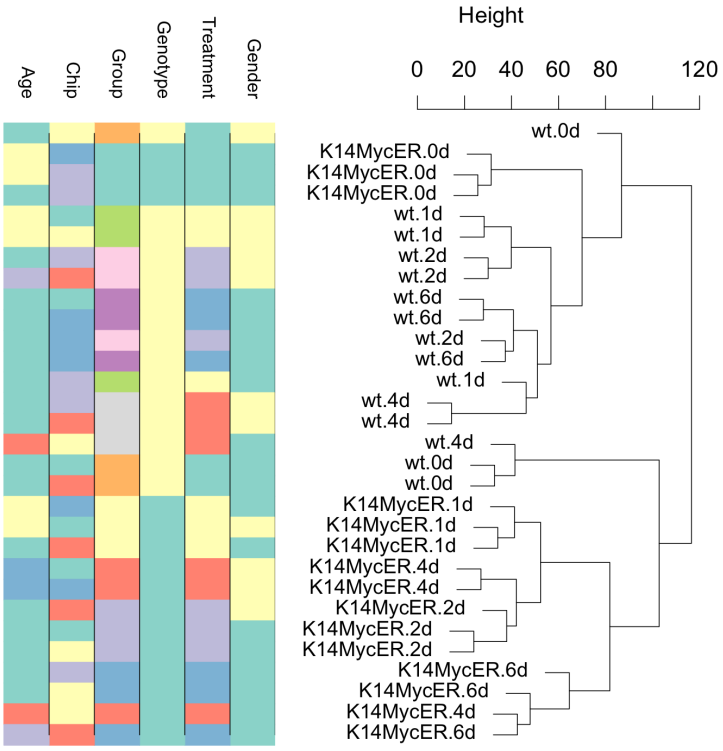

Figure 3.12: MYC activation in epidermal keratinocytes triggers a specific gene expression profile. Hierarchical clustering of gene expression data shows wild-type (WT) and K14MycER tamoxifen treated skin samples as two independent groups. Within each group, additional clusters based on the duration of tamoxifen (4-OHT) treatment were also generated (0d,1d,2d,4d,6d corresponds to days of treatment). Untreated K14MycER, with no MYC activation, clustered with wild-type littermates. Clustering was not affected by gender, age or array platform, but it was dependent on genotype and duration of treatment.

In addition, the clustering analysis grouped samples which had been treated with 4-OHT for the same amount of time. Exceptions were observed for three wild-type skin samples treated with 4-OHT for zero and four days, as these samples clustered with K14MycER 4-OHT treated mice. In addition, a sample of K14MycER treated for four days clustered with six days 4-OHT treated samples of the same strain, probably due to a severe phenotype. Factors such as age, array platform (ChIP) and gender did not affect the clustering outcome, however, the growth phase of the HF cycle appeared to determine patterns of expression in the epidermis. Histological analysis of H&E sections of dorsal epidermis from

the outliers, revealed that these wild-type samples were obtained from mice in which the HFs had entered the early anagen growth phase (*data not shown*) and were not in telogen (resting phase of the HF), as all the other samples used in the experiment. Increased *Myc* expression during anagen, possibly due to proliferation of the HF matrix cells, might have contributed to a gene expression pattern closely resembling the one observed for K14MycER mice. These results strengthen the idea that all samples analyzed, in order to be comparable, must be collected at the same phase of the HF cycle. All the subsequent data generation and analysis performed was based on skin samples collected at the telogen phase of the HF cycle. Gene expression data from skin samples of K14MycER mice treated for four days with 4-OHT was compared with previous generated ChIP-on-chip data for MYC binding in the mouse genome. I identified 2187 putative MYC target genes in epidermis which corresponded to 30% of the differentially expressed genes observed upon MYC activation (Figure 3.13).

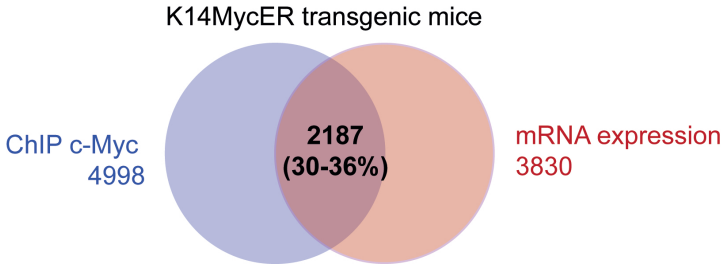

Figure 3.13: MYC binds and trancriptionally regulates thousands of genes in keratinocytes. The Venn diagram depicts an overlap between MYC bound genes in K14MycER mice treated for four days with tamoxifen (4-OHT) and the resulting gene expression changes. Upon MYC induction, 2187 genes (30% binding events) were shown to be bound and regulated by MYC.

3.3.3 KEGG and Gene Ontology (GO) analysis

Functional analysis using bioinformatic tools on MYC target genes in epidermis shows that MYC is involved in a diverse set of biological pathways such as: MAPK, WNT, TGFβ, TP53, SHH and NOTCH signaling, as well as apoptosis, cell cycle, ribosome biogenesis and DNA replication (Figure 3.14).

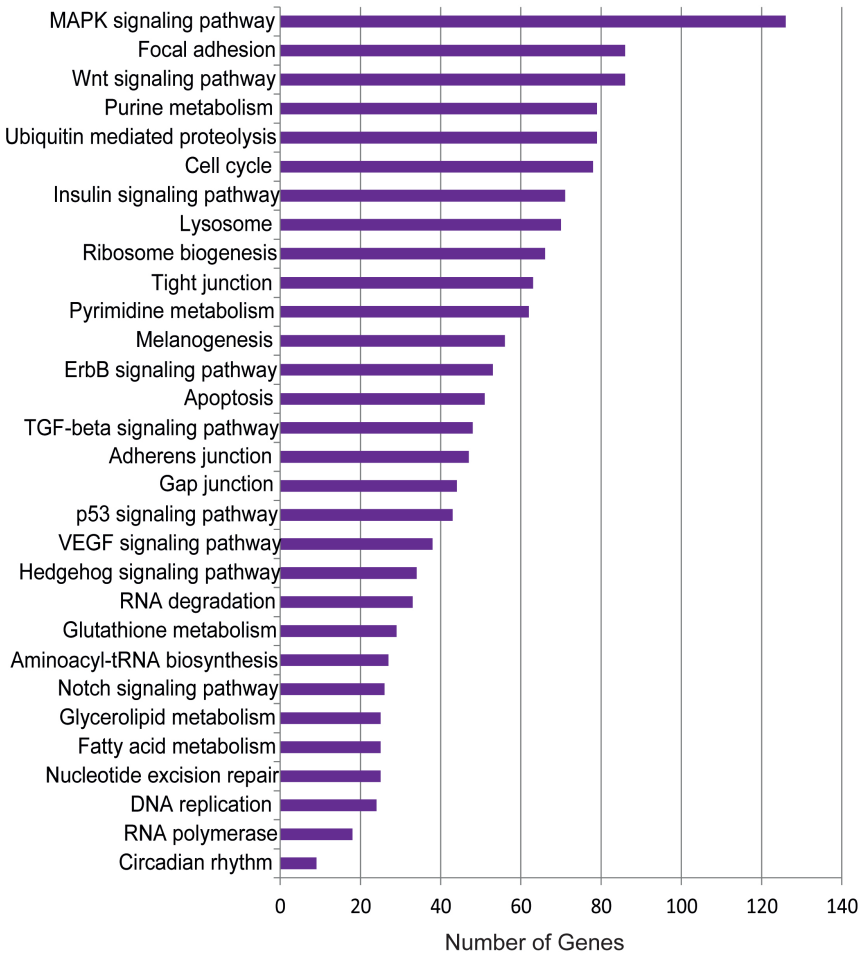

Figure 3.14: KEGG pathway analysis of putative MYC target genes. The number of genes for each KEGG category is depicted in the y-axis and a P-value <0.05 was used. Data was obtained using the David Functional Annotation Bioinformatic Microarray Analysis tool available online (http://david.abcc.ncifcrf.gov/). Only selected KEGG pathways are shown.

These results confirm the notion that MYC regulates genes involved in a plethora of biological functions as it has been suggested by several groups [Dang et al., 2006; Eilers and Eisenman, 2008; Zeller et al., 2003].

Gene ontology (GO) analysis on putative MYC target genes revealed as over-represented gene categories metabolism, protein translation, morphogenesis, cell cycle, chromatin modification and DNA damage, amongst others (Figure 3.15, A red bars). The categories for biological functions were diverse and have all been documented [Dang et al., 2006; Eilers and Eisenman, 2008; Zeller et al., 2003]. It is worth mentioning some of the genes that appear in the over-represented categories, such as *Polr2a*. Recently, MYC has been involved in the release of the pause of DNA polymerase II [Rahl et al., 2010], facilitating transcriptional elongation, therefore it is not surprising that MYC might modulate *Polr2a* expression. Also worth mentioning is the fact that MYC regulates several genes involved in chromatin remodeling such as *Ruvbl1*, *Cbx3*, *Hdac2*, *Eed*, *Dnmt3b*, *Suz12*, *Mbd3* and *Ezh2*, confirming the role of MYC in regulation of global chromatin structure [Knoepfler et al., 2006]. MYC also targets genes encoding for important regulators of the epidermal differentiation program such as OVOL1 and KLF4 [Segre et al., 1999; Teng et al., 2007]. This data also confirms MYC regulation of the gene encoding for RNA methyltransferase NSun2, *Nsun2*, which has been shown to mediate MYC-induced proliferation [Frye and Watt, 2006]. Finally, I also analyzed genes located in under-represented GO categories (Figure 3.15, B green bars) and found that most of these were related with signal transduction through G-coupled receptors as well as ECM. Several of these genes have been described as potential targets for MYC repression [Frye et al., 2003]. This group also represented the stem cell marker, *Lrig1*, which was shown to be regulated by MYC [Jensen et al., 2009].

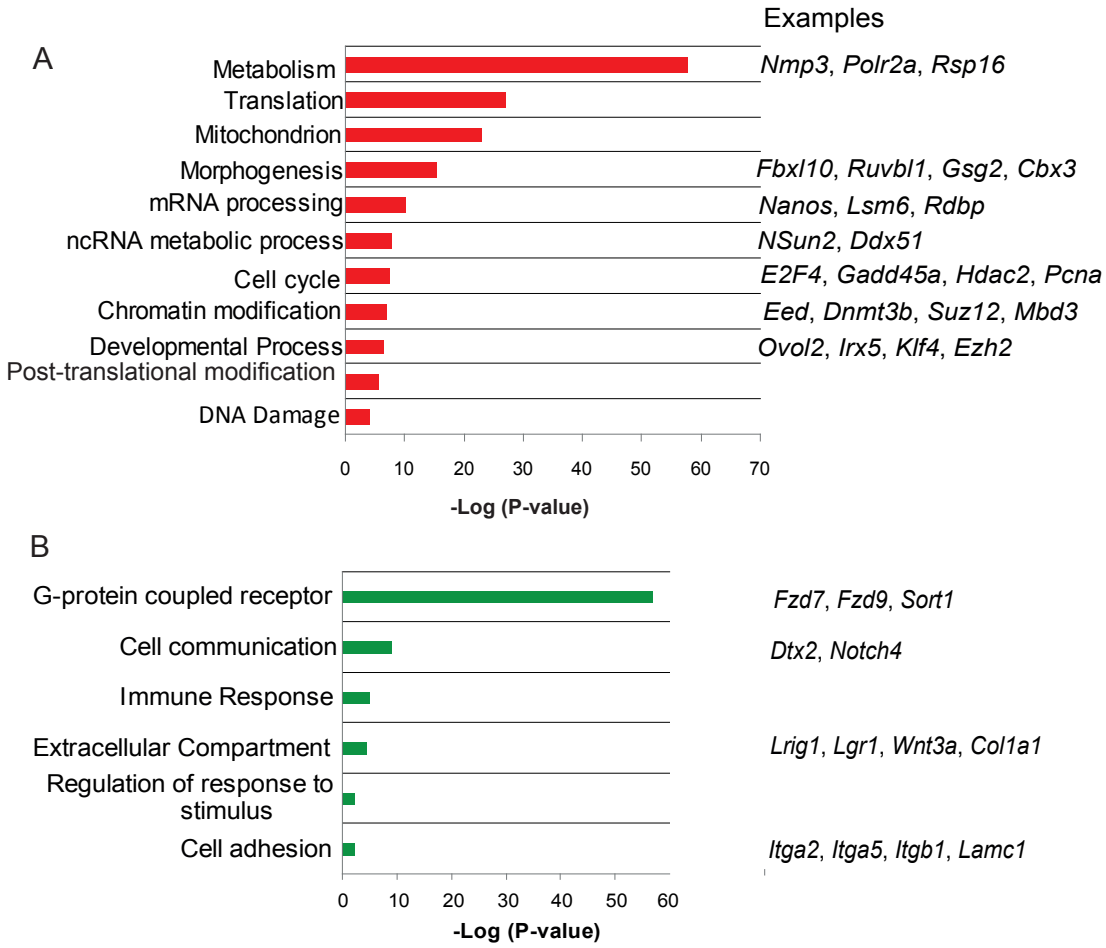

Figure 3.15: Functional categories of putative MYC target genes. Gene ontology (GO) categories were obtained using the bioinformatic tool GeneTrail (http://genetrail.bioinf.uni-sb.de/). Over-represented groups are listed on the top panel (A, red bars) and under-represented categories at the bottom panel (B, green bars). Examples of genes in each of the categories can be found on the right side of each graph. Only selected GO categories are shown.

3.3.4 Motif analysis

In order to understand if the phenotypic changes observed in the epidermis upon MYC activation relied solely on MYC induction or were achieved in cooperation with other TFs, I performed motif analysis on the list of 2187 MYC target genes shown in (Figure 3.13). I used the bioinformatic tool *Pscan* to scans through the set of sequences where MYC was bound to assess which TF motifs were significantly over- or under-represented [Zambelli et al., 2009]. MYC-bound and regulated genes revealed enrichment in consensus binding motifs for KLF4, TCFAP2, E2F1, SP1 and MYC. All these TFs's promoters were bound (Figure 3.16) and regulated by MYC, which is known to negatively regulate its own expression [Penn et al., 1990].

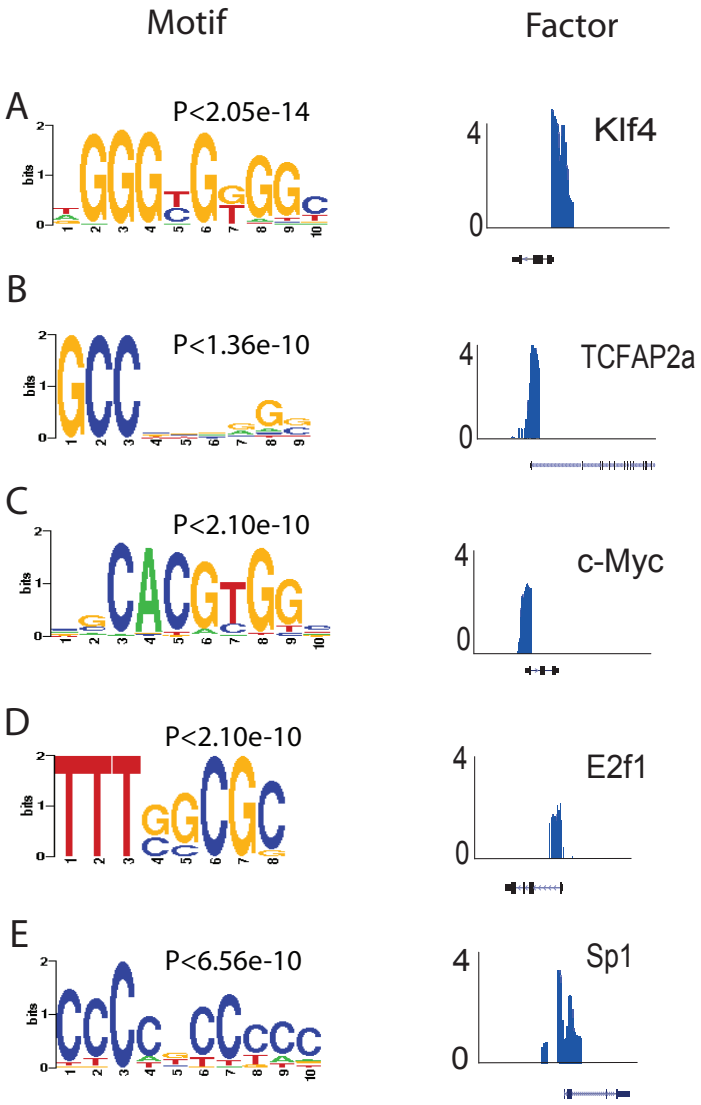

Figure 3.16: MYC putative cooperation with other transcription factors. Motif analysis using the bioinformatic tool Pscan (http://159.149.109.9/pscan/) shows that MYC binding regions are enriched in consensus motifs for KLF4, TCFAP2, MYC, E2F1 and SP1 (A-E). In addition, MYC binds to the promoter region of the genes encoding for these transcription factors, in K14MycER mice, as seen on the right hand side of the panel. Enchiment values depicted from 0 to 4 represent the log2 FC of the MYC enriched DNA fractions relative to background.

3.4 Summary

Genome-wide location of MYC by ChIP-on-chip was successfully performed in epidermal keratinocytes isolated from K14MycER mice following activation of MYC by tamoxifen treatment. MYC was shown to bind and regulate an unusually large and diverse set of biological functions, such as cell cycle (e.g *E2f4* and *Pcna*), metabolism (e.g *Nmp3* and *Rsp16*), mRNA processing (e.g *Nanos*, *Lsm6* and *Rdbp*) and chromatin remodelers (e.g *Eed*, *Suz12* and *Mbd3*). It has been postulated that activation of MYC in the epidermal basal layer, induces exit of the stem cells from the niche through downregulation of genes involved in adhesion, amplification of the progenitor's pool and subsequent lineage specific differentiation [Frye et al., 2003]. My data supports this hypothesis and shows that MYC directly binds to the promoter region of these genes (e.g *Itga2*, *Itga5*, *Itgb1* and *Lamc1*) and affects their expression. Proliferation of the epidermal progenitors can be explained by the fact that MYC regulates cell cycle related genes, while increased differentiation might be attributed to the fact that MYC also binds and induces upregulation of epidermal differentiation genes such as *S100a1*, *Sprr1a* and *S100a11* and regulators (e.g *Ovol2*, *Klf4* and *Ezh2*), as seen in (Figures 3.9, 3.10 and 3.15). MYC was also found to preferentially bind to promoter regions carrying the histone mark H3K4me3, usually associated with transcriptionally active genes. In addition, MYC induction does not affect the distribution of H3K4me3 at the genome, as roughly the same number and location of sites enriched in this histone mark are found in wild-type and K14MycER mice. This observation, combined with the fact that MYC target genes are also enriched for consensus motifs for binding of known epidermal differentiation regulators, TCFAP2, KLF4 and E2F1(Figure 3.16), led to the assumption that MYC might contribute to the activation not only of genes involved in growth, proliferation and metabolism, but also genes determining lineage fate. Due to the fact that very low peak resolution for MYC binding was observed in wild-type epidermal cells, the majority of the analysis presented, as well as subsequent experiments, were focused on the data obtained using the K14MycER mice.

Chapter 4

MYC determines tissue-specific transcriptional networks

4.1 MYC transcriptional regulation at the EDC

As outlined in chapter 3, I found that MYC was bound to promoters of genes involved in differentiation (*S100a1*, *S100a11* and *Sprr1a*) and thought MYC might be directly involved in the regulation of epidermal differentiation genes. The epidermis is an excelent model to study the effect of MYC in lineage determination, firstly because MYC activation induces a terminal differentiation program in the IFE, and secondly because several of the genes encoding for proteins involved in the differentiation process (cornification), are clustered in a region of the mouse genome designated as epidermal differentiation complex (EDC) (Figure 4.1, A). As previously mentioned, this region constitutes a 2.2 Mb (mega base) locus located on mouse chromosome 3 and encodes 61 genes known to be important for epidermal maturation.

4.1.1 MYC associates with promoters of EDC genes

To assess whether MYC might be involved in the direct regulation of keratinocyte's differentiation I performed ChIP-on-chip where again, I used basal undifferentiated keratinocytes isolated from the dorsal skin of K14MycER mice treated for four days with 4-OHT and focused the ChIP-on-chip analysis on the EDC region.

MYC binding profile at the EDC revealed occupancy over more than 80% of the gene promoters (Figure 4.1, B blue peaks). The majority of binding sites overlapped with H3K4me3, similarly to what had been observed when using mouse genome-wide proximal promoter arrays (Figure 4.1, purple peaks). MYC binding generaly excluded H3K27me3, a histone mark usually associated with silencing (exceptions included *Lor* and *Tchh* promoters) (Figure 4.1, B green peaks).

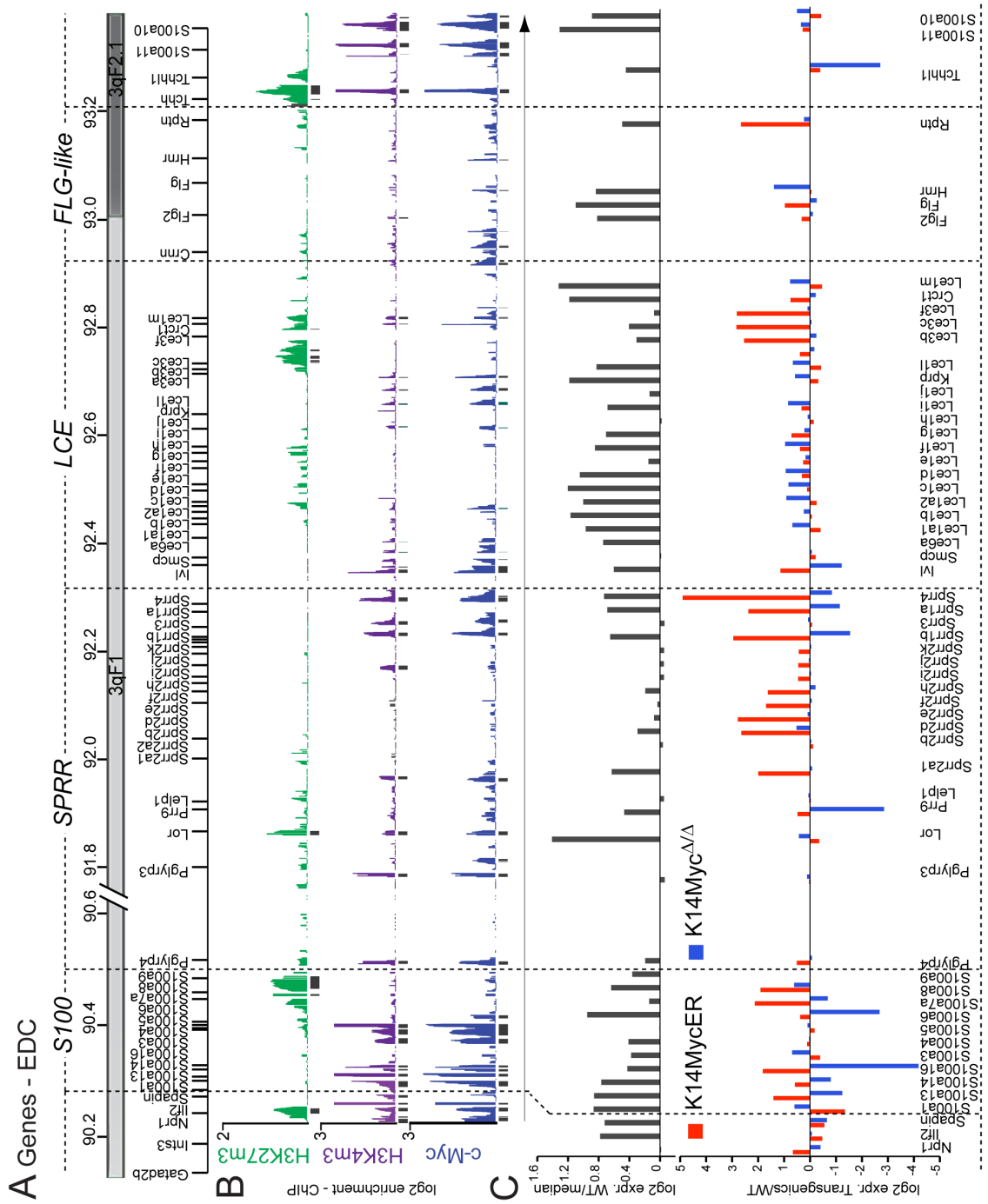

Figure 4.1: MYC binds and regulates epidermal differentiation genes. (A) Genomic organization of the mouse EDC; (B) schematic overview of H3K27me3 (green), H3K4me3 (purple) and c-Myc (blue) binding to EDC genes; mRNA expression levels of EDC genes in wild-type epidermis (C, upper panel, grey bars); fold change of EDC gene expression in K14MycER (C, lower panel, red bars) and K14Myc$^{\Delta/\Delta}$ epidermis (C, lower panel, blue bars) normalized to wild-type. Data was extracted from mRNA expression arrays where a minimum of three biological replicates (n=3) was used. ChIP-on-chip data is presented as a log2 fold change in signal between MYC or histone marks (H3K27me3 or H3K4me3) enriched genomic DNA fragments and the background.

To evaluate if MYC binding at the EDC resulted in a direct regulation of these genes at the transcriptional level, I compared MYC binding to the previous obtained mRNA gene expression data for wild-type and K14MycER treated for four days with 4-OHT. In wild-type epidermis, more than 80% of the genes at the EDC were expressed above background level (Figure 4.1, C upper panel grey bars). Activation of MYC resulted in a two to four fold increase in mRNA gene expression for 17 out of the 55 EDC genes (Figure 4.1, C lower panel blue bars). Importantly, 12 EDC genes were downregulated, with a significant mRNA decrease for only for *S100a1*. To further confirm MYC induced upregulation of EDC genes, I performed RT-qPCR using mRNA samples isolated from 4-OHT treated dorsal skin of wild-type and K14MycER mice (Figure 4.2). For this purpose, I selected a group of genes representing the EDC protein families S100A (purple bars) and LCE (pink bars): *S100* (*S100a1*, *S100a16* and *S100a11*) and *Lce* (*Lce1e*, *Lce1g*, *Lce3f*). The *Sprr* family had already been represented by confirmation of upregulation of *Sprr1a* upon MYC induction (Figure 3.10).

Activation of MYC induced upregulation of all genes analyzed compared to wild-type, except for *S100a1* which was downregulated, confirming the mRNA global gene expression data obtained.

4.1.2 MYC directly regulates epidermal and keratin related genes

I performed mRNA gene expression arrays for K14Myc$^{\Delta/\Delta}$ mice and compared the results obtained for MYC ChIP-on-Chip at the EDC. I found that conditional deletion of *Myc* in the epidermis resulted in repression of at least 11 EDC genes (e.g *S100a13*, *S100a14*, *S100a16*, *S100a6*, *S100a7*, *Prr9*, *Sprr1a*, *Sprr1b*, *Sprr4*, *Ivl*, and *Tchhl1*) (Figure 4.1, C lower panel blue bars). This effect on the expression level of EDC genes, suggests a direct role for MYC regulating epidermal differentiation. Functional analysis on global mRNA expression data obtained from *Myc* depleted epidermal samples shows that 48% of all genes repressed upon *Myc* deletion were either epidermal or keratin associated (see Appendix) (Figure 4.3, A-C).

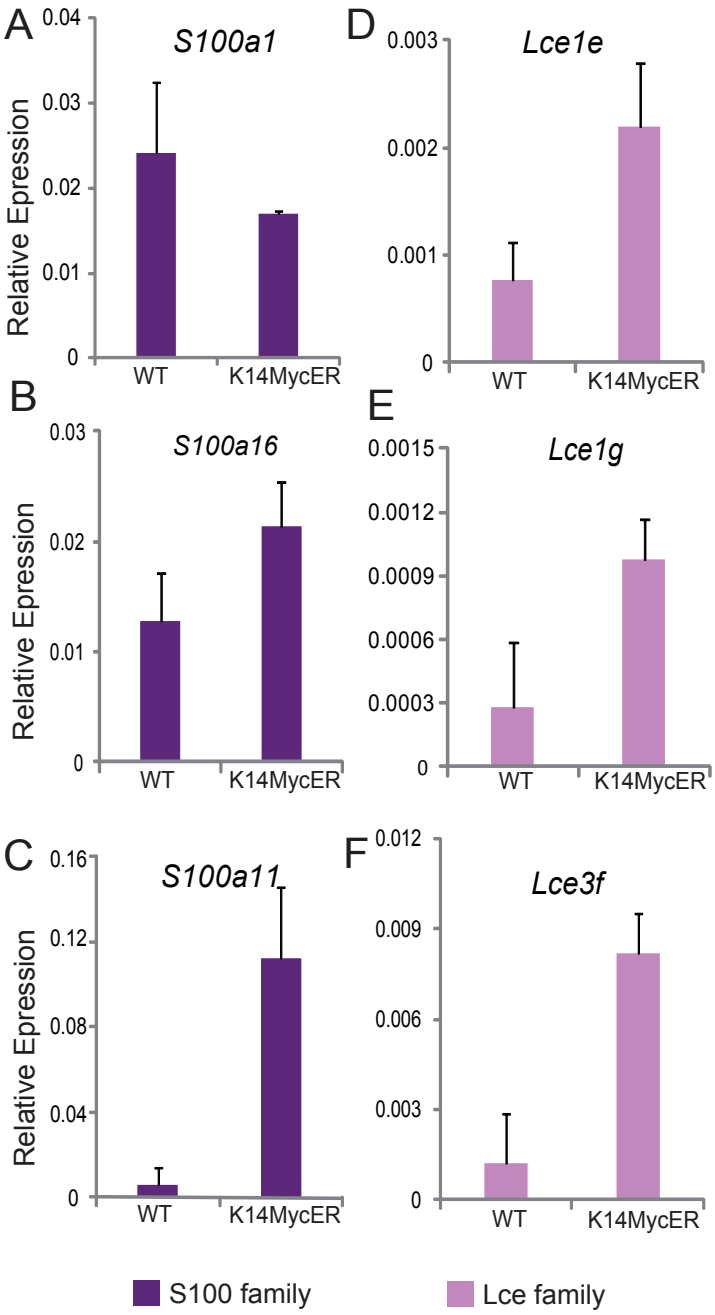

Figure 4.2: MYC regulates *S100* and *Lce* genes. Gene expression for *S100a* (purple bars) and *Lce* (pink bars) family genes shows that MYC induction in K14MycER mice results in upregulation of these genes when compared to wild-type, WT (except for *S100a1*). mRNA levels were calculated relative to *Gapdh* and represent mean values for three biological replicates (n = 3). Bars represent the standard deviation of the mean.

A

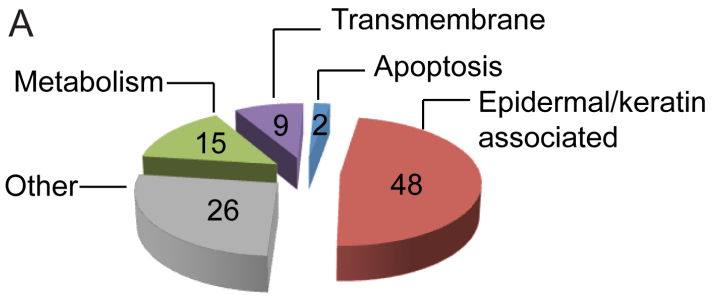

B

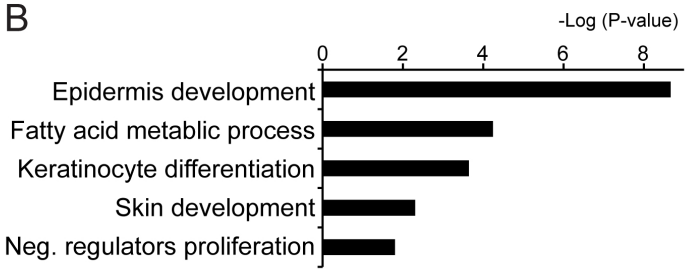

C

Epidermis:	*Fatty acid :*	*Kerat. diff:*	*Skin dev.:*	*Neg. prolif.:*
KRTAP16-7,	ACSM3,	SPRR1A,	TGM3,	MSX2,
SFN,	ACAA2,	SPRR1B,	KRTAP16-7,	WNT5A,
SHH,	TYRP1,	CNFN,	SFN,	GPC3,
FOXQ1,	ACOT7,	TGM3,	SHH	MSX1,
KRT27,	PTGDS,	SFN,		GJB6,
SPRR1A,	CYP2D22,	IVL		SFN,
HOXC13,	EDN2,			SHH,
SPRR1B,	FADS3,			ALOX8
OVOL1,	ACOT1,			
CNFN,	LYPLA2,			
FOXE1,	ALOX8			
TGM3,				
IVL,				
KRT71				

Figure 4.3: Transcriptional changes upon *Myc* deletion in epidermis. (A) Percentages of genes associated with each gene ontology category (GO; http://david.abcc.ncifcrf.gov/) repressed for more than 2 fold upon *Myc* deletion. (B) Functional categories and examples of genes corresponding to each functional category. (C) Several of the genes which are repressed upon *Myc* deletion are either epidermal or keratino-associated.

4.2 Dynamic expression of EDC genes in response to MYC activation

To understand how MYC dynamically regulated EDC genes, I performed hierarchical clustering on global mRNA expression levels obtained for isolated from K14MycER keratinocytes, where MYC had been induced zero to six days. A distinct group of EDC genes was upregulated only after four to six days; whereas few genes were downregulated (Figure 4.4, A). Because MYC binds to a large number of genes in the genome, corresponding to up to 15% of all expressed genes, I confirmed MYC specifically regulated EDC genes by comparing the changes in mRNA expression levels over the time-course with genes randomly chosen outside the EDC region (non-EDC genes) (Figure 4.4, B). In general, MYC activation resulted in an increase in the mRNA levels of EDC genes when compared to randomly selected genes outside the EDC. This behaviour in gene expression dynamics was statistically significant for EDC genes only, specifically on days four and six of 4-OHT treament; a result that was not observed for non-EDC genes.

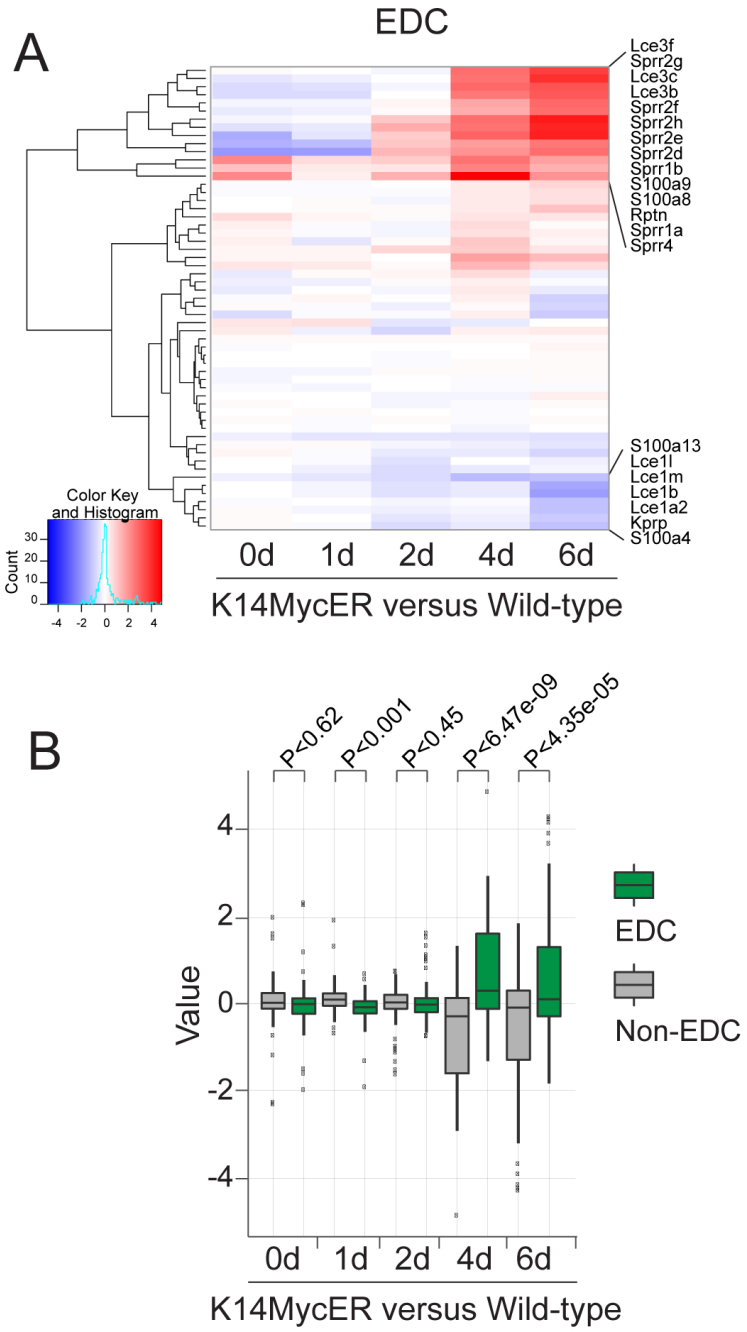

Figure 4.4: Distinct expression profile of epidermal differentiation complex genes (EDC) genes upon MYC activation.(A) Cluster analysis of mRNA expression levels of EDC genes in K14MycER mice relative to wild-type littermates following tamoxifen (4-OHT) treatment for the indicated time points in days, d. (B) Comparison of EDC gene expression from (A) *versus* randomly selected non-EDC genes across mouse chromosome 3. Heatmaps show upregulated mRNA expression levels in red, unchanged in white and downregulated in blue, with the corresponding fold change values depicted in the color key legend on the left of the heatmap.

In addition I also analyzed the mRNA expression profiles of the 5000 genes with most significant variation in mRNA levels following MYC induction (Figure 4.5). The expression level of *Rasd2* is shown as an example for the 46% genes that were immediately upregulated after 1 day of 4-OHT treatment (mRNA levels kept increasing until 6 days of treatment). Similarly, *Alox12* represents 46% of the genes with immediate reduction in mRNA levels after 1 day treatment, whereas *Lcn2* represents the group of 1.7% of genes which were upregulated only after 4 days of MYC induction. This group of genes comprised several EDC genes (e.g *S100a9*, *Sprr2g*, *Sprr2e*, *Sprr2d*, *Sprr2h* and *Lce3c*).

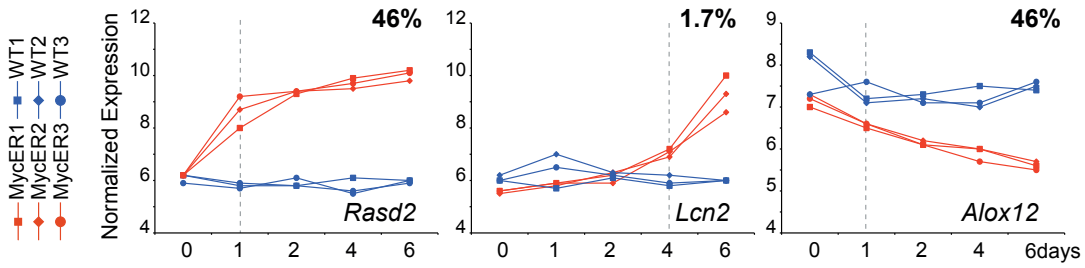

Figure 4.5: Representation of the expression profiles of 5000 genes in MYC induced epidermis. These profiles represent the most common transcriptional responses in a MYC induced time-course where triplicates samples of K14MycER (MycER 1-3, red) and wild-type (1-3, blue) murine skin mRNA samples were used. *Rasd2*, represents one example for the 46% of genes upregulated after 1 day of tamoxifen (4-OHT) treatment (left hand panel). *Lcn2* represents the small group of genes (1.7%) upregulated after 4 days 4-OHT treatment (middle panel). *Alox12* is as an example for 46% of genes downregulated after 1 day treatment with 4-OHT (right hand panel).

As activation of MYC after 1 day 4-OHT treatment induced changes in the mRNA levels of 92% of 5000 genes, I decided to perform a ChIP-on-Chip experiment at this time point to confirm that the oncoprotein was in fact bound to the promoter of EDC genes and directly regulating their mRNA expression levels (Figure 4.6). Binding location of MYC after 1 day 4-OHT treatment confirmed that the protein was already bound to the promoter of at least 80% of the transcriptional active EDC genes observed at day 4. Analysis of MYC binding after a longer induction period increased the resolution of the peaks and the number

of binding events, demonstrating that the consequences of MYC activation in epidermal cells are very dynamic and change in a low and high MYC microenvironment. Histological sections of dorsal skin of wild-type and K14MycER mice treated for 1 day with 4-OHT were stained with H&E and the phenotype was analyzed under the microscope (Figure 4.6). Low levels of MYC activation did not phenotypically affected epidermal differentiation or proliferation, suggesting that activation of MYC in the epidermis might exert a unique regulatory network at the EDC cluster, possibly through cooperation with additional tissue-specific TFs.

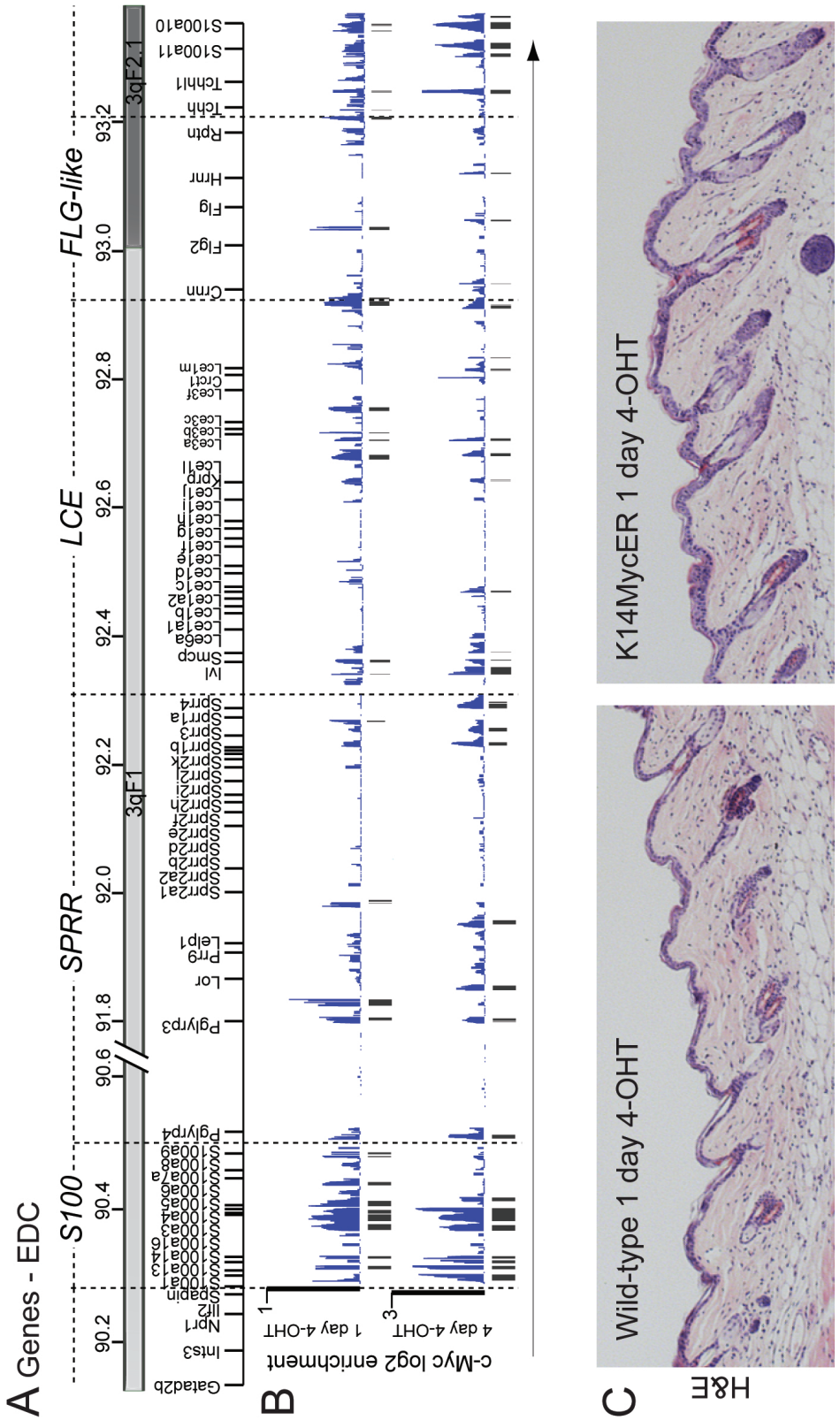

Figure 4.6: MYC location at the EDC after 1 day 4-OHT induction. (A) Genomic organisation of EDC genes in the mouse chromosome 3. ChIP-on-chip data is presented as a log2 fold change in signal between MYC enriched genomic DNA fragments and the background. (B) Comparison of MYC binding (blue) to EDC genes in K14MycER mice following 1 day and 4 days treatment with tamoxifen (4-OHT). (C) Hematoxylin and eosin (H&E) stained skin sections from wild-type (left hand panel) and K14MycER (right hand panel) mice treated 1 day with 4-OHT.

4.2.1 MYC regulates EDC transcription by modulating a tissue-specific regulatory network

To try to understand if the late transcriptional response of EDC genes upon MYC activation, required additional tissue specific TFs, I performed clustering analysis of ChIP-on-Chip data obtained for MYC, H3K4me3, H3K27me3, RBP2 and 8 transcription factors previously shown to be important for epidermal differentiation (TCFAP2γ, SIN3A, MXI1, CEBPα, CEBPβ, KLF4, OVOL1 and OVOL2). The goal was to identify genes co-regulated by MYC and 1 or more tissue-specific TFs. This analysis was performed over part of mouse chromosome 3 and demonstrated that MYC activation dramatically affected the overall transcription factor binding profiles (Figure 4.7 A,B).

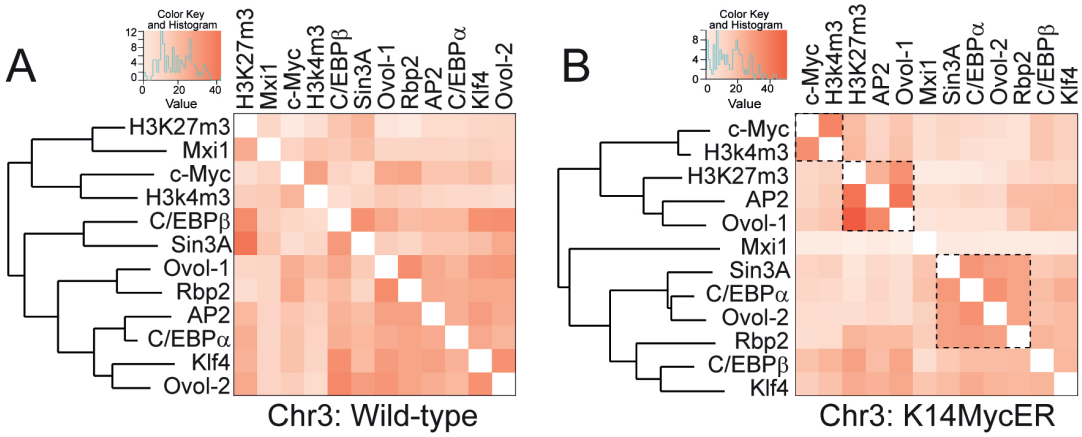

Figure 4.7: MYC determines specific regulatory networks. (A) Cluster analysis of binding events of the indicated tissue-specific transcription factors (TFs) to chromosome 3 (Chr3) before - wild-type - and after - K14MycER - MYC induction (B). Activation of MYC in epidermal keratinocytes completely remodels the binding of tissue-specific TFs. Heatmaps show the number of shared binding events between two TFs (light orange: low similarity and dark orange: high similarity). Highlighted dashed boxes represent the TFs that most likely share a vast proportion of binding sites.

A more detailed analysis at the EDC region upon MYC induction revealed two distinct clusters of TFs: one containing KLF4, OVOL1 and MYC and the other containing SIN3A, MXI1 and CEBPα (Figure 4.8 A,B). The level of occupancy of these TFs at the EDC was strongly dependent on the levels of MYC, contrarily to what was observed for histone marks H3K4me3 and H3K27me3, which remained unchanged and comparable in keratinocytes from wild-type and K14MycER mice (Figure 4.8 C). In wild-type animals, with low levels of endogenous MYC, binding of KLF4 and OVOL1 to the EDC *S100a* family of genes was low when compared with the high occupancy of CEBPα, MXI1 and SIN3A (Figure 4.8 C, left hand panel). Conversely, MYC induction favoured KLF4 and OVOL1 binding and depleted SIN3A, CEBPα and MXI1 occupancy at the EDC (Figure 4.8 C, right hand panel).

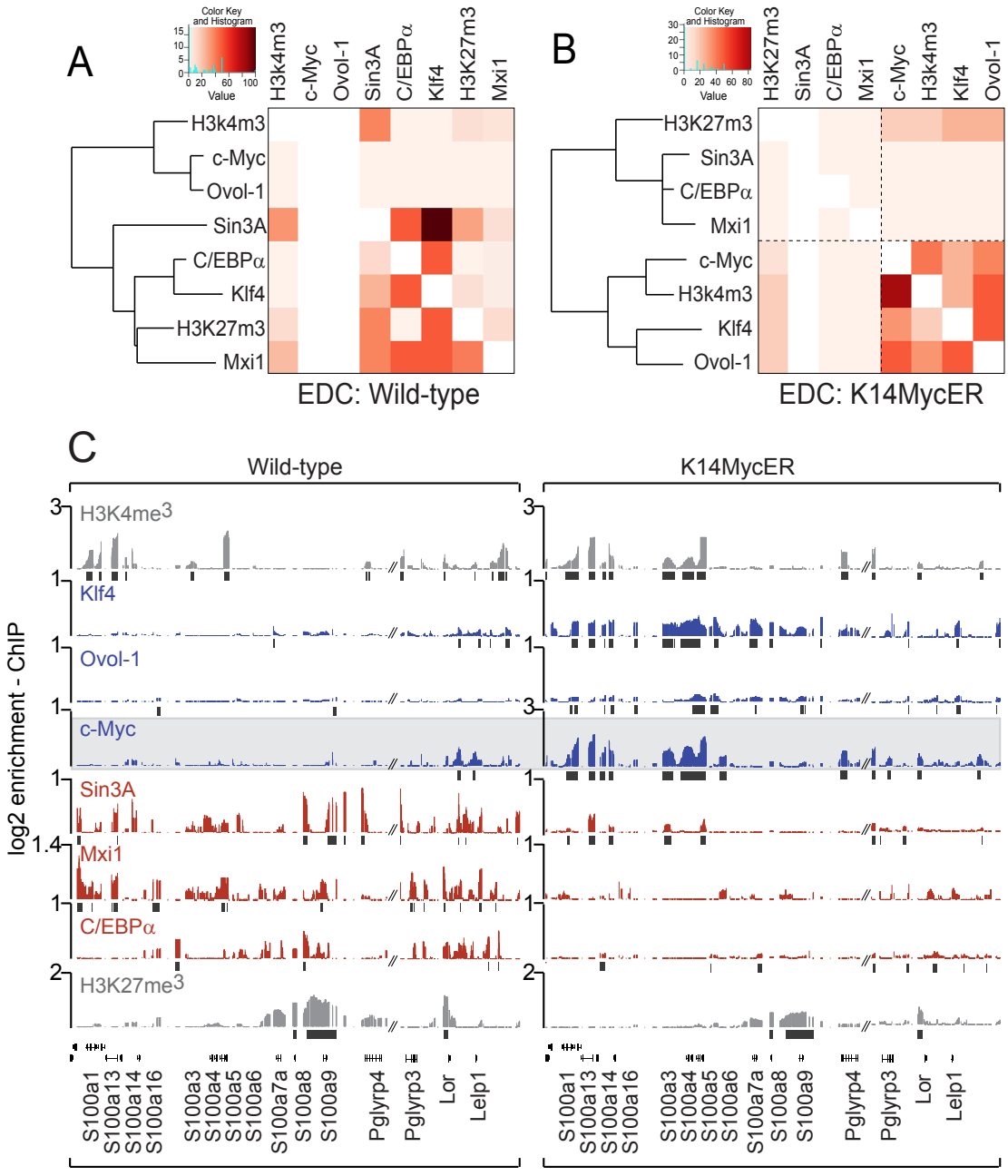

Figure 4.8: MYC favours occupancy of KLF4 and OVOL1 at EDC. (A,B) Cluster analysis of binding events of the indicated transcription factors to the EDC. Heatmaps show the number of shared binding events between two TFs (light orange: low similarity and dark orange: high similarity). (C) Occurrency of H3K4me3 (grey), H3K27me3 (grey) and occupancy of the transcription factors (TF) indicated, to the *S100a* family of genes from the EDC in wild-type (C, left hand panel) and K14MycER (C, right hand panel) keratinocytes. Activation of MYC in K14MycER keratinocytes enhances binding of KLF4 and OVOL1 (blue) and loss of SIN3A, MXI1 and CEBPα (red).

4.2.2 MYC tissue-specific regulator's remodeling at EDC does not occur via transcriptional regulation

To understand if binding or exclusion of CEBPα, SIN3A, KLF4 and OVOL1 to the EDC was directly dependent on MYC transcriptional regulation, I performed RT-qPCR analysis on tissue isolated from wild-type and K14MycER mice. Binding of KLF4 and OVOL1 in the transgenic mice was not directly dependent on MYC activation as correspondent mRNA levels decreased upon MYC activation (Figure 4.9 B,C). Moreover, *Cebpα* mRNA levels remained unchanged in wild-type or transgenic animals, but interestingly *Sin3a* mRNA levels were higher in homeostasis, probably due to an indirect effect as MYC does not bind to the *Sin3a* promoter by genome-wide ChIP-on-chip analysis (*data not shown*) (Figure 4.9 D,E).

I also confirmed that the different TFs were expressed in the same cellular populations during epidermal differentiation. I used flow cytometry combined with staining for the surface marker ITGα6 to isolate basal undifferentiated (High ITGα6), differentiated (Low ITGα6) and progenitor (Mid ITGα6) epidermal cell populations in wild-type and K14MycER transgenic mice (Figure 4.10 A,B). RNA samples were obtained from each population and RT-qPCR analysis was performed for assessing the expression levels of *Itgα6* and *Ivl*, here used as controls for undifferentiated and differentiated cells, respectively. I also measured the mRNA levels in each cellular compartment for *Myc*, *Klf4*, *Sin3a* and *Cebpα* with the purpose of assessing if both lineage specific TFs were expressed in the expected cell compartments (Figure 4.10 C-H). In wild-type epidermis there was a clear distinction between high, medium and low *Itgα6* populations which disappeared upon MYC activation (Figure 4.10 C). *Ivl* expression was higher in the progenitor's and differentiated epidermal cells (Mid and Low Itgα6) for both wild-type and K14MycER transgenic mice (Figure 4.10 D). While *Myc* expression levels did not change in basal, suprabasal or progenitor populations in wild-type epidermis, MYC activation in the basal cells induced, as expected, higher levels of the *Myc* oncogene in these cells when compared to progenitor or differentiated cells (Figure 4.10 F). *Sin3a* mRNA levels were high in basal wild-type keratinocytes but upon MYC activation the expression increased in the progenitor population by

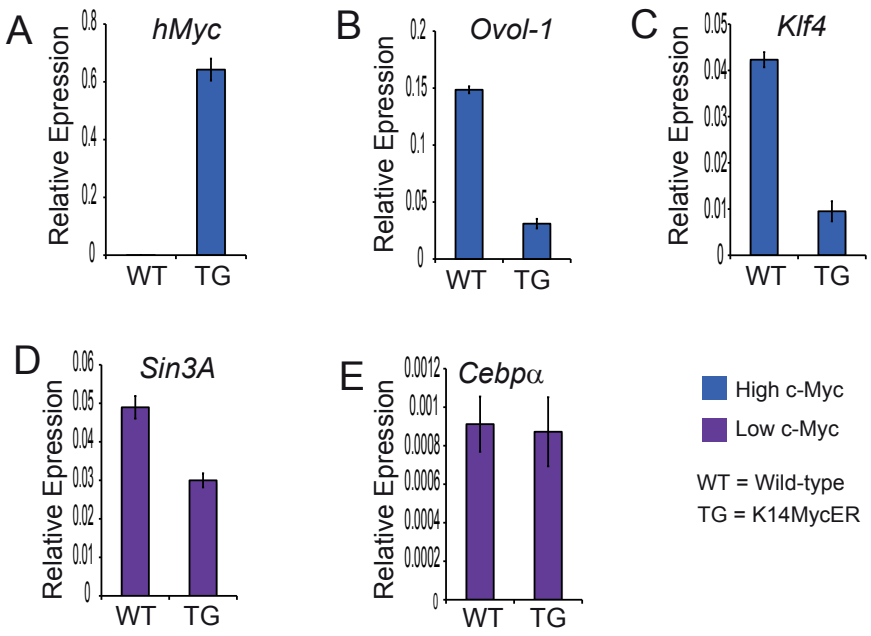

Figure 4.9: Effect of activated MYC on mRNA levels of epidermal specific transcription factors. mRNA levels for the genes indicated, in skin of wild-type (WT) and K14MycER (TG) mice in response to tamoxifen (4-OHT) treatment for 4 days. The colours represent the increased binding of the correspondent proteins in a high (blue) or low (purple) MYC microenvironment (i.e wild-type or K14MycER). mRNA levels were calculated relative to *Gapdh*. Data represents the mean values for three biological replicates (n = 3) and bars the standard deviation of the mean.

two fold, when compared to basal undifferentiated K14MycER epidermal cells (Figure 4.10 F). *Cebpα* was mainly expressed in the differentiated suprabasal wild-type keratinocytes, whereas after MYC activation it was shown to be more expressed in the population of progenitors (Figure 4.10 G). *Klf4* expression in the wild-type was observed mainly in the basal and progenitor's population, whereas upon MYC activation it changed to the suprabasal cells, as seen in (Figure 4.10 H and 4.11).

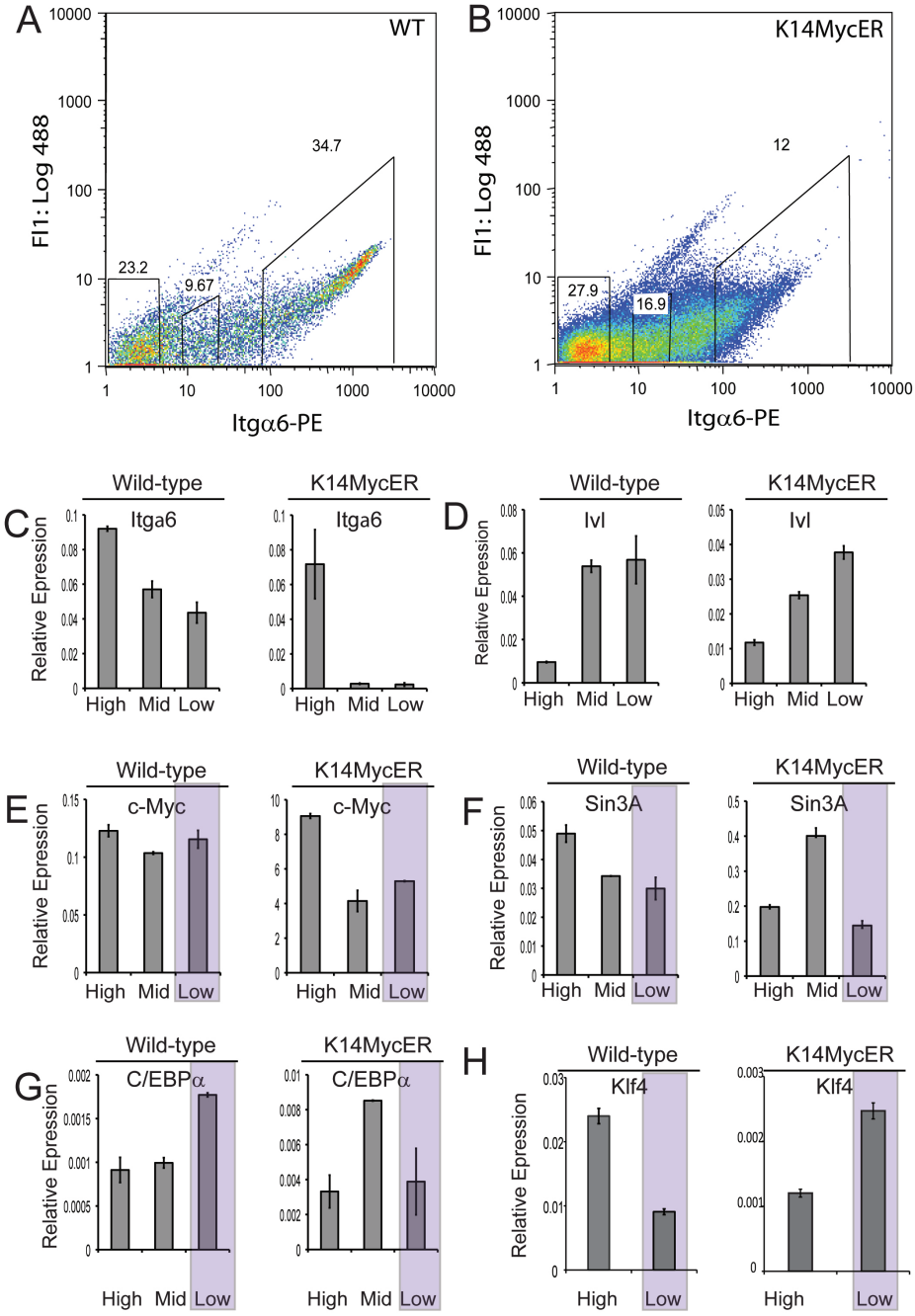

Figure 4.10: mRNA gene expression levels of MYC and skin specific regulators at distinct cellular compartments. mRNA levels of the genes indicated in the flow sorted epidermal populations in wild-type (A) and K14MycER (B) mouse skin, with high, middle (mid) and low surface levels of ITGα6. Purple indicates co-expression of the respective factors in differentiated epidermal populations (C-H). Mice were treated for 4 days with tamoxifen (4-OHT). mRNA levels were calculated relative to *Gapdh*. Data represents mean values for two independent biological replicates (n = 2). Bars represent the standard deviation of the mean.

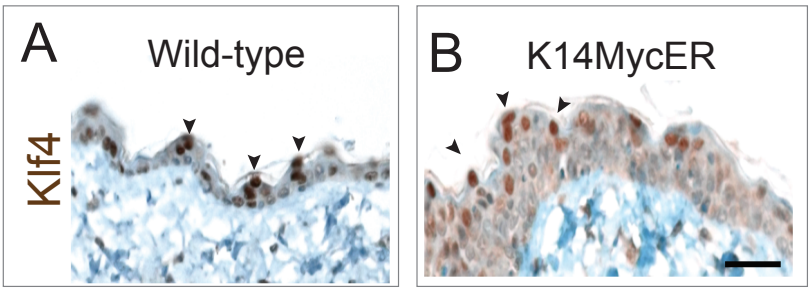

Figure 4.11: KLF4 expression in suprabasal epidermal layers upon MYC activation. Skin sections from wild-type (A) and K14MycER (B) mice labelled with KLF4 antibody. Arrow heads indicate cells expressing KLF4. Scale bar: 25μm.

4.2.3 MYC enriched regions at the EDC present consensus motifs for additional tissue-specific regulators

Motif discovery analysis for regions enriched in MYC at the EDC revealed that the sequences bound by MYC also present consensus motifs for CEBPα, KLF4 and TCFAP2α (Figure 4.12).

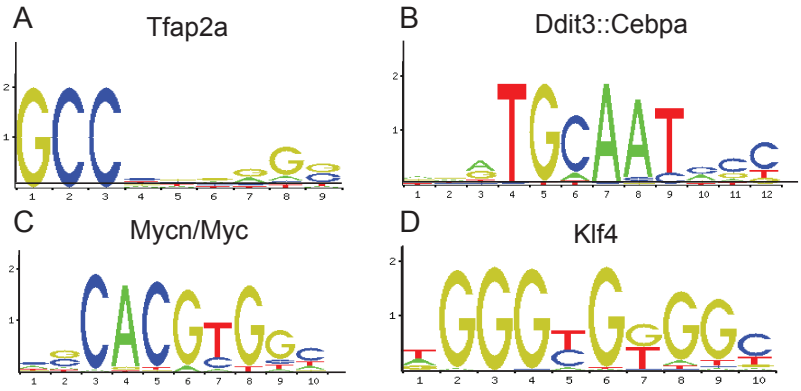

Figure 4.12: Motif analysis for MYC enriched promoter regions. Analysis was performed using the bioinformatic tool *Pscan* (http://159.149.109.9/pscan/) . Motifs shown were calculated by an algoritm that retrieved a P-value<0.05 and performed on a list of genes shown to be bound and regulated by MYC in K14MycER mice treated with 4-OHT. The CEBPA motif was detected in MYC bound regions in wild-type mice, whereas KLF4 and TCFAP2α were enriched in MYC bound genes in K14MycER mice treated with tamoxifen for 4 days.

4.3 Summary

In summary, I have shown that MYC binds to the promoter of EDC genes and regulates their mRNA expression. The binding of this oncoprotein is generally associated with active transcription and indeed MYC preferentially binds to H3K4me3 enriched promoters positively affecting the expression of 17 of 55 EDC genes by inducing an increase in mRNA levels from two to four fold. On the other hand, MYC activation also results in a slight repression of 12 EDC genes, but mRNA levels do not decrease more than two fold (with exception of *S100a1*). There is also no changes in H3K4me3 or in H3K27me3 histone marks at the promoter of EDC genes upon MYC activation (Figure 4.1 B,C). Confirmation of these results (which have been obtained through global gene expression analysis) was shown by RT-qPCR where eight out of the nine genes analyzed were upregulated in K14MycER mice compared to wild-type (Figure 3.10).

MYC was bound to promoters of genes important for epidermal specific lin-

eage/differentiation/homeostasis and data obtained for mRNA gene expression levels in epidermis depleted of *Myc* has shown that several of the genes repressed are genes essential for establishment of the cornified envelope (Figure 4.3, A-C). In addition, MYC induced genome-wide changes at the mRNA level after 1 day of 4-OHT treatment, however expression of EDC genes was only affected after four to six days of induction, even though MYC was already bound at their promoters after one day (Figure 4.4, 4.5 and 4.6).

Moreover, ChIP-on-chip analysis focused on the EDC region for a set of specific differentiation regulators has shown that MYC activation completely remodels the occupancy of each of the TF regulators analyzed, favoring binding of KLF4 and OVOL1 and excluding occupancy of CEBPα, SIN3A and MXI1 (Figure 4.8 C). Gene expression analysis in wild-type and K14MycER mice for *Klf4*, *Ovol1*, *Sin3a*, *Cebpα* and *Myc* was performed to understand if MYC induced TF remodelling at the EDC was due to regulation of these genes at the transcriptional level. This analysis has shown that this was not the case, even though *Sin3a* expression was repressed upon MYC activation (Figure 4.9). This effect however must occur post-transcriptionally as MYC was not bound to the *Sin3a* promoter in the ChIP-on-chip whole genome promoter analysis performed.
It is also important to mention the fact that MYC binding to the EDC might be evolutionary conserved as ChIP-seq experiments in human epidermal keratinocytes grown *in vitro* and retrovirally infected with the contruct MYCER that induces expression of the MYCER protein upon 4-OHT treatment, have shown that MYC also binds to the promoter of genes from the *S100A*, *LCE* and *FLG*-like families (Figure 4.13).
In order to assess if TF binding correlated with expression at the same cellular compartments in the epidermis, gene expression analysis was performed on sorted cells from the basal, progenitor's and suprabasal epidermal populations (Figure 4.10). In normal wild-type epidermis, *Cebpα* was shown to be more expressed in the suprabasal layers of epidermis; *Sin3a* was more expressed in the basal layer, but generally expressed in all cell compartments, as well as *Myc*. Subsequent MYC activation and amplification of the progenitor's cell population has shown that *Myc* remained highly expressed in undifferentiated keratinocytes

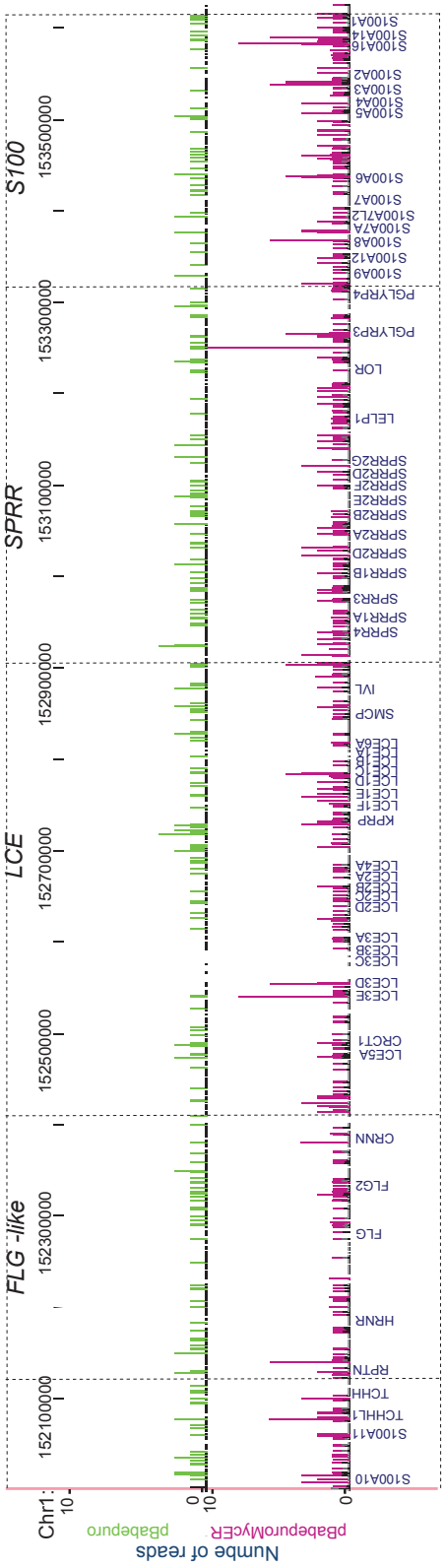

Figure 4.13: MYC binding at the human EDC. ChIP-seq experiments performed in human epidermal keratinocytes grown in culture and retrovirally infected with a MYCER construct that induces expression of MYC upon addition of tamoxifen (pBabeMycER, magenta) and correspondent empty vector control (pBabe, green) and focused on the epidermal differentiation complex (EDC) in chromosome 1. Binding of MYC is observed at the *S100A*, *LCE* and *FLG-like* family genes.

whereas *Cebpα* and *Sin3a* were co-expressed in the progenitor's cell populations. *Klf4* expression was only assessed in populations sorted for high and low ITGα6, and therefore it was difficult to address from the gene expression data if MYC and KLF4 were co-expressed in the same cellular compartments. However, immunohistochemistry images of KLF4 labelled epidermal cells on skin sections of wild-type and K14MycER mice, clearly demonstrated that expression of KLF4 occurred in the suprabasal layers of the epidermis upon MYC induction, correlating with the mRNA gene expression data obtained. It is possible a scenario where MYC induction would favor KLF4 binding to the EDC, and the later would then induce the expression of EDC genes, such as the *Sprr* family. This would explain the lag in activation of these genes upon MYC induction (Figure 4.11).
In conclusion, the consequences of MYC induction in the epidermis were very dynamic and changes in the MYC protein levels exposed certain TF sequence motifs, as oppose to others at the EDC. Endogenous levels of MYC favored regions where, for example CEBPα was co-bound, whereas in a high MYC microenvironment, binding motifs for KLF4 and TCFAP2α where more enriched (Figure 4.12). Interestingly, this MYC tissue-specific function might be evolutionary conserved as, ChIP-seq experiments for enrichment of MYC in human keratinocytes overexpressing a pBabeMycER retroviral construct, where MYC activation was induced by 4-OHT treatment, also revealed binding of MYC at the human EDC cluster in chromosome 1.

Chapter 5

Transcriptional repression at the epidermal differentiation complex (EDC)

5.1 SIN3A as a repressor of MYC target genes

The drastic changes in occupancy of epidermal specific regulators (KLF4, CEBPα, MXI1, SIN3A) upon MYC induction, suggested that one or more of these TFs might regulate MYC transcriptional activity. A likely candidate would be SIN3A, a multiprotein complex with deacetylase activity that is known to interact with MYC antagonists (MXD/MNT family of proteins). A hypothetical scenario would predict that SIN3A might induce MYC displacement at the EDC in order to antagonize its function (i.e to repress MYC target genes). In line with this hypothesis the binding sites occupied by both TFs at the *S100a* cluster target the same promoters (Figure 4.8 C).

5.1.1 MYC-SIN3A interaction targets MYC for degradation

Work in collaboration with Shobbir Hussain [1] involving co-immunoprecipitation experiments using flag-tagged MycER (MycER-Flag) constructs, measurement of MYC acetylation levels, as well as, cycloheximide experiments to determine MYC's half-life in the presence of SIN3A, have shown that SIN3A interacts with MYC at the protein level targeting it for degradation (Figure 5.1 A-C). Degradation of MYC happens most likely via de-acetylation. Overexpression of the acetyltransferases *GCN5* and *TIP60* led to an increase in MYC acetylation levels compared to controls (Figure 5.1 B, Ac-Lys), whereas MYC acetylation was decreased when *SIN3A* was also overexpressed (Figure 5.1 B, Ac-Lys).

Moreover, when protein translation was inhibited via treatment with cycloheximide, the half-life of the MYC protein was reduced when *SIN3A* was overexpressed in combination with *GCN5* (Figure 5.1 C). Interestingly, when the Myc-mutant construct, Mycmt, that cannot be acetylated by GCN5 at lysines positioned at locations 323 and 417 (K323 and K417) was used, no substantial changes in the half-life of the protein were observed compared to cells overexpressing *GCN5* alone, or in presence of *GCN5* and *Sin3a* (Figure 5.1 D).

[1] Wellcome Trust Centre for Stem Cell Research, University of Cambridge

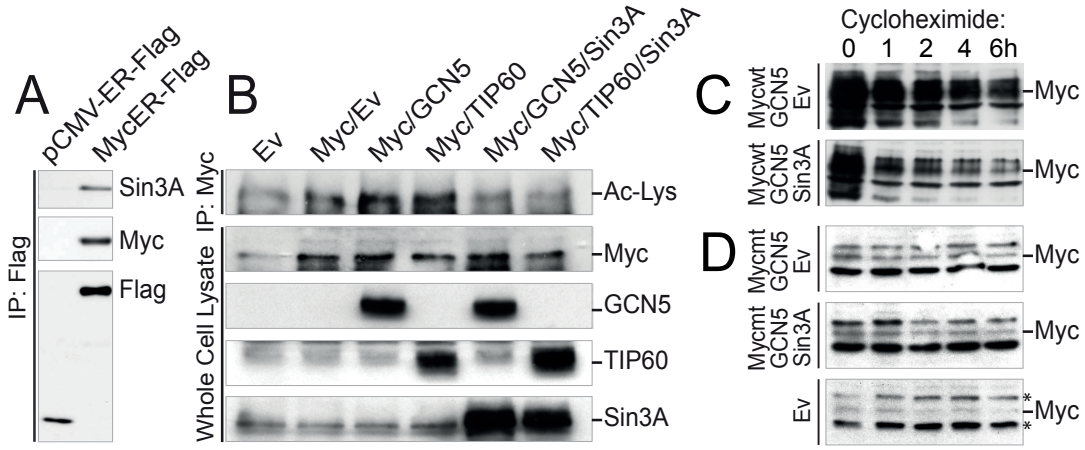

Figure 5.1: MYC de-aceylation and degradation is mediated by SIN3A. (A) SIN3A co-immunoprecipitates with Flag-tagged MycER (MycER-Flag) but not with Flag-tagged ER (pCMV-ER-Flag); western-blots were labelled using antibodies for SIN3A, MYC and Flag. (B) Overexpression of *SIN3A* inhibits acetylation of MYC by GCN5 and TIP60. Cos-7 cells transfected with the indicated constructs were immunoprecipitated for MYC (IP: Myc). Protein levels of MYC, GCN5, TIP60 and SIN3A were detected in whole cells lysates by western-blot and were found to be comparable. (C) Western-blot for MYC in Cos-7 cells overexpressing endogenous MYC and empty vector control (Ev), wild-type MYC (Mycwt) and GCN5 or MYC, GCN5 and SIN3A, following cycloheximide treatment for the indicated hours. (D) Western-blot of MYC of Cos-7 cells overexpressing a MYC-mutant construct (Mycmt) and GCN5 or Mycmt, GCN5 and SIN3A. The empty vector (Ev) was used as a negative control and Mycmt cannot be acetylated by GCN5 at lysines 323 and 417 (*Courtesy of Shobbir Hussain*).

Acetylation of the MYC protein by GCN5 is known to increase MYC stability [Patel et al., 2004], therefore I performed a luciferase reporter assay for MYC and the Myc-mutant construct, Mycmut to confirm that the mutant form of MYC exhibited reduced transactivation activity when compared to the wild-type protein. Indeed, decreased acetylation of the MYC protein affected its transactivation activity more than two fold when compared to the wild-type protein.

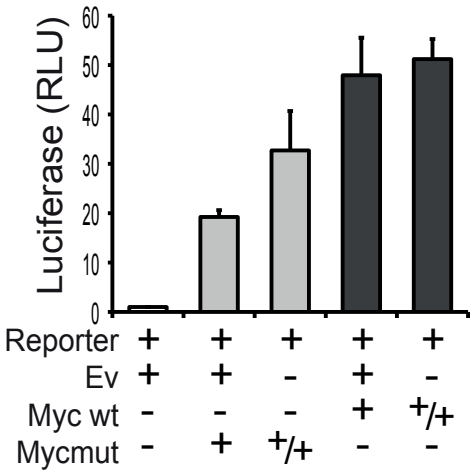

Figure 5.2: Decreased acetylation of MYC affects its transactivation activity. A MYC reporter assay in HEK-293 cells expressing the empty vector control (Ev), a wild-type *Myc* (Myc wt) or a mutant *Myc* contruct (Mycmut) which cannot be acetylated by GCN5 at lysine 323 positions and 417. (+) indicates that cells were transfected with the indicated constructs; (-) indicates non-transfected cells and (+/+) indicates that the double concentration of the construct was used for transfection. The transactivation activity of Mycmut is lower compared with the wild-type protein (Myc wt).

According to these results I speculated that deletion of *Sin3a* in the epidermis would lead to a stabilization of the MYC protein.

5.1.2 Loss of *Sin3a* in the epidermis results in hyperproliferation of the IFE

In wild-type skin, SIN3A is expressed in the IFE, HF and SGs (Figure 5.3, A). Deletion of *Sin3a* in the epidermis, by crossing mice carrying a floxed *Sin3a* allele with mice expressing *Cre*-recombinase (K14Sin3a$^{\Delta/\Delta}$), resulted in increased thickening of the IFE compared to wild-type (Figure 5.3 B-D), a phenotype similar to the one observed for *Myc* overexpressing skin (Figure 3.1).

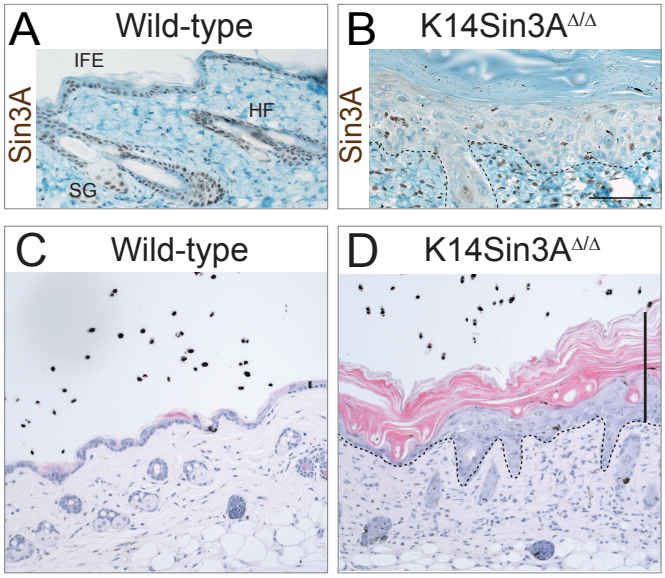

Figure 5.3: Deletion of *Sin3a* in skin causes increased thickening of the epidermis. (A,B) Skin sections from wild-type and K14Sin3A$^{\Delta/\Delta}$ mice where *Sin3a* was deleted in KRT14 positive cells from the epidermis, labelled with a SIN3A specific antibody. (C,D) Hematoxilin and eosin stained skin sections of wild-type and K14Sin3A$^{\Delta/\Delta}$ mice. Sin3a is expressed in the interfollicular epidermis (IFE), sebaceous glands (SG) and hair follicle (HF) and its deletion causes thicknening of the IFE, shown by vertical bar. Dotted lines in B and D mark the basement membrane of the epidermis. Scale bar: 100μm.

The increase in thickness of the IFE, following *Sin3a*, deletion resulted from an increase in proliferation, as seen by the higher number of KI67 positive cells in K14Sin3A$^{\Delta/\Delta}$ epidermis compared to wild-type skin (Figure 5.4 A,B).

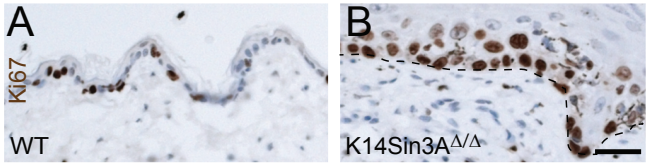

Figure 5.4: *Sin3a* deletion in the epidermis increases proliferation. Skin sections of wild-type (A) and K14Sin3A$^{\Delta/\Delta}$ (B) where *Sin3a* was deleted in basal KRT14 positive epidermal cells labelled with a KI67 antibody. Scale bar: Scale bar: 25μm.

This increase in proliferation upon *Sin3a* deletion also resulted in an increase in MYC expression, due to increase acetylation of MYC in epidermis from K14Sin3A$^{\Delta/\Delta}$ (*data not shown*), a phenotype similar to the one observed for K14MycER upon MYC activation (Figure 5.5 B,D). These results were confirmed at the protein and mRNA levels (Figure 5.5 E-G). At the mRNA level, the *Sin3a* and *Myc* deletions were observed by comparison with wild-type littermates skin samples containing epidermis and dermis. As *Sin3a* or *Myc* deletion was targeted only to the epidermis, significant mRNA expression values for both genes were still observed in dermal cells. However, protein obtained from epidermal sample preparations, as well as immunohistochemistry using back skin samples of mice where one or both proteins were deleted, revealed complete loss of MYC or SIN3A.

So far, the data presented confirmed that conditional deletion of *Sin3a* or overexpression of MYCER in KRT14 positive epidermal cells resulted in a similar phenotype.

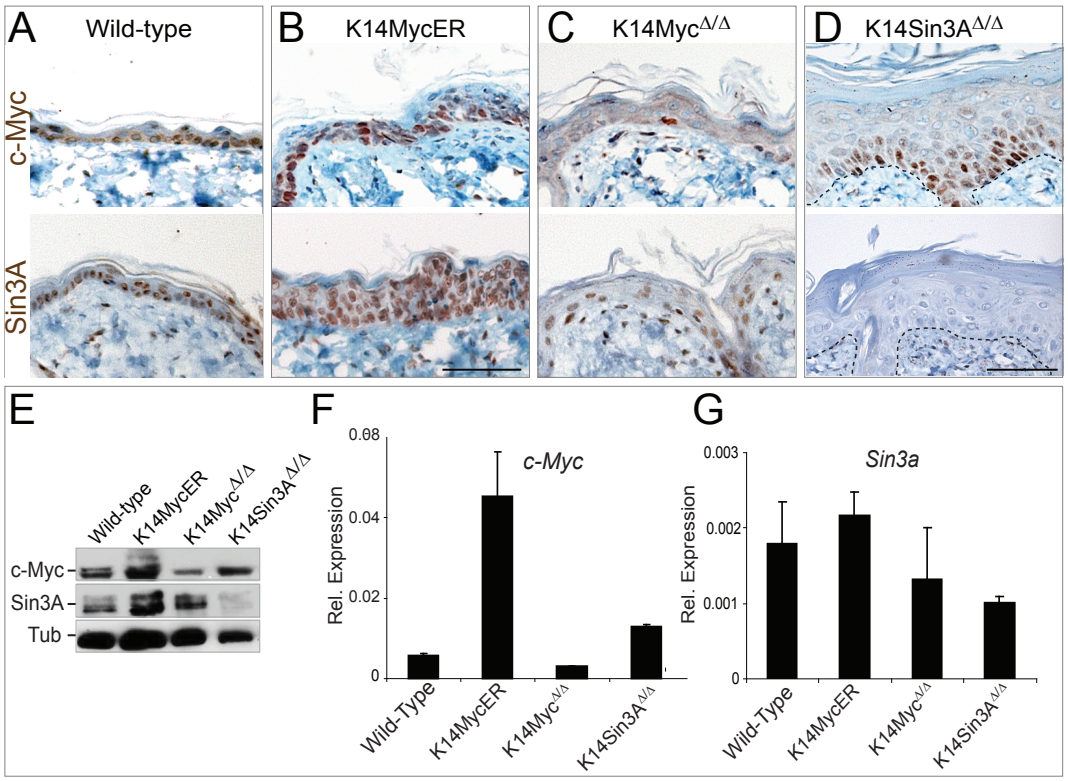

Figure 5.5: MYC expression increases upon loss of *Sin3a* in the epidermis. Skin sections of wild-type (A) and indicated transgenic mice (B-D) labelled for MYC (upper panels) and SIN3A (lower panels). Dotted lines in D mark the basement membrane. Scale bars: 100μm. (E) Western-blots show protein expression levels of MYC and SIN3A in the skin of wild-type and indicated transgenic mice. Tubulin (Tub) was used as a loading control. (F,G) mRNA levels of *Myc* and *Sin3a* in skin samples from wild-type and the indicated transgenic mice, relative to *Gapdh*. Data represents the mean values for three biological replicates (n = 3) and bars the standard deviation of the mean.

5.2 Loss of *Sin3a* in the epidermis increases MYC occupancy at the EDC

As deletion of *Sin3a* in the epidermis led to an increase in MYC expression, this suggested that upregulation of MYC target genes was a likely outcome.

5.2.1 Effects of MYC overexpression or *Sin3a* deletion in TF occupancy

To test wether loss of *Sin3a* would increase MYC occupancy at its target genes, I performed ChIP-on-chip experiments on chromossome 3 for MYC in *Sin3a* depleted epidermis of K14Sin3A$^{\Delta/\Delta}$ mice. I found that the number of MYC bound genes, as well as the peak signal (maximum and averaged), increased when compared to wild-type epidermis (Figure 5.6 A-C blue bars). Conversely, SIN3A binding was also assessed in epidermis from *Myc* depleted (K14Myc$^{\Delta/\Delta}$) or overexpressed (K14MycER) skin, as well as wild-type (Figure 5.6 A-C red bars). As expected, the number and signal intensity obtained for SIN3A binding events in wild-type epidermis was higher than in *Myc* depleted or overexpressed epidermis. In addition, the number of MYC bound genes commonly found in K14Sin3A$^{\Delta/\Delta}$ and K14MycER epidermis was two fold higher when compared to the same number in wild-type *versus* K14MycER mice (Figure 5.6 D, red numbers). These results suggest that K14MycER and K14Sin3A$^{\Delta/\Delta}$ mice share a significant number of identical genes regulated by MYC.

The number of SIN3A binding sites in wild-type epidermis was higher than in either *Myc* overexpressing or depleted epidermis, suggesting a that large proportion of MYC target genes requires the presence of MYC Examples of SIN3A and MYC binding in wild-type and each of the transgenic mouse lines analysed are shown in (Figure 5.7).

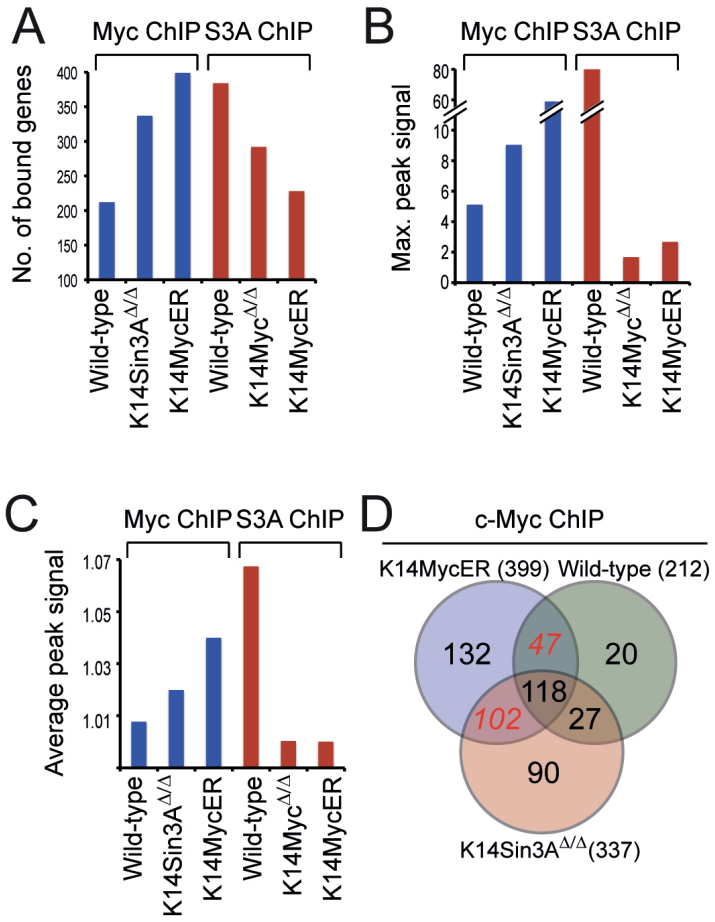

Figure 5.6: Enhanced SIN3A binding in the absence of *Myc*. ChIP-on-chip analysis on chromossome 3 using SIN3A and MYC antibodies. The total number of binding events (A) as well as maximum (B) and average (C) peak signals of the combined replicates in epidermis of K14MycER, K14Myc$^{\Delta/\Delta}$, wild-type and K14Sin3A$^{\Delta/\Delta}$ mice is shown.

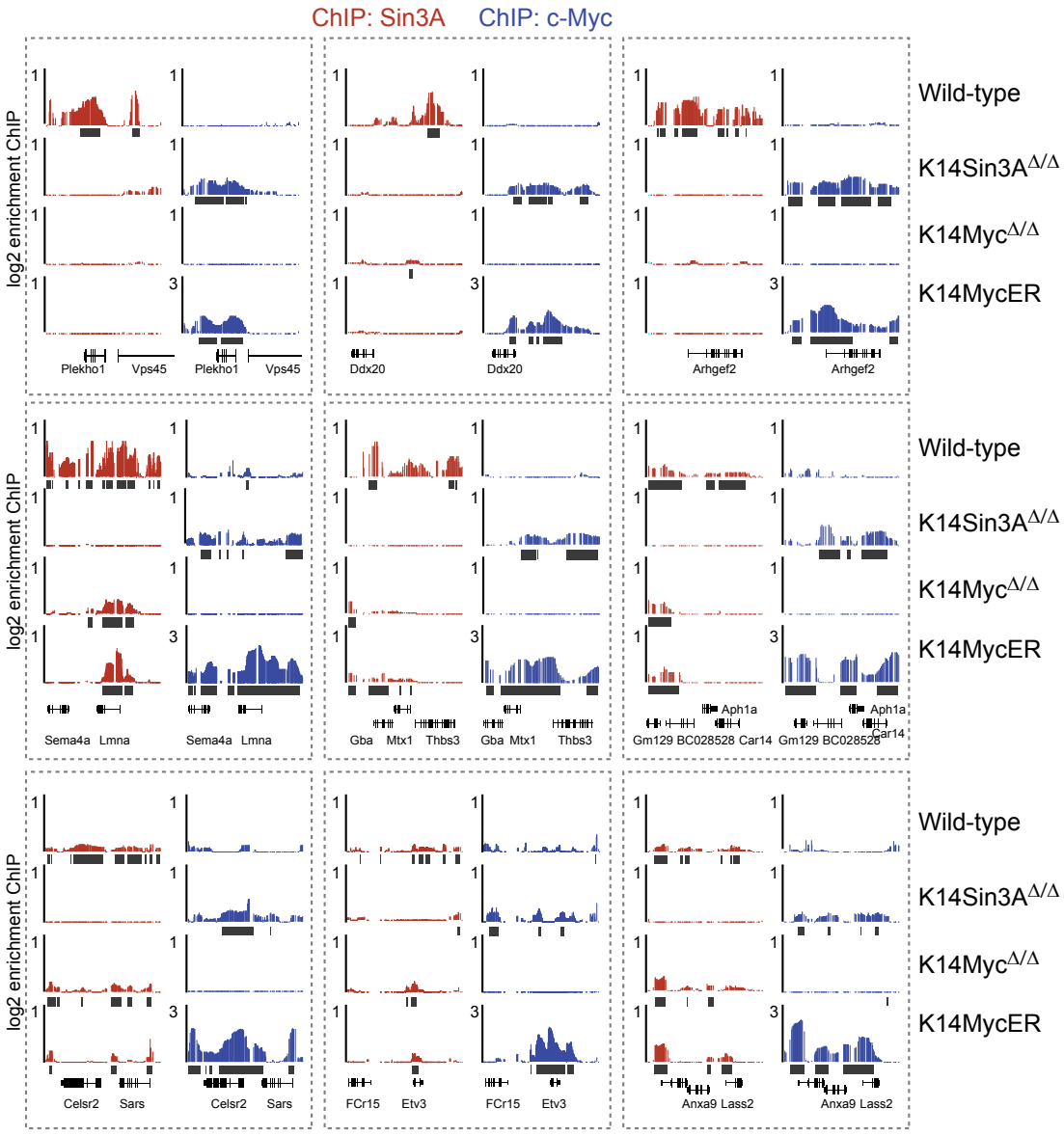

Figure 5.7: Enrichment of SIN3A (red) and MYC (blue) on genes located on chromosome 3. Location of SIN3A and MYC on the promoter region of genes on chromosome 3, located outside the epidermal differentiation complex (EDC) in wild-type, K14Sin3A$^{\Delta/\Delta}$, K14Myc$^{\Delta/\Delta}$ and K14MycER mice.

So far, I have shown that SIN3A interacts with MYC, targets MYC for degradation and occupies the promoter regions of MYC's target genes, possibly repressing them. Because SIN3A mediated repression relies on the recruitment of MXD/MNT proteins, I performed ChIP-on-chip for MXI1 (known to interact with SIN3A), in order to identify if MXI1 location was dependent on MYC levels, as it had been observed for SIN3A. I found that the number and signal of MXI1 binding events was not affected by *Sin3a* loss, remaining unchanged in wild-type and K14Sin3A$^{\Delta/\Delta}$ epidermis (Figure 5.8 A-C).

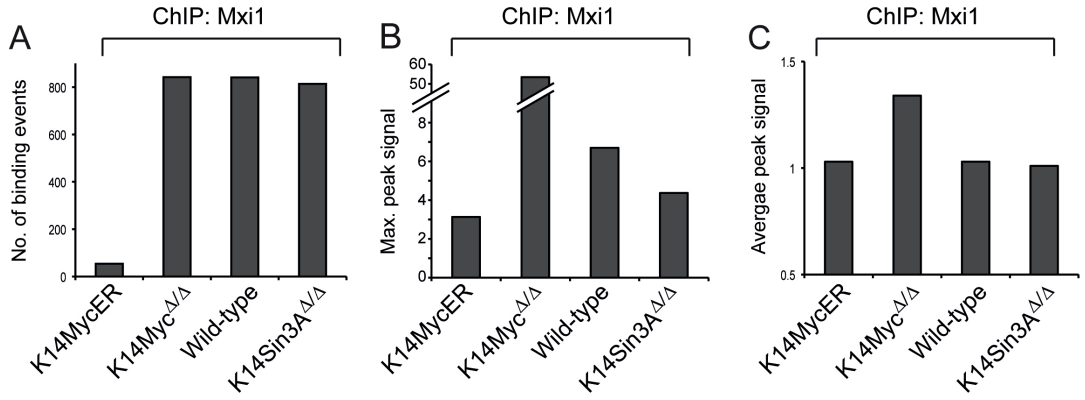

Figure 5.8: Binding of MXI1 is independent of SIN3A. ChIP-on-chip analysis on chromossome 3 using a antibody specific for MXI1. The total number of binding events (A) and maximum (B) and average (C) peak signals of the combined replicates in epidermis of K14MycER, K14Myc$^{\Delta/\Delta}$, wild-type and K14Sin3A$^{\Delta/\Delta}$ mice is shown. The number of MXI1 binding events is largely dependent on MYC levels.

Analysis of the binding of MXI1 at the EDC revealed that, as it had been observed for SIN3A, MXI1 was preferentially enriched in wild-type epidermis (Figure 5.9 C) when compared to *Myc* depleted or overexpressing skin (Figure 5.9 A,B). In addition, binding of MXI1 remained unchanged upon *Sin3a* deletion, where the endogenous levels of MYC increased (Figure 5.9 D).

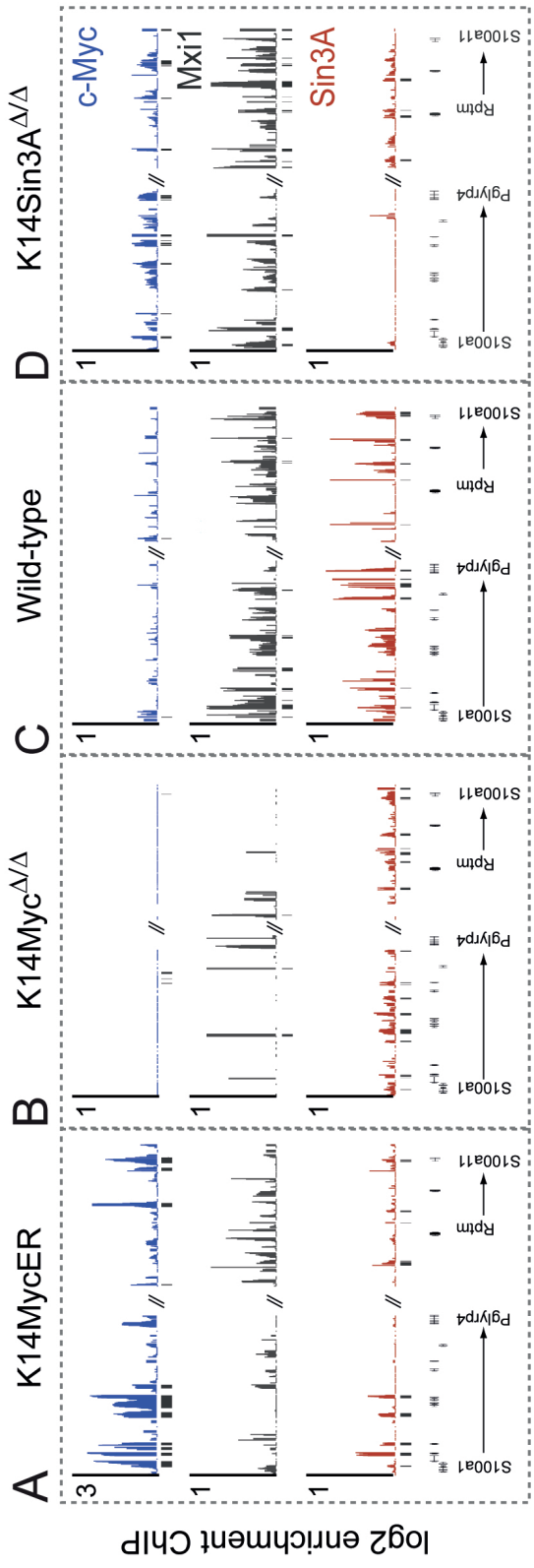

Figure 5.9: MXI1 occupancy at the EDC. Occurence of MXI1 binding to EDC genes in epidermis of K14MycER mice, K14Myc$^{\Delta/\Delta}$, wild-type and K14Sin3A$^{\Delta/\Delta}$ (A-D). MXI1 occupancy was mainly observed in wild-type and *Sin3a* depleted epidermis and was dependent on MYC levels.

Because *Sin3a* deletion in the epidermis resulted in an increase of the endogenous levels of MYC, it seemed plausible to assume that the increased number of differentiated suprabasal layers observed in the epidermis of K14Sin3A$^{\Delta/\Delta}$ mice resulted from increased differentiation, due to de-repression of MYC target genes at the EDC (Figure 5.3, D). For this reason I analysed the mRNA gene expression levels of EDC genes in samples of epidermis depleted from *Sin3a*. The fold change observed was similar to the expression profile of K14MycER mice (Figure 5.10).

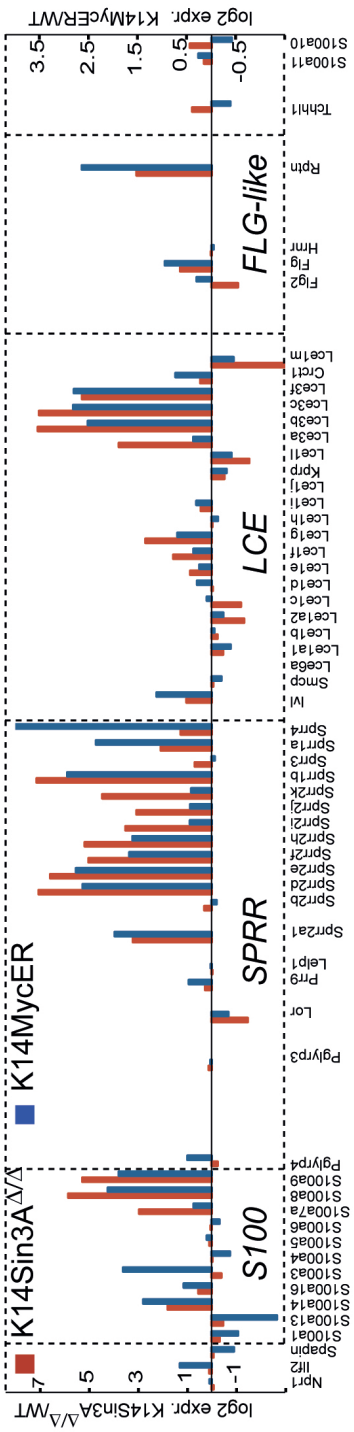

Figure 5.10: De-repression of MYC target genes upon *Sin3a* deletion. mRNA expression levels of epidermal differentiation complex (EDC) genes upon *Sin3a* deletion in the epidermis of K14Sin3A$^{\Delta/\Delta}$ (red bars) mice. Comparison with gene expression data obtained for K14MycER mice (blue bars) shows that both expression profiles are comparable. Data was extracted from mRNA expression arrays, measured relative to wild-type and a minimum of three biological samples (n=3) were used.

Further evidence that MYC and SIN3A targeted the same group of genes was observed following the overlap of SIN3A binding events in wild-type skin, compared to MYC in K14Sin3A$^{\Delta/\Delta}$ at chromosome 3. I found that in this situation there was a 71% overlap of binding events for both transcription factors, whereas only a small percentage (18%) of all MYC bound genes was never targeted by SIN3A in wild-type and MYC transgenic skin (Figure 5.11 A,B).

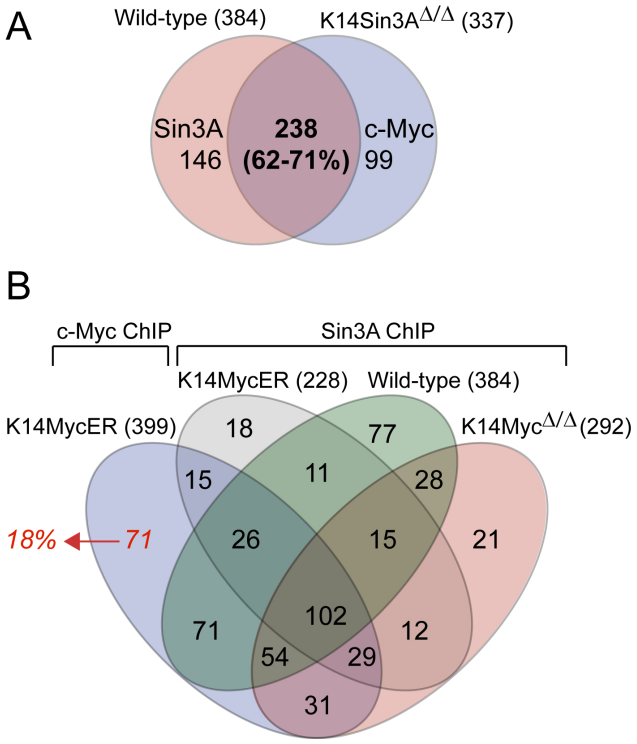

Figure 5.11: SIN3A targets MYC bound genes. (A) The top Venn diagram shows that 71% of MYC bound genes in K14Sin3A$^{\Delta/\Delta}$ epidermis was also bound by SIN3A in wild-type mice. (B) The bottom 4-way Venn diagram (http://bioinfogp.cnb.csic.es/tools/venny/index.html) was used for identification of a small percentage of MYC target genes in K14MycER mice which were never bound by SIN3A in the conditions analysed: SIN3A ChIP-on-chip on chromossome 3 in wild-type, K14MycER and K14Myc$^{\Delta/\Delta}$ murine epidermis.

This data indicates that in the absence of the multiprotein repressor complex SIN3A in the epidermis, MYC genomic occupancy at the EDC genes is facilitated.

5.2.2 SIN3A cooperates in regulating genes involved in proliferation

In addition to an increase in differentiation, loss of SIN3A also induced proliferation in the epidermis (Figure 5.4, B). To understand if SIN3A also repressed MYC target genes involved in cell growth and proliferation, I compared the differentially expressed genes in skin of K14Sin3A$^{\Delta/\Delta}$ mice with the MYC 2187 functional target genes which had been identified in K14MycER mice by genome-wide ChIP-on-chip (Figure 3.13). From this comparison, 512 genes were found to be targets of MYC as well as differentially expressed in K14Sin3A$^{\Delta/\Delta}$ skin (Figure 5.12). Functional analysis revealed that MYC-SIN3A regulated genes over-representated GO categories were related with metabolism, cell cycle, cell growth and RNA processing, as previously shown for MYC-only target genes (Figure 3.15 and 5.12). Furthermore, motif discovery analysis on the common 512 genes, revealed enrichment for the Myc-Max binding consensus motif, E-box, with high statistical significance.

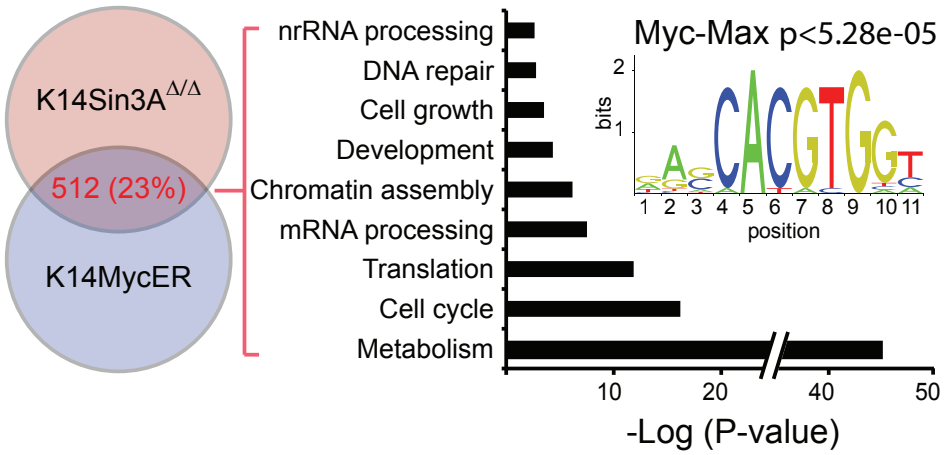

Figure 5.12: SIN3A target genes involved in cell growth and proliferation. Comparison of MYC functional target genes with differentially expressed genes in K14Sin3A$^{\Delta/\Delta}$ epidermis, followed by gene ontology (GO) analysis of MYC and SIN3A regulated genes. Expression data for K14Sin3A$^{\Delta/\Delta}$ was calculated relative to wild-type after treatment with tamoxifen (4-OHT) for 14 days. The P-value for the over-representation of Myc-Max binding sites in the 512 MYC and SIN3A-regulated genes is shown.

5.3 Summary

In this chapter I have shown that SIN3A is one of the epidermal differentiation regulators that affects MYC transcriptional activity. MYC and SIN3A binding to the EDC, at least in the conditions analysed, is mutually exclusive. Work in collaboration with Shobbir Hussain has shown that SIN3A and MYC interact at the protein level, and that when SIN3A is overexpressed, MYC acetylation and therefore stability are decreased. As a consequence, MYC is targeted for degradation and displaced from its target genes, which are then occupied by SIN3A, as well as MXI1. In fact, I have shown that SIN3A and MXI1 occupancy at the EDC genes is dependent on MYC levels. Because SIN3A is a known transcriptional repressor that recruits MXD/MNT proteins, it seems likely that it's function in the epidermis is to repress MYC target genes. Indeed, when *Sin3a* was deleted from the basal undifferentiated layers of the epidermis, it induced an increase in the thickness of the IFE as well as the number of differentiation suprabasal layers. I have shown that this was due to de-repression of EDC, as well as proliferation genes. Genome-wide motif analysis of MYC target and SIN3A regulated genes in the epidermis, has shown that the MYC-MAX consensus motif was highly enriched. Lastly, functional analysis revealed that both MYC and SIN3A control genes involved in cell growth, proliferation, metabolism and mRNA processing, in addition to epidermal differentiation. In conclusion, I have shown that SIN3A and MYC cooperate in the maintenance of epidermal homeostasis by regulating genes involved in differentiation and proliferation.

Chapter 6

Epidermal homeostasis is controlled by SIN3A and MYC

6.1 Deletion of MYC rescues the phenotype of K14Sin3A$^{\Delta/\Delta}$ mice

To understand if the hyperproliferation and increased differentiation observed in K14Sin3A$^{\Delta/\Delta}$ epidermis was solely dependent on MYC, deletion of *Myc* in this context was paramount. Analysis of skin sections of mice where *Sin3a* and *Myc* were deleted in undifferentiated epidermal cells (K14Myc$^{\Delta/\Delta}$K14Sin3a$^{\Delta/\Delta}$) demonstrated that upon *Myc* deletion, the epidermal morphology was largely rescued (Figure 6.1 A-C).

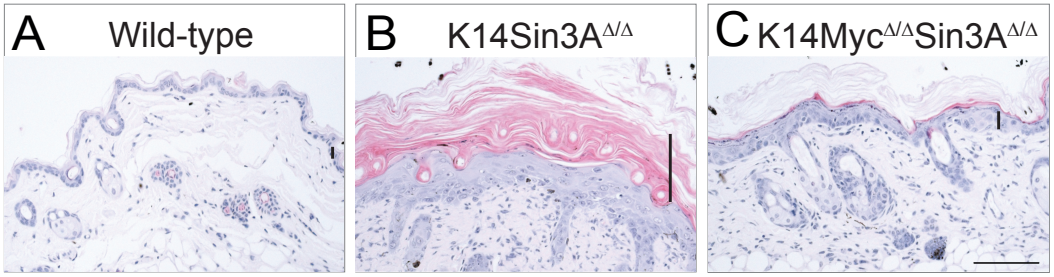

Figure 6.1: Deletion of *Myc* reverts K14Sin3a$^{\Delta/\Delta}$ phenotype. Hematoxilin and eosin staining of sections of wild-type (A), *Sin3a* deleted (K14Sin3a$^{\Delta/\Delta}$, B), and *Myc* and *Sin3a* deleted (K14Myc$^{\Delta/\Delta}$Sin3a$^{\Delta/\Delta}$, C) epidermis. Deletion of *Myc* in K14Sin3a$^{\Delta/\Delta}$ reverted the thickness of the interfollicular epidermis to levels comparable to wild-type skin. Scale bar:150μm.

Confirmation of *Myc* mRNA gene expression levels in epidermis from K14Myc$^{\Delta/\Delta}$Sin3a$^{\Delta/\Delta}$ mice was performed by RT-qPCR and shows that the mRNA levels of *Myc* decreased to half when compared to wild-type control or *Sin3a* depleted epidermis. (K14Sin3a$^{\Delta/\Delta}$) (Figure 6.2).

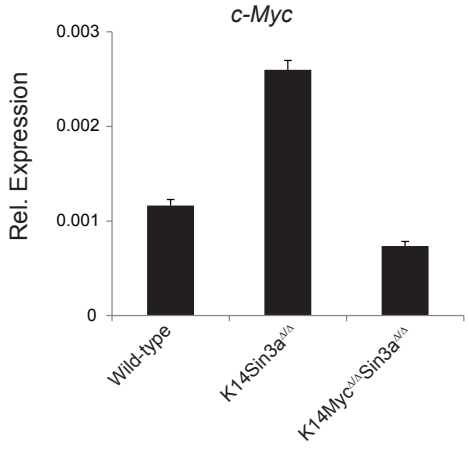

Figure 6.2: *Myc* levels decrease in K14Myc$^{\Delta/\Delta}$Sin3a$^{\Delta/\Delta}$ skin. mRNA expression levels of *Myc* measured by reversetranscriptase semi-quantitative PCR for wild-type and the indicated transgenic mice. Results were calculated relative to *Gapdh*. Data represents the mean values for three biological replicates (n = 3) and bars the standard deviation of the mean.

6.2 Loss of *Myc* in K14Sin3A$^{\Delta/\Delta}$ restores proliferation

Functional analysis performed on genes differentially expressed in K14Sin3a$^{\Delta/\Delta}$ and K14Myc$^{\Delta/\Delta}$Sin3a$^{\Delta/\Delta}$ murine skin samples, confirmed that genes related to proliferation and cell cycle that initially were two fold upregulated in *Sin3a* depleted epidermis, where either restored to wild-type levels or repressed in K14Sin3a$^{\Delta/\Delta}$ epidermis (Figure 6.3).

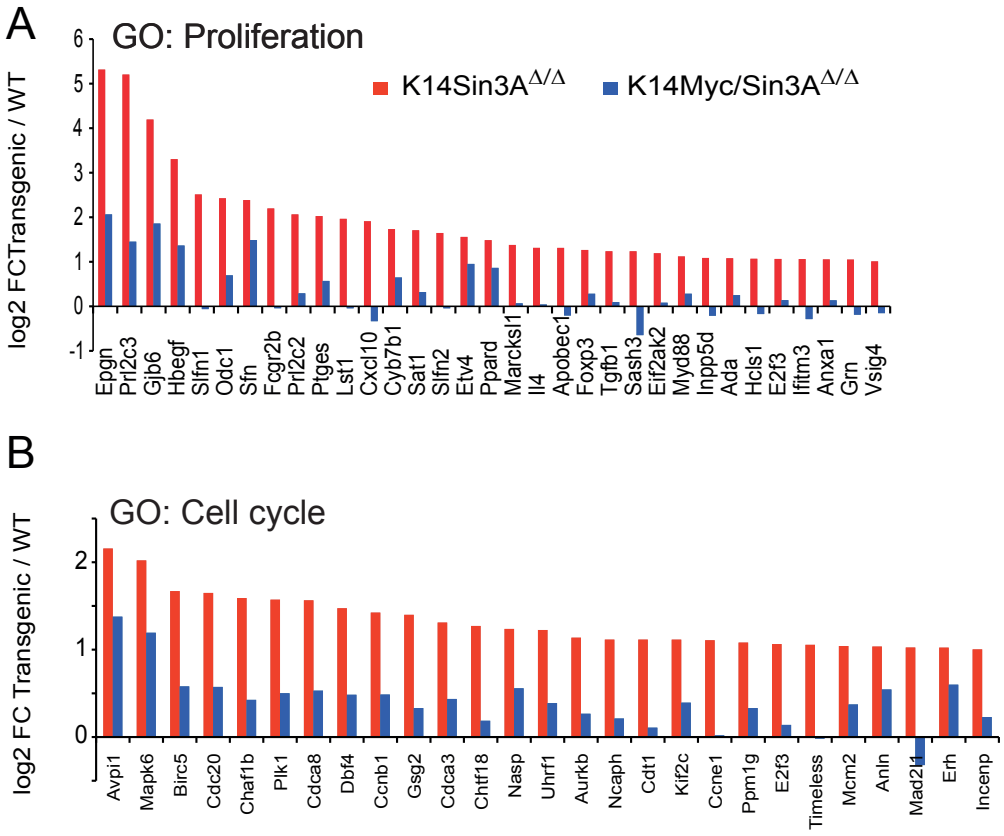

Figure 6.3: *Myc* deletion in K14Sin3a$^{\Delta/\Delta}$ restored normal proliferation. Log2 fold change of genes categorized as cell proliferation (A) and cell cycle (B) in *Sin3a* depleted skin (K14Sin3a$^{\Delta/\Delta}$, red bars) or *Myc* and *Sin3a* depleted skin (K14Myc$^{\Delta/\Delta}$Sin3a$^{\Delta/\Delta}$, blue bars). mRNA levels were normalized to wild-type (WT) controls. Data was obtained from gene expression arrays where at least 4 biological replicates were used.

6.3 Loss of *Myc* in K14Sin3A$^{\Delta/\Delta}$ restores differentiation

Similarly, the expression pattern of epidermal differentiation regulators CEBPα and KLF4 in K14Myc$^{\Delta/\Delta}$Sin3a$^{\Delta/\Delta}$ murine epidermis was restored to levels observed in the wild-type (Figure 6.4 A-G). Analysis of the mRNA expression levels of EDC genes was also found to be more comparable to wild-type than to K14Sin3a$^{\Delta/\Delta}$ epidermis (Figure 6.4 H).

Figure 6.4: *Myc* deletion in K14Sin3a$^{\Delta/\Delta}$ restores differentiation. Skin sections of wild-type and the indicated transgenic mice stained with specific antibodies for CEBPα and KLF4. Sections reveal that the pattern of expression was more comparable to wild-type epidermis and K14Myc$^{\Delta/\Delta}$Sin3a$^{\Delta/\Delta}$ (A,E,G) than to K14Sin3a$^{\Delta/\Delta}$ (D,F). Scale bars: 100μm (upper panel) and original magnification 20x (lower panel). (H) Log2 fold change of epidermal differentiation genes (EDC) genes in *Sin3a* depleted skin (K14Sin3a$^{\Delta/\Delta}$, red bars) or *c-Myc* and *Sin3a* depleted skin (K14Myc$^{\Delta/\Delta}$Sin3a$^{\Delta/\Delta}$, blue bars). mRNA levels were normalized to wild-type (WT) controls. Data was obtained from gene expression arrays where at least 4 biological replicates were used.

Confirmation of the restored mRNA levels of selected EDC genes *S100a1*, *S100a10* and *Lce1a2* was performed by RT-qPCR analysis (Figure 6.5). Comparison of mRNA levels of the indicated genes in acetone treated (negative control correspondent to wild-type) and K14Myc$^{\Delta/\Delta}$Sin3a$^{\Delta/\Delta}$ murine epidermis does not show significant differences in expression when compared to K14MycER, K14Myc$^{\Delta/\Delta}$, or K14Sin3a$^{\Delta/\Delta}$ (Figure 6.5, D).

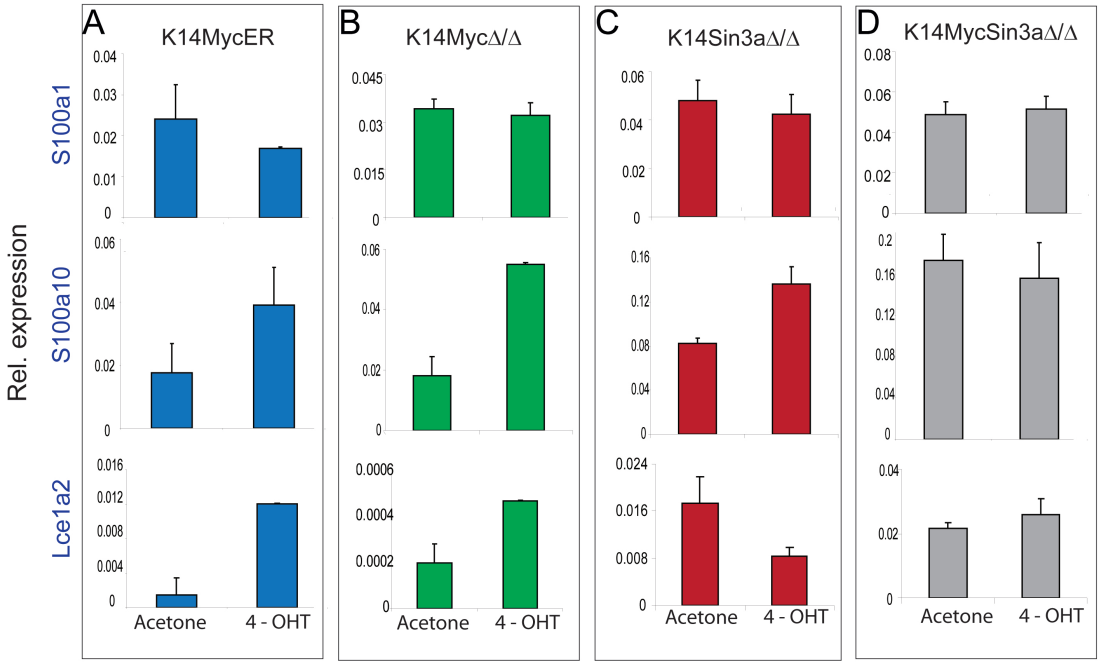

Figure 6.5: mRNA expression levels of EDC genes restored in K14Myc$^{\Delta/\Delta}$Sin3a$^{\Delta/\Delta}$ epidermis. Reverse transcriptase semi-quantitative PCR (RT-qPCR) for the indicated transgenic mice treated with tamoxifen (4-OHT) for either 4 days (K14MycER) , 14 days (K14Sin3a$^{\Delta/\Delta}$ and K14Myc$^{\Delta/\Delta}$Sin3a$^{\Delta/\Delta}$) or 21 days (K14Myc$^{\Delta/\Delta}$) compared to acetone treated mice (negative controls). Results were calculated relative to *Gapdh*. Data represents the mean values for three biological replicates (n = 3) and bars the standard deviation of the mean.

6.4 Summary

My data revealed that the effect of increased proliferation and differentiation observed upon *Sin3a* deletion in epidermis, is a consequence of an increase in *Myc* levels. This was confirmed when deletion of *Myc* in the epidermis of a K14Sin3a$^{\Delta/\Delta}$ background mouse line, resulted in restoration of the abnormal proliferation and differentiation phenotype, previously observed at the IFE. This effect was also confirmed at the genetic level when EDC genes, as well as genes involved in growth and differentiation, were either restored to wild-type level or repressed in K14Myc$^{\Delta/\Delta}$Sin3a$^{\Delta/\Delta}$ mice. In summary, a dramatic reduction of both undifferentiated proliferating and differentiated epidermal cells in skin of K14Myc$^{\Delta/\Delta}$Sin3a$^{\Delta/\Delta}$ mice was observe. These results suggest that MYC and SIN3A target the same group of genes required for normal epidermal homeostasis, but their roles in this process are antagonistic. MYC acts primarily as an activator of proliferation and differentiation related genes, while SIN3A act as a repressor.

Chapter 7

Conclusions and Future Perspectives

MYC functions have been extensively studied in cancer, but few reports have addressed the biological function of MYC in normal cells and tissues. Studies in cell lines dramatically changed the view of MYC as a gene-specific transcription factor, when genome-wide binding studies revealed widespread binding of MYC to tens of thousands of sites in the genome (reviewed in Knoepfler [2007]). Consistent with this I have shown that in epidermal stem and progenitor cells, MYC modulates the transcriptional response of 2187 genes involved in processes as diverse as cell growth and proliferation, metabolism, apoptosis, mRNA processing, non-coding RNA processing, differentiation and chromatin remodeling. In addition, MYC has been shown to modulate adhesion and opposing processes such as proliferation and differentiation. While MYC induced proliferation has been shown to be directly regulated at the promoter of cell cycle regulators such as CDK4, the underlying mechanisms for MYC induced differentiation were thought to be indirect. My work indicates that indeed MYC binds and transcriptionally regulates the promoters of at least 15% of the genes in the genome of mouse epidermal cells, including genes involved in epidermal differentiation, as shown by the widespread binding of MYC to the epidermal differentiation complex (EDC) in mouse chromosome 3. In particular, as it has been shown by others [Guccione et al., 2006], MYC binding was widespread accross the genome and at the EDC, in particular, overlapping with a chromatin mark generally found at active genes, H3K4me3. My work shows, that enrichment for this chromatin mark in the epi-

dermis, does not change following MYC activation, supporting a model where the deposition of H3K4me3 is independent of MYC.

Overall, MYC induces rapid transcriptional changes to a large proportion of genes in undifferentiated proliferating keratinocytes. This was observed following analysis of the gene expression profiles of K14MycER mice, where MYC was induced either one to six days, revealing that most target genes were up- or downregulated immediately after 1 day induction. Interestingly, EDC genes comprised the only group of genes with a substantial delay in activation upon MYC induction (only after 4 days). This observation led to the hypothesis that the EDC cluster might require remodeling before initiating a transcriptional response. I have shown that upon MYC activation, a selected set of epidermal differentiation-specific regulators is removed, while another set is placed at the promoters of EDC genes. These observations suggest that MYC controls the trancription of these genes by direct binding to the promoter regions following recruitment of a differentiation specific regulatory TF network. I observed that KLF4 and OVOL1 were some of the regulators involved in this network. Both TFs were recruited to the EDC upon MYC induction, suggesting that these might replace MYC at the promoter of the EDC genes. In particular, KLF4 has been shown to possibly regulate the *Sprr* family of genes. In addition, previous work demonstrated that KLF4 [Segre et al., 1999] and OVOL1 [Teng et al., 2007] are essential for establishment of the barrier function of the skin, negatively regulating Myc expression.

In my work I have also shown that there is a group of regulators that is displaced from the EDC upon MYC activation, which comprises CEBPα, MXI1 and SIN3A. My data revealed that SIN3A and MYC target a large proportion of common genes, known to be involved in proliferation and differentiation in the skin. Previously, SIN3A has been defined as an important regulator of testis [Payne et al., 2010] and adult muscle homeostasis [VanOevelen et al., 2010] as well as a regulator of the myotube differentiation process, therefore it does not seem surprising that SIN3A might as well have a role on epidermal homeostasis. Although the biological role of SIN3A in the epidermal differentiation specific network has not been fully elucidated, one possible mechanism of action might

be through detection of DNA-bound MYC at the EDC and removal via deacetylation, since MYC acetylation decreases upon SIN3A overexpression, as well as its half-life. Removal of MYC from the promoter regions of EDC genes facilitates recruitment of MYC antagonists by SIN3A. One of MYC antagonists, MXI1, correlated with SIN3A in terms of location across the EDC and was enriched in wild-type and absent in K14MycER epidermis. Binding of MXI1 appears to strongly depend on the availability of its binding motif, the E-box (for which it competes with MYC), rather than on the levels of SIN3A, as MXI1 enrichment in *Sin3a* depleted cells was comparable to wild-type.

The fact that overexpression of *Myc* in the epidermis prevents SIN3A binding, indicates that in these conditions SIN3A is unable to form a stable complex with MYC in order to induce it's degradation, or stoichiometrically the number of molecules for SIN3A and MYC is largely unbalanced, in a way that not enough MYC molecules are targeted for degradation. It is possible that the interaction between MYC and SIN3A is indirect, via other core-proteins mediating the deacetylase enzymatic activity, and not directly via the PAH2 domain of SIN3A, as it has been described for MXD proteins. One possible candidate mediating MYC deacetylation via SIN3A would be YY1, which has been shown to directly interact with both proteins and to also cause degradation of MYC, although this is still under debate [Gordon et al., 2006; Parija and Das, 2003; Yang et al., 1996].

SIN3A constitutes one of the few chromatin remodelers for which a direct link with a TF has been described during epidermal stratification. Indeed, the process of how chromatin remodelers (e.g DNA methyltransferase 1 DNMT1, histone demethylase JMJD3, histone acetylases 1 and 2, chromatin modifying enzymes Brg1 and Mi-2β and the polycomb group Ezh2) and TFs are coordinately regulated to establish a skin specific regulatory network has been poorly understood. Recently, in an effort to elucidate these interactions, Botchkarev and colleagues have shown that deletion of the higher order genome organizer *Satb1* in epidermal progenitors, prevents activation of genes in the EDC locus [Truong et al., 2006]. In the absence of SATB1, decompression of the EDC locus is observed, specifically in the central domain, resulting in a marked downregulation of termi-

nal differentiation-associated genes. As a consequence of *Satb1* deletion, specific morphogical changes in the epidermis are observed, such as: thinning of the granular layer and decrease of the epidermal thickness. Interestingly, Botchkarev work also identified *Satb1* as a direct downstream target of the TF p63, a known master regulator of epidermal development and homeostasis. At the same time, Driskell and colleagues identified another chromatin remodeler and known target of MYC, SETD8 (monomethyltransferase of H4K20), which is also required for normal p63 expression in skin [Driskell et al., 2011]. The role of SATB1 is to induce remodeling of the chromatin architecture of the EDC by compression of the central domain of the locus containing differentiation associated genes, but this information is still lacking for SETD8. Neverthless, it is possible a scenario where SETD8, in combination with SATB1 cooperatively bind to a region of the EDC designated as the 'gene desert'. This region might contain evolutionary conserved regulatory sequences important for the formation of 3 dimensional (3D) loop structures. The 3D loops allow the interaction of distal- and promoter-regions and are important for gene transcriptional regulation. In skin, information regarding the role of the 'gene desert' present in the EDC is limited, but studies in the *Hoxd* cluster during limb development have shown that gene desert regions, also designated as 'regulatory archipelagos' , contain several enhancer like-sequences that contribute to gene expression [Montavon et al., 2011]. Presumably, such enhancer-like sequences might be present in the EDC 'gene desert' and therefore it would be interesting to identify enhancer regions (for example using H3K4me1 or H3K27Ac as markers) as well apply the use of the chromosome conformation capture technique (3C) with ChIP (ChIP-3C) [Fullwood and Ruan, 2009] to identify potential interaction spots between distal- and promoter-regions at the EDC during epidermal maturation.

Overall this study identified that MYC transcriptional functions in the epidermis are controlled by SIN3A. The activity of both proteins appears crucial for maintenance of epidermal homeostais, as perturbation of these proteins expression affects epidermal morphology. The right balance between MYC and SIN3A prevents hyperproliferation or differentiation, therefore rescuing the skin from diseases such as cancer or psoriasis. In the future, it would be interesting to

study if the specific process of degradation of MYC via deacetylation, possibly exploring the ubiquitin proteosome pathway. Also, it would be exciting to explore if overexpression of SIN3A *in vivo* in basal undifferentiated keratinocytes is able to prevent differentiation and/or proliferation and wether mutations in the *Sin3a* locus might predispose to the formation of epidermal tumours. Lastly, the possibility that other TFs, such as KLF4 and OVOL1, might also interact with the MYC protein is very likely, and therefore it would be valuable to perform TF location at various time-points to understand the tissue specific regulatory networks, during the differentiation process in skin, as well as sequential chromatin immunoprecipitation experiments to identify other MYC interactors important in the process.

In summary my work has shown that:

1. MYC directly regulates genes involved in cell adhesion and proliferation in mouse epidermal stem and progenitor cells.
2. MYC regulates genes involved in epidermal specific differentiation.
3. MYC binding induces remodeling of the occupancy of tissue-specific transcriptional regulators, an effect that is enhanced at the promoter of epidermal lineage specific genes.

Appendix

Gene	**$\log_2$ fold-change**
Krtap16-4	-4.406094451
Krtap16-9	-4.369305888
Krt33b	-4.319155808
Krt33a	-4.274609987
Krt81	-4.247673801
Krt86	-4.167640493
S100a3	-4.160445546
Krtap9-1	-4.160125002
Krtap16-9	-4.136371955
Krtap5-1	-4.092171413
Krtap4-1	-4.086366855
Krtap11-1	-4.044824358
Krtap6-2	-4.04300514
Krt34	-4.008367231
Krtap3-1	-3.981801044
Krt86	-3.977885451
Krt73	-3.962887702
Krtap6-1	-3.955978334
Krtap4-16	-3.922609954
Krtap6-2	-3.896878614
Krtap17-1	-3.895732922
AK173067	-3.892441163

Gene	$\log_2$ fold-change
Krtap2-4	-3.873521483
Krtap7-1	-3.871735756
Krtap16-7	-3.871420502
Vsig8	-3.832521374
Krt86	-3.773462007
AK020703	-3.721535688
Krt71	-3.713099818
Krtap16-8	-3.698839829
Krtap1-5	-3.684733773
Krtap16-10	-3.667033255
Krt31	-3.661278777
Krtap5-2	-3.63879009
Krtap31-2	-3.628625449
Krtap4-7	-3.610565271
Krtap31-2	-3.582216079
AY026312	-3.576947317
Krt35	-3.567152982
Krtap4-13	-3.553960528
Cryba4	-3.547299745
2310033E01Rik	-3.441872202
RP23-212C14.7	-3.439127269
Krtap10-10	-3.433411048
Ly6g6d	-3.425286804
Krtap1-4	-3.395323943
AK020694	-3.393646475
Cyp2g1	-3.390027167
LOC100040214	-3.386898776
Psors1c2	-3.367115852
Krt28	-3.366392537
Krt72	-3.320526507
Krt27	-3.308350788

Gene	$\log_2$ fold-change
Krt83	-3.265051131
Krt26	-3.232622758
Krt86	-3.146452147
LOC100040201	-3.143534867
AK017438	-3.119866462
Krtap26-1	-3.09026475
Adh6b	-3.035552698
Lrrc15	-3.03306489
Crym	-2.981082108
Krtap26-1	-2.978715784
AK020696	-2.966013187
Cpm	-2.957236435
Krtap13-1	-2.945094031
Gjb2	-2.923630369
Krt73	-2.921231518
Krtap9-3	-2.898023266
Gjb2	-2.876692122
Krtap6-3	-2.856134382
Prr9	-2.834858389
Sct	-2.817960419
AK220314	-2.748579524
Ctse	-2.738962071
Si	-2.712885358
Tchhl1	-2.690342596
A030003K21Rik	-2.662221347
S100a7a	-2.661157797
BC048518	-2.65727806
Padi1	-2.648052855
D730001G18Rik	-2.631668835
Cpm	-2.610117529
Gjb2	-2.589816667

Gene	**$\log_2$ fold-change**
Cyp2g1	-2.571638167
AK009595	-2.536481843
NR001463	-2.487222583
Krt84	-2.442914182
Gnmt	-2.415183936
Fam26d	-2.402116649
Krtap14	-2.371758828
Gjb6	-2.337016334
Krtap16-7	-2.311637567
Krtap16-5	-2.307255311
Si	-2.304274608
Krt36	-2.289411262
Dlx3	-2.276098249
Mlana	-2.245948402
BC039632	-2.240736683
Chac1	-2.184681333
Krt82	-2.14577175
Ctps	-2.125399737
2310007B03Rik	-2.113100904
Ctps	-2.072317051
AK009595	-2.023613005
Dclk3	-2.008677417
Krtap16-10	-1.996617509
Ctps	-1.990219768
Slc7a8	-1.970057002
Dct	-1.957346269
Krt82	-1.9340153
Fbp1	-1.923199106
Eef2	-1.899222393
NR001463	-1.881815084
AK037168	-1.875285882

Gene	$\log_2$ fold-change
Tmem90a	-1.868944521
BC042411	-1.859516166
Krtap16-1	-1.835449142
Hspa8	-1.82749694
Slc40a1	-1.822658096
Dusp2	-1.792051514
Akr1c18	-1.783154767
AK173067	-1.782584613
Upp1	-1.769756477
Otop2	-1.760150203
Tyrp1	-1.756218973
Erdr1	-1.735490805
Krtap15	-1.733706352
Sytl2	-1.727567885
2310033E01Rik	-1.723180785
Vsig8	-1.707512732
Ppp1ca	-1.704595687
Bhlha9	-1.70459358
Dusp14	-1.701908657
Fxyd4	-1.684756511
Mt4	-1.681362374
Dct	-1.669290134
Eif5a	-1.66108632
Atp13a4	-1.657298575
Gp9	-1.627712717
Eef2	-1.627619225
EG433923	-1.601780498
Casp14	-1.586549749
Fam46b	-1.582392579
4930438A08Rik	-1.57116359
Foxe1	-1.567077225

Gene	$\log_2$ fold-change
Alox8	-1.557238761
Slc39a8	-1.556398185
Lyg2	-1.549592805
Krtap31-1	-1.539568232
Tro	-1.53909724
Pitrm1	-1.537337291
Sprr1b	-1.522700856
Sfn	-1.518027649
Slc4a1	-1.517745223
Ass1	-1.506479479
Dnase1l2	-1.505609081
Msx2	-1.500298966
Eraf	-1.493270608
Sp6	-1.492466906
Eef2	-1.488002939
Dnajc6	-1.483089091
Msx1	-1.479856359
Mlf2	-1.472757887
Gpnmb	-1.472542841
Fzd5	-1.434833335
D12Ertd553e	-1.419990904
Sp6	-1.419120718
Tyrp1	-1.414240573
Gabrp	-1.399854425
6330442E10Rik	-1.399150495
Rtkn2	-1.392510144
Krt36	-1.392055711
Hnrnpa2b1	-1.387855001
Fam26d	-1.387030389
Fdps	-1.383267304
Dnase1l2	-1.382429465

Gene	**$\log_2$ fold-change**
Mycl1	-1.376456394
Rab15	-1.376335597
Hnrnpa1	-1.375451707
Cct3	-1.366837538
Ovol1	-1.359112001
Slc5a5	-1.358949143
Tagln3	-1.358313477
Cnfn	-1.355636961
Eif5a	-1.354616748
Otub2	-1.354539253
Krtap12-1	-1.348906882
Wnt5a	-1.347344574
Zdhhc13	-1.346015865
Mfsd2	-1.339305332
Nkd2	-1.338315702
Slc7a5	-1.335802548
AI646023	-1.331901864
Rnf222	-1.330337048
Spint1	-1.325041113
Zdhhc13	-1.319867671
Fgf22	-1.317585038
AK003073	-1.315967683
Rnaset2b	-1.315064878
Cnfn	-1.31190376
Slc6a13	-1.311683375
Gcat	-1.306003204
Krtap8-2	-1.292335361
Shh	-1.292299123
Mup2	-1.28756728
Gng13	-1.287497159
Ptbp1	-1.286699036

Gene	**$\log_2$ fold-change**
Slc39a6	-1.283150789
Bmp8a	-1.281430259
Serinc2	-1.281380419
Edn2	-1.277450255
Krtap5-4	-1.272545192
Tubb6	-1.269879462
Serinc2	-1.267810497
Nop58	-1.267409942
Eif4a1	-1.264260105
Lmnb1	-1.259126341
AK137397	-1.256515702
Erdr1	-1.253432504
Rars	-1.25144353
Dnase1l2	-1.246488416
Mki67	-1.243872968
AK082735	-1.241038183
Rps27a	-1.234746142
Actb	-1.230763404
Calr	-1.23047366
1110012J17Rik	-1.229225933
Cdc2a	-1.228338285
S100a14	-1.227315443
Krt75	-1.227136572
Cited4	-1.224296137
NR001463	-1.222655277
Tyrp1	-1.217248529
Otub2	-1.208183753
4732456N10Rik	-1.208175132
Cyp2d22	-1.205668831
Ivl	-1.202504913
ASK2	-1.195744553

Gene	**$\log_2$ fold-change**
Ranbp1	-1.186329269
Cyp17a1	-1.184797116
Tpm1	-1.184514584
Dnajc6	-1.182243267
Lsr	-1.179539666
Hnrnpk	-1.179520469
AK031134	-1.173947995
Hmgb2	-1.172664605
Nfil3	-1.172202172
Tnc	-1.16890659
Hist1h2ak	-1.167115782
Sqle	-1.165340017
Hist1h2ah	-1.164319131
Ccbl1	-1.164097665
Cux1	-1.162710542
Pik3r3	-1.162070704
Gnmt	-1.161504626
Gprc5a	-1.160743864
Krtap5-5	-1.158313245
AK008417	-1.157498305
Fzd10	-1.148479177
BC003885	-1.142955319
D4Bwg0951e	-1.14118881
Pla2g2e	-1.140170907
Mfap3l	-1.138526417
Npm3	-1.136696225
Rnd3	-1.135318406
Ccbl1	-1.132050033
Atp6v0d1	-1.130820049
AK079261	-1.130716432
Sprr1a	-1.129493205

Gene	**$\log_2$ fold-change**
Krt36	-1.129159387
Mrpl3	-1.126900297
Acot7	-1.126866243
St14	-1.126088013
Fads3	-1.124300718
Nup210	-1.122380191
Acsm3	-1.122242658
AK052609	-1.122051536
Uck2	-1.12064945
2610029G23Rik	-1.117250918
Gpc3	-1.116597488
Fzd10	-1.115804231
Hspd1	-1.114763083
Eif2s3x	-1.110135182
AK034531	-1.108778614
Slc25a37	-1.106269191
Atp12a	-1.105233172
Tgm3	-1.10516005
Ephb1	-1.100751373
Acaa2	-1.100690687
Upp1	-1.099319558
Lyg2	-1.096166404
Birc5	-1.094057833
Vangl2	-1.093921633
Top2a	-1.090717172
Ivl	-1.08939805
Ptbp1	-1.087294325
Fabp5	-1.085636736
Hist1h2ad	-1.085328792
Nme1	-1.085219693
Ard1a	-1.081185638

Gene	**$\log_2$ fold-change**
C330005M16Rik	-1.080866798
Upp1	-1.079064966
Eif3i	-1.078798482
Cxcl14	-1.076886316
Rnaset2b	-1.076343244
Cdk4	-1.075316741
Hoxc13	-1.075153438
Krtap5-4	-1.073134498
Ctse	-1.067900515
Hopx	-1.066619091
Slc25a37	-1.063207038
Hist1h2af	-1.060739035
ENV	-1.060045996
Acot1	-1.058592562
Krt82	-1.053108776
Mup2	-1.052838957
Cytsb	-1.051989696
Hnrnpa1	-1.049051306
Hist1h2ah	-1.048233524
Rpl13a	-1.047588935
Cenpa	-1.045776855
Lypla2	-1.043644171
H2afx	-1.038912234
Abhd2	-1.038585344
Oca2	-1.037314046
Tspan6	-1.035560718
Psmd7	-1.034437506
Acpl2	-1.034313482
Cxcl14	-1.033682484
Npm3	-1.033374583
Unc5b	-1.032435227

Gene	$\log_2$ fold-change
E2f2	-1.030809693
Ptbp1	-1.029961801
Frag1	-1.028222774
Rpgrip1	-1.025489508
Fzr1	-1.025463977
Tpm1	-1.025328855
Rbbp7	-1.024228811
Acaa2	-1.021185653
Pbk	-1.018999491
Rab1b	-1.018907391
Otub2	-1.018037178
Eif2b4	-1.017827053
Dnase1l2	-1.017664334
Clu	-1.015135375
Actn4	-1.014558124
Slc1a4	-1.013841419
1700019N12Rik	-1.013280876
Acot7	-1.013177076
Cldn10	-1.01167167
Nhp2	-1.011492892
Foxq1	-1.009518251
Birc5	-1.008187431
Rab25	-1.005347967
5730437N04Rik	-1.004548525
Ptgds	-1.004437679
Tspan3	-1.004435242
Cdh6	-1.003234531
Uck2	-1.002638023

Gene	$\log_2$ fold-change

Table 1: List of genes repressed in K14Myc$^{\Delta/\Delta}$ mice. Majority of the genes are either related to keratins or to regulators of the differentiation process in the epidermis. Data represents normalized Log2 fold changes of a minimum of four biological replicates (n=4) and P-values below 0.05.

References

J Adams and S Cory. Myc oncogene activation in B and T lymphoid tumours. *Proceedings of the Royal Society of London*, 226(1242):59–72, 1985. 40

S Adhikary and M Eilers. Transcriptional regulation and transformation by Myc proteins. *Nature Reviews in Molecular Cell Biology*, 6(8):635–645, 2005. 28, 30, 33, 41

M Akiyama, T Smith, and H Shimizu. Changing patterns of localization of putative stem cells in developing human hair follicles. *The Journal of Investigative Dermatology*, 114(2):321–327, 2000. 4

I Alboran, R O'Hagan, F Gärtner, B Malynn, L Davidson, R Rickert, K Rajewsky, R DePinho, and F Alt. Analysis of C-MYC function in normal cells via conditional gene-targeted mutation. *Immunity*, 14(1):45–55, 2001. 46

L Alland, R Muhle, H Hou, J Potes, L Chin, N Schreiber-Agus, and R DePinho. Role for N-CoR and histone deacetylase in Sin3-mediated transcriptional repression. *Nature*, 387(1):49–55, 1997. 31

M Allen, M Grachtchouk, H Sheng, V Grachtchouk, A Wang, L Wei, J Liu, A Ramirez, D Metzger, P Chambon, J Jorcano, and A Dlugosz. Hedgehog signaling regulates sebaceous gland development. *Cancer Research*, 163(6): 2173–2178, 2003. 9

S Alowami, G Qing, E Emberley, L Snell, and P Watson. Psoriasin (S100A7) expression is altered during skin tumorigenesis. *BioMed Central Dermatology*, 3:1, 2003. 22

B Amati, S Dalton, M Brooks, T Littlewood, G Evan, and H Land. Transcriptional activation by the human c-Myc oncoprotein in yeast requires interaction with Max. *Nature*, 359(1):432–425, 1992. 29

N Ambartsumian, J Klingelhöfer, M Grigorian, C Christensen, M Kriajevska, E Tulchinsky, G Georgiev, V Berezin, E Bock, J Rygaard, R Cao, Y Cao, and E Lukanidin. The metastasis-associated Mts1(S100A4) protein could act as an angiogenic factor. *Oncogene*, 20(34):4685–4695, 2001. 22

C Amin, A Wagner, and N Hay. Sequence-specific transcriptional activation by Myc and repression by Max. *Molecular and Cellular Biology*, 13(1):383–390, 1993. 29

Y Amoh, L Li, K Katsuoka, S Penman, and R Hoffman. Multipotent nestin-positive, keratin-negative hair-follicle bulge stem cells can form neurons. *Proceedings of the National Academy of Sciences of the United States of America*, 102(15):5530–5534, 2005. 8

B Andersen, W Weinberg, O Rennekampff, R McEvilly, J Bermingham, F Hooshmand, V Vasilyev, J Hansbrough, M Pittelkow, S Yuspa, and M Rosenfeld. Functions of the POU domain genes Skn-1a/i and Tst-1/Oct-6/SCIP in epidermal differentiation. *Genes & Development*, 11(14):1873–1884, 1997. 25

T Andl, K Ahn, A Kairo, E Chu, L Wine-Lee, S Reddy, N Croft, J Cebra-Thomas, D Metzger, P Chambon, K Lyons, Y Mishina, J Seykora, E Crenshaw, and S Millar. Epithelial Bmpr1a regulates differentiation and proliferation in postnatal hair follicles and is essential for tooth development. *Development*, 131(10):2257–2268, 2004. 8

D Armstrong, K McKenna, and A Hughes. A novel insertional mutation in loricrin in Vohwinkel's Keratoderma. *The Journal of Investigative Dermatology*, 111 (4):702–704, 1998. 20

I Arnold and F Watt. c-Myc activation in transgenic mouse epidermis results in mobilization of stem cells and differentiation of their progeny. *Current Biology*, 11(8):558–568, 2001. 9, 24, 37, 39, 42, 45, 46

W Atchley and W Fitch. Myc and Max: molecular evolution of a family of proto-oncogene products and their dimerization partner. *Proceedings of the National Academy of Sciences of the United States of America of the United States of America*, 92(22):10217–10221, 1995. 28

D Ayer, L Kretzner, and R Eisenman. Mad: a heterodimeric partner for Max that antagonizes Myc transcriptional activity. *Cell*, 72(2):211–222, 1993. 31

D Ayer, Q Lawrence, and R Eisenman. Mad-Max transcriptional repression is mediated by ternary complex formation with mammalian homologs of yeast repressor Sin3. *Cell*, 80(5):767–776, 1995. 31

S Balasubramanian, T Efimova, and R Eckert. Green tea polyphenol stimulates a Ras, MEKK1, MEK3, and p38 cascade to increase activator protein 1 factor-dependent involucrin gene expression in normal human keratinocytes. *The Journal of Biological Chemistry*, 277(3):1828–1836, 2002. 19

S Banks-Schlegel and H Green. Involucrin synthesis and tissue assembly by keratinocytes in natural and cultured human epithelia. *The Journal of Cell Biology*, 90(3):732–737, 1981. 19

Y Barrandon and H Green. Three clonal types of keratinocyte with different capacities for multiplication. *Proceedings of the National Academy of Sciences of the United States of America*, 84(8):2302–2306, 1987. 11

T Baudino, C McKay, H Pendeville-Samain, J Nilsson, K Maclean, E White, A Davis, J Ihle, and J Cleveland. c-Myc is essential for vasculogenesis and angiogenesis during development and tumor progression. *Genes & Development*, 16(19):2530–2543, 2002. 35

R Baxter and J Brissette. Role of the nude gene in epithelial terminal differentiation. *The Journal of Investigative Dermatology*, 118(2):303–309, 2002. 26

S Benitah, M Frye, M Glogauer, and F Watt. Stem cell depletion through epidermal deletion of Rac1. *Science*, 309(5736):933–935, 2005. 9

S Berberich and M Cole. Casein kinase II inhibits the DNA-binding activity of Max homodimers but not Myc/Max heterodimers. *Genes & Development*, 6 (2):166–176, 1992. 29, 33

J Bickenbach. Identification and Behavior of Label-retaining Cells in Oral Mucosa and Skin. *Journal of Dental Research*, 60(3 Suppl):1611–1620, 1981. 3

J Bickenbach and E Chism. Selection and extended growth of murine epidermal stem cells in culture. *Experimental Cell Research*, 244(1):184–195, 1998. 3

D Bikle, D Ng, C Tu, Y Oda, and Z Xie. Calcium and vitamin D-regulated keratinocyte differentiation. *Molecular and Cellular Endocrinology*, 177(1-2): 161–71, 2001. 19

T Blackwell, J Huang, A Ma, L Kretzner, F Alt, R Eisenman, and H Weintraub. Binding of myc proteins to canonical and noncanonical DNA sequences. *Molecular and Cellular Biology*, 13(9):5216–5224, 1993. 29

E Blackwood, L Kretzner, and R Eisenman. Myc and Max function as a nucleoprotein complex. *Current Opinion in Genetics & Development*, 2(2):227–235, 1992. 29, 32

C Blanpain and E Fuchs. Epidermal stem cells of the skin. *Annual Review of Cell and Developmental Biology*, 22:339–373, 2006. 10

C Blanpain and E Fuchs. Epidermal homeostasis: a balancing act of stem cells in the skin. *Nature Reviews in Molecular Cell Biology*, 10(3):207–217, 2009. 4, 23, 41

C Blanpain, W Lowry, A Geoghegan, L Polak, and E Fuchs. Self-renewal, multipotency, and the existence of two cell populations within an epithelial stem cell niche. *Cell*, 118(5):635–648, 2004. 5

K Blyth, A Terry, M O'Hara, E Baxter, M Campbell, M Stewart, L Donehower, D Onions, J Neil, and E Cameron. Synergy between a human c-myc transgene and p53 null genotype in murine thymic lymphomas: contrasting effects of homozygous and heterozygous p53 loss. *Oncogene*, 10(9):1717–1723, 1995. 40

C Bouchard, K Thieke, A Maier, R Saffrich, J Hanley-Hyde, W Ansorge, S Reed, P Sicinski, J Bartek, and M Eilers. Direct induction of cyclin D2 by Myc contributes to cell cycle progression and sequestration of p27. *The European Molecular Biology Organization Journal*, 18(19):5321–5333, 1999. 40

C Bouchard, O Dittrich, A Kiermaier, K Dohmann, A Menkel, M Eilers, and B Lüscher. Regulation of cyclin D2 gene expression by the Myc/Max/Mad network: Myc-dependent TRRAP recruitment and histone acetylation at the cyclin D2 promoter. *Genes & Development*, 15(16):2042–2047, 2001. 34

D Brash and J Pontén. Skin precancer. *Cancer Surveys*, 32:69–113, 1998. 41

K Braun and D Prowse. Distinct epidermal stem cell compartments are maintained by independent niche microenvironments. *Stem Cell Reviews*, 2(3):221–231, 2006. 4, 8

K Braun, C Niemann, U Jensen, J Sundberg, V Silva-Vargas, and F Watt. Manipulation of stem cell proliferation and lineage commitment: visualisation of label-retaining cells in wholemounts of mouse epidermis. *Development*, 130 (21):5241–55, 2003. 9

M Broome, D Ryan, and R Eckert. S100 Protein Subcellular Localization During Epidermal Differentiation and Psoriasis. *Journal of Histochemistry & Cytochemistry*, 51(5):675–685, 2003. 22

S Brown, C Tilli, B Jackson, A Avilion, M MacLeod, L Maltais, R Lovering, and C Byrne. Rodent Lce gene clusters; new nomenclature, gene organization, and divergence of human and rodent genes. *The Journal of Investigative Dermatology*, 127(7):1782–1786, 2007. 18

M Buck and J Lieb. ChIP-chip: considerations for the design, analysis, and application of genome-wide chromatin immunoprecipitation experiments. *Genomics*, 83(3):349–60, 2004. 42

J Bull, S Pelengaris, S Hendrix, C Chronnell, M Khan, and M Philpott. Ectopic expression of c-Myc in the skin affects the hair growth cycle and causes an

enlargement of the sebaceous gland. *The British Journal of Dermatology*, 152 (6):1125–1133, 2005. 9

E Candi, G Melino, G Mei, E Tarcsa, S Chung, L Marekov, and P Steinert. Biochemical, structural, and transglutaminase substrate properties of human loricrin, the major epidermal cornified cell envelope protein. *The Journal of Biological Chemistry*, 270:26382–26390, 1995. 19, 21

E Candi, R Schmidt, and G Melino. The cornified envelope: a model of cell death in the skin. *Nature Reviews in Molecular Cell Biology*, 6(4):328–340, 2005. 2, 16, 19, 20

R Cao, L Wang, H Wang, L Xia, H Erdjument-Bromage, P Tempst, R Jones, and Y Zhang. Role of histone H3 lysine 27 methylation in Polycomb-group silencing. *Science*, 298(5595):1039–1043, 2002. 24

T Chang, D Yu, YS Lee, E Wentzel, D Arking, K West, C Dang, A Thomas-Tikhonenko, and J Mendell. Widespread microRNA repression by Myc contributes to tumorigenesis. *Nature Genetics*, 40(1):43–50, 2008. 29, 86

P Channavajhala and D Seldin. Functional interaction of protein kinase CK2 and c-Myc in lymphomagenesis. *Oncogene*, 21(34):5280–5288, 2002. 33

E Clayton, D Doupé, A Klein, D Winton, B Simons, and P Jones. A single type of progenitor cell maintains normal epidermis. *Nature*, 446(7132):185–189, 2007. 13, 15

J Connelly, J Gautrot, B Trappmann, D Tan, G Donati, W Huck, and F Watt. Actin and serum response factor transduce physical cues from the microenvironment to regulate epidermal stem cell fate decisions. *Nature Cell Biology*, 12 (7):711–718, 2010. 12

G Cotsarelis. Gene expression profiling gets to the root of human hair follicle stem cells. *Journal of Clinical Investigation*, 116(1):19–22, 2006. 7

G Cotsarelis, T Sun, and R Lavker. Label-retaining cells reside in the bulge area of pilosebaceous unit: implications for follicular stem cells, hair cycle, and skin carcinogenesis. *Cell*, 61(7):1329–1337, 1990. 4, 5

M Couillard and M Trudel. c-myc as a modulator of renal stem/progenitor cell population. *Developmental Dynamics*, 238(2):405–414, 2009. 36

C Cowan and A Hyman. Asymmetric cell division in C. elegans: cortical polarity and spindle positioning. *Annual Review of Cell and Developmental Biology*, 20: 427–453, 2004. 11

V Cowling and M Cole. The Myc transactivation domain promotes global phosphorylation of the RNA polymerase II carboxy-terminal domain independently of direct DNA binding. *Molecular and Cellular Biology*, 27(6):2059–2073, 2007. 30

J Crish, J Howard, T Zaim, S Murthy, and R Eckert. Tissue-specific and differentiation-appropriate expression of the human involucrin gene in transgenic mice: an abnormal epidermal phenotype. *Differentiation*, 53(3):191–200, 1993. 19

X Dai and J Segre. Transcriptional control of epidermal specification and differentiation. *Current Opinion in Genetics & Development*, 14(5):485–491, 2004. 10, 25, 26, 41

M Dajee, M Lazarov, J Zhang, T Cai, C Green, A Russell, M P Marinkovich, S Tao, Q Lin, Y Kubo, and P Khavari. NF-kappaB blockade and oncogenic Ras trigger invasive human epidermal neoplasia. *Nature*, 421(6923):639–643, 2003. 41

C Dang, K O'Donnell, K Zeller, T Nguyen, R Osthus, and F Li. The c-Myc target gene network. *Seminars in Cancer Biology*, 16(4):253–264, 2006. 29, 34, 95

J Dannenberg, G David, S Zhong, J Torre, W Wong, and R Depinho. mSin3A corepressor regulates diverse transcriptional networks governing normal and neoplastic growth and survival. *Genes & Development*, 19(13):1581–1595, 2005. 46

A Davis, M Wims, G Spotts, S Hann, and A Bradley. A null c-myc mutation causes lethality before 10.5 days of gestation in homozygotes and reduced fer-

tility in heterozygous female mice. *Genes & Development*, 7(4):671–682, 1993. 35

C D'Cruz, E Gunther, R Boxer, J Hartman, L Sintasath, S Moody, J Cox, S Ha, G Belka, A Golant, R Cardiff, and L Chodosh. c-MYC induces mammary tumorigenesis by means of a preferred pathway involving spontaneous Kras2 mutations. *Nature Medicine*, 7(2):235–239, 2001. 41

C DeGuzmanStrong, S Conlan, C Deming, J Cheng, K Sears, and J Se. A milieu of regulatory elements in the epidermal differentiation complex syntenic block: implications for atopic dermatitis and psoriasis. *Human Molecular Genetics*, 19(8):1453–1460, 2010. 18

M Delehedde, S Cho, M Sarkiss, S Brisbay, M Davies, A El-Naggar, and T McDonnell. Altered expression of bcl-2 family member proteins in nonmelanoma skin cancer. *Cancer*, 85(7):1514–1522, 1999. 41

A Deucher, T Efimova, and R Eckert. Calcium-dependent involucrin expression is inversely regulated by protein kinase C (PKC)alpha and PKCdelta. *The Journal of Biological Chemistry*, 277(19):17032–17040, 2002. 19

P Djian, K Easley, and H Green. Targeted Ablation of the Murine Involucrin Gene. *The Journal of Cell Biology*, 151(2):381–388, 2000. 19

A Dlugosz and S Yuspa. Coordinate changes in gene expression which mark the spinous to granular cell transition in epidermis are regulated by protein kinase C. *The Journal of Cell Biology*, 120(1):217–225, 1993. 19

R Donato. Functional roles of S100 proteins, calcium-binding proteins of the EF-hand type. *Biochimica et Biophysica Acta*, 1450(3):191–231, 1999. 21

K Downs, G Martin, and J Bishop. Contrasting patterns of myc and N-myc expression during gastrulation of the mouse embryo. *Genes & Development*, 3 (6):860–869, 1989. 27

I Driskell, H Oda, S Blanco, E Nascimento, P Humphreys, and M Frye. The histone methyltransferase Setd8 acts in concert with c-Myc and is required to

maintain skin. *The European Molecular Biology Organization journal*, pages 1–14 doi:10.1038/emboj.2011.421, 2011. 152

S Eberhardy and P Farnham. Myc recruits P-TEFb to mediate the final step in the transcriptional activation of the cad promoter. *The Journal of Biological Chemistry*, 277(42):40156–40162, 2002. 30, 34

R Eckert, M Yaffe, J Crish, S Murthy, E Rorke, and J Welter. Involucrin–structure and role in envelope assembly. *The Journal of Investigative Dermatology*, 100 (5):613–617, 1993. 19

R Eckert, J Crish, T Efimova, S Dashti, A Deucher, F Bone, G Adhikary, G Huang, R Gopalakrishnan, and S Balasubramanian. Regulation of involucrin gene expression. *The Journal of Investigative Dermatology*, 123(1):13–22, 2004. 18, 22, 25

M Eilers and R Eisenman. Myc's broad reach. *Genes & Development*, 22(20): 2755–2766, 2008. 27, 28, 29, 95

M Eilers, S Schirm, and J Bishop. The MYC protein activates transcription of the alpha-prothymosin gene. *The European Molecular Biology Organization Journal*, 10(1):133–141, 1991. 31

R Eisenman. Deconstructing myc. *Genes & Development*, 15(16):2023–2030, 2001. 42

A Elson, C Deng, J Campos-Torres, L Donehower, and P Leder. The MMTV/c-myc transgene and p53 null alleles collaborate to induce T-cell lymphomas, but not mammary carcinomas in transgenic mice. *Oncogene*, 11(1):181–190, 1995. 40

G Evan, A Wyllie, C Gilbert, T Littlewood, H Land, M Brooks, C Waters, L Penn, and D Hancock. Induction of apoptosis in fibroblasts by c-myc protein. *Cell*, 69(1):119–128, 1992. 40

E Ezhkova, H Pasolli, J Parker, N Stokes, I Su, G Hannon, A Tarakhovsky, and E Fuchs. Ezh2 orchestrates gene expression for the stepwise differentiation of tissue-specific stem cells. *Cell*, 136(6):1122–1135, 2009. 24, 43

X Feng, YY Liang, M Liang, W Zhai, and X Lin. Direct interaction of c-Myc with Smad2 and Smad3 to inhibit TGF-beta-mediated induction of the CDK inhibitor p15(Ink4B). *Molecular Cell*, 9(1):133–143, 2002. 30

P Fernandez, S Frank, L Wang, M Schroeder, S Liu, J Greene, A Cocito, and B Amati. Genomic targets of the human c-Myc protein. *Genes & Development*, 17(9):1115–1129, 2003. 29, 40

C Ferraris, B Bernard, and D Dhouailly. Adult epidermal keratinocytes are endowed with pilosebaceous forming abilities. *The International Journal of Developmental Biology*, 41(3):491–498, 1997. 13

D Fischer, S Gibbs, P van De Putte, and C Backendorf. Interdependent transcription control elements regulate the expression of the SPRR2A gene during keratinocyte terminal differentiation. *Molecular and Cellular Biology*, 16(10): 5365–5374, 1996. 21

K Foley, G McArthur, C Quéva, P Hurlin, P Soriano, and R Eisenman. Targeted disruption of the MYC antagonist MAD1 inhibits cell cycle exit during granulocyte differentiation. *The European Molecular Biology Organization Journal*, 17(3):774–785, 1998. 31

S Frank, T Parisi, S Taubert, P Fernandez, M Fuchs, HM Chan, D Livingston, and B Amati. MYC recruits the TIP60 histone acetyltransferase complex to chromatin. *The European Molecular Biology Organization Journal*, 4(6):575–580, 2003. 31, 34

M Frye and F Watt. The RNA methyltransferase Misu (NSun2) mediates Myc-induced proliferation and is upregulated in tumors. *Current Biology*, 16(10): 971–981, 2006. 95

M Frye, C Gardner, E Li, I Arnold, and F Watt. Evidence that Myc activation depletes the epidermal stem cell compartment by modulating adhesive interactions with the local microenvironment. *Development*, 130(12):2793–2808, 2003. 9, 13, 24, 29, 42, 77, 95, 99

M Frye, A Fisher, and F Watt. Epidermal stem cells are defined by global histone modifications that are altered by Myc-induced differentiation. *PloS One*, 2(1): e763, 2007. 24

E Fuchs. Scratching the surface of skin development. *Nature*, 445(7130):834–842, 2007. 1

E Fuchs. Finding one's niche in the skin. *Cell Stem Cell*, 4(6):499–502, 2009a. 2, 16

E Fuchs. The tortoise and the hair: slow-cycling cells in the stem cell race. *Cell*, 137(5):811–819, 2009b. 4

E Fuchs and V Horsley. More than one way to skin . . . *Genes & Development*, 22(8):976–985, 2008. 5, 9, 10

M Fullwood and Y Ruan. ChIP-based methods for the identification of long-range chromatin interactions. *Journal of Cellular Biochemistry*, 107(1):30–49, 2009. 152

P Gallant and D Steiger. Myc's secret life without Max. *Cell Cycle*, 8(23): 3848–3853, 2009. 29

G Gallico, N O'Connor, C Compton, O Kehinde, and H Green. Permanent coverage of large burn wounds with autologous cultured human epithelium. *The New England Journal of Medicine*, 311(7):448–851, 1984. 11

A Gandarillas and F Watt. c-Myc promotes differentiation of human epidermal stemcells. *Genes & Development*, 11(21):2869–2882, 1997. 24

A Gandarillas, L Goldsmith, S Gschmeissner, I Leigh, and F Watt. Evidence that apoptosis and terminal differentiation of epidermal keratinocytes are distinct processes. *Experimental Dermatology*, 8(1):71–79, 1999. 40

M Garmyn, M Yaar, N Boileau, C Backendorf, and B Gilchrest. Effect of aging and habitual sun exposure on the genetic response of cultured human keratinocytes to solar-simulated irradiation. *The Journal of Investigative Dermatology*, 99(6):743–748, 1992. 21

U Gat, R DasGupta, L Degenstein, and E Fuchs. De Novo hair follicle morphogenesis and hair tumors in mice expressing a truncated beta-catenin in skin. *Cell*, 95(5):605–614, 1998. 8, 9, 12

A Gazdar. *Anticancer Research*, (1B):261–267. 40

A Gebhardt, M Frye, S Herold, S Benitah, K Braun, B Samans, F Watt, H-P Elsässer, and M Eilers. Myc regulates keratinocyte adhesion and differentiation via complex formation with Miz1. *The Journal of Cell Biology*, 172(1):139–149, 2006. 13, 29

R Gentleman, V Carey, D Bates, B Bolstad, M Dettling, S Dudoit, B Ellis, L Gautier, Y Ge, J Gentry, K Hornik, T Hothorn, W Huber, S Iacus, R Irizarry, F Leisch, C Li, M Maechler, A Rossini, G Sawitzki, C Smith, G Smyth, L Tierney, J Yang, and J Zhang. Bioconductor: open software development for computational biology and bioinformatics. *Genome Biology*, 5(10):R80, 2004. 62

S Ghazizadeh and L Taichman. Multiple classes of stem cells in cutaneous epithelium: a lineage analysis of adult mouse skin. *The European Molecular Biology Organization Journal*, 20(6):1215–1222, 2001. 3, 9

S Gibbs, R Fijneman, J Wiegant, A Van Kessel, P Van De Putte, and C Backendorf. Molecular characterization and evolution of the SPRR family of keratinocyte differentiation markers encoding small proline-rich proteins. *Genomics*, 16(3):630–637, 1993. 21

N Gomez-roman, C Grandori, R Eisenman, and R White. Direct activation of RNA polymerase III transcription by c-Myc. *Nature*, 421(6920):1698–1701, 2003. 29

J Goodliffe, E Wieschaus, and M Cole. Polycomb mediates Myc autorepression and its transcriptional control of many loci in Drosophila. *Genes & Development*, 19(24):2941–2946, 2005. 87

S Gordon, G Akopyan, H Garban, and B Bonavida. Transcription factor YY1: structure, function, and therapeutic implications in cancer biology. *Oncogene*, 25(8):1125–1142, 2006. 151

P Greasley, C Bonnard, and B Amati. Myc induces the nucleolin and BN51 genes: possible implications in ribosome biogenesis. *Nucleic Acids Research*, 28(2):446–453, 2000. 87

A Grinberg, C Hu, and T Kerppola. Visualization of Myc / Max / Mad Family Dimers and the Competition for Dimerization in Living Cells . *Molecular Cell Bilogy*, 24(10):4294–4308, 2004. 31

E Guccione, F Martinato, G Finocchiaro, L Luzi, L Tizzoni, V Dall' Olio, G Zardo, C Nervi, L Bernard, and B Amati. Myc-binding-site recognition in the human genome is determined by chromatin context. *Nature Cell Biology*, 8(7):764–770, 2006. 30, 85, 149

Y Guo, C Niu, P Breslin, M Tang, S Zhang, W Wei, A Kini, G Paner, S Alkan, S Morris, M Diaz, P Stiff, and J Zhang. c-Myc-mediated control of cell fate in megakaryocyte-erythrocyte progenitors. *Blood*, 114(10):2097–2106, 2009. 36

G Hagens, I Masouye, E Augsburger, R Hotz, J Saurat, and G Siegenthaler. Calcium-binding protein S100A7 and epidermal-type fatty acid-binding protein are associated in the cytosol of human keratinocytes. *Biochemical Journal*, 339 (Pt 2):419–427, 1999. 22

P Hall and F Watt. Stem cells: the generation and maintenance of cellular diversity. *Development*, 106(4):619–633, 1989. 3

M Hampsey and D Reinberg. Tails of intrigue: phosphorylation of RNA polymerase II mediates histone methylation. *Cell*, 113(4):429–432, 2003. 83

G Han, A Li, Y-Y Liang, P Owens, W He, S Lu, Y Yoshimatsu, D Wang, P Ten Dijke, X Lin, and X Wang. Smad7-induced beta-catenin degradation alters epidermal appendage development. *Developmental Cell*, 11(3):301–312, 2006. 9

M Hardy. The secret life of the hair follicle. *Trends in Genetics*, 8(2):55–61, 1992. 4

C Hassig, T Fleischer, A Billin, S Schreiber, and D Ayer. Histone deacetylase activity is required for full transcriptional repression by mSin3A. *Cell*, 89(3): 341–347, 1997. 31

B Hatton, P Knoepfler, A Kenney, D Rowitch, I Alborán, J Olson, and R Eisenman. N-myc is an essential downstream effector of Shh signaling during both normal and neoplastic cerebellar growth. *Cancer Research*, 66(17):8655–8661, 2006. 36

K Hatton, K Mahon, L Chin, F Chiu, H Lee, D Peng, S Morgenbesser, J Horner, and R DePinho. Expression and activity of L-Myc in normal mouse development. *Molecular and Cellular Biology*, 16(4):1794–1804, 1996. 27, 35

C Heizmann, G Fritz, and B Schäfer. S100 proteins: structure, functions and pathology. *Frontiers in Bioscience : a journal and virtual library*, 7:d1356–68, 2002. 21

M Hemann, A Bric, J Teruya-Feldstein, A Herbst, J Nilsson, C Cordon-Cardo, J Cleveland, W Tansey, and S Lowe. Evasion of the p53 tumour surveillance network by tumour-derived MYC mutants. *Nature*, 436(7052):807–11, 2005. 34

H Hermeking, C Rago, M Schuhmacher, Q Li, J Barrett, A Obaya, B O'Connell, M Mateyak, W Tam, F Kohlhuber, C Dang, J Sedivy, D Eick, B Vogelstein, and K Kinzler. Identification of CDK4 as a target of c-MYC. *Proceedings of the National Academy of Sciences of the United States of America*, 97(5): 2229–2234, 2000. 40

S Herold, M Wanzel, V Beuger, C Frohme, D Beul, T Hillukkala, H-P Saluz, F Haenel, and M Eilers. Negative regulation of the mammalian UV response by Myc through association with Miz-1. *Molecular Cell*, 10(3):509–521, 2002. 30

S Hoffjan and S Stemmler. On the role of the epidermal differentiation complex in ichthyosis vulgaris, atopic dermatitis and psoriasis. *The British Journal of Dermatology*, 157(3):441–449, 2007. 20

D Hohl, U Lichti, D Breitkreutz, P Steinert, and D Roop. *The Journal of Investigative Dermatology*, (4). 19

D Hohl, P de Viragh, F Amiguet-Barras, S Gibbs, C Backendorf, and M Huber. The small proline-rich proteins constitute a multigene family of differentially regulated cornified cell envelope precursor proteins. *The Journal of Investigative Dermatology*, 104(6):902–909, 1995. 21

K Honeycutt, M Koster, and D Roop. Genes involved in stem cell fate decisions and commitment to differentiation play a role in skin disease. *The Journal of Investigative Dermatology. Symposium Proceedings*, 9(3):261–268, 2004. 40

C Hooker and P Hurlin. Of Myc and Mnt. *Journal of Cell Science*, 119(Pt 2): 208–216, 2006. 32

V Horsley, D O'Carroll, R Tooze, Y Ohinata, M Saitou, T Obukhanych, M Nussenzweig, A Tarakhovsky, and E Fuchs. Blimp1 defines a progenitor population that governs cellular input to the sebaceous gland. *Cell*, 126(3): 597–609, 2006. 9, 10

J Huelsken, R Vogel, B Erdmann, G Cotsarelis, and W Birchmeier. beta-Catenin controls hair follicle morphogenesis and stem cell differentiation in the skin. *Cell*, 105(4):533–545, 2001. 8

P Hurlin, C Quéva, P Koskinen, E Steingrímsson, D Ayer, N Copeland, N Jenkins, and R Eisenman. Mad3 and Mad4: novel Max-interacting transcriptional repressors that suppress c-myc dependent transformation and are expressed during neural and epidermal differentiation. *The European Molecular Biology Organization Journal*, 15(8):5646–5659, 1995. 31

P Hurlin, C Queva, and R Eisenman. Mnt, a novel Max-interacting protein is coexpressed with Myc in proliferating cells and mediates repression at Myc binding sites. *Genes & Development*, 11(1):44–58, 1997. 31

P Hurlin, ZQ Zhou, K Toyo-oka, S Ota, W Walker, S Hirotsune, and A Wynshaw-Boris. Deletion of Mnt leads to disrupted cell cycle control and tumorigene-

sis. *The European Molecular Biology Organization Journal*, 22(18):4584–4596, 2003. 31

A Indra, X Warot, J Brocard, J Bornert, J Xiao, P Chambon, and D Metzger. Temporally-controlled site-specific mutagenesis in the basal layer of the epidermis: comparison of the recombinase activity of the tamoxifen-inducible Cre-ER(T) and Cre-ER(T2) recombinases. *Nucleic Acids Research*, 27(22): 4324–4327, 1999. 37

A Ishida-Yamamoto, J McGrath, H Lam, H Iizuka, R Friedman, and A Christiano. The molecular pathology of progressive symmetric erythrokeratoderma: a frameshift mutation in the loricrin gene and perturbations in the cornified cell envelope. *The American Journal of Human Genetics*, 61(3):581–589, 1997. 20

M Ito and K Kizawa. Expression of calcium-binding S100 proteins A4 and A6 in regions of the epithelial sac associated with the onset of hair follicle regeneration. *The Journal of Investigative Dermatology*, 116(6):956–963, 2001. 22

M Ito, K Kizawa, K Hamada, and G Cotsarelis. Hair follicle stem cells in the lower bulge form the secondary germ, a biochemically distinct but functionally equivalent progenitor cell population, at the termination of catagen. *Differentiation*, 72(9-10):548–557, 2004. 16

M Ito, Y Liu, Z Yang, J Nguyen, F Liang, R Morris, and G Cotsarelis. Stem cells in the hair follicle bulge contribute to wound repair but not to homeostasis of the epidermis. *Nature Medicine*, 11(12):1351–1354, 2005. 13

V Iyer, C Horak, C Scafe, D Botstein, M Snyder, and P Brown. Genomic binding sites of the yeast cell-cycle transcription factors SBF and MBF. *Nature*, 409 (6819):533–538, 2001. 42

V Jaks, N Barker, M Kasper, J Es, H Snippert, H Clevers, and R Toftgå rd. Lgr5 marks cycling, yet long-lived, hair follicle stem cells. *Nature Genetics*, 40(11): 1291–1299, 2008. 5, 7

V Jaks, M Kasper, and R Toftgå rd. The hair follicle-a stem cell zoo. *Experimental Cell Research*, 316(8):1422–1428, 2010. 5, 6, 7

S Jang and P Steinert. Loricrin expression in cultured human keratinocytes is controlled by a complex interplay between transcription factors of the Sp1, CREB, AP1, and AP2 families. *The Journal of Biological Chemistry*, 277(44): 42268–42279, 2002. 25

M Jarnik, P DeViragh, E Schärer, D Bundman, M Simon, D Roop, and Alasdair C Steven. Quasi-normal cornified cell envelopes in loricrin knockout mice imply the existence of a loricrin backup system. *The Journal of Investigative Dermatology*, 118(1):102–109, 2002. 19

K Jensen and F Watt. Single-cell expression profiling of human epidermal stem and transit-amplifying cells: Lrig1 is a regulator of stem cell quiescence. *Proceedings of the National Academy of Sciences of the United States of America*, 103(32):11958–11963, 2006. 12, 40

K Jensen, C Collins, E Nascimento, D Tan, M Frye, S Itami, and F Watt. Lrig1 expression defines a distinct multipotent stem cell population in mammalian epidermis. *Cell Stem Cell*, 4(5):427–439, 2009. 7, 9, 15, 79, 95

K Jensen, R Driskell, and F Watt. Assaying proliferation and differentiation capacity of stem cells using disaggregated adult mouse epidermis. *Nature Protocols*, 5(5):898–911, 2010. 47

U Jensen, X Yan, C Triel, SH Woo, R Christensen, and D Owens. A distinct population of clonogenic and multipotent murine follicular keratinocytes residing in the upper isthmus. *Journal of Cell Science*, 121(Pt 5):609–617, 2008. 5, 41

T Jinquan, H Vorum, C Larsen, P Madsen, H Rasmussen, B Gesser, M Etzerodt, B Honoré, J Celis, and K Thestrup-Pedersen. Psoriasin: a novel chemotactic protein., 1996. 22

P Jones and F Watt. Separation of human epidermal stem cells from transit amplifying cells on the basis of differences in integrin function and expression. *Cell*, 73(4):713–724, 1993. 11

P Jones, B Simons, and F Watt. Sic transit gloria: farewell to the epidermal transit amplifying cell? *Cell Stem Cell*, 1(4):371–381, 2007. 15

S Kanazawa, L Soucek, G Evan, T Okamoto, and B Peterlin. c-Myc recruits P-TEFb for transcription, cellular proliferation and apoptosis. *Oncogene*, 22 (36):5707–5711, 2003. 34

T Kartasova, G Muijen, H Pelt-Heerschap, and P Putte. Novel protein in human epidermal keratinocytes: regulation of expression during differentiation. *Molecular and Cellular Biology*, 8(5):2204–2210, 1988. 21

K Kelly, B Cochran, C Stiles, and P Leder. Cell-specific regulation of the c-myc gene by lymphocyte mitogens and platelet-derived growth factor. *Cell*, 35(3 Pt 2):603–610, 1983. 31, 32

P Khavari. Profiling epithelial stem cells. *Nature Biotechnology*, 22(4):393–394, 2004. 2, 6

J Kim, A Woo, J Chu, J Snow, Y Fujiwara, C Kim, A Cantor, and S Orkin. A Myc network accounts for similarities between embryonic stem and cancer cell transcription programs. *Cell*, 143(2):313–324, 2010. 30, 41

K King, R Ponnamperuma, T Yamashita, T Tokino, L Lee, M Young, and W Weinberg. deltaNp63alpha functions as both a positive and a negative transcriptional regulator and blocks in vitro differentiation of murine keratinocytes. *Oncogene*, 22(23):3635–3644, 2003. 23

A Klein, D Doupé, P Jones, and B Simons. Kinetics of cell division in epidermal maintenance. *Physical Review E*, 76(2):1–13, August 2007. 15

P Knoepfler. Myc goes global: new tricks for an old oncogene. *Cancer Research*, 67(11):5061–5063, 2007. 149

P Knoepfler, P Cheng, and R Eisenman. N-myc is essential during neurogenesis for the rapid expansion of progenitor cell populations and the inhibition of neuronal differentiation. *Genes & Development*, 16(20):2699–2712, 2002. 29, 36

P Knoepfler, XY Zhang, P Cheng, P Gafken, S McMahon, and R Eisenman. Myc influences global chromatin structure. *The European Molecular Biology Organization Journal*, 25(12):2723–2734, 2006. 95

K Kobielak, H Pasolli, L Alonso, L Polak, and E Fuchs. Defining BMP functions in the hair follicle by conditional ablation of BMP receptor IA. *The Journal of Cell Biology*, 163(3):609–623, 2003. 8

P Koch, P Viragh, E Scharer, D Bundman, M Longley, J Bickenbach, Y Kawachi, Y Suga, Z Zhou, M Huber, D Hohl, T Kartasova, M Jarnik, A Steven, and D Roop. Lessons from loricrin-deficient mice: compensatory mechanisms maintaining skin barrier function in the absence of a major cornified envelope protein. *The Journal of Cell Biology*, 151(2):389–400, 2000a. 22

P Koch, P Viragh, E Scharer, D Bundman, M Longley, J Bickenbach, Y Kawachi, Y Suga, Z Zhou, M Huber, D Hohl, T Kartasova, M Jarnik, A Steven, and D Roop. Lessons from loricrin-deficient mice: compensatory mechanisms maintaining skin barrier function in the absence of a major cornified envelope protein. *The Journal of Cell Biology*, 151(2):389–400, 2000b. 22

B Kopnin. Genetic events responsible for colorectal tumorigenesis: achievements and chultrapure waterges. *Tumori*, 79(4), 1993. 40

B Korge, A Ishida-Yamamoto, C Pünter, P Dopping-Hepenstal, H Iizuka, A Stephenson, R Eady, and C Munro. Loricrin mutation in Vohwinkel's keratoderma is unique to the variant with ichthyosis. *The Journal of Investigative Dermatology*, 109(4):604–610, 1997. 20

M Koster and D Roop. Sorting out the p63 signaling network. *The Journal of Investigative Dermatology*, 128(7):1617–1619, 2008. 23

M Koster, S Kim, A Mills, F DeMayo, and D Roop. P63 Is the Molecular Switch for Initiation of an Epithelial Stratification Program. *Genes & Development*, 18(2):126–131, 2004. 23

L Kretzner, E Blackwood, and R Eisenman. Transcriptional activities of the Myc and Max proteins in mammalian cells. *Current topics in Microbiology and Immunology*, 182:435–443, 1992. 29

A Krippner-Heidenreich, R Talanian, R Sekul, R Kraft, H Thole, H Ottleben, and B Lüscher. Targeting of the transcription factor Max during apoptosis: phosphorylation-regulated cleavage by caspase-5 at an unusual glutamic acid residue in position P1. *The Biochemical journal*, 358(Pt 3):705–715, 2001. 33

H Kulessa, G Turk, and B Hogan. Inhibition of Bmp signaling affects growth and differentiation in the anagen hair follicle. *The European Molecular Biology Organization Journal*, 19(24):6664–6674, 2000. 8

C Laherty, W Yang, J Sun, J Davie, E Seto, and R Eisenman. with the mSin3 Corepressor Mediate Mad Transcriptional Repression. *Cell*, 89:349–356, 1997. 31

L Lajtha. Stem cell concepts. *Differentiation*, 14(1-2):23–34, 1979. 3

E Laurenti, B Varnum-Finney, A Wilson, I Ferrero, W Blanco-Bose, A Ehninger, P Knoepfler, P-F Cheng, H MacDonald, R Eisenman, I Bernstein, and A Trumpp. Hematopoietic stem cell function and survival depend on c-Myc and N-Myc activity. *Cell Stem Cell*, 3(6):611–624, 2008. 36

J Laurikkala, M Mikkola, M James, M Tummers, A Mills, and I Thesleff. p63 regulates multiple signalling pathways required for ectodermal organogenesis and differentiation. *Development*, 133(8):1553–1563, 2006. 23

R Lavker and T Sun. Heterogeneity in epidermal basal keratinocytes: morphological and functional correlations. *Science*, 215(4537):1239–1241, 1982. 11

E Lawlor, L Soucek, L Brown-Swigart, K Shchors, C Bialucha, and G Evan. Reversible kinetic analysis of Myc targets in vivo provides novel insights into Myc-mediated tumorigenesis. *Cancer Research*, 66(9):4591–4601, 2006. 29, 37

T Lechler and E Fuchs. Asymmetric cell divisions promote stratification and differentiation of mammalian skin. *Nature*, 437(7056):275–280, 2005. 11, 13

S Lee, I Kim, L Marekov, E O'Keefe, D Parry, and P Steinert. The structure of human trichohyalin. Potential multiple roles as a functional EF-hand-like calcium-binding protein, a cornified cell envelope precursor, and an intermediate filament-associated (cross-linking) protein. *The Journal of Biological Chemistry*, 268(16):12164–12176, 1993. 21

J Legg, U Jensen, S Broad, I Leigh, and F Watt. Role of melanoma chondroitin sulphate proteoglycan in patterning stem cells in human interfollicular epidermis. *Development*, 130(24):6049–6063, 2003. 11

G Legube, L Linares, C Lemercier, M Scheffner, S Khochbin, and D Trouche. Tip60 is targeted to proteasome-mediated degradation by Mdm2 and accumulates after UV irradiation. *The European Molecular Biology Organization Journal*, 21(7):1704–1712, 2002. 72

N Lehr, S Johansson, S Wu, F Bahram, A Castell, C Cetinkaya, P Hydbring, I Weidung, K Nakayama, K Nakayama, O Söderberg, T Kerppola, and L Larsson. The F-box protein Skp2 participates in c-Myc proteosomal degradation and acts as a cofactor for c-Myc-regulated transcription. *Molecular Cell*, 11(5): 1189–1200, 2003. 34

W Leśniak, Somnicki, and J Kuźnicki. Epigenetic control of the S100A6 (calcyclin) gene expression. *The Journal of Investigative Dermatology*, 127(10): 2307–2314, 2007. 22

D Levens. You Don't Muck with MYC. *Genes & Cancer*, 1(6):547–554, 2010. 32

L Levy, S Broad, A Zhu, J Carroll, I Khazaal, B Péault, and F Watt. Optimised retroviral infection of human epidermal keratinocytes: long-term expression of transduced integrin gene following grafting on to SCID mice. *Gene Therapy*, 5 (7):913–22, 1998. 70

V Levy, C Lindon, B Harfe, and B Morgan. Distinct stem cell populations regenerate the follicle and interfollicular epidermis. *Developmental Cell*, 9(6): 855–861, 2005. 13

A Li, P Simmons, and P Kaur. Identification and isolation of candidate human keratinocyte stem cells based on cell surface phenotype. *Proceedings of the National Academy of Sciences of the United States of America*, 95(7):3902–3907, 1998. 11

E Li, D Owens, P Djian, and F Watt. Expression of involucrin in normal, hyperproliferative and neoplastic mouse keratinocytes. *Experimental Dermatology*, 9 (6):431–8, 2000a. 68

L Li and H Clevers. Coexistence of quiescent and active adult stem cells in mammals. *Science*, 327(5965):542–555, 2010. 5

M Li, A Indra, X Warot, J Brocard, N Messaddeq, S Kato, D Metzger, and P Chambon. Skin abnormalities generated by temporally controlled RXRalpha mutations in mouse epidermis. *Nature*, 407(6804):633–636, 2000b. 12

Y Li, A Pirro, M Amling, G Delling, R Baron, R Bronson, and M Demay. Targeted ablation of the vitamin D receptor: an animal model of vitamin D-dependent rickets type II with alopecia. *Proceedings of the National Academy of Sciences of the United States of America*, 94(18):9831–9835, 1997. 12

W Lien, X Guo, L Polak, L Lawton, R Young, D Zheng, and E Fuchs. Genome-wide Maps of Histone Modifications Unwind In Vivo Chromatin States of the Hair Follicle Lineage. *Cell Stem Cell*, 9(3):219–232, 2011. 43

K Lin, V Kumar, M Geyfman, D Chudova, A Ihler, P Smyth, J Paus, Rand Takahashi, and B Andersen. Circadian Clock Genes Contribute to the Regulation of Hair Follicle Cycling. *PLoS Genetics*, 5(7):14, 2009. 12

T Littlewood, B Amati, H Land, and G Evan. Max and c-Myc/Max DNA-binding activities in cell extracts. *Oncogene*, 7(9):1783–1792, 1992. 29

T Littlewood, D Hancock, P Danielian, M Parker, and G Evan. A modified oestrogen receptor ligand-binding domain as an improved switch for the regulation of heterologous proteins. *Nucleic Acids Research*, 23(10):1686–1690, 1995. 37, 72

C LoCelso, D Prowse, and F Watt. Transient activation of beta-catenin signalling in adult mouse epidermis is sufficient to induce new hair follicles but continuous activation is required to maintain hair follicle tumours. *Development*, 131(8): 1787–1799, 2004. 8, 9, 12

C LoCelso, M Berta, K Braun, M Frye, S Lyle, C Zouboulis, and F Watt. Characterization of bipotential epidermal progenitors derived from human sebaceous gland: contrasting roles of c-Myc and beta-catenin. *Stem Cells*, 26(5):1241–1252, 2008. 9

F Lohman, J Medema, S Gibbs, M Ponec, P Putte, and C Backendorf. Expression of the SPRR cornification genes is differentially affected by carcinogenic transformation. *Experimental Cell Research*, 231(1):141–148, 1997. 21

L Loo, J Secombe, J Little, LS Carlos, C Yost, PF Cheng, E Flynn, B Edgar, and R Eisenman. The Transcriptional Repressor dMnt Is a Regulator of Growth in Drosophila melanogaster . *Molecular Cell Biology*, 25(16):7078–7091, 2005. 31

R Lopez, S Garcia-Silva, S Moore, O Bereshchenko, A Martinez-Cruz, O Ermakova, E Kurz, J Paramio, and C Nerlov. C/EBPalpha and beta couple interfollicular keratinocyte proliferation arrest to commitment and terminal differentiation. *Nature Cell Biology*, 11(10):1181–1190, 2009. 26

N Lopez-Bigas, T Kisiel, D Dewaal, K Holmes, T Volkert, S Gupta, J Love, H Murray, R Young, and E Benevolenskaya. Genome-wide analysis of the H3K4 histone demethylase RBP2 reveals a transcriptional program controlling differentiation. *Molecular Cell*, 31(4):520–530, 2008. 49

T López-Rovira, V Silva-Vargas, and F Watt. Different consequences of beta1 integrin deletion in neonatal and adult mouse epidermis reveal a context-dependent role of integrins in regulating proliferation, differentiation, and in-

tercellular communication. *The Journal of Investigative Dermatology*, 125(6): 1215–1227, 2005. 12

B Lüscher, E Kuenzel, E Krebs, and R Eisenman. Myc oncoproteins are phosphorylated by casein kinase II. *The European Molecular Biology Organization Journal*, 8(4):1111–1119, 1989. 33

S Lyle, M Christofidou-Solomidou, Y Liu, D Elder, S Albelda, and G Cotsarelis. The C8/144B monoclonal antibody recognizes cytokeratin 15 and defines the location of human hair follicle stem cells. *Journal of Cell Science*, 111 (Pt 2): 3179–3188, 1998. 4, 7

I Mackenzie. Relationship between mitosis and the ordered structure of the stratum corneum in mouse epidermis. *Nature*, 226(5246):653–655, 1970. 13, 15

B Malynn, I Alboran, R O'Hagan, R Bronson, L Davidson, R DePinho, and F Alt. N-myc can functionally replace c-myc in murine development, cellular growth, and differentiation. *Genes & Development*, 14(11):1390–1399, 2000. 36

R Marcotte, JF Qian, J Chen, and E Wang. hMad4, c-Myc endogenous inhibitor, induces a replicative senescence-like state when overexpressed in human fibroblasts. *Journal of Cellular Biochemistry*, 89(3):576–588, 2003. 31

I Marenholz, C Heizmann, and G Fritz. S100 proteins in mouse and man: from evolution to function and pathology (including an update of the nomenclature). *Biochemical and biophysical Research Communications*, 322(4):1111–1122, 2004. 22

D Markowitz, S Goff, and A Bank. Construction and use of a safe and efficient amphotropic packaging cell line. *Virology*, 167(2):400–406, 1988. 71

D Marshall, M Hardman, K Nield, and C Byrne. Differentially expressed late constituents of the epidermal cornified envelope. *Proceedings of the National Academy of Sciences of the United States of America*, 98(23):13031–13036, 2001. 18

M Mateyak, A Obaya, S Adachi, and J Sedivy. Phenotypes of c-Myc-deficient rat fibroblasts isolated by targeted homologous recombination. *Cell growth & Differentiation*, 8(10):1039–1048, 1997. 35

S McMahon, H VanBuskirk, K Dugan, T Copeland, and M Cole. The novel ATM-related protein TRRAP is an essential cofactor for the c-Myc and E2F oncoproteins. *Cell*, 94(3):363–374, 1998. 31

S McMahon, M Wood, and M Cole. The essential cofactor TRRAP recruits the histone acetyltransferase hGCN5 to c-Myc. *Molecular and Cellular Biology*, 20 (2):556–562, 2000. 31

G Meroni, A Reymond, M Alcalay, G Borsani, A Tanigami, R Tonlorenzi, C Lo Nigro, S Messali, M Zollo, D Ledbetter, R Brent, A Ballabio, and R Carrozzo. Rox, a novel bHLHZip protein expressed in quiescent cells that heterodimerizes with Max, binds a non-canonical E box and acts as a transcriptional repressor. *The European Molecular Biology Organization Journal*, 16(10):2892–2906, 1997. 31

B Merrill, U Gat, R DasGupta, and E Fuchs. Tcf3 and Lef1 regulate lineage differentiation of multipotent stem cells in skin. *Genes & Development*, 15(13): 1688–1705, 2001. 8

D Mischke, B Korge, I Marenholz, A Volz, and A Ziegler. Genes encoding structural proteins of epidermal cornification and S100 calcium-binding proteins form a gene complex ("epidermal differentiation complex") on human chromosome 1q21. *The Journal of Investigative Dermatology*, 106(5):989–992, 1996. 18

T Montavon, N Soshnikova, B Mascrez, E Joye, L Thevenet, E Splinter, W de Laat, F Spitz, and D Duboule. A Regulatory Archipelago Controls Hox Genes Transcription in Digits. *Cell*, 147:1132–1145, 2011. 152

R Monzon, J LaPres, and L Hudson. Regulation of involucrin gene expression by retinoic acid and glucocorticoids. *Cell Growth & Differentiation*, 7:1751–1759, 1996. 19

M Morasso. Regulation of epidermal differentiation by a Distal-less homeodomain gene. *The Journal of Cell Biology*, 135(6):1879–1887, 1996. 26

J Morgenstern and H Land. Choice and manipulation of retroviral vectors. *Methods in Molecular Biology*, 7:181–206, 1991. 72

R Morris and C Potten. Highly persistent label-retaining cells in the hair follicles of mice and their fate following induction of anagen. *The Journal of Investigative Dermatology*, 112(4):470–475, 1999. 5

R Morris, Y Liu, L Marles, Z Yang, C Trempus, S Li, J Lin, J Sawicki, and G Cotsarelis. Capturing and profiling adult hair follicle stem cells. *Nature Biotechnology*, 22(4):411–417, 2004. 5

V Muncan, O Sansom, L Tertoolen, T Phesse, H Begthel, E Sancho, A Cole, A Gregorieff, I de Alboran, H Clevers, and A Clarke. Rapid loss of intestinal crypts upon conditional deletion of the Wnt/Tcf-4 target gene c-Myc. *Molecular and Cellular Biology*, 26(22):8418–8426, 2006. 35

D Murphy, M Junttila, L Pouyet, A Karnezis, K Shchors, D Bui, L Brown-Swigart, L Johnson, and G Evan. Distinct thresholds govern Myc's biological output in vivo. *Cancer Cell*, 14(6):447–457, 2008. 32, 37

L Nagy, H Kao, D Chakravarti, R Lin, C Hassig, D Ayer, S Schreiber, and R Evans. Nuclear receptor repression mediated by a complex containing SMRT, mSin3A, and histone deacetylase. *Cell*, 89(3):373–380, 1997. 87

M Nair, A Teng, V Bilanchone, A Agrawal, B Li, and X Dai. Ovol1 regulates the growth arrest of embryonic epidermal progenitor cells and represses c-myc transcription. *The Journal of Cell Biology*, 173(2):253–264, 2006. 25, 49

M Nair, V Bilanchone, K Ortt, S Sinha, and X Dai. Ovol1 represses its own transcription by competing with transcription activator c-Myb and by recruiting histone deacetylase activity. *Nucleic Acids Research*, 35(5):1687–1697, 2007. 25

M Nakamura, J Sundberg, and R Paus. Mutant laboratory mice with abnormalities in hair follicle morphogenesis, cycling, and/or structure: annotated tables. *Experimental Dermatology*, 10(6):369–390, 2001. 9

H Nakhai, J Siveke, L Mendoza-Torres, and R Schmid. Conditional inactivation of Myc impairs development of the exocrine pancreas. *Development*, 135:3191–3196, 2008. 36

S Nass and R Dickson. Defining a role for c-Myc in breast tumorigenesis. *Breast Cancer Research and Treatment*, 44(1):1–22, 1997. 40

S Nass, M Li, L Amundadottir, P Furth, and R Dickson. Role for Bcl-xL in the regulation of apoptosis by EGF and TGF beta 1 in c-myc overexpressing mammary epithelial cells. *Biochemical and biophysical Research Communications*, 227(1):248–256, 1996. 41

C Nesbit, J Tersak, and E Prochownik. MYC oncogenes and human neoplastic disease. *Oncogene*, 18(19):3004–3016, 1999. 32

R Newton and N Hogg. The human S100 protein MRP-14 is a novel activator of the beta 2 integrin Mac-1 on neutrophils. *Journal of Immunology*, 160(3): 1427–1435, 1998. 22

H Nguyen, M Rendl, and E Fuchs. Tcf3 governs stem cell features and represses cell fate determination in skin. *Cell*, 127(1):171–183, 2006. 9

C Niemann and F Watt. Designer skin: lineage commitment in postnatal epidermis. *Trends in Cell Biology*, 12(4):185–192, 2002. 12, 13

C Niemann, A Unden, S Lyle, C Zouboulis, R Toftgå rd, and F Watt. Indian hedgehog and beta-catenin signaling: role in the sebaceous lineage of normal and neoplastic mammalian epidermis. *Proceedings of the National Academy of Sciences of the United States of America*, 100 Suppl 1:11873–11880, 2003. 9

J Nilsson, K Maclean, U Keller, H Pendeville, T Baudino, and J Cleveland. Mnt Loss Triggers Myc Transcription Targets , Proliferation , Apoptosis , and Transformation. *Molecular and Cellular Biology*, 24(4):1560–1569, 2004. 31

E Nishimura, S Jordan, H Oshima, H Yoshida, M Osawa, M Moriyama, I Jackson, Y Barrandon, Y Miyachi, and S Nishikawa. Dominant role of the niche in melanocyte stem-cell fate determination. *Nature*, 416(6883):854–860, 2002. 8

J Nowak, L Polak, H Pasolli, and E Fuchs. Hair follicle stem cells are specified and function in early skin morphogenesis. *Cell Stem Cell*, 3(1):33–43, 2008. 7

D Odom, N Zizlsperger, D Gordon, G Bell, N Rinaldi, H Murray, T Volkert, J Schreiber, P Rolfe, D Gifford, E Fraenkel, G Bell, and R Young. Control of pancreas and liver gene expression by HNF transcription factors. *Science*, 303 (5662):1378–1381, 2004. 26

K O'Donnell, E Wentzel, K Zeller, C Dang, and J Mendell. c-Myc-regulated microRNAs modulate E2F1 expression. *Nature*, 435(7043):839–843, 2005. 29

J O'Driscoll, G Muston, J McGrath, H Lam, J Ashworth, and A Christiano. A recurrent mutation in the loricrin gene underlies the ichthyotic variant of Vohwinkel syndrome. *Clinical and Experimental Dermatology*, 27(3):243–246, 2002. 19

M Ohyama, A Terunuma, C Tock, M Radonovich, C Pise-Masison, S Hopping, J Brady, M Udey, and J Vogel. Characterization and isolation of stem cell-enriched human hair follicle bulge cells. *Journal of Clinical Investigation*, 116(1): 249–260, 2006. 7

A Orian, B Steensel, J Delrow, H Bussemaker, L Li, T Sawado, E Williams, L Loo, S Cowley, C Yost, S Pierce, B Edgar, S Parkhurst, and R Eisenman. Genomic binding by the Drosophila Myc, Max, Mad/Mnt transcription factor network. *Genes & Development*, 17(9):1101–114, 2003. 31

T Oskarsson, M Essers, N Dubois, S Offner, C Dubey, C Roger, D Metzger, P Chambon, E Hummler, P Beard, and A Trumpp. Skin epidermis lacking the c-Myc gene is resistant to Ras-driven tumorigenesis but can reacquire sensitivity upon additional loss of the p21Cip1 gene. *Genes & Development*, 20(15): 2024–2029, 2006. 39, 41

D Owens and F Watt. Contribution of stem cells and differentiated cells to epidermal tumours. *Nature Reviews in Cancer*, 3(6):444–451, 2003. 40

C Palmer, A Irvine, A Terron-Kwiatkowski, Y Zhao, H Liao, S Lee, D Goudie, A Sandilands, L Campbell, F Smith, G O'Regan, R Watson, J Cecil, S Bale, J Compton, J DiGiovanna, P Fleckman, S Lewis-Jones, G Arseculeratne, A Sergeant, C Munro, B El Houate, K McElreavey, L Halkjaer, H Bisgaard, S Mukhopadhyay, and W McLean. Common loss-of-function variants of the epidermal barrier protein filaggrin are a major predisposing factor for atopic dermatitis. *Nature Genetics*, 38(4):441–446, 2006. 20

T Parija and B Das. Involvement of YY1 and its correlation with c-myc in NDEA induced hepatocarcinogenesis, its prevention by d-limonene. *Molecular Biology Reports*, 30(1):41–46, 2003. 151

J Patel, Y Du, P Ard, C Phillips, B Carella, C Chen, C Rakowski, C Chatterjee, P Lieberman, W Lane, and S McMahon. The c-MYC oncoprotein is a substrate of the acetyltransferases hGCN5/PCAF and TIP60. *Molecular and Cellular Biology*, 24(24):10826–10834, 2004. 34, 72, 126

C Payne, S Gallagher, O Foreman, J Dannenberg, R DePinho, and Braun R. Sin3a is required by sertoli cells to establish a niche for undifferentiated spermatogonia, germ cell tumors, and spermatid elongation. *Stem Cells*, 28(8): 1424–1434, 2010. 150

S Pelengaris, T Littlewood, M Khan, G Elia, and G Evan. Reversible activation of c-Myc in skin: induction of a complex neoplastic phenotype by a single oncogenic lesion. *Molecular Cell*, 3(5):565–577, 1999. 37, 39

S Pelengaris, M Khan, and G Evan. Suppression of Myc-induced apoptosis in beta cells exposes multiple oncogenic properties of Myc and triggers carcinogenic progression. *Cell*, 109(3):321–334, 2002a. 37, 40

S Pelengaris, M Khan, and G Evan. c-MYC: more than just a matter of life and death. *Nature Reviews in Cancer*, 2(10):764–776, 2002b. 28

G Pellegrini, R Ranno, G Stracuzzi, S Bondanza, L Guerra, G Zambruno, G Micali, and M DeLuca. The control of epidermal stem cells (holoclones) in the treatment of massive full-thickness burns with autologous keratinocytes cultured on fibrin. *Transplantation*, 68(6):868–879, 1999. 11

L Penn, M Brooks, E Laufer, and H Land. Negative autoregulation of c-myc transcription. *The European Molecular Biology Organization Journal*, 9(4): 1113–1121, 1990. 97

J Perez-Losada and A Balmain. Stem-cell hierarchy in skin cancer. *Nature reviews in Cancer*, 3(6), 2003. 40

C Pincelli and A Marconi. Keratinocyte stem cells: friends and foes. *Journal of Cellular Physiology*, 225(2):310–315, 2010. 1, 7, 40

N Popov, T Wahlström, P Hurlin, and M Henriksson. Mnt transcriptional repressor is functionally regulated during cell cycle progression. *Oncogene*, 24 (56):8326–8337, 2005. 32

C Potten and C Booth. Keratinocyte stem cells: a commentary. *The Journal of Investigative Dermatology*, 119(4):888–899, 2002. 13, 14

Y Poumay, F Herphelin, P Smits, I Potter, and M Pittelkow. High-cell-density phorbol ester and retinoic acid upregulate involucrin and downregulate suprabasal keratin 10 in autocrine cultures of human epidermal keratinocytes. *Molecular Cell Biology Research Communications*, 2(2):138–144, 1999. 19

R Presland, D Boggess, S Lewis, C Hull, P Fleckman, and J Sundberg. Loss of normal profilaggrin and filaggrin in flaky tail (ft/ft) mice: an animal model for the filaggrin-deficient skin disease ichthyosis vulgaris. *The Journal of Investigative Dermatology*, 115(6):1072–1081, 2000. 20

C Quéva, P Hurlin, K Foley, and R Eisenman. Sequential expression of the MAD family of transcriptional repressors during differentiation and development. *Oncogene*, 16(8):967–977, 1998. 31

P Rabbitts, A Forster, M Stinson, and T Rabbitts. Truncation of exon 1 from the c-myc gene results in prolonged c-myc mRNA stability. *The European Molecular Biology Organization Journal*, 4(13B):3727–3733, 1985. 31, 32

P Rahl, C Lin, A Seila, R Flynn, S McCuine, C Burge, P Sharp, and R Young. c-Myc regulates transcriptional pause release. *Cell*, 141(3):432–445, 2010. 29, 30, 89, 95

B Ren, F Robert, J Wyrick, O Aparicio, E Jennings, I Simon, J Zeitlinger, J Schreiber, N Hannett, E Kanin, T Volkert, C Wilson, S Bell, and R Young. Genome-wide location and function of DNA binding proteins. *Science*, 290 (5500):2306–2309, 2000. 42, 54

A Reynolds and C Jahoda. Cultured dermal papilla cells induce follicle formation and hair growth by transdifferentiation of an adult epidermis. *Development*, 115(2):587–593, 1992. 12, 13

J Rheinwald and H Green. Serial cultivation of strains of human epidermal keratinocytes: the formation of keratinizing colonies from single cells. *Cell*, 6 (3):331–343, 1975. 11, 70

G Robertson, M Hirst, M Bainbridge, M Bilenky, Y Zhao, T Zeng, G Euskirchen, B Bernier, R Varhol, A Delaney, N Thiessen, O Griffith, A He, M Marra, M Snyder, and S Jones. Genome-wide profiles of STAT1 DNA association using chromatin immunoprecipitation and massively parallel sequencing. *Nature Methods*, 4(8):651–657, 2007. 43

A Rochat, K Kobayashi, and Y Barrandon. Location of stem cells of human hair follicles by clonal analysis. *Cell*, 76(6):1063–1073, 1994. 11

E Rorke, G Adhikary, R Jans, J Crish, and R Eckert. AP1 factor inactivation in the suprabasal epidermis causes increased epidermal hyperproliferation and hyperkeratosis but reduced carcinogen-dependent tumor formation. *Oncogene*, 29(44):5873–5882, 2010. 25

E Rosen, P Sarraf, A Troy, G Bradwin, K Moore, D Milstone, B Spiegelman, and R Mortensen. PPAR gamma is required for the differentiation of adipose tissue in vivo and in vitro. *Molecular Cell*, 4(4):611–617, 1999. 10

J Rothnagel and G Rogers. Trichohyalin, an intermediate filament-associated protein of the hair follicle. *The Journal of Cell Biology*, 102(4):1419–1429, 1986. 21

R Rounbehler, R Schneider-Broussard, C Conti, and D Johnson. Myc lacks E2F1's ability to suppress skin carcinogenesis. *Oncogene*, 20(38):5341–5349, 2001. 39

S Ruiz, C Segrelles, A Bravo, M Santos, P Perez, H Leis, J Jorcano, and J Paramio. Abnormal epidermal differentiation and impaired epithelial-mesenchymal tissue interactions in mice lacking the retinoblastoma relatives p107 and p130. *Development*, 130(11):2341–2353, 2003. 24

T Sandmann, J Jakobsen, and E Furlong. ChIP-on-chip protocol for genome-wide analysis of transcription factor binding in Drosophila melanogaster embryos. *Nature Protocols*, 1(6):2839–2855, 2006. 80

M Sark, D Fischer, E Meijer, P Putte, and C Backendorf. AP-1 and ETS transcription factors regulate the expression of the human SPRR1A keratinocyte terminal differentiation marker. *The Journal of Biological Chemistry*, 273(38): 24683–24692, 1998. 25

R Schofield. The stem cell system. *Biomedicine & Pharmacotherapy*, 37(8): 375–380, 1983. 3

N Schreiber-Agus, L Chin, K Chen, R Torres, G Rao, P Guida, A Skoultchi, and R DePinho. An amino-terminal domain of Mxi1 mediates anti-Myc oncogenic activity and interacts with a homolog of the yeast transcriptional repressor SIN3. *Cell*, 80(5):777–786, 1995. 31

N Schreiber-Agus, Y Meng, T Hoang, H Hou, K Chen, R Greenberg, C Cordon-Cardo, H Lee, and R DePinho. Role of Mxi1 in ageing organ systems and the regulation of normal and neoplastic growth. *Nature*, 393:483–487, 1998. 31

R Sears. The life cycle of C-myc: from synthesis to degradation. *Cell Cycle*, 3 (9):1133–1137, 2004. 33

J Segre. Epidermal differentiation complex yields a secret: mutations in the cornification protein filaggrin underlie ichthyosis vulgaris. *The Journal of Investigative Dermatology*, 126(6):1202–1204, 2006. 20

J Segre, C Bauer, and E Fuchs. Klf4 is a transcription factor required for establishing the barrier function of the skin. *Nature Genetics*, 22(4):356–360, 1999. 26, 95, 150

S Selleri, H Seltmann, S Gariboldi, Y Shirai, A Balsari, C Zouboulis, and C Rumio. Doxorubicin-induced alopecia is associated with sebaceous gland degeneration. *The Journal of Investigative Dermatology*, 126(4):711–720, 2006. 8

P Shrestha, Y Muramatsu, W Kudeken, M Mori, Y Takai, E Ilg, B Schafer, and C Heizmann. Localization of Ca(2+)-binding S100 proteins in epithelial tumours of the skin. *Virchows Archiv International Journal of Pathology*, 432 (1):53–59, 1998. 22

M Sieber-Blum, M Grim, Y Hu, and V Szeder. Pluripotent neural crest stem cells in the adult hair follicle. *Developmental Dynamics*, 231(2):258–269, 2004. 8

V Silva-Vargas, C LoCelso, A Giangreco, T Ofstad, D Prowse, K Braun, and F Watt. Beta-catenin and Hedgehog signal strength can specify number and location of hair follicles in adult epidermis without recruitment of bulge stem cells. *Developmental Cell*, 9(1):121–31, 2005. 8

B Simons and H Clevers. Strategies for homeostatic stem cell self-renewal in adult tissues. *Cell*, 145(6):851–862, 2011. 15

F Smith, A Irvine, A Terron-Kwiatkowski, A Sandilands, L Campbell, Y Zhao, H Liao, A Evans, D Goudie, S Lewis-Jones, G Arseculeratne, C Munro, A Sergeant, G O'Regan, S Bale, J Compton, J DiGiovanna, R Presland, P Fleckman, and W McLean. Loss-of-function mutations in the gene encoding filaggrin cause ichthyosis vulgaris. *Nature Genetics*, 38(3):337–342, 2006. 20

G Smyth. Limma: linear models for microarray data. *Bioinformatics and Computational Biology solutions using R and bioconductor*, (2005):397–420, 2005. 62

H Snippert, A Haegebarth, M Kasper, V Jaks, J Es, N Barker, M Wetering, M Born, H Begthel, R Vries, D Stange, and Clevers H Toftgrd R. Lgr6 marks stem cells in the hair follicle that generate all cell lineages of the skin. *Science*, 327(March):1385–1389, 2010. 7, 9, 13, 15

N Sodir and G Evan. Nursing some sense out of Myc. *Journal of Biology*, 8(8): 77, 2009. 27, 36

L Soucek, S Nasi, and G Evan. Omomyc expression in skin prevents Myc-induced papillomatosis. *Cell Death and Differentiation*, 11(9):1038–1045, 2004. 36

A Spradling, D Drummond-Barbosa, and T Kai. Stem cells find their niche. *Nature*, 414(6859):98–104, 2001. 12

P Staller, K Peukert, A Kiermaier, J Seoane, J Lukas, H Karsunky, T Möröy, J Bartek, J Massagué, F Hänel, and M Eilers. Repression of p15INK4b expression by Myc through association with Miz-1. *Nature Cell Biology*, 3(4): 392–399, 2001. 29, 40

D Steiger, M Furrer, D Schwinkendorf, and P Gallant. Max-independent functions of Myc in Drosophila melanogaster. *Nature Genetics*, 40(9):1084–1091, 2008. 29

M Stewart and D Downing. Chemistry and function of mammalian sebaceous lipids. *Advances In Lipid Research*, 24:263–301, 1991. 8

T Stoelzle, P Schwarb, A Trumpp, and N Hynes. c-Myc affects mRNA translation, cell proliferation and progenitor cell function in the mammary gland. *BioMed Central Biology*, 7:63, 2009. 36

A Strasser, A Harris, M Bath, and S Cory. Novel primitive lymphoid tumours induced in transgenic mice by cooperation between myc and bcl-2. *Nature*, 348 (6299):331–333, 1990. 40

S Swift, J Lorens, P Achacoso, and G Nolan. Rapid production of retroviruses for efficient gene delivery to mammalian cells using 293T cell-based systems. *Current Protocols in Immunology*, Chapter 10:Unit 10.17C, 2001. 70

Y Tai and T Speed. On gene ranking using replicated microarray time course data. *Biometrics*, 65(1):40–51, 2009. 62

K Takahashi and S Yamanaka. Induction of pluripotent stem cells from mouse embryonic and adult fibroblast cultures by defined factors. *Cell*, 126(4):663–676, 2006. 44

H Tani, R Morris, and P Kaur. Enrichment for murine keratinocyte stem cells based on cell surface phenotype. *Proceedings of the National Academy of Sciences of the United States of America*, 97(20):10960–10965, 2000. 11

E Tarcsa, L Marekov, J Andreoli, W Idler, E Candi, S Chung, and P Steinert. The fate of trichohyalin. Sequential post-translational modifications by peptidyl-arginine deiminase and transglutaminases. *The Journal of Biological Chemistry*, 272(44):27893–27901, 1997. 21

G Taylor, M Lehrer, P Jensen, T Sun, and R Lavker. Involvement of follicular stem cells in forming not only the follicle but also the epidermis. *Cell*, 102(4): 451–461, 2000. 13

A Teng, M Nair, J Wells, J Segre, and X Dai. Strain-dependent perinatal lethality of Ovol1-deficient mice and identification of Ovol2 as a downstream target of Ovol1 in skin epidermis. *Biochimica et Biophysica Acta*, 1772(1):89–95, 2007. 95, 150

J Toedling, O Skylar, T Krueger, J Fischer, S Sperling, and W Huber. Ringo an R/Bioconductor package for analyzing ChIP-chip readouts. *BioMed Central Bioinformatics*, 8(1):443, 2007. 54

C Trempus, R Morris, C Bortner, G Cotsarelis, R Faircloth, J Reece, and R Tennant. Enrichment for living murine keratinocytes from the hair follicle bulge with the cell surface marker CD34. *The Journal of Investigative Dermatology*, 120(4):501–511, 2003. 5

C Trempus, H Dang, M Humble, S Wei, M Gerdes, R Morris, C Bortner, G Cotsarelis, and R Tennant. Comprehensive microarray transcriptome profiling of CD34-enriched mouse keratinocyte stem cells. *The Journal of Investigative Dermatology*, 127(12):2904–2907, 2007. 5

N Trivedi, Z Cong, A Nelson, A Albert, L Rosamilia, S Sivarajah, K Gilliland, W Liu, D Mauger, R Gabbay, and D Thiboutot. Peroxisome proliferator-activated receptors increase human sebum production. *The Journal of Investigative Dermatology*, 126(9):2002–2009, 2006. 10

A Truong, M Kretz, T Ridky, R Kimmel, and P Khavari. P63 Regulates Proliferation and Differentiation of Developmentally Mature Keratinocytes. *Genes & development*, 20(22):3185–3197, 2006. 151

T Tumbar, G Guasch, V Greco, C Blanpain, W Lowry, M Rendl, and E Fuchs. Defining the epithelial stem cell niche in skin. *Science*, 303(5656):359–363, 2004. 3, 4, 5, 13

A Vaezi, C Bauer, V Vasioukhin, and E Fuchs. Actin cable dynamics and Rho/Rock orchestrate a polarized cytoskeletal architecture in the early steps of assembling a stratified epithelium. *Developmental Cell*, 3(3):367–381, 2002. 10

A Valouev, David S J, A Sundquist, C Medina, E Anton, S Batzoglou, Richard M M, and A Sidow. Genome-wide analysis of transcription factor binding sites based on ChIP-Seq data. *Nature Methods*, 5(9):829–834, 2008. 43

D VanMater, F Kolligs, A Dlugosz, and E Fearon. Transient activation of beta -catenin signaling in cutaneous keratinocytes is sufficient to trigger the active growth phase of the hair cycle in mice. *Genes & Development*, 17(10):1219–1224, 2003. 8, 9, 12

C VanOevelen, C Bowman, J Pellegrino, P Asp, J Cheng, F Parisi, M Micsinai, Y Kluger, A Chu, A Blais, G David, and B Dynlacht. The mammalian Sin3 proteins are required for muscle development and sarcomere specification. *Molecular and Cellular Biology*, 30(24):5686–5697, 2010. 150

I Västrik, A Kaipainen, T Penttilä, A Lymboussakis, R Alitalo, M Parvinen, and K Alitalo. Expression of the mad gene during cell differentiation in vivo and its inhibition of cell growth in vitro. *The Journal of Cell Biology*, 128(6): 1197–1208, 1995. 31

J Vervoorts, J Lüscher-Firzlaff, S Rottmann, R Lilischkis, G Walsemann, K Dohmann, M Austen, and B Lüscher. Stimulation of c-MYC transcriptional activity and acetylation by recruitment of the cofactor CBP. *The European Molecular Biology Organization Journal*, 4(5):484–490, 2003. 31

J Vervoorts, J Lüscher-Firzlaff, and B Lüscher. The ins and outs of MYC regulation by posttranslational mechanisms. *The Journal of Biological Chemistry*, 281(46):34725–34729, 2006. 33, 34

V Vidal, M Chaboissier, S Lützkendorf, G Cotsarelis, P Mill, C Hui, N Ortonne, J Ortonne, and A Schedl. Sox9 is essential for outer root sheath differentiation and the formation of the hair stem cell compartment. *Current Biology*, 15(15): 1340–1351, 2005. 7

R Waikel, X Wang, and D Roop. Targeted expression of c-Myc in the epidermis alters normal proliferation, differentiation and UV-B induced apoptosis. *Oncogene*, 18(34):4870–4878, 1999. 39

R Waikel, Y Kawachi, P Waikel, X Wang, and D Roop. Deregulated expression of c-Myc depletes epidermal stem cells. *Nature Genetics*, 28(2):165–168, 2001. 9, 13, 24, 39

W Walker, ZQ Zhou, S Ota, A Wynshaw-Boris, and P Hurlin. Mnt-Max to Myc-Max complex switching regulates cell cycle entry. *The Journal of Cell Biology*, 169(3):405–413, 2005. 31, 32

X Wang, H Pasolli, T Williams, and E Fuchs. AP-2 factors act in concert with Notch to orchestrate terminal differentiation in skin epidermis. *The Journal of Cell Biology*, 183(1):37–48, 2008. 25

G Warnes, B Bolker, and T Lumley. gplots: Various R programming tools for plotting data. R package version 2.6.0. 62

F Watt. Involucrin and other markers of keratinocyte terminal differentiation. *The Journal of Investigative Dermatology*, 81(1 Suppl):100s–103s, 1983. 18

F Watt and B Hogan. Out of Eden: stem cells and their niches. *Science*, 287 (5457):1427–1430, 2000. 12

F Watt, M Frye, and S Benitah. MYC in mammalian epidermis: how can an oncogene stimulate differentiation? *Nature Reviews in Cancer*, 8(3):234–242, 2008. 27, 28, 29, 39, 40

A Webb, A Li, and P Kaur. Location and phenotype of human adult keratinocyte stem cells of the skin. *Differentiation*, 72(8):387–395, 2004. 11

C Wei, Q Wu, V Vega, K Chiu, P Ng, T Zhang, A Shahab, H Yong, Y Fu, Z Weng, J Liu, X Zhao, JL Chew, Y Lee, V Kuznetsov, WK Sung, L Miller, B Lim, E T Liu, Q Yu, HH Ng, and Y Ruan. A global map of p53 transcription-factor binding sites in the human genome. *Cell*, 124(1):207–219, 2006. 43

J Wells, B Lee, A Cai, A Karapetyan, WJ Lee, E Rugg, S Sinha, Q Nie, and X Dai. Ovol2 suppresses cell cycling and terminal differentiation of keratinocytes by directly repressing c-Myc and Notch1. *The Journal of Biological Chemistry*, 284(42):29125–29135, 2009. 49

J Welter. Fos-related Antigen (Fra-1), junB, and junD activate Human Involucrin Promoter Transcription by Binding to Proximal and Distal AP1 sites to Mediate Phorbol Ester Effects on Promoter Activity. *The Journal of Biological Chemistry*, 270(21):12614–12622, 1995. 19

R Williams, S Broad, D Sheer, and J Ragoussis. Subchromosomal positioning of the epidermal differentiation complex (EDC) in keratinocyte and lymphoblast interphase nuclei. *Experimental Cell Research*, 272(2):163–175, 2002. 17, 18

A Wilson, M Murphy, T Oskarsson, K Kaloulis, M Bettess, G Oser, A Pasche, C Knabenhans, H Macdonald, and A Trumpp. c-Myc controls the balance between hematopoietic stem cell self-renewal and differentiation. *Genes & Development*, 18(22):2747–2763, 2004. 29, 36

A Wodarz. Molecular control of cell polarity and asymmetric cell division in Drosophila neuroblasts. *Current Opinion in Cell Biology*, 17(5):475–481, 2005. 11

D Wong, H Liu, T Ridky, D Cassarino, E Segal, and H Chang. Module map of stem cell genes guides creation of epithelial cancer stem cells. *Cell Stem Cell*, 2(4):333–344, 2008. 41

H Xu, L Handoko, X Wei, C Ye, J Sheng, CL Wei, F Lin, and WK Sung. A signal-noise model for significance analysis of ChIP-seq with negative control. *Bioinformatics*, 26(9):1199–1204, 2010. 58

M Yaar, M Eller, J Bhawan, D Harkness, P DiBenedetto, and B Gilchrest. In vivo and in vitro SPRR1 gene expression in normal and malignant keratinocytes. *Experimental Cell Research*, 217(2):217–226, 1995. 21

W Yang, C Inouye, Y Zeng, D Bearss, and E Seto. Transcriptional repression by YY1 is mediated by interaction with a mammalian homolog of the yeast global regulator RPD3. *Proceedings of the National Academy of Sciences of the United States of America*, 93(23):12845–12850, 1996. 151

Y Yokota, A Mansouri, and S Mori. Development of peripheral lymphoid organs and natural killer cells depends on the helix loop helix inhibitor Id2. *Nature*, 397:702–706, 1999. 25

K Yoneda and P Steinert. Overexpression of human loricrin in transgenic mice produces a normal phenotype. *Proceedings of the National Academy of Sciences of the United States of America*, 90(22):10754–10758, 1993. 19

K Youssef, A Keymeulen, G Lapouge, B Beck, C Michaux, Y Achouri, P Sotiropoulou, and C Blanpain. Identification of the cell lineage at the origin of basal cell carcinoma. *Nature Cell Biology*, 12(3):299–305, 2010. 40

F Zambelli, G Pesole, and G Pavesi. Pscan: finding over-represented transcription factor binding site motifs in sequences from co-regulated or co-expressed genes. *Nucleic acids research*, 37(Web Server issue):W247–W252, 2009. 97

J Zanet, S Pibre, C Jacquet, A Ramirez, I Alborán, and A Gandarillas. Endogenous Myc controls mammalian epidermal cell size, hyperproliferation, endoreplication and stem cell amplification. *Journal of Cell Science*, 118:1693–1704, 2005. 36, 39

K Zeller, A Jegga, B Aronow, K O'Donnell, and C Dang. An integrated database of genes responsive to the Myc oncogenic transcription factor: identification of direct genomic targets. *Genome Biology*, 4(10):R69, 2003. 29, 95

A Zervos, J Gyuris, and J Brent. Mxi1, a protein that specifically interacts with Max to bind Myc-Max recognition sites. *Cell*, 72(2):223–232, 1993. 31

X Zhang, W Huang, S Yang, LD Sun, FY Zhang, QX Zhu, FR Zhang, C Zhang, WH Du, XM Pu, H Li, FL Xiao, ZX Wang, Y Cui, F Hao, J Zheng, XQ Yang, Hui C, Xiao-Ming L, LiM X, HF Zheng, SM Zhang, JZ Zhang, HY Wang, YL Cheng, BH Ji, QY Fang, YZ Li, FS Zhou, JW Han, C Quan, B Chen, JL Liu, D Lin, L Fan, A Zhang, S Liu, C Yang, P Wang, W Zhou, G Lin, W Wu, X Fan, M Gao, B Yang, W Lu, Z Zhang, KJ Zhu, SK Shen, M Li, XY Zhang, TT Cao, W Ren, X Zhang, J He, XF Tang, S Lu, JQ Yang, L Zhang, DN Wang, F Yuan, XY Yin, HF Wang, XY Lin, and JJ Liu. Psoriasis genome-wide association study identifies susceptibility variants within LCE gene cluster at 1q21. *Nature Genetics*, 41(2):205–210, 2009. 22

Y Zhang, T Liu, C Meyer, J Eeckhoute, D Johnson, B Bernstein, C Nusbaum, R Myers, M Brown, W Li, and X Liu. Model-based analysis of ChIP-Seq (MACS). *Genome Biology*, 9(9):R137, 2008. 58

X Zhao and J Elder. Positional cloning of novel skin-specific genes from the human epidermal differentiation complex. *Genomics*, 45(2):250–258, 1997. 18

D Zimmer and J Dubuisson. Identification of an S100 target protein: glycogen phosphorylase. *Cell Calcium*, 14(4):323–332, 1993. 22

F Zindy, C Eischen, D Randle, T Kamijo, J Cleveland, C Sherr, and M Roussel. Myc signaling via the ARF tumor suppressor regulates p53-dependent apoptosis and immortalization. *Genes & Development*, 12(15):2424–2433, 1998. 34